CORROSION
IN NATURAL ENVIRONMENTS

STP 558

AMERICAN SOCIETY FOR TESTING AND MATERIALS

CORROSION IN NATURAL ENVIRONMENTS

Three symposia
presented at the
Seventy-sixth Annual Meeting
AMERICAN SOCIETY FOR
TESTING AND MATERIALS
Philadelphia, Pa. 24–29 June 1973

ASTM SPECIAL TECHNICAL PUBLICATION 558

List Price $29.75
04-558000-27

AMERICAN SOCIETY FOR TESTING AND MATERIALS
1916 Race Street, Philadelphia, Pa. 19103

Library of Congress Catalog Card Number: 74-77097

Printed in Lutherville-Timonium, Md.
August 1974

Foreword

The papers in this special technical publication were presented during three symposia at the Seventy-sixth Annual Meeting of the American Society for Testing and Materials held in Philadelphia, Pa., 24–29 June 1973. The three symposia were:

1. Atmospheric Corrosion
   S. W. Dean, Jr., Olin Corporation, chairman
   V. P. Pearson, Inland Steel Company, cochairman
2. Metal Corrosion in Seawater
   W. H. Ailor, Reynolds Metals Company, chairman
3. Statistical Planning and Analysis of Corrosion Experiments
   F. H. Haynie, Environmental Protection Agency, chairman
   E. H. Jebe, Ann Arbor, Mich., cochairman

These three symposia are included in this publication.

Related ASTM Publications

Localized Corrosion—Cause of Metal Failure, STP 516 (1972), $22.50 (04-516000-27)

Stress Corrosion Cracking of Metals—A State of the Art, STP 518 (1972), $11.75 (04-518000-27)

Manual of Industrial Corrosion Standards and Control, STP 534 (1973), $16.75 (04-534000-27)

Contents

TESTING IN NATURAL ATMOSPHERES

SEAWATER ENVIRONMENTS

LABORATORY AND STATISTICAL TECHNIQUES

Introduction

As part of its on-going program for "collection of engineer-data and the development of methods of test," Committee G-1 on Corrosion of Metals sponsored three symposia in 1973. These symposia included papers on atmospheric corrosion, seawater corrosion, and statistical planning and analysis of corrosion experiments.

The papers in this book have been arranged into three groups to permit easier reference. These groupings are:

Part 1—Testing in Natural Atmospheres
Part 2—Seawater Environments
Part 3—Laboratory and Statistical Techniques

The papers concerned with atmospheric corrosion in this volume were part of the Symposium on Atmospheric Corrosion, which was organized to update the existing knowledge in the field. The impetus for this effort was twofold. The efforts of governments and industries to reduce atmospheric pollution, especially in urban areas, have changed the nature of atmospheric corrosion in these areas. Also, many agencies are now collecting a range of atmospheric data, and this information is now available to correlate with atmospheric corrosion results. Furthermore, a variety of new materials has been developed since the last ASTM symposium on this subject in 1967,[1] and it was of interest to have at least early performance data on these materials.

Papers on atmospheric corrosion have been assembled covering a wide range of subjects. Five of the papers are concerned with the effects of various weather factors on atmospheric corrosion. These cover a range of topics, including estimating the effects of various weather factors in quantitative terms and selecting sites to give an accurate assessment of the performance of materials. Other subjects of interest include the effects of various alloying elements in steel on its atmospheric corrosion resistance and a new electrochemical technique for measuring instantaneous atmospheric corrosion rates.

Four papers deal with the performance of specific materials in atmospheric sites. These include some early results on new copper-base alloys and data on the exfoliation of aluminum alloys containing zinc, magnesium, and copper. One paper is concerned with the correlation of

---

[1] *Metal Corrosion in the Atmosphere, ASTM STP 435*, American Society for Testing and Materials, 1968.

atmospheric corrosion with the performance of aluminum alloys in accelerated tests.

ASTM Committee G-1 is now responsible for the 20-year test program initiated in 1957 by its predecessor, Committee B-3. Many of the original seven-year exposure panels from Point Reyes, California were lost through vandalism, making it necessary to prepare a second set of panels for a seven-year exposure. These panels have now been retrieved, and the results are given in this volume.

The Symposium on Seawater Corrosion represented a timely mix of several alloys and metal coatings exposed at surface seawater, deep ocean, and sea-floor locations. Some galvanic corrosion data for ferritic stainless steels in seawater were also presented.

The Symposium on Statistical Planning and Analysis of Corrosion Experiments was organized to stimulate greater use of a valuable mathematical tool by corrosion researchers. For this reason, two basic statistics educational lectures were presented during the symposium that were not appropriate for inclusion in this volume. The remaining presentations represented examples of how some researchers are presently using statistics to plan their corrosion experiments and analyze their data. Two of these papers dealt with corrosion in natural environments and are included in this volume.

The information in this book should be useful to engineers interested in the performance of materials in natural environments; to environmentalists interested in obtaining information on the effects of pollution factors on material performance; and to research workers who are developing new materials intended for service in natural environments.

Statistically designed experiments provide the researcher with a maximum amount of desired information from a set amount of work. Decisions based on statistically analyzed data can be accepted with a measurable degree of confidence. These papers should suggest to the reader how he may be able to enhance the results through statistical design and analysis of corrosion experiments.

W. H. Ailor, Jr.

Metallurgical Research Division,
Reynolds Metals Company,
Richmond, Va. 23219;
symposium chairman,
Seawater Corrosion.

S. W. Dean, Jr.

Olin Corporation,
New Haven, Conn. 06504;
symposium chairman,
Atmospheric Corrosion.

F. H. Haynie

National Environmental Research Center,
Research Triangle Park, N. C. 27711;
symposium chairman,
Statistical Planning and Analysis of
Corrosion Experiments.

Testing in Natural Atmospheres

P. J. Sereda[1]

Weather Factors Affecting Corrosion of Metals

REFERENCE: Sereda, P. J., "**Weather Factors Affecting Corrosion of Metals,**" *Corrosion in Natural Environments, ASTM STP 558*, American Society for Testing and Materials, 1974, pp. 7–22.

ABSTRACT: Various weather factors are assessed in relation to corrosion of metals. Published data are discussed and new results presented to show that time-of-wetness is a very important factor and that reasonable values may be obtained from analysis of meteorological records. These are applicable for predicting long-range corrosion effects. For short-term corrosion, data must be collected for the particular exposure conditions. Results are presented to show the effect of orientation on time-of wetness, and recommendations are made for increasing this type of study.

A summary of data on pollution by SO_2 in major cities of Canada is presented and the distribution in Metro Toronto given. It indicates that pollution by SO_2 has been decreasing in many areas of the world. The effects on corrosion of chlorides, corrosion products, and temperature are also discussed.

KEY WORDS: corrosion, metals, weather factors, natural environments, atmospherics, pollution, sulfur dioxide, moisture content, corrosion products, chlorides

Study of the atmospheric corrosion of metals has been an important activity of ASTM for most of its history [*1–4*],[2] and of many other private and public agencies [*5,6*]. Information has been obtained of corrosion loss of numerous metal samples exposed at sites throughout the world. It is therefore ironic that in spite of this volume of accumulated data and experience it is possible to predict the performance of any metal in a particular application in only a very limited way. Unexpected failures resulting from corrosion continue to be a serious problem.

One of the main reasons why the results of atmospheric corrosion testing cannot be used directly for design purposes may be seen from data collected by Larrabee and Ellis and compiled by ASTM Committee G-1, Subcommittee IV [*7*]. Variation in the corrosion rate of steel for 46 sites is very great (Norman Wells to Kure Beach 80-ft lot, 1:1570); the ratio

---

[1] Head, Building Materials Section, Division of Building Research, National Research Council of Canada, Ottawa, Ont., Canada.

[2] The italic numbers in brackets refer to the list of references appended to this paper.

for corrosion rates of steel and zinc varies from 2 for Norman Wells to 118 for Kure Beach. It should be realized that the corrosion rate for a given metal at a given site will depend upon the time of year or even upon the particular weather conditions when the exposure test is initiated [*8*].

Many studies measuring and correlating various weather factors with corrosion rates have attempted to account for these variations and to improve prediction [*9–12*]. It was realized, however, that if reasonable correlations were found it would be somewhat fortuitous because other factors in the system were not being accounted for, especially the effect of corrosion products. Figure 1 attempts to represent the system involved in the prediction of atmospheric corrosion and identifies the area to be dealt with in the present paper. It is clear that complete predictability would have to be based on understanding of the total system, including quantitative interrelations of the many factors. This ideal is far from being realized, but it does not follow that the designer must wait for the final stage before he can use accumulated experience and data to assist him in the selection of materials to be exposed to outdoor environment. This paper assesses to what extent measurement of weather factors has advanced the prediction of the corrosion behavior of metal and what needs to be done in the future.

Moisture

It is over 40 years since Vernon [*13*] found that only beyond a "critical humidity" will rapid acceleration of corrosion occur. The significance of this fact was not fully appreciated until a method was developed for measuring the percentage of time when this critical humidity is exceeded [*9*]. This period is called the time-of-wetness. Subsequent study has shown [*10–16*] that it is the most important factor promoting atmospheric corrosion of metals.

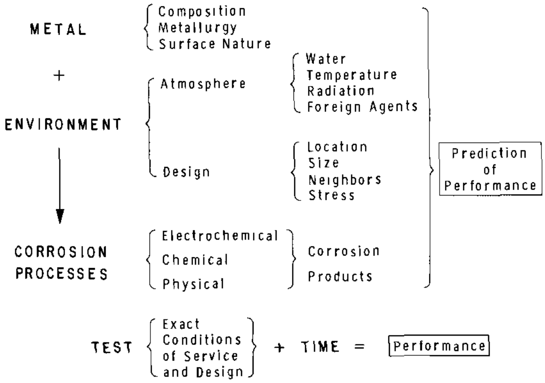

FIG. 1—*Diagrammatic representation of the system in atmospheric corrosion of metals.*

Because of this it is necessary to have a strict definition of time-of-wetness. It should be realized that what is being attempted is a definition in terms of conditions of relative humidity that will result in an adequate film of water on a metal surface to facilitate the highest rate of electrochemical reaction. This condition is obviously influenced by surface contaminants (soluble ions which depress vapor pressure) and the nature of the corrosion products that may render the surfaces hydroscopic or provide pores into which water may condense. Vernon [*13*] showed that in the presence of 0.01 percent sulfur dioxide (SO_2) iron shows a sharp increase in corrosion rate at 60 percent relative humidity (RH) for constant humidity conditions, but that for increasing humidity the sharp increase in the rate begins in the range 70 to 80 percent RH. He also showed that the critical humidity is different for different metals. Tomashov [*17*] suggested classification of atmospheric corrosion by the degree of dampness of the corroding surface. He postulated, first, that under visible moisture films or highly wetted corrosion products the corrosion process proceeds with predominantly cathodic control, and second, that under conditions of thin adsorbed films (below 100 percent RH) control is predominantly by the anodic process.

Although it must be accepted that the effect of humidity on the corrosion process is very complex, it is reasonable to expect that levels of relative humidity can be designated to define the interval during which metal corrodes at a high rate. The approach taken by the author to define this level is based on measurement of the potential developed between platinum and zinc under normal atmospheric conditions [*18,19*]. Time-of-wetness is the interval during which this potential exceeds 0.2 V. In the strictest sense it might be argued that it should apply only to the atmospheric corrosion of zinc, but adequate correlation of steel [*10*] and steel copper and zinc [*11,12*] indicates that this measurement can be used for other metals.

Guttman [*12*] used measuring equipment developed by the author in studying corrosion of zinc and showed that the time-of-wetness measured by this instrumentation corresponded to the time during which humidity exceeded 86.5 percent, based on 4-year averages. The author has measured time-of-wetness at a number of exposure sites (Table 1). These results were compared with the results of RH measurements compiled to show the durations of intervals of humidity.

A computer analysis has been carried out of meteorological data collected by the Department of Environment, Atmospheric Environment Service, for the period 1957 to 1966 to provide the percentage duration of the different levels of RH for 112 stations across Canada. Data for a selected number of stations are presented in Fig. 2, which shows that the data fall roughly into two bands identified as coastal and inland locations. From Table 1 it may be seen that the interval of 87 to 100 percent RH for

TABLE 1—*Percentage time-of-wetness for Canadian exposure sites as measured by the "dew detector."*

	Halifax ARL 1961–1972	Halifax Y.R. 1962–1968	Ottawa 1961–1970	Saskatoon 1962–1970	Esquimalt 1961–1969
Yearly average	39.1	44.1	35.3	30.3	42.5
SD	4.9	3.9	4.9	4.5	4.7
Max	48.4	48.9	41.8	39.5	52.8
Min	30.7	37.3	29.6	25.4	35.7
RH[a] Equivalent 1955–1966	89.0	87.0	80.0	83.0	87.0
Monthly average					
Dec.	44.4	52.0	51.6	47.5	61.5
SD	11.6	8.5	9.6	18.0	9.5
Max	72.3	67.4	71.5	74.8	71.5
Min	29.1	43.0	38.5	26.2	43.8
Monthly average					
June	29.5	36.2	26.8	21.4	23.2
SD	6.8	7.6	11.7	7.0	7.4
Max	47.6	50.4	52.2	29.2	29.5
Min	21.6	24.4	13.7	8.6	7.0

[a] RH value derived from meteorological records (Fig. 2) so that duration of humidity above this value corresponds to the measured time-of-wetness.

Dartmouth and Victoria (both coastal sites) corresponds to the time-of-wetness measured at the York Redoubt and Esquimalt sites (also coastal sites). Intervals of 80 to 100 percent RH for Ottawa and 83 to 100 percent RH for Saskatoon correspond to the measured time-of-wetness.

It should be noted that variations in measured time-of-wetness are very large from year to year (Table 1). Variations from month to month are even larger, and results for December and June are given in Table 1. The significance of the monthly variations in long-term corrosion has not, however, been resolved except that the high rates of corrosion of steel observed at New York for autumn exposures correspond to periods of high time-of-wetness and high SO_2 levels. There is evidence dating back to Vernon [13], Ellis [8], and Guttman [12] that the conditions at time of exposure have an influence on subsequent corrosion rate. This aspect will be discussed later in connection with the effect of corrosion products.

Although there is still doubt regarding the level of humidity that should be taken in determining percentage time-of-wetness and whether it is different for each metal, it is clear that the corrosion process is definitely related to it and that prediction of relative corrosivity at a given site can be improved if time-of-wetness can be predicted. It is now possible to make such a prediction for a locality by using pertinent meteorological data. What is not known, however, is the effect of orientation and location

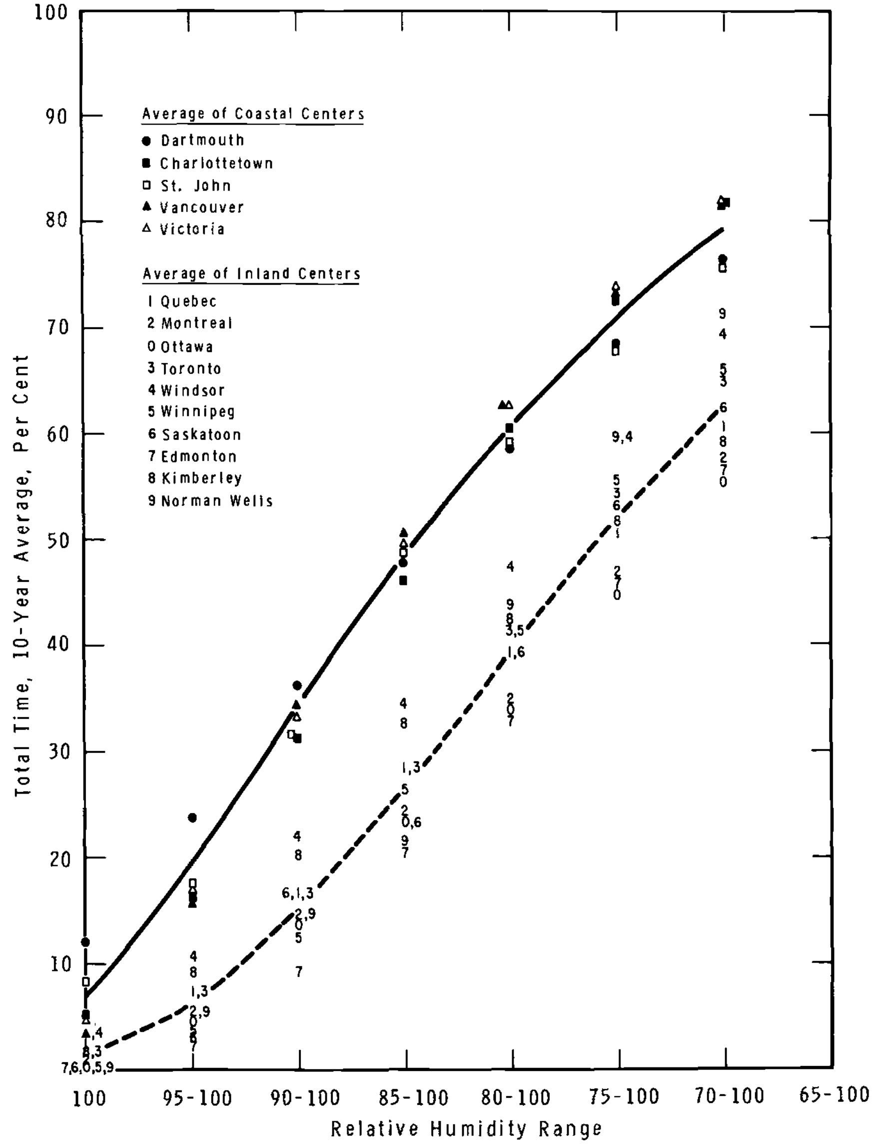

FIG. 2—*Duration of humidity ranges in the atmosphere for major centers in Canada.*

of the metal on a structure. Some work to resolve this question has been carried out by Larrabee [*1*], who showed a threefold variation in the corrosion loss of carbon steel among samples having different degrees of shelter and different orientations. It is suggested that these variations could be largely accounted for by differences in time-of-wetness, as was done by Guttman for different times of exposure [*12*]. Guttman [*20*] also collected

TABLE 2—*Percentage time-of-wetness on galvanized sheet metal exterior walls and roof of a storage building, Trail, B. C. (data collected by Guttman* [20]).

West Exposure	South Exposure			North Exposure		
Wall (midheight)	Roof (overhang)	Wall (near roof overhang)	Wall (midheight)	Roof (overhang)	Wall (near roof overhang)	Wall (midheight)
23.6	50.3	14.6	18.5	51.1	23.2	21.1

data at Trail on the distribution of time-of-wetness of the various exterior surfaces of a galvanized sheet steel wall cladding and roof on a storage building. The metal sheet was insulated on the inside face with foamed-in-place polyurethane. The average percentage time-of-wetness for a period of about one year for a number of measuring points is given in Table 2.

The author has installed dew detector cells behind the precast concrete exterior panels in the vent space at the top and bottom of the north and south walls of a three-storey National Research Council (NRC) laboratory building located in Halifax. The results are given in Table 3 for a period of three years (1968 to 1970). It may be seen that the average time-of-wetness for all the measurements in the walls is close to the value of the average of the outside measurements. There are locations such as those near the top of the building, however, where time-of-wetness is about 50 percent higher than it is near the bottom. There is no doubt that metal ties and brackets, etc., would corrode much faster at the top of the wall than at the bottom. Many specific design features can influence these results and for this reason they should be used with caution until a number of buildings sufficient to indicate a trend have been measured.

It can be stated that time-of-wetness is a very important factor in atmospheric corrosion, and it is recommended that it should be measured to account for the large variations that can occur when short-term corrosion tests are made. Estimates of time-of-wetness for long-term exposures may be predicted with adequate precision from meteorological data. More data should be obtained for time-of-wetness for exposures of metals on structures where the effects of design and orientation can be very large.

TABLE 3—*Percentage time-of-wetness in wall space of ARL building, Halifax, N. S. (3-year average, 1968–1970).*

Location	December	June	Yearly
Outdoors	42.5	26.1	33.7
Average for all walls in building	59.0	27.8	32.2
North wall	61.4	26.1	37.0 (top) 27.7 (bottom)
South wall	56.6	29.5	38.8 (top) 25.6 (bottom)

Pollution

The agents constituting pollution that have been identified with corrosion can be listed as SO_2, hydrogen sulphide (H_2S), ammonia (NH_4), nitrite (NO_2), nitrate (NO), sodium chloride (NaCl) and particulate matter. Of these, only SO_2 and NaCl have been measured or controlled to any extent with the idea of correlating their effects on the corrosion of metals. In most of these cases other factors such as time-of-wetness were not taken into account.

Sulfur Dioxide

Vernon [*13*] was the first to show the serious corrosion-accelerating effect of sulfur dioxide in conjunction with humidity. The correlation between the atmospheric concentration of sulfur dioxide and corrosion of iron and zinc has since been demonstrated by Sereda [*10*], Guttman [*12*], Schikorr [*21*], Hudson and Stanners [*22*], and Barton et al [*23*]. Recently Sydberger and Vannerberg [*24*] have shown that the adsorption rate of SO_2 on polished as well as on corroded samples of metals is greatly influenced by relative humidity. For polished steel the rate increases from 0.1 to 1.4 $mg/cm^2\ h \times 10^{-4}$ as the relative humidity increases from 85 to 95 percent. This work shows that once corrosion products are formed there is a decrease in the level of humidity at which high rates of adsorption of SO_2 may be observed. This fact coupled with observations of Ross and Callaghan [*25*], who showed that sulfate is found in bands at the metal-rust interface during active corrosion, suggests a complex interaction between SO_2 in the atmosphere and the metal in which the corrosion product plays an important part, being itself influenced by the process. The work of McLeod and Rogers [*26*] is also relevant to this subject.

There has been very little work to show the combined effects of various pollutants. Some evidence exists of the effect of ammonia in promoting the wetting of the metal surface, and subsequent involvement of a greater area of the metal [*27*]. Results obtained by Scott and Hobbs [*28*] show that water droplets contain a much higher concentration of sulfates in the presence of ammonia than without it for the same concentration of SO_2.

There can be no doubt that SO_2 pollution is an important factor in atmospheric corrosion of metals, and testing and evaluation of corrosion must involve measurement of SO_2. This was done when the corrosion program was conducted in Canada [*6*] and the results reproduced in Table 4 have been of great help in interpreting these corrosion data. The greatest value, however, lies in predicting the level of corrosion to be expected in other areas for which SO_2 records have been obtained.

Fortunately, various agencies have been measuring pollution by SO_2 for health purposes and a compilation of data has been made for the major cities in Canada (Fig. 3). These data were obtained through the

TABLE 4—*Average amount of sulfur dioxide in the atmosphere at each test site, 1954–1964.*

Site no.	Location	mg SO_3/100 cm^2/day
4	Halifax (Federal building)	6.36
3	Montreal	1.71
8	Trail	0.68
1	Ottawa	0.52
5	York Redoubt	0.28
2	Saskatoon	0.16
7	Esquimalt	0.06
6	Norman Wells	0.01

kind cooperation of the following agencies: Department of Energy and Resources Management, Ontario Government; Department of Health, Air Pollution Control Section, Alberta Government; Department of Health, Government of Manitoba; City of Montreal; Department of Health and Department of Environment, Federal Government of Canada. It should be noted that values of SO_2 listed in the diagram represent dif-

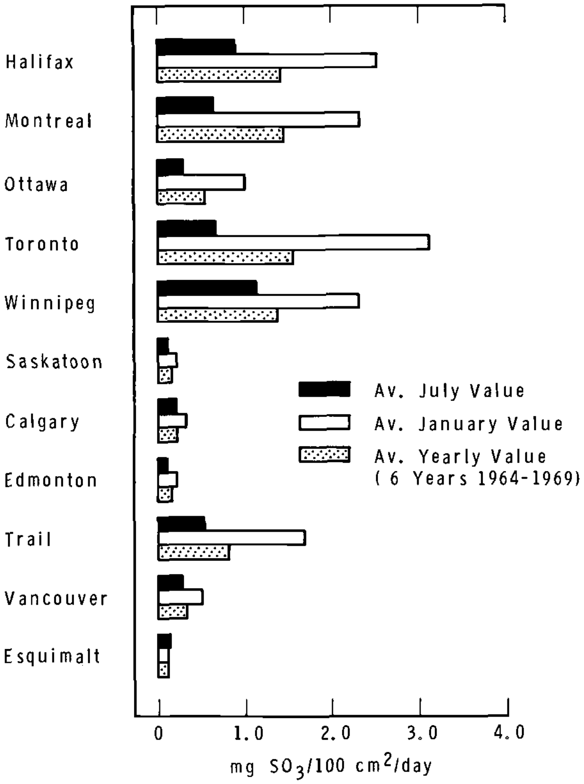

FIG. 3—*Levels of pollution by SO_2 in major cities in Canada.*

ferent numbers of sampling points for the different localities and no assurance can be given that the values are truly representative of the whole area. Some values have quite adequate numbers of sampling points. As an example, the data for the Toronto area are derived from 45 sampling stations, and a contour map has been constructed to show the distribution for 1967 (Fig. 4). (The SO_2 values are in units of mg SO_3/100 cm^2/day.) This is the kind of information that is required for predicting corrosion, although it should be noted that the contour map for 1972 (Fig. 5) shows at least a threefold decrease in air pollution by SO_2. Although prediction becomes less definite with such changing situations, the estimates should have a larger factor of safety if the trend continues. The decreasing SO_2 pollution observed for Toronto was also found for New York. Eisenbud [*29*] reports that the annual maximum hourly concentration was reduced from 2.2 to 0.8 ppm between 1965 and 1969.

It has been reported that SO_2 levels in England have been decreasing for nearly 20 years and Ross [*30*] indicates that the average concentration of SO_2 in the air at ground level seems to have gone down by about 40 percent. Such decreases should certainly begin to reflect on the corrosion of metals. It seems evident that adequate data are now being collected on the levels of SO_2 by agencies concerned with pollution, and that these data can be

Credit
Prov. of Ontario
Dept. of Energy and Resources Management

FIG. 4—*Distribution of pollution by SO_2 in Metro Toronto for 1967.*

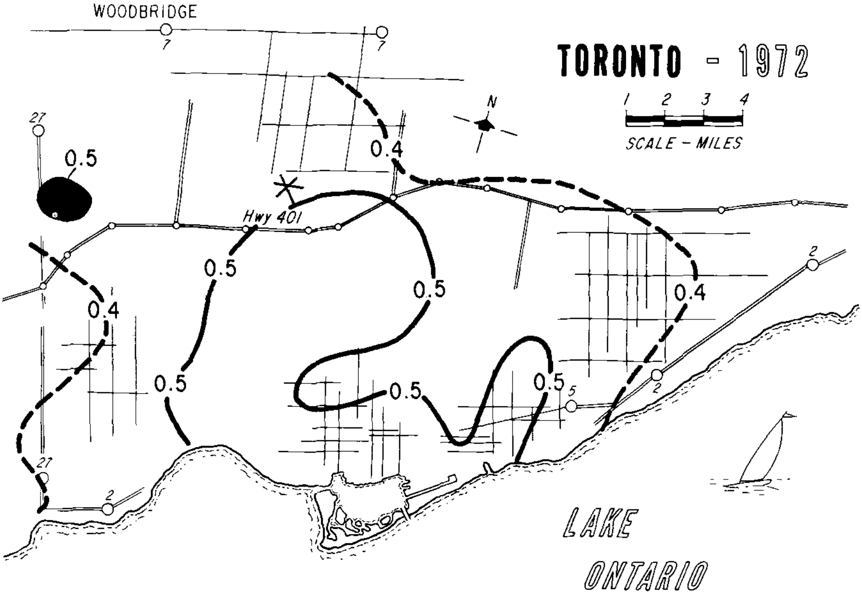

FIG. 5—*Distribution of pollution by SO_2 in Metro Toronto for 1972.*

equally useful to those concerned with corrosion. The necessary liaison is essential.

Chlorides

The accelerated corrosion rate of metals exposed to direct sea spray is well known, and the classic case involves the two exposure sites at Kure Beach, North Carolina, one 80 ft and the other 800 ft from the ocean, where the one-year average weight loss for iron specimens (2 by 4 by ⅛ in.) was found to be 70.5 and 5.8 g, respectively [*1*]. This very clearly shows both the influence of sea salts and the rapid decay of their effect with distance from the sea. Decreasing influence with distance was explored by a special technique called "wire-on-bolt" by Doyle and Godard [*31*], who concluded that the corrosivity of a marine atmosphere is reduced several fold only 1 to 2 km inland. An important question remains unanswered, however; to what extent do sea salts affect corrosion inland? This question is valid when one examines the distribution of sea salts compiled by Brierly [*32*], who shows large variations and high saltfall (average 3.8 lb/acre/year) across North America. What is very surprising is the chloride content found in corrosion products after exposure of steel samples at corrosion sites in Canada and the United States (Table 5).

TABLE 5—*Concentration of chlorides in corrosion products collected from steel samples exposed for one year.*

Location	Chlorides, ppm	
	1st Series 1960	2nd Series 1961–1962
Halifax City, N. S.	796	...
Halifax—York Redoubt	216	...
Montreal, Que.	230	...
Ottawa, Ont.	161	640
Saskatoon, Sask.	359	...
Norman Wells, N. W. T.	568	...
Trail, B. C.	146	369
Esquimalt, Vancouver Island	307	...
Cleveland, Ohio	...	447
South Bend, Pa.	...	507
Kure Beach, N. C. (80-ft lot)	...	1746
Kure Beach, N. C. (800-ft lot)	...	1225

Table 5 shows that the high values of chlorides in corrosion products cannot be readily accounted for in locations such as Norman Wells and Ottawa (2nd series). The fact that values for Halifax and the coastal site at York Redoubt were the reverse of those expected is also unexplained.

Because reasonable correlation was obtained for inland sites without including chlorides [*10–12*], it is thought that a threshold level of chloride is always present at all sites, giving a constant effect, and that only when this level is greatly increased does the effect of corrosion increase significantly. This would account for the rapid decay of the effect with distance from the sea, but more detailed study is clearly needed. A bibliography recently compiled by Brierly [*33*] should prove valuable in this respect.

Corrosion Products

Over 40 years ago Patterson and Hebbs [*34*] showed the relation between moisture in rust and the critical corrosion humidity. This was the first recognition of the effect of the physical nature of corrosion products. La Que [*1*] has related the color of rust to resistance to atmospheric corrosion, indicating that both the physical and chemical natures of the products have an effect upon corrosion rate. In fact, it is logical to consider the products as the barrier or buffer between the atmosphere and the metal surface where the electrochemical processes must occur. The product can act as a protective coating by virtue of its nature, as in weathering steels. This was discussed by Misawa et al [*35*], who showed that copper and phosphorus in steel act as a catalyst in fostering the formation of amorphous δ-Fe O(OH). Under cycles of wetting and drying it becomes stable and forms a protective dense layer on the metal surface. Ross and

Callaghan [*25*] have also made an important contribution to the understanding of the nature of corrosion products.

Thus, there is considerable evidence of the influence of the composition [*36*] as well as the physical nature of corrosion products [*37,38*], but an adequate connection has not yet been made between atmospheric factors and the resulting corrosion products in a given corrosion process.

During one of the exposure programs sponsored by Committee B-3 of ASTM, specimens of steel were exposed to the atmosphere at six selected sites for a period of one year. The author collected the corrosion products and had analyses made for sulfate and chloride ions. The concentrations were determined by the Division of Applied Chemistry, National Research Council. These results were computed to give total sulfate and chloride collected in the corrosion products, based on weight loss and complete conversion to Fe_2O_3. A plot of the results is given in Figs. 6 and 7. The curve for sulfate versus weight loss definitely shows no correlation; that for chloride versus weight loss may be considered to show a trend, but data are incomplete for a definite relation.

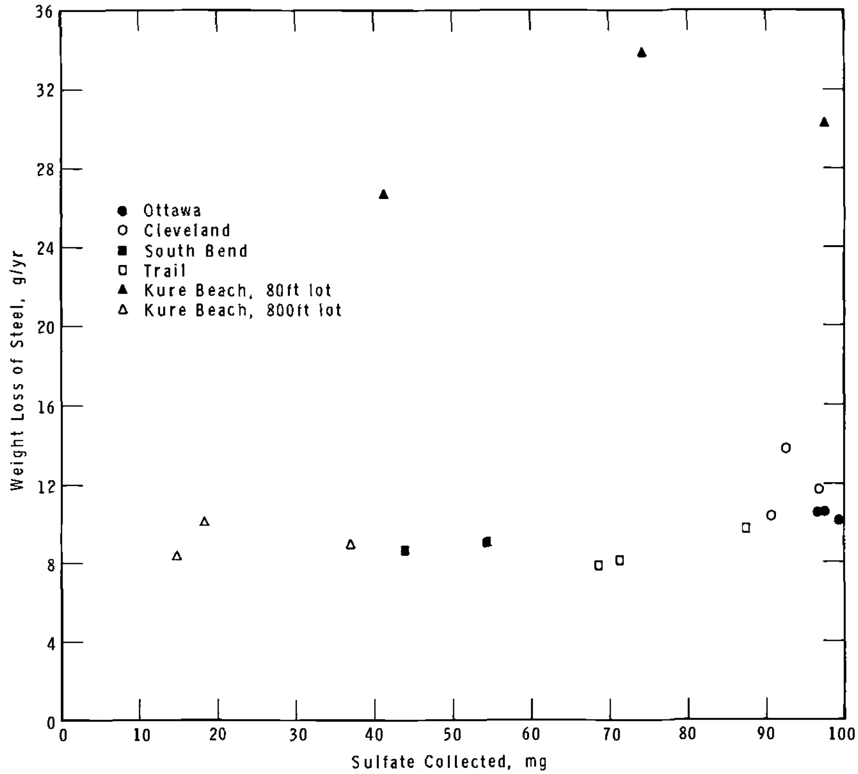

FIG. 6—*Sulfate collected on corrosion specimens related to weight loss.*

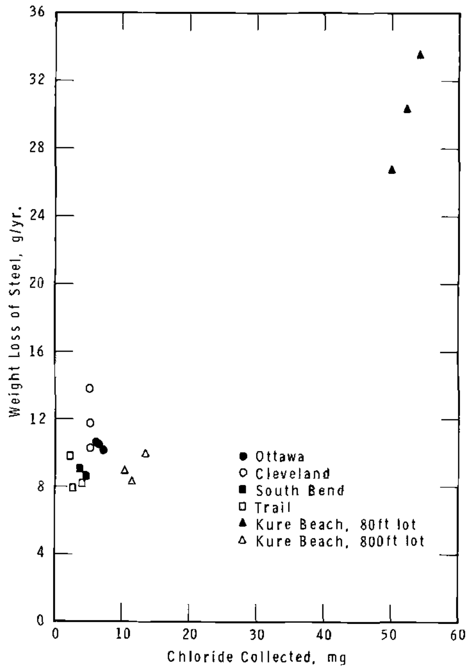

FIG. 7—*Chloride collected on corrosion specimens related to weight loss.*

Temperature

Although it might be expected that temperature would be an important factor in metal corrosion, this has been confirmed only in the work of the author [*10*] and in separate analysis by Grossman [*39*] of data presented by Guttman and Sereda [*11*]. It is not clear why multiple regression analysis of corrosion data and corresponding weather factors does not always indicate a significant correlation with temperature. It may be that the close coupling of the factor of the time-of-wetness associated with dew, hoarfrost, and snow during periods of low temperature may mask the true significance of temperature on corrosion. Early work often showed higher rates of corrosion in winter (than in summer) for some areas where longer periods of time-of-wetness and higher SO_2 pollution prevail in winter. Because these factors were not accounted for, however, there remained an impression that temperature was not a factor because higher rates of corrosion were associated with lower temperature.

In estimating the time when the surface of metal is moistened in a given area, Golubev and Kadyrov [*40*] assumed that a film of water would not serve as an electrolyte at a temperature below −1°C (30°F). Results from the author's work using the potential developed between platinum and zinc to indicate the presence of an electrolyte show that there is no "freezing" point at which corrosion would cease. Potentials were measured at temperatures as low as −20°C (−4°F) and (since time-of-wetness measured in this way, including conditions of low temperature, correlates with corrosion rate) confirmed that there is no "freezing" point in this process.

It is believed that temperature is an important factor but that its effect is manifested through other factors. The author believes that the low average temperature at Norman Wells accounts for a significant part of the very low corrosion rate there for steel and zinc, as shown by Gibbons [6] and by the report of ASTM Committee G-1, Subcommittee IV Section 1 [7]. Now that major industrial development is taking place in the Far North the effect of temperature on corrosion may be investigated more closely to resolve this question.

Summary

Assessment of the measurement and correlation of atmospheric factors affecting the corrosion of metals has shown that such measurements are useful in predicting levels of corrosion in a given area from data obtained in other areas. The importance of the time-of-wetness value is also stressed. For long-term exposures it can be derived from meteorological records.

Most areas may be classed as either coastal or inland, but more data are required to take account of precise orientation, location and design of the metal on a structure.

Data already collected with regard to pollution are useful in corrosion technology and should be made more widely available. Evidence that pollution is on the decrease in many major centers provides an added factor of safety in design. If the trend continues it should result in major savings.

It is recognized that much work remains to be done before a full understanding of the system involved in atmospheric corrosion is achieved, but the end is in sight. In the meantime, prediction is more reliable.

Acknowledgment

The author is grateful to the Provincial and Federal Departments of Health and Environment and to the City of Montreal for supplying data on pollution by SO_2; to the Department of the Environment, Atmospheric Environment Service, for meteorological data; and to H. Guttman and P. Grossman, who provided private data.

The author also acknowledges with thanks the assistance of G. A. O'Doherty and H. F. Slade, DBR/NRC, for supervising the collection of data and installing the instrumentation; and that of the Regional Stations, officers in charge, J. J. Hamilton and D. C. Tibbetts, and their staffs for attending to the operation of equipment at the field stations.

This paper is a contribution from the Division of Building Research, National Research Council of Canada, and is published with the approval of the Director of the Division.

References

[*1*] La Que, F. L., "Corrosion Testing," *Edgar Marburg Lecture*, American Society for Testing and Materials, 1951.

[*2*] *Atmospheric Corrosion of Non-ferrous Metals, ASTM STP 75*, American Society for Testing and Materials, 1956.

[*3*] *20-year Atmospheric Corrosion Investigation of Zinc-Coated and Uncoated Wire and Wire Products, ASTM STP 290*, American Society for Testing and Materials, 1961.

[*4*] *Metal Corrosion in the Atmosphere, ASTM STP 435*, American Society for Testing and Materials, 1968.

[*5*] Hudson, J. C., *Iron and Steel*, Nov. 1947, pp. 507–518.

[*6*] Gibbons, E. V., "The Corrosion Behaviour of the Major Architectural and Structural Metals in Canadian Atmospheres. Summary of Ten-year Results of Group 1," National Research Council of Canada, Division of Building Research, NRC 11630, Oct. 1970.

[*7*] "Corrosiveness of Various Atmospheric Test Sites as Measured by Specimens of Steel and Zinc," *Metal Corrosion in the Atmosphere, ASTM STP 435*, American Society for Testing and Materials, 1968.

[*8*] Ellis, O. B., *ASTM Proceedings*, American Society for Testing and Materials, Vol. 49, 1949, p. 152.

[*9*] Sereda, P. J., "Measurement of Surface Moisture and Sulfur Dioxide Activity at Corrosion Sites," *ASTM Bulletin*, American Society for Testing and Materials, No. 246, May 1960, pp. 47–48.

[*10*] Sereda, P. J., *Industrial and Engineering Chemistry*, Vol. 52, No. 2, Feb. 1960, pp. 157–160.

[*11*] Guttman, H. and Sereda, P. J., *Metal Corrosion in the Atmosphere, ASTM STP 435*, American Society for Testing and Materials, 1968, pp. 326–359.

[*12*] Guttman, H., *Metal Corrosion in the Atmosphere, ASTM STP 435*, American Society for Testing and Materials, 1968, pp. 223–239.

[*13*] Vernon, W. H. J., *Transactions*, Faraday Society, Vol. 27, 1931, pp. 265–277, and *Faraday Society*, Vol. 31, 1935, pp. 1668–1700.

[*14*] Sanyal, B., Singhania, G. K., and Nanda, J. N., *Proceedings*, 3rd International Congress on Metallic Corrosion, Moscow, 1966, Vol. 4, 1969, pp. 542–553.

[*15*] Addanki, S. R., Mukherjee, K. P., Lahiri, A. K., and Banerjee, T., *Proceedings*, 3rd International Congress on Metallic Corrosion, Moscow, 1966, Vol. 4, 1969, pp. 554–563.

[*16*] Golubev, A. I. and Kadyrov, M. K., *Proceedings*, 3rd International Congress on Metallic Corrosion, Moscow, 1966, Vol. 4, 1969, pp. 522–531.

[*17*] Tomashov, N. D., in *The Science of Corrosion*, Macmillan, New York, 1966.

[*18*] Sereda, P. J., "Measurement of Surface Moisture—A Progress Report," *ASTM Bulletin*, No. 228, American Society for Testing and Materials, Feb. 1958, pp. 53–55.

[*19*] Sereda, P. J., "Measurement of Surface Moisture—Second Progress Report," *ASTM Bulletin*, No. 238, American Society for Testing and Materials, May 1959, pp. 61–63.

[*20*] Guttman, H., private communication.

[*21*] Schikorr, G. and Schikorr, I., *Zeitschrift für Metallkunde*, Vol. 35, No. 9, Sept. 1943, pp. 175–181.

[*22*] Hudson, J. C. and Stanners, J. F., *Journal of Applied Chemistry*, Vol. 3, 1953, p. 86.

[*23*] Barton, K., Beranek, E., and Akimov, G. V., *Werkstoffe und Korrosion*, Vol. 10, No. 6, 1959, pp. 377–383.

[*24*] Sydberger, T. and Vannerberg, N. G., *Corrosion Science*, Vol. 12, 1972, pp. 775–784.

[*25*] Ross, T. K. and Callaghan, B. G., *Corrosion Science*, Vol. 6, 1966, pp. 337–343.

[*26*] McLeod, W. and Rogers, R. R., *Electrochemical Technology*, Vol. 6, 1968, pp. 231–235.

[*27*] Ross, T. K. and Callaghan, B. G., *Nature*, Vol. 211, No. 5044, July 1966, pp 25–26.

[*28*] Scott, W. D. and Hobbs, P. V., *Journal of Atmospheric Science*, Vol. 24, No. 1, Jan. 1967, pp. 54–57.

[*29*] Eisenbud, M., *Science*, Vol. 170, No. 13, 1970, pp. 706–712.

[*30*] Ross, F., *New Scientist and Science Journal*, Vol. 13, May 1971, pp. 373–378.

[*31*] Doyle, D. P. and Godard, H. P., *Proceedings*, 3rd International Congress on Metallic Corrosion, Moscow, 1966, Vol. 4, 1969, pp. 429–437.

[*32*] Brierly, W. B., *Journal of Environmental Sciences*, Vol. 8, No. 5, 1965, pp. 15–23.

[33] Brierly, W. B., "Bibliography of Atmospheric (Cyclic) Sea-salts," U.S. Army, Natick Laboratories, Technical Report 70-63-ES, April 1970.
[34] Patterson, W. S. and Hebbs, L., *Tranasctions*, Faraday Society, Vol. 27, 1931, pp. 277–283.
[35] Misawa, T., Kyuno, T., Suetaka, W., and Shimodaira, S., *Corrosion Science*, Vol. 11, 1971, pp. 35–48.
[36] Horton, J. B., Goldberg, M. M., and Watterson, K. F., *Proceedings*, 4th International Congress on Metallic Corrosion, Amsterdam, 1969, pp. 385–391.
[37] Okada, Hideya, Hosoi, Yuzo, Yukawa, Ken-ichi, and Naito, Hiromitsu, *Proceedings*, 4th International Congress on Metallic Corrosion, Amsterdam, 1969, pp. 392–398.
[38] Fyfe, D., Shanahan, C. E. A., and Shreir, L. L., *Proceedings*, 4th International Congress on Metallic Corrosion, Amsterdam, 1969, pp. 399–407.
[39] Grossman, P., private communication.
[40] Golubev, A. I. and Kadyrov, M. Kh., *Proceedings*, 3rd International Congress on Metallic Corrosion, Moscow, 1966, Vol. 4, 1969, pp. 522–531.

In the later stages of preparation of this paper, the following translation of a Russian book was published: "Atmospheric Corrosion of Metals" by I. L. Rozenfeld, National Association of Corrosion Engineers, Houston, Texas, 1973, 238 p (translated by Boris Tytel; edited by E. C. Greco). This book is considered an important contribution to the subject and is therefore cited here in this way.

J. F. Stanners[1]

Selecting Testing Conditions Representative of the Atmospheric Environment

REFERENCE: Stanners, J. F., "**Selecting Testing Conditions Representative of the Atmospheric Environment,**" *Corrosion in Natural Environments, ASTM STP 558*, American Society for Testing and Materials, 1974, pp. 23–32.

ABSTRACT: The main environmental factors that affect atmospheric corrosion of metals are examined and their range and distribution are related to steel utilization. From the data available, recommendations are made for the selection of exposure sites in Great Britain likely to be more representative of conditions in which steel is used than are present sites. A method is suggested for examining pollution data in this context. The implications for natural atmospheric exposure testing are discussed.

KEY WORDS: air pollution, atmospheric corrosion, field tests, test sites, corrosion

This paper describes a method of deciding what environmental conditions should be looked for in choosing exposure sites. Atmospheric corrosion tests are usually conducted either to compare performances in an arbitrary environment or to investigate absolute performance in a given environment. In the former case, experience shows that different orders of merit are found at different exposure sites; the selection of sites significantly affects the result. In the latter case, it is important to choose environments such that results there can be related to performance in practice. The technique of selection is illustrated by the example of testing steels or coated steels in Great Britain but should have wider validity.

Many prominent authorities, including ASTM, have a wide range of exposure sites at which to carry out atmospheric corrosion tests. While in most cases these sites can be related to the environment in general terms, little is known quantitatively about the relationship between the conditions found at these test sites and the range of conditions that has to be withstood in service. This paper describes an attempt to collect such data and hence to find a method of selecting sites that would be in a meaningful way representative of the conditions to which steel is exposed when in use.

---

[1] Head, Corrosion Control Section, Corporate Engineering Laboratory, British Steel Corporation, London, England.

The need was for exposure conditions ranging from the best to worst, special exceptions apart, that the steel is likely to encounter in service in the market under consideration. Tests at sites exhibiting such a range would then show how far corrosion resistance or coatings durability could be reduced so as to avoid adding unduly to product cost. Such trials would also show whether the product were capable of withstanding the worst conditions for a reasonable period of time.

In the United Kingdom, about 50 percent of all the corrosion rate results for steel recorded in the literature relate to one atmosphere, that at Sheffield. This has given the impression that steel corrodes at a much greater rate in the United Kingdom than it would in many districts at the present time. Moreover, there is no way of correcting this bias in the results.

An attempt was made, therefore, to reexamine the way in which exposure sites might be selected. Two main steps proved necessary. The first was to investigate the distribution of the utilization of steel and steel products throughout the country, and the second was to elucidate what specific environmental factors affect the corrosion of metals or the breakdown of coatings, and how these factors vary from place to place.

As will be described, the procedure then adopted was to use the estimates of the geographical distribution of steel utilization as a means of weighting the importance to be attached to the level of each environmental factor found in each particular locality. These weighted importances were then used to construct cumulative frequency curves of the probability of steel being exposed to successive levels of each factor through the country as a whole. The principal factors studied were duration of wetness, kind and degree of atmospheric pollution, extent of sea-salt contamination, temperature, and amount of solar radiation.

Estimating the Distribution of Steel Utilization

The first step was to estimate the likelihood of steel being exposed to various levels of each parameter. To have attached equal weight to every part of the country would have been to place too much stress on rural and highland conditions where least steel is used, so some method had to be found of weighting the data to allow for this. Local records were not available of the amount of steel used in different localities. The sales in different localities were no guide, since steel objects are often made in one place and used in another. A simple postulate that steel consumption is proportional to population of a given locality seemed to be the only one that could be used. From this it was further assumed that the probability of steel being exposed to the atmosphere at a particular place (or the amount of steel exposed there in a given period of time) would also be roughly related to population. This approximation breaks down if the unit areas become too small, but it seemed reasonable to expect it to hold true for natural units of population such as towns. The approximation is also weakened by the use of steel (for example, for communications) outside centers of population, and by a proportionally greater use of steel per head of population in large towns. These criticisms, though valid, are believed not to be fatal to the present application of the method. The magnitude of the effect of this weighting, to lay most emphasis on places where steel is most used, can be immediately recognized when it is realized that, even in the relatively crowded island of Great Britain, 78 percent of the people live in only 10 percent of the area (that designated "urban").

Environmental Factors to be Taken into Account

Though it will be recognized that the severity of the conditions of exposure of a piece of steel depends very much upon design, such matters need not be taken into account directly in the original selection of exposure sites. Earlier studies *[1]*[2] have indicated that the factors that must be taken into account include duration of wetness of surfaces, their temperature, the ultraviolet radiation reaching them, industrial air pollution, and the sea salt in the air at marine sites. To find the distribution of the factors of interest over the whole country it was necessary to select measures of them that had already been widely made throughout the country. For each environmental factor one or more such parameters was chosen that reflected its magnitude, often in a simplified fashion. Thus, to represent "duration of wetness," one of the parameters chosen was the number of hours per year when the atmospheric relative humidity was 90 percent or more. For each of the 1800 local authorities, one average value only was estimated of each parameter used to represent wetness, temperature, or solar radiation.

For the following reasons this procedure could not be adopted for sulphur pollution or for sea-salt concentrations in the air. While meteorological records cover most of the country, measurements of domestic and industrial air pollution are restricted mainly to towns and, even so, in a fashion which does not adequately reflect the range of pollution found over the whole country. Local variability is also too great to allow the use of one average value for each locality. Because of this, it has been necessary to examine the sulphur pollution records by a different method from that used for the meteorological records. This method will be described later. There is also a problem relating to the salinity of the atmospheres near the sea. Practially no measurements of this factor have been made and it has, therefore, regretfully, been necessary to exclude marine atmospheres from the present study.

[2] The italic numbers in brackets refer to the list of references appended to this paper.

Variability of the Selected Environmental Factors

The data shown in Table 1 were extracted from the records [*2–8*] for every local authority in Great Britain. The *regions* were the statistical regions for census purposes. The *classes* were based on population, according to size, one *type* of local authority, namely 'Rural Districts', being placed in the lowest population class whatever its actual population. Available records showed *temperatures* at sea level, so the mean *height* of each locality was needed to convert these back to temperatures at the elevation in question.

TABLE 1—*Environmental data selected.*

For each:

Local Authority	Pollution Measuring Site
Region	Region
Class	Class of local authority
Type	Type of local authority
Population	Population of local authority
Coastal or inland	Coastal or inland local authority
Duration of:	Site classification (Warren Spring Laboratory System)
-bright sunshine	
-relative humidity of 90 percent or more	Sulfur dioxide concentrations:
-rain	-annual average of daily readings
Height above sea level	-highest monthly average in the year
Annual average of daily:	
-mean temperature	-highest daily reading in the year
-maximum temperature	

Histograms were made of the distribution of the level of the meteorological variables with respect to population, using a single value of each factor to represent each local authority.

Figure 1 shows the data for duration of periods of high relative humidity. The histogram has been converted to a cumulative frequency curve (the upper curve). The corresponding curve produced on the basis of land area affected, instead of population affected, has been added for comparison purposes (the lower curve). It will be seen from the shaded sectors that the range of conditions required to cover 95 percent of the population corresponds to the range for much less than 95 percent of the area. Thus, by weighting the observations on population, the range of conditions that has to be considered is narrowed from the full range occurring (between the solid vertical lines) to that between the two broken verticals. Had area been used as the criterion, a different, and wider, range would have had to be taken into account.

Figure 2 shows the appearance of an original histogram. The one shown is for sulphur pollution, in the Greater London Region, not for a meteoro-

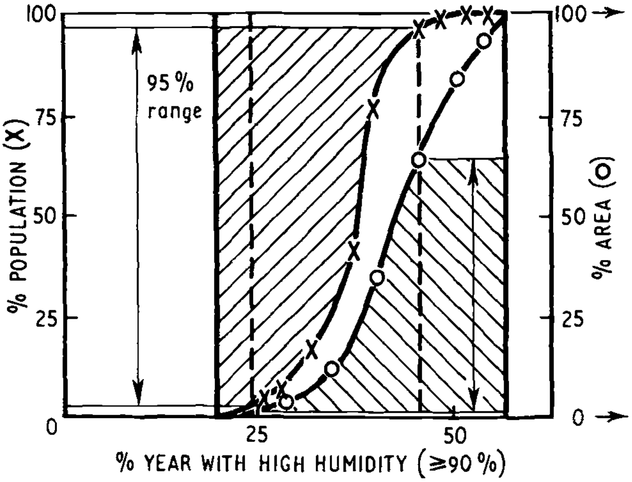

FIG. 1—*Cumulative frequency curve for periods of high relative humidity (on population, on area) effect of deleting extremes, Great Britain.*

logical factor over the whole country, though these appeared similar. The method of estimating such a histogram for sulphur pollution will now be described.

Sulphur dioxide concentration as measured by the daily volumetric method was used for the survey. It was found that there were some 721 sites in the country at which full pollution records were available from the

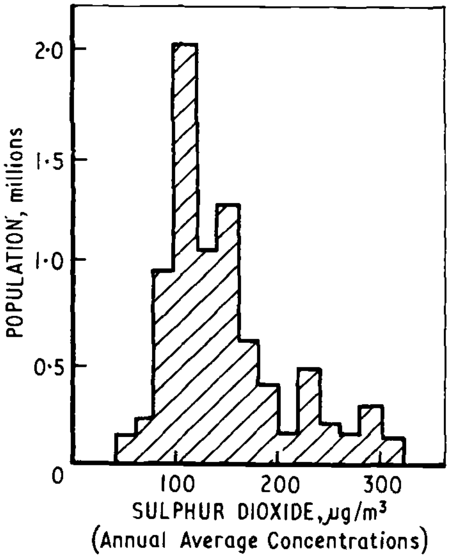

FIG. 2—*Histogram of annual average concentrations of sulfur dioxide to which the population of Greater London was exposed (estimated from 1969 to 1970 records).*

year April 1969 to March 1970. It was necessary to take a single year for the studies, since pollution changes from year to year. This means that a reexamination of the pollution influence on the selection of sites will have to be made at reasonably frequent intervals. The records available related to most of the large towns, to smaller proportions of the medium sizes of towns, and to about 8 percent of the small towns of 5000 to 20 000 inhabitants. In addition, rural areas and towns of less than 5000 inhabitants were represented by at least one such town or village in each major county and by 20 isolated sites. Since a single value of pollution could clearly not be selected for each local authority, a separate study was made of the distribution of pollution in each of the five classes of local authority in each of the eleven statistical regions. The assumption was made that, taken as a whole, the pollution records available were representative of the range and distribution of pollution to which the whole population in that class of local authority in that region of the country was exposed. The records for each local authority were considered individually. A weight was assigned to each available sulphur pollution reading, proportional to the population of that local authority, except that, if there was more than one pollution site in any single local authority, the population was assigned equally among the pollution sites and the weighting thus shared among them. This was done to avoid giving excessive weight to a few towns that had been more extensively studied than usual. For each class of local authority in each region, a histogram was thus plotted of the population exposed to each level of sulphur pollution in steps of 20 $\mu g/m^3$. To get the same vertical scale on all the histograms for each class and region, a further weighting was then applied, increasing the populations assigned to each pollution level in the ratio of the total population of the class to the population of those local authorities in the class and region from which pollution data had actually been obtained. The result for annual average sulphur dioxide concentrations in Greater London (that is, Region 1, Class 1) is illustrated in Fig. 2. The histograms were then added together to form a composite histogram representative of the country as a whole.

Selection of Conditions Required at Exposure Sites

At this stage in the work, histograms were available for the country to show the relationship between the levels of the main environmental conditions and the population exposed to these levels. For interest, the population-weighted median conditions found outdoors in Great Britain are shown in Table 2. It seems reasonable to assume that in making a selection of exposure sites the absolute extremes would be avoided. It was arbitrarily decided to remove the 2½ percent 'tails' from each distribution as derived in the foregoing. It was found that 95 percent of the people in Great Britain lived (and therefore, according to the assumptions of this study, most steel surfaces occur) in places exposed in an average year to between

TABLE 2—*Estimate of median environmental conditions to which the population of Great Britain is exposed outdoors.*

Duration of bright sunshine, h/year	1400
Duration of relative humidities of 90 percent or more, h/year	3500
Duration of rain, h/year	550
Annual average of daily mean temperature, °C	9.2 (49°F)
Annual average of daily maximum temperature, °C	13.3 (56°F)
Sulfur dioxide concentrations (1969 to 1970):	
-average, μg/m^3	85
-highest monthly average, μg/m^3	140

450 and 850 h of rain, 1150 and 1700 h of bright sunshine, and 2250 and 4000 h of relative humidities of 90 percent or more. The corresponding 95 percent ranges of annual averages of daily mean and daily maximum temperatures were 7.2 to 10.4°C (45 to 51°F) and 11.6 to 14.4°C (53 to 58°F), respectively. The sulfur dioxide concentrations in the air in 1969 to 1970 had a population-weighted 95 percent range of yearly averages of 25 to 231 μg/m^3.

At first sight, it might seem to be the next logical step to select exposure sites that represent certain combinations (say the upper level of each) of all of these factors simultaneously. If taken literally, such a step would be doomed to failure. First of all, the factors are not independent of one another. Secondly, even if they were, this would not fully represent the conditions to which steel is exposed, since the factors interact in their influence on corrosion or coatings breakdown. What is really required is some overall measure of severity of the environment as related to the factors that cause it. As summarized in an earlier paper [9], models of atmospheric corrosion have been attempted by several workers. There have been several improved versions since, but none has succeeded in producing a model that has a wide enough application to be acceptable for the present purpose. It is clear that to produce such a model is the next step toward refining the selection of exposure sites. Until this can be done, the best that seems possible is to attempt to make a selection based on the 95 percent range of each factor, but considering them successively and not

TABLE 3—*Range of conditions required for test sites in Great Britain for bare steel.*

	95 percent—Range for Bare Steel	
Factor	Annual Averages and Parameter Used	
Pollution:	25 to 231	SO_2, μg/m^3
Wetness:	2250 to 4000	relative humidity of 90 percent or more, h
Rain washing:	850 to 450	rain, h
Temperature:	7.2 to 10.4 (45 to 51)	daily means, °C (daily means, °F)

simultaneously, using common sense to decide which factors have the most important influence on corrosion.

One suitable method is illustrated by taking the case of bare steel as in Table 3 with the ranges mentioned earlier (although these specific values may be modified for the real selection). For the corrosion of bare steel in Great Britain, the variable causing the greatest change in corrosion between its lowest and highest levels is probably sulfur dioxide concentration. This is set, therefore, for two groups of sites, at about 25 and about 230 $\mu g/m^3$, respectively. Hours of high humidity might be taken next as being of almost equal importance. Within each of the two levels of sulfur pollution, sites should be found with hours of humidities of 90 percent or more as near as possible to 2250 and 4000, respectively. (In fact, the combination of low hours of high humidity and low sulfur pollution is hard to find, because almost all the dry areas of the country are highly industrialized and thus polluted.) It would suffice finally, since the influence on corrosion across their range is smaller, to take high and low levels of rain simultaneously with low and high daily mean temperatures, respectively, ignoring sunshine altogether. Thus, within practical limits, 850 h of rain per year would be taken with 7.2°C (45°F) daily mean temperature, and 450 h of rain per year with 10.4°C (51°F). The number of sites so chosen is two (for low and high sulfur pollution), times two (for short and long durations of wetness), times two (for high rainfall with low temperature and for low low rainfall with high temperature). This is a total of eight sites to represent the country.

Feasibility of Selecting Sites

The final step in the operation is to select localities for exposure sites where (according to the same records used in the survey) the conditions match sufficiently closely those defined for the (for bare steel) eight sites. There obviously will be a wide choice of such places, and other factors such as accessibility, freedom from vandalism and security of tenure must then be taken into account [*1*]. It is to be hoped that many of the existing sites in Great Britain will prove suitable, but it is already known that some of the combinations described do not in fact exist as exposure sites at the present time. As was said earlier, a further selection will have to be made of marine sites, the marine factor being superimposed upon those already mentioned.

Discussion

One aspect of this study that may not immediately be recognized is that it is not necessary to know, for example, the absolute time of wetness of surfaces in selecting sites by this method. All that is needed is a relative array (weighted by population) of some factor that is directly related to the variable causing degradation. The relationship between this factor and the variable need not be linear to give sufficiently correct cutoff points for the 95 percent range. This is why it is possible to use duration of humidities 90 percent or more even though it is evident that the absolute values so obtained will differ from the durations of wetness measured by more direct methods. The same may be said of any of the factors. It should be noted that mathematical models of aggressivity have usually been related as closely as possible to the actual durations of wetness or other more direct measures of conditions causing degradation at specimen surfaces. In order to use a model in this present application, it would be necessary to produce one relating corrosion rates to the less direct factors actually available in the widespread meteorological and pollution records.

The implications of using this method of site selection on corrosion testing are as follows. Given that sites can be so chosen as to be in some meaningful way representative of the conditions to which steel is exposed in service, it is possible to consider exposing a product at the range of sites in question and making from the results a good estimate of the range of service performance that will actually be obtained. Such data should give the customer far more confidence in the use of his selected product than he can get at present from tests carried out at arbitrarily described exposure sites. Moreover, if the tests concerned, conducted at the newly selected range of sites, also take into account simultaneously the effect of microclimate, orientation, design and so on, it should be possible to provide the user of the product with far more adequate and reliable data as to service performance than he can possibly obtain at present.

If used for short-term tests, an added requirement of a site is that the conditions shall vary little from year to year, so that tests conducted over a single year can be said to be representative of a longer term. Given this, the selection of exposure sites near the extremes of the service range will help to ensure that the results of such short-term studies are most effectively interpreted.

It is important not to fall into the trap of conducting tests only in the most aggressive combination of conditions found. This will give a biased impression of the product under test, which is bad for the supplier and also bad for the user, who will be tempted to use products that are more durable than he needs. A far more reasonable assessment of the right material to use can be made if tests are carried out in good conditions as well as bad. If, in addition, statistically designed tests can be carried out in intermediate situations, where only one factor is good, or only one factor is bad, then the individual influence of the various factors can be assessed more effectively than hitherto.

Conclusions

The study here described has in reality been an investigation of the feasibility of making a selection of exposure sites that relates more nearly than at present to the range of conditions in which metals are used in practice. Not all the problems exposed have been overcome. Nevertheless, it does seem, as a result of this first work, that it should be possible to make a reasonable selection of exposure site conditions that more faithfully represent the conditions of metals in use. Further work in refining the concepts might well be worthwhile if it allows more rapid development of improved metals and protective coatings by making it possible to conduct short-term exterior durability tests under the proper conditions. The lack of data on atmospheric salinity needs overcoming, expecially now that the use of metals in maritime conditions is increasing. Without such measurements we may soon be faced with the situation of being able to select representative sites for inland conditions, in which the durability of products is already moderately well known from empirical observations, and of not being able to make a corresponding proper selection of conditions for coastal areas, in which the durability of products is far less well defined.

Acknowledgments

The author is grateful to the American Society for Testing and Materials for the opportunity of presenting this experiment in public. While recognizing that it falls far short of being a complete answer to the problems identified, its presentation may enable others to take the discussion a stage further. Thanks are also expressed to L. Kenworthy, who undertook the arduous task of interpreting and collating the original meteorological and pollution data, to P. Sereda for commenting on the method of estimating time of wetness, to the Meteorological Office for providing additional data, and to the British Steel Corporation for permission to publish this paper.

References

[*1*] Stanners, J. F., *La Tribune de CEBEDEAU*, 1970, Vol. 24, No. 324, pp. 512–519.

[*2*] The Municipal Year Book and Public Utilities Directory, London, England, Municipal Journal, 1971.

[*3*] "Mean Annual Duration of Rainfall (in hours) 1951–60," 1970; "Average Number of Hours per Year with Relative Humidity of 90 percent or more, 1957–66," 1971, private communications, The Meteorological Office, Bracknell, England.

[*4*] Booth, R. E., 1931–60 Monthly, Seasonal and Annual Maps of Mean Daily Maximum, Mean Daily Minimum, Mean Temperature and Mean Temperature-Range over the British Isles, Climatological Memorandum No. 43A, The Meteorological Office, Bracknell, England (undated).

[*5*] Booth, R. E., 1931–60 Average Monthly, Seasonal and Annual Maps of Bright Sunshine over the British Isles, Climatological Memorandum No. 42A, The Meteorological Office, Bracknell, England, 1966.

[*6*] The Investigation of Air Pollution, National Survey Smoke and Sulphur Dioxide, April 1969–March 1970, Warren Spring Laboratory, Department of Trade and Industry, Stevenage, England, (undated).

[*7*] Half-Inch *Contoured Maps* (Great Britain Series), John Bartholomew & Son Ltd, Edinburgh, Scotland.

[*8*] Administrative Areas (of Great Britain) Maps, North and South Sheets (approx 10 miles to one inch), Ordnance Survey, Southampton, England.

[*9*] Stanners, J. F., *British Corrosion Journal*, Vol. 5, No. 3, May 1970, pp. 117–121.

F. H. Haynie[1] *and J. B. Upham*[1]

Correlation Between Corrosion Behavior of Steel and Atmospheric Pollution Data

---

REFERENCE: Haynie, F. H. and Upham, J. B., "**Correlation Between Corrosion Behavior of Steel and Atmospheric Pollution Data,**" *Corrosion in Natural Environments, ASTM STP 558*, American Society for Testing and Materials, 1974, pp. 33–51.

ABSTRACT: Specimens of an enameling steel were exposed at 57 sites of the National Air Sampling Network (NASN). Weight losses for one and two years of exposure at each site were determined. Available climatic data were collected and average relative humidities and average temperatures were calculated. Average levels of pollutants were determined from collected NASN data. The pollutants of interest were gaseous sulfur dioxide, total suspended particulate, sulfate in suspended particulate, and nitrate in suspended particulate.

Multiple linear regression and nonlinear curve fitting techniques were used to analyze the relationship between corrosion behavior of this steel and the collected atmospheric data. The resulting best empirical function has the form:

$$cor = a_0 \sqrt{t}\, e^{[a_1 sul \;\; a_2/\mathrm{RH}]}$$

where

cor = depth of corrosion, μm
t = time, years
sul = average level of sulfate in suspended particulate (μg/m^3) or average level of sulfur dioxide (μg/m^3)
RH = average relative humidity

According to statistical analysis, differences in average temperature, average total suspended particulate, and average nitrate in suspended particulate caused insignificant changes in this steel's corrosion behavior. Sulfur dioxide was a significant variable only when sulfate in suspended particulate was not included in the regression analysis. The levels of these two pollutants generally change together from site to site (exhibit a high degree of covariance). Therefore, sulfate in suspended particulate may be a substitute variable for sulfur dioxide.

KEY WORDS: corrosion, steel corrosion, air pollution, sulfates, sulfur dioxide, humidity, atmospheric corrosion tests, maintenance, frequencies

It has been fairly well established that atmospheric pollutants accelerate the corrosion of steel. ASTM has done much to show differences in corrosion behavior between rural and industrial exposures [*1*].[2] Both field and

---

[1] Chief and chemical engineer, respectively, Materials Section, Environmental Protection Agency, National Environmental Research Center, Research Triangle Park, N. C. 27711.

[2] The italic numbers in brackets refer to the list of references appended to this paper.

laboratory studies have shown that sulfur dioxide is a corrosion accelerating factor [*2–13*].

The rate of corrosion is also affected by relative humidity [*2,10*]. More precisely, relative humidity affects the amount of moisture on the surface of the steel [*9,12*]. Normally, a specific relative humidity must be exceeded before the surface becomes wet and corrodes.

Particulate matter has been identified as a likely contributing factor in accelerating steel corrosion [*2,14*]. Past field experience, however, has not conclusively established a correlation between particulate levels and corrosion behavior [*11*]. In many industrial areas sulfur dioxide levels and particulate levels are covariant, that is, they vary together in the same direction. In such cases it becomes impossible (using mathematical correlation techniques) to ascertain which variable actually causes a change in corrosion behavior.

This field study was performed so that a large amount of corrosion data could be accumulated simultaneously with air pollution data collected at National Air Sampling Network sites. With sufficient data on several variables, multiple regression techniques may be used to indicate the corrosion causing factors.

Experimental Procedure

Material

An enameling steel with nominal 0.019 percent carbon and 0.028 percent copper was selected for exposure because of its susceptibility to atmospheric corrosion. The 890-μm-thick steel was cut into 10-cm by 15-cm specimens which were cleaned, coded, and weighed prior to exposure.

Exposure Sites

Both urban and rural exposure sites were selected from the National Air Sampling Network. The 57 selected sites represent normal and extremes of climatic and pollution conditions. The specimens were boldly exposed to wind, rain, and sunlight facing south at a 30-deg angle from the horizontal.

Atmospheric Measurements

The National Air Sampling Network was established in 1957 to monitor suspended particulate levels in both urban and rural America [*15*]. Measurement of other pollutants has since been added to this operation. The pollutant level data used in this study were taken from "Air Quality Data" for 1964–1965, and 1966 [*15,16*].

Sulfur dioxide was measured by continuous monitoring instruments in San Francisco, Denver, Washington, Chicago, New Orleans, Detroit, Cincinnati, and Philadelphia. The sulfur dioxide levels at the remaining sites are based on partially randomized biweekly, 24-h samples. In this method of sampling, the sulfur dioxide is collected by bubbling air through a 50-ml solution of potassium tetrachloromercurate at a flow rate of approximately 150 to 200 cm^3/min.

The particulate levels at all sites are also based on biweekly 24-h samples. Approximately 2300 m^3 of air are filtered through 414 cm^2 of fiber glass filter area. The details for the sampling and analytical procedures for both sulfur dioxide and particulate matter are given in Ref *16*.

The same pollutants were not measured at all sites. Sulfur dioxide concentrations were measured at less than one half (27) of the 57 selected sites. At over 90 percent of the selected sites, measurements were available on total suspended particulate matter and the amounts of sulfate and nitrate in the particulate.

Average temperatures and relative humidities for each site were calculated from available local climatological data from the nearest weather stations or from published norms for nearest cities [*17*].

Corrosion Measurements

Two steel panels were exposed at each site beginning in October and November of 1964. Exposure of one panel was normally terminated at one year and the other at two years. Corrosion products were removed with concentrated hydrochloric acid inhibited with 5 percent by volume stannous chloride and 0.2 percent by volume commercial inhibitor solution.[3] The panels then were weighed to the nearest milligram and the weight losses calculated. Weight losses in grams per panel were converted to depths of corrosion in micrometers by multiplying by a factor or 4. No attempt was made to differentiate between amounts of corrosion on upper and lower surfaces. The calculated depths are, therefore, an average for both surfaces.

Results and Analysis

Data Range

The collected data are presented in Table 3 of the Appendix. Average relative humidities ranged from 29 to 76 percent. Average temperatures ranged from 4°C to 21°C (39°F to 70°F). Average sulfur dioxide levels were as low as 9 $\mu g/m^3$ and as high as 374 $\mu g/m^3$; the median was 44 $\mu g/m^3$. Average total suspended particulate levels ranged from 11 $\mu g/m^3$ to 182 $\mu g/m^3$. The calculated depths of corrosion on the steel panels ranged from a fraction of micrometer to 100 μm. Thus, with the exception of average temperature, the data for each variable cover a wide range of values. This type of data is desirable where multiple regression techniques are to be used in analyzing variable relationships.

---

[3] Rodine No. 213. Mention of company name of commercial products does not constitute endorsement by the Environmental Protection Agency.

Theoretical Considerations

Analysis of these data should be consistent with physical corrosion behavior. For example, the effects of different variables should be multiplicative rather than additive because corrosion is primarily an interaction effect of moisture (relative humidity), temperature, and time. Thus, statistical analysis should be performed on the logarithms of the corrosion data.

Theoretically and empirically the logarithm of depth of corrosion is directly proportional to the logarithm of time, and approaches a parabolic relationship in the early stages of corrosion product film growth [*13*]. Based on kinetic theory, the logarithm of corrosion rate should be negatively proportional to the reciprocal of the absolute temperature. The logarithm of the depth of corrosion also is expected to be proportional to various pollutants.

Corrosion, being an electrochemical process, will not occur when steel is not wet; therefore, some critical relative humidity must be exceeded to produce wetness that will allow corrosion. In this study average relative humidity and time were the measured variables that are proxies for the unmeasured expected causative variable, time-of-wetness. The logarithm of depth of corrosion, negatively proportional to the reciprocal of relative humidity, is an empirical relationship consistent with this fact as can be seen in a plot of probability of wetness as a function of relative humidity [*18*].

Assuming a parabolic rate function, the corrosion loss divided by the square root of exposure time can also be considered the dependent variable. The logarithm of this value should then be a function of the other variables.

Correlation Analysis

Simple correlation coefficients can be used to indicate how closely variables are mathematically associated or covariant [*19*]. Values of -1 and 1 for coefficients represent perfect linear negative and positive association or covariance, respectively. A value of zero indicates there is no association. When two independent variables have a high degree of association (high absolute value for correlation coefficient) it becomes difficult or impossible to separate the effects on a dependent variable using multiple regression techniques. Thus, correlation coefficients between independent variables can be used to indicate where possible troubles may arise when using multiple regression analysis.

Table 1 is a correlation matrix for the variables considered in this study. The least significant variable is the reciprocal of the absolute temperature. This behavior may be a result of the relatively narrow range of values and not because the effect is nonexistent. As might be expected, some negative covariance was found between the reciprocal of relative humidity and the reciprocal of the absolute temperature. This behavior is likely because relative humidity is a function of absolute humidity and temperature.

TABLE 1—*Correlation matrix.*

	Correlation Coefficients/Probability that $\lvert R \rvert = 0$ (No Correlation)/Number of Observations							
	$\ln\left(\frac{\text{corrosion}}{\sqrt{\text{time}}}\right)$	ln (time)	Reciprocal of Relative Humidity	Sulfur Dioxide	Suspended Particulates	Sulfate	Nitrate	Reciprocal of Absolute ture, °R
ln (corrosion)	0.992168 0.0001 111	0.169317 0.0720 111	−0.722226 0.0001 111	0.448010 0.0013 51	0.441162 0.0001 111	0.68165 0.0001 103	0.243029 0.0137 101	0.104120 0.2763 111
$\ln\left(\frac{\text{corrosion}}{\sqrt{\text{time}}}\right)$		0.044880 0.6452 111	−0.728857 0.0001 111	0.436252 0.0017 51	0.453802 0.0001 111	0.704156 0.0001 103	0.259909 0.0085 101	0.112980 0.2359 111
ln (time)			−0.025333 0.7879 111	0.060852 0.6749 51	−0.052295 0.5925 111	−0.073478 0.5325 103	−0.111046 0.2681 101	−0.058704 0.5477 111
Reciprocal of relative humidity				0.020052 0.8839 51	−0.066121 0.5024 111	−0.381942 0.0002 103	−0.172131 0.0814 101	−0.253867 0.0072 111
Sulfur dioxide					0.288498 0.0377 51	0.696098 0.0001 51	−0.139852 0.6605 49	0.031331 0.8218 51
Suspended particulates						0.682643 0.0001 103	0.467937 0.0001 101	−0.111757 0.2412 111
Sulfate							0.327552 0.0012 101	0.087828 0.06186 103
Nitrate								−0.190781 0.0529 101

The most significant independent variable with respect to its affect on corrosion is the reciprocal of relative humidity. Fortunately, little covariance was found between this variable and sulfur dioxide and suspended particulates. The covariance between sulfur dioxide and total suspended particulate is also weak; therefore, it should be possible to separate the effects of these variables. A strong covariance was found between sulfate in suspended particulate and sulfur dioxide, as well as between sulfate and total suspended particulate. Therefore, separating these effects mathematically using multiple regression techniques will be difficult.

The sulfate-total suspended particulate-sulfur dioxide relationship is probably due to a chemical reaction either in the air or on the sampler filter. Suspended particulate probably absorbs some SO_2 which eventually becomes sulfate. The type of filter used during this time could also contribute to the conversion reaction [*20*]. Therefore, particulate sulfate level is probably a very strong indicator of atmospheric sulfur dioxide levels, and a mathematically observed sulfate effect may be a proxy for a true sulfur dioxide effect.

The short duration of this study caused time to be a relatively insignificant variable. It should be noted, however, that using corrosion divided by the square root of time, rather than corrosion, as the dependent variable, improves the correlation coefficients for five of the six remaining independent variables. Time, therefore, should be considered in any regression analysis.

Multiple Regression Analysis

Multiple regression analysis is a statistical technique used to analyze empirical relationships between a dependent variable and several independent variables. Values for each variable to be studied are needed to perform the analysis. Only 49 of the sets of data are complete in this sense, primarily because of the lack of SO_2 data at many of the sites. The initial analysis was performed on these data.

Five different multiple linear regression techniques were used to determine the best empirical relationships between ln (corrosion) and ln [(corrosion)/($\sqrt{\text{time}}$)] as dependent variables for all the independent variables. Based on the criterion that all independent variables have coefficients with 0.95 or greater probability that they are different from zero, the resulting regression equations from each technique were the same. The resulting analysis of variance and regression coefficients are presented in Table 4 of the Appendix.

The results from the foregoing analysis indicate that corrosion of steel is primarily a function of both sulfate and nitrate levels in suspended particulate, relative humidity, and time. Temperature, total suspended particulate, and sulfur dioxide concentration appear to be insignificant variables. However, based on the observed covariance between sulfate and sulfur dioxide, as well as the good relationship between SO_2 and corrosion found in previous studies, the sulfate level is likely a useful proxy variable for atmospheric sulfur dioxide. When the sulfate data are excluded from the multiple linear regression, nearly as good a fit is produced with sulfur dioxide replacing the sulfate as a significant variable.

The assumption that the depth of corrosion is a parabolic function of time is apparently correct because the coefficient for ln (t) in the first regression is not significantly different from 0.5, and in the second regression ln $[(\text{corrosion})/(\sqrt{\text{time}})]$ is not significantly affected by ln (t).

Less than half of the data were used in this initial analysis because of the necessity to have complete data sets. This narrowed the range of some of the variables. If only relative humidity, sulfate, nitrate, and time are considered as independent variables, more than double the previous number of complete data sets can be used and a wider range of values can be covered. Analysis of variance and regression coefficients for these variables including and excluding nitrate are presented in Table 5 of the Appendix.

The inclusion of a larger number of data sets increased the significance of time and average relative humidity and decreased the significance of sulfate and nitrate. The nitrate variable no longer had any statistical significance, and a regression equation excluding nitrate as a variable can account for as much variability as one including it. The coefficient for ln (t) again is not significantly different from 0.5; therefore, the parabolic rate function is apparently applicable.

Therefore, based on this study, the best empirical relationship between corrosion behavior of this particular steel and atmospheric pollution that is consistent with theoretical considerations has the form:

$$cor = a_0\sqrt{t}\,[e^{(a_1 sul - a_2/\mathrm{RH})}] \tag{1}$$

where

cor = depth of corrosion, μm
sul = average level of sulfate in suspended particulate, $\mu g/m^3$
RH = average relative humidity, percent
t = time, years

A nonlinear least-squares fit gives the values (for the coefficients and their standard deviations) presented in Table 2.

Plots of cumulative distribution of residuals and residuals versus fitted corrosion values reveal normal behavior and indicate that the empirical relationship is as good a fit as can be expected from the available data.

A plot of observed depths of corrosion as a function of the "best fit" predicted depths of corrosion is presented in Fig. 1. A perfect fit would produce a line of points at a 45-deg angle. As it is, approximately 23 percent of the variability is unaccounted for by the functional relationship.

TABLE 2—*Nonlinear least-squares fit of Equation* 1: cor $= a_0 \sqrt{t}\ [e^{(a_1 sul - a_2/RH)}]$.[a]

Coefficient		Standard Deviation	95% Confidence Limits	
Name	Value		Lower	Upper
a_0	183.5	85.0	13.4	353
a_1	0.06421	0.00451	0.0552	0.0732
a_2	163.21	32.8	97.6	229
Residual root mean square = 12.6				
$R^2 = 0.774$				

[a] A total of 103 complete data sets was used.

Very little error is associated with the measurement of corrosion data. Therefore, approximately half of the error is probably associated with the sampling and analysis of the sulfate in suspended particulate. Most of the remaining error is probably associated with assuming that average relative humidity is a good proxy variable for fraction of exposure time the steel surface is wet.

Discussion

Enameling steel is not made for unprotected, atmospheric exposure. These results, however, are generally consistent with exposure data for

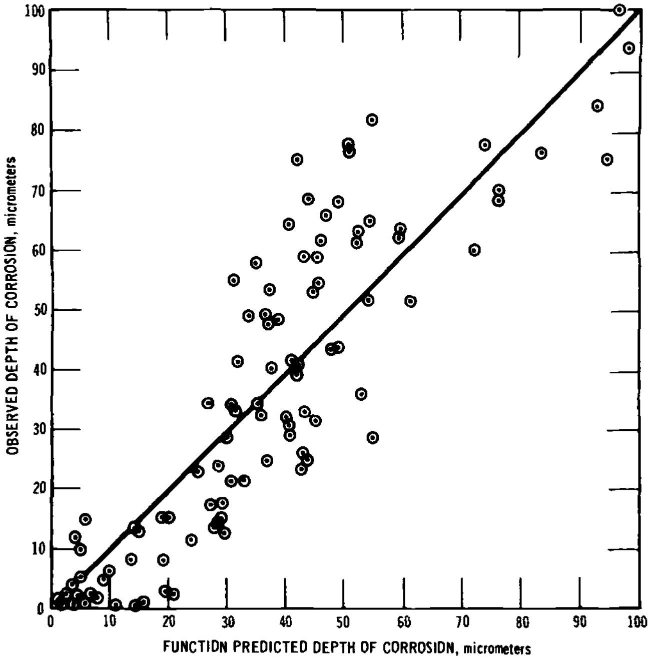

FIG. 1—*Functional fit of steel corrosion data.*

other steels [9,13]. Thus the qualitative environmental effects are probably applicable to many steels.

Although it is theoretically possible that particulate sulfates cause accelerated corrosion of steel, it is more likely that sulfur dioxide is the causative factor, and sulfate is a good proxy variable for SO_2.

A linear regression between sulfate and SO_2 using 51 sets of data yields the following relationship:

$$
\begin{aligned}
sul &= 8.9 + 0.0429SO_2 \qquad (2)\\
\pm 2S &= 8.2
\end{aligned}
$$

where *sul* and SO_2 are respectively average sulfate and SO_2 concentrations in $\mu g/m^3$ and S is the estimated standard deviation.

Substituting this relationship for sulfate concentrations in Eq 1 using the coefficients in Table 2 gives the following function:

$$cor = 325\sqrt{t}\,e^{[0.00275SO_2-(163.2/RH)]} \qquad (3)$$

where the units are the same as in Eq 1.

Equation 3 is a four-dimensional relationship and is therefore difficult to visualize. The elimination of one variable makes it possible to graphically portray the function. The corrosion rate ($d\,cor/dt$) is inversely proportional to $\sqrt{t}$; that is, the corrosion rate decreases as the exposure time increases. Thus, using true corrosion rate as the dependent variable does not eliminate a dimension. However, assuming a pseudo-corrosion rate ($cor/\sqrt{t}$) reduces the total number of variables to three, which can be handled graphically. Figure 2 is an example of such a presentation. This figure shows the interaction effect of average relative humidity and average sulfur dioxide. It also shows that corrosion occurs in the absences of sulfur dioxide. The converse is not true, as is illustrated in Fig. 3. One may expect negligible corrosion of steel at average relative humidities below 30 percent, regardless of the average concentration of sulfur dioxide.

The average relative humidity is a measure of the probability that some critical relative humidity for wetting the steel has been exceeded. Thus, 30 percent is not this critical relative humidity. For example, if 80 percent is the critical relative humidity and the average relative humidity is 40 percent, the probability that 80 percent has been exceeded is approximately 0.08 or very low. At an average relative humidity of 100 percent, the critical humidity of 80 percent will always be exceeded.

The value of 30 percent is useful, however, in that in arid regions where this average relative humidity is not exceeded, no steel corrosion problems are to be expected.

Maintenance Frequency

It is evident from these results that corrosion-caused maintenance of steel structures must be performed more often in sulfur dioxide polluted

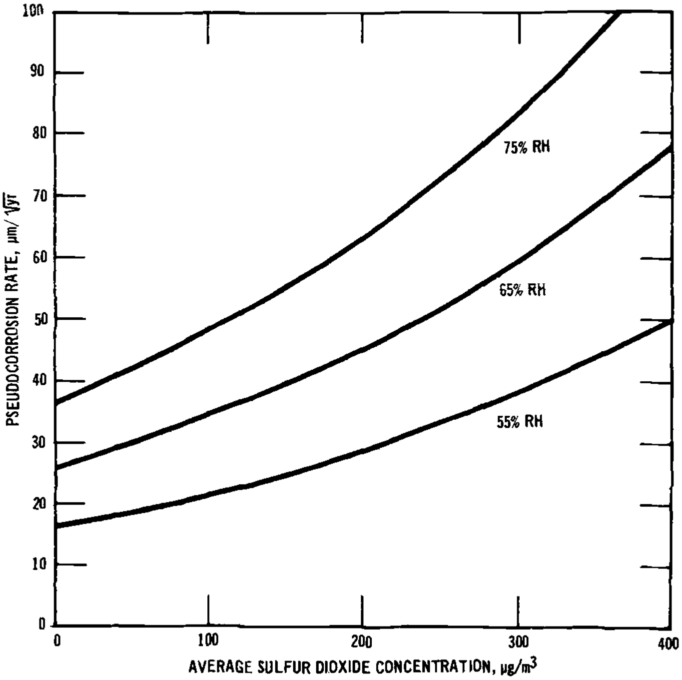

FIG. 2—*Steel corrosion behavior as a function of average sulfur dioxide concentration and average relative humidity.*

atmospheres than in clean environments. Thus, as ambient levels of SO_2 are reduced, one may expect the frequency of maintenance and replacement of steel products to also be reduced.

Because of the complex factors that are involved in the maintenance of steel structures, it is difficult to assess the magnitude of this benefit. The durability of protective organic coatings as a function of substrate corrosion is such a factor. However, by assuming that maintenance frequency is inversely proportional to the time required to corrode to some specific depth, a crude estimate of the ratio of the maintenance frequency in a polluted environment to that in the same environment without pollution can be determined. This relationship is:

$$\text{maintenance frequency ratio (MFR)} = e^{0.0055\text{SO}_2} \tag{4a}$$

with estimated 95 percent confidence limits of

$$\text{MFR}_{\text{low}} = e^{0.0043\text{SO}_2} \tag{4b}$$

and

$$\text{MFR}_{\text{high}} = e^{0.0069\text{SO}_2} \tag{4c}$$

These equations are graphically presented in Fig. 4. Both the magnitude and error increase exponentially with increasing SO_2 concentrations.

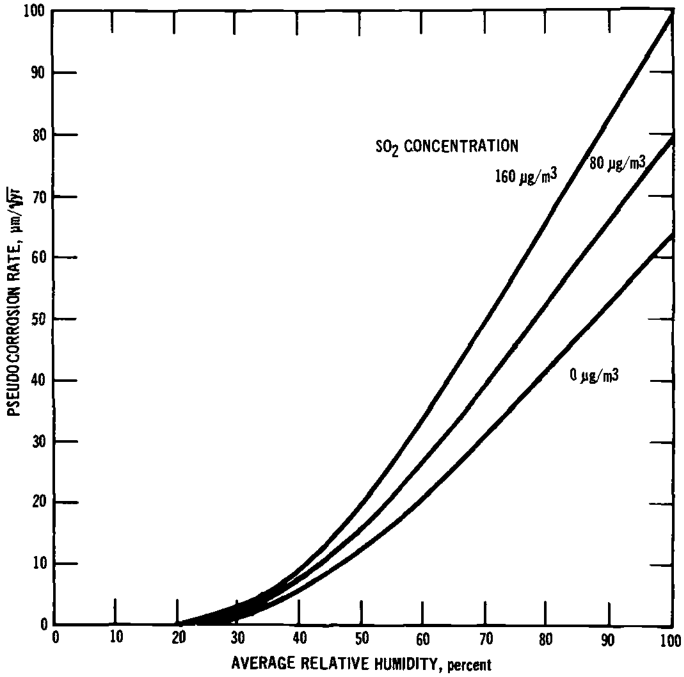

FIG. 3—*Steel corrosion behavior as a function of average relative humidity at three average concentration levels of sulfur dioxide.*

Ratios of maintenance frequencies between different levels of SO_2 are simply

$$MFR = e^{0.0055(SO_{2_1} - SO_{2_2})} \tag{5}$$

This equation can be used to calculate approximate savings from lowering pollution levels. For example, if a city (*a*) presently spends 5.0 million dollars a year on atmospheric-corrosion-of-steel maintenance in an atmosphere containing an average SO_2 concentration of 200 $\mu g/m^3$, and (*b*) lowers the average level to 60 $\mu b/m^3$, it can lower its cost to 2.3 million dollars a year. The savings or benefit would then be the difference, or 2.7 million dollars.

Conclusions

The conclusions based on the results of this study are:

1. Total suspended particulate, nitrate in suspended particulate, and average temperature are relatively unimportant factors in the corrosion behavior of steel.

2. Either sulfate in suspended particulate, atmospheric sulfur dioxide, or both accelerate steel corrosion. Sulfur dioxide is known to be a causative factor based on previous studies. The possible sulfate effect should be

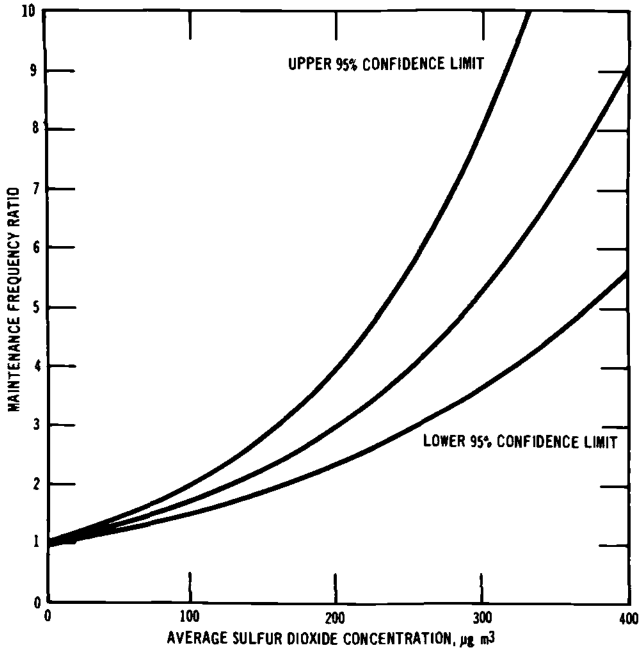

FIG. 4—*Effect of average sulfur dioxide concentration on steel corrosion maintenance frequency.*

verified with laboratory-controlled experiments where there is no problem of covariance between SO_2 and sulfate.

3. Corrosion of steel should not be a problem in arid regions where the average relative humidity does not exceed 30 percent.

4. Savings from reduced corrosion of steel maintenance can be an appreciable benefit of reduced ambient levels of sulfur dioxide.

Acknowledgment

The authors gratefully acknowledge the assistance provided by individuals in local and state agencies that operated the selected National Air Sampling Network sites during the exposure of the steel specimens.

APPENDIX

Data

The collected atmospheric and corrosion data are presented in Table 3.

Multiple Linear Regression

The results of various multiple linear regressions on the data are presented in Tables 4 and 5. Also given is the analysis of variance for these regressions.

TABLE 3—*Atmospheric and corrosion data.*

			Normal Climatic Conditions			Average Levels of Pollutants During Exposure Period (μg/m³)				
State	Site	Type[a]	Relative Humidity, %	Temperature, °C(°F)	Exposure Period, years	Sulfur Dioxide	Total Suspended Particulate	Sulfate in Particulate	Nitrate in Particulate	Depth of Steel Corrosion, μm
Alabama	Birmingham	U	73	17 (64)	1	...	172	12.2	2.8	23.5
			73	17 (64)	2	...	157	10.6	2.9	28.6
	Mobile	U	71	19 (68)	1	...	111	8.1	1.2	55.1
			71	19 (68)	2	...	122	8.1	1.2	68.7
Arizona	Phoenix	U	39	19 (69)	1	...	162	4.5	2.9	0.7
			39	19 (69)	2	...	157	4.6	2.8	5.0
	Maricopa Co.	U	39	19 (69)	1	...	68	4.1	1.2	3.8
			39	19 (69)	2	...	68	4.1	1.2	9.8
	Grand Canyon	R	34	16 (62)	1	...	22	2.1	0.5	0.9
			34	16 (62)	2	...	27	2.5	0.4	2.4
California	Los Angeles	U	55	16 (62)	1	39	171	14.4	13.5	11.6
			55	16 (62)	2	39	145	11.2	9.3	17.3
	Sacramento	U	67	15 (60)	1	...	78	2.8	3.5	8.2
			67	15 (60)	2	...	72	2.8	3.5	17.3
	San Diego	U	69	17 (64)	1	...	78	8.2	5.3	18.0
			69	17 (64)	2	...	74	8.0	4.0	29.0
	San Francisco	U	73	13 (57)	2	44	68	6.5	2.7	41.0
			73	13 (57)	2	44	68	6.5	2.7	39.6
Colorado	Denver	U	51	9 (50)	1	52	156	4.7	4.2	6.2
			51	9 (50)	2	41	151	4.4	2.8	8.2
	Montezuma	R	45	14 (58)	1	...	13	2.5	0.3	0.6
			45	14 (58)	2	...	16	2.5	0.3	1.8
Connecticut	Hartford	U	68	9 (50)	1	72	92	13.8	3.3	64.5
			68	9 (50)	2	67	91	13.1	2.2	82.1

(*continued*)

TABLE 3—*Continued*

			Normal Climatic Conditions			Average Levels of Pollutants During Exposure Period ($\mu g/m^3$)				
State	Site	Type[a]	Relative Humidity, %	Temperature, °C(°F)	Exposure Period, years	Sulfur Dioxide	Total Suspended Particulate	Sulfate in Particulate	Nitrate in Particulate	Depth of Steel Corrosion, μm
D. C.	Washington	U	63	13 (57)	1	121	98	15.4	3.5	53.4
			63	13 (57)	2	119	77	13.2	2.7	59.2
Florida	Orlando	U	76	21 (71)	2	...	66	...	...	38.0
			76	21 (71)	2	...	66	...	...	38.5
Florida	Tampa	U	72	21 (72)	1	...	80	...	...	35.9
			72	21 (72)	2	...	66	...	...	46.3
Illinois	Chicago	U	65	10 (51)	2	280	132	13.7	2.2	77.2
			65	10 (51)	2	280	132	13.7	1.9	78.0
Iowa	Delaware Co.	R	73	9 (49)	1	...	33	5.3	1.7	13.7
			73	9 (49)	2	...	37	4.4	1.4	24.8
Iowa	Des Moines	U	73	9 (49)	1	11	142	6.7	2.7	28.8
			73	9 (49)	2	12	133	7.0	2.2	33.0
Kentucky	Ashland	U	69	12 (55)	1	...	179	22.3	2.3	60.2
			69	12 (55)	2	...	173	19.2	2.3	76.8
Louisiana	New Orleans	U	75	19 (69)	1	25	95	8.5	3.4	32.4
			75	19 (69)	2	24	94	7.6	2.8	43.6
Maryland	Baltimore	U	68	12 (55)	1	83	132	16.0	2.9	66.0
			68	12 (55)	2	95	139	17.8	2.6	78.1
Michigan	Detroit	U	69	5 (41)	1	120	165	14.8	3.4	53.2
			69	5 (41)	2	119	163	14.0	3.6	63.7

Minnesota	Minneapolis	U	71	6 (44)	1	34	70	5.9	1.8	34.6
			71	6 (44)	1.9	39	78	6.1	1.4	40.4
Missouri	Kansas City	U	64	13 (57)	2	9	131	6.6	2.2	34.2
	St. Louis	U	66	12 (55)	1	113	152	15.2	2.6	41.7
Montana	Glacier Park	R	61	6 (44)	1	. . .	22	3.4	0.2	0.6
			61	6 (44)	2	. . .	19	2.4	0.1	2.5
	Helena	U	57	7 (45)	1	. . .	73	4.9	1.0	13.4
			57	7 (45)	2	. . .	63	3.9	0.8	15.2
Nebraska	Thomas Co.	R	59	10 (51)	1	. . .	21	3.5	0.7	0.7
			59	10 (51)	2	. . .	24	2.8	0.6	3.0
Nevada	Las Vegas	U	29	16 (63)	1	. . .	150	5.6	2.8	0.3
			29	16 (63)	2	. . .	125	4.6	2.1	1.5
Nevada	White Pine	R	46	11 (52)	1	. . .	29	3.8	0.4	2.7
			46	11 (52)	2	. . .	19	2.7	0.3	4.7
New Hampshire	Coos Co.	R	73	4 (40)	1	. . .	21	6.1	1.2	15.3
			73	4 (40)	2	. . .	25	6.0	0.8	30.6
New Mexico	Rio Arriba	R	43	13 (57)	1	. . .	24	2.4	0.3	1.9
			43	13 (57)	2	. . .	25	2.3	0.3	2.3
New York	Buffalo	U	72	8 (47)	1	40	127	16.2	. . .	51.7
			72	8 (47)	2	33	133	16.2	. . .	68.6
	Cape Vincent	R	67	12 (55)	1	. . .	40	10.0	2.5	21.1
			67	12 (55)	2	. . .	36	10.0	2.5	26.2
	New York	U	65	12 (55)	1	374	179	28.8	2.4	75.5
			65	12 (55)	2	360	157	23.7	2.1	100.1
	Niagara Falls	U	75	8 (47)	1	. . .	137	. . .	. . .	53.8
			75	8 (47)	2	. . .	138	. . .	. . .	73.1
North Carolina	Fayetteville	U	68	15 (60)	1	. . .	63	. . .	. . .	33.2
			68	15 (60)	2	. . .	63	. . .	. . .	46.9

(continued)

TABLE 3—*Continued.*

			Normal Climatic Conditions			Average Levels of Pollutants During Exposure Period ($\mu g/m^3$)				
State	Site	Type^a	Relative Humidity, %	Temperature, °C(°F)	Exposure Period, years	Sulfur Dioxide	Total Suspended Particulate	Sulfate in Particulate	Nitrate in Particulate	Depth of Steel Corrosion, μm
Ohio	Cincinnati	U	69	12 (55)	1	79	141	13.6	3.4	41.9
			69	12 (55)	2	80	148	14.3	2.7	51.7
	Youngstown	U	73	10 (51)	1	47	141	15.8	2.9	65.3
Oregon	Portland	U	75	11 (53)	1	18	132	11.5	7.4	24.8
			75	11 (53)	2	20	104	9.1	5.3	36.0
Pennsylvania	Clarion Co.	R	70	9 (49)	1	...	57	9.0	1.8	41.7
			70	9 (49)	2	...	49	8.3	1.0	59.0
	Philadelphia	U	67	12 (54)	1	223	182	24.3	3.0	70.2
			67	12 (54)	2	231	168	21.9	2.6	84.1
	Pittsburgh	U	69	9 (50)	1	89	149	15.0	2.9	54.4
			69	9 (50)	2	91	149	13.8	2.5	62.2
Rhode Island	Providence	U	65	9 (50)	1	110	125	14.1	2.4	47.7
			65	9 (50)	2	118	123	14.1	1.8	63.5
	Washington Co.	R	66	9 (50)	1	...	64	12.6	2.5	58.0
			66	9 (50)	2	...	55	10.2	1.6	75.5
South Carolina	Columbia	U	70	17 (64)	1	...	85	7.3	1.2	24.0
			70	17 (64)	2	...	81	7.3	1.2	32.2

	Richland	R	70	17 (64)	1	...	33	5.4	0.6	22.5
			70	17 (64)	2	...	35	5.4	0.6	34.5
Tennessee	Nashville	U	69	15 (60)	1	23	114	9.4	3.1	33.4
			69	15 (60)	2	26	115	10.9	2.7	44.0
Texas	Dallas	U	64	18 (66)	2	...	111	5.8	3.3	12.6
			64	18 (66)	2	...	111	5.2	2.5	14.2
	El Paso	U	38	16 (63)	1	65	188	8.0	1.2	11.8
			38	16 (63)	2	64	190	8.0	1.2	14.8
	Houston	U	75	19 (69)	1	...	128	7.0	3.1	21.5
			75	19 (69)	2	...	115	6.6	2.8	31.9
Utah	Salt Lake	U	54	10 (51)	1	12	114	8.0	2.3	13.1
			54	10 (51)	2	16	104	7.4	1.9	15.4
Vermont	Orange Co.	R	71	6 (54)	1	...	39	6.2	1.6	34.5
			71	6 (44)	2	...	42	6.1	1.0	48.4
Washington	Seattle	U	75	8 (48)	1	35	95	7.4	2.0	49.2
			75	8 (48)	2	35	86	6.9	1.7	61.8
West Virginia	Charleston	U	69	13 (57)	1	17	187	16.2	1.5	68.4
			69	13 (57)	2	23	207	21.7	1.3	93.7
Wisconsin	Milwaukee	U	73	7 (45)	1	15	142	9.6	2.6	49.5
			73	7 (45)	2	22	146	9.8	2.4	61.6
Wyoming	Yellowstone	R	56	7 (45)	1	...	12	1.7	0.2	0.4
			56	7 (45)	2	...	11	1.8	0.2	1.3

[a] Type: U = urban; R = rural.

TABLE 4—*Results of multiple linear regressions, considering seven variables and eliminating those not significant at the 95 percent confidence level.*[a]

ln (cor) as Dependent Variable	Source of Variability	Partial Sum of Squares	F Value	Regression Coefficient	Standard Deviation, $\pm S$
	$\frac{1}{RH}$	5.985	87.25	−129.2	13.8
$F = 64.18$	sulfate	6.214	90.60	0.06744	0.00709
$R^2 = 0.854$	nitrate	2.200	32.07	−0.1051	0.0186
	ln (time)	0.576	8.40	0.3215	0.1109
	mean	...	...	5.090	...
	error	3.018			
$\ln\left[\frac{cor}{\sqrt{t}}\right]$ as dependent variable	$\frac{1}{RH}$	6.540	92.09	−128.7	14.1
	sulfate	5.942	83.66	0.06874	0.00716
	nitrate	2.049	28.85	−0.0999	0.0186
$F = 79.86$	mean			4.985	...
$R^2 = 0.842$	error	3.195	...	...	...

[a] A total of 49 complete data sets used. Sulfur dioxide, suspended particulate, and reciprocal of absolute temperature were not significant sources of variability at the 95 percent confidence level.

TABLE 5—*Multiple linear regressions for* ln (*cor*) *as a function of* ln (*time*), *1/RH, sulfate, with and without nitrate as an independent variable.*[a]

	Source of Variability	Partial Sum of Squares	F Value	Regression Coefficient	Standard Deviation, $\pm S$
$F = 70.81$	$\frac{1}{RH}$	47.556	88.46	−162.76	17.31
$R^2 = 0.747$	sulfate	39.560	73.59	0.1253	0.0146
	nitrate	0.027	0.05	0.00965	0.0429
	ln (time)	7.771	14.46	0.8091	0.2128
	mean	...	...	4.220	0.387
	error	51.609	...	...	...
	$\frac{1}{RH}$	47.875	89.93	−162.00	17.19
$F = 95.33$	sulfate	43.587	81.88	0.1263	0.0140
$R^2 = 0.747$	ln (time)	7.754	14.57	0.8046	0.2108
	mean	...	...	4.239	0.376
	error	51.636	...	...	...

[a] A total of 101 complete data sets used.

The partial sum of squares is a measure of the variability associated with a particular variable having considered the variability associated with the remaining variables being studied. The column of F values is the ratio of the partial sum of squares for a particular variable to the partial sum of squares for error. The higher the F value the greater the probability that a particular variable is causing an effect.

The estimated standard deviations (S) are a measure of the accuracy of the individual regression coefficients. Plus or minus two standard deviations are considered 95 percent confidence limits for large samples. That is, we would expect the regression coefficient to lie within the range of its value $\pm 2S$, ninety-five percent of the time if the experiment were repeated a large number of times.

The F and R^2 values on the left in Tables 4 and 5 are measures of the degree of fit for the total regression. The R^2 represents the fraction of the variability accounted for by the regression.

References

[*1*] "Corrosiveness of Various Atmospheric Test Sites as Measured by Specimens of Steel and Zinc," A report of Committee G-1, *Metal Corrosion in the Atmosphere, ASTM STP 435*, American Society for Testing and Materials, 1968, p. 360.

[*2*] Vernon, W. H. J., *Faraday Society Transactions*, Vol. 31, 1935, p. 1668.

[*3*] Vernon, W. H. J., *Society of Chemical Industry, Chemical Engineering Group, Proceedings*, Vol. 19, 1937, p. 15.

[*4*] Vernon, W. H. J., *Journal of the Society of Chemical Industry*, Vol. 62, 1943, p. 314.

[*5*] Preston, R. St. J., *Journal of the Iron and Steel Institute*, Vol. 158, Nov. 1948, p. 289.

[*6*] Vernon, W. H. J., *Journal of the Royal Society of Arts*, Vol. 97, 1949, p. 578.

[*7*] Hudson, J. C. and Stanner, J. F., *Journal of Applied Chemistry*, Vol. 3, Feb. 1953, p. 36.

[*8*] Greenburg, L. and Jacobs, M. B., *American Paint Journal*, Vol. 39, 1955, p. 64.

[*9*] Sereda, P. J., *Industrial and Engineering Chemistry*, Vol. 52, 1960, p. 157.

[*10*] Tice, E. A., *Journal of the Air Pollution Control Association*, Vol. 12, 1962, p. 533.

[*11*] Upham, J. B., *Journal of the Air Pollution Control Association*, Vol. 17, No. 6, June 1967, p. 398.

[*12*] Guttman, H. and Sereda, P. J., *Metal Corrosion in the Atmosphere, ASTM STP 435*, American Society for Testing and Materials, 1968, p. 326.

[*13*] Haynie, F. H. and Upham, J. B., *Materials Protection and Performance*, Vol. 10, Nov. 1971, p. 18.

[*14*] Preston, R. St. J. and Sanyal, B., *Journal of Applied Chemistry*, Vol. 6, 1956, p. 28.

[*15*] Division of Air Pollution, Department of Health, Education, and Welfare, "Air Quality Data from the National Air Sampling Networks and Contributing State and Local Networks," 1964–1965 ed., Cincinnati, Ohio, 1966.

[*16*] National Air Polution Control Administration, Department of Health, Education, and Welfare, "Air Quality Data from the National Air Sampling Networks and Contributing State and Local Networks," 1966 ed., Durham, N. C., 1968.

[*17*] U. S. Bureau of the Census, "Statistical Abstracts of the United States 1970," 91st ed., Washington, D. C., 1970, p. 176, 184.

[*18*] Guttman, H., *Metal Corrosion in the Atmosphere, ASTM STP 435*, American Society for Testing and Materials, 1968, p. 237.

[*19*] Ostle, B., *Statistics in Research*, Iowa State University Press, Ames, Iowa, 1963, p. 222.

[*20*] Lee, R. E., Jr. and Wagman, J., *American Industrial Hygiene Association Journal*, Vol. 27, June 1966, p. 266.

D. Knotková-Čermáková,[1] *B. Bošek,*[2] *and J. Vlčková*[1]

Corrosion Aggressivity of Model Regions of Czechoslovakia

REFERENCE: Knotková-Čermáková, D., Bošek, B., and Vlčková, J., "**Corrosion Aggressivity of Model Regions of Czechslovakia,**" *Corrosion in Natural Environments, ASTM STP 558,* American Society for Testing and Materials, 1974, pp. 52–74.

ABSTRACT: A comprehensive research program was started in Czechoslovakia five years ago for a systematic investigation of the corrosion aggressivity of selected industrial regions. The corrosion tests were performed on 19 corrosion stations in the North-Bohemian model region. Principal technical metals were tested.

The characteristics of climate and air pollution and also the combined index of the corrosion aggressivity were suggested and numerically expressed.

The hyperbolic function has most closely approximated the law of the time-dependent course of the corrosion process of metals. The regression analysis was performed with the use of various forms of the climate characteristics, and the most favorable function was expressed.

The cybernetic model of the atmospheric corrosion process was suggested.

KEY WORDS: corrosion, atmospheric corrosion, iron, zink, copper, aluminum, meteorological data, aerochemical characteristics, time dependence, regression (statistics), cybernetics

The process of advanced civilization is accompanied by a number of negative consequences which manifest themselves in particular by the worsening of our environment.

The most serious losses in the nonbiological sphere must be ascribed to corrosion. The pollution caused by industrial plants and household heating equipment involves corrosion-stimulating constituents (sulfur dioxide (SO_2), hydrochloric acid (HCl), hydrogen sulfide (H_2S)) which distinctly increase the aggressivity of the atmosphere. For this reason, a comprehensive research program was started in Czechoslovakia five years ago for a systematic investigation of the corrosion aggressivity of selected industrial regions. The program is a part of extensive activities aimed at understanding the influence of industry on the environment.

---

[1] National Research Institute for Protection of Materials, Prague, Czechoslovakia.

[2] Czech Technical University, Department of Automation, Prague, Czechoslovakia.

Eight model regions were selected, differing in the degree of industrialization, population density, climatic conditions, and geographic situation. A network of measuring points was already established in some of these regions for a systematic observation of the action of climatic factors and air pollution.

At present, the work in the North-Bohemian model region is in its final stage. This industrial agglomeration is characterized by brown-coal mines, highly developed industry, especially chemical factories, and a high population density. The measuring network here comprises about 100 points, 16 of which were sites for performing corrosion tests on principal metals. Selected localities were used for examining various types of surface treatment (coating, metallization, cement covers). Further tests proceed in the district of Frýdlant, which is strongly affected by emissions from power plants, and in the industrialized Ostrava district.

The tests proceed in close cooperation with the Geographic Institute of the Czechoslovak Academy of Sciences and with the Hydrometeorological Institute. Mathematical treatment of the results offers the possibility of formulating the dependence of corrosion on time and external factors.

Analysis of the Problem

We started with the basic simple concept that atmospheric corrosion of metals is a discontinuous process, taking place in periods of favorable moisture conditions on the surface. The average corrosion rate in these periods, V_k, is a function of time and the level of external factors

$$V_{k(t)} = f\,[a_{\mathrm{H_2O}(t)}, a_{\mathrm{SO_4^{2-}}\,(t)}, T_{(t)}] \qquad (1)$$

These activities of water and SO_4^{2-}, as given in Eq 1, or the pollution in general are not directly measurable; they are functionally in connection with the state of atmospheric moisture and the pollution, by means of which they must be expressed.

The actual aim of research into atmospheric corrosion of metals, followed theoretically and practically, is to find and express the interrelations between the meteorological and the aerochemical characteristics of various types of atmospheres and the long-term process of atmospheric corrosion.

The methods by which individual research workers endeavor to attain this aim are various. Most frequently they utilize methods of regression analysis [*1*,*2*][3] in which the experimental material is given by the results of short-term tests for localities differing in their aggressivity. The analyses are usually concerned with results of tests during a period in which a stationary state of corrosion has not yet been attained. The influence of

---

[3] The italic numbers in brackets refer to the list of references appended to this paper.

TABLE 1—*Characteristics of climate.*

No.	Station Name	Program	Time of Exposure, days	Characteristic							
				V_1	V_2	T_1	T_2	T_3	Z_1	Z_2	Z_3
North-Bohemian Region:											
10	Práhly	I	350	51.2	41.5	7.9	264	75.6	0.06	24 786	70.81
10	Práhly	II	377	43.8	37.4	8.7	335	86.3	0.01	23 694	62.8
5	Kopisty	I	385	53.0	43.7	6.9	296	75.5	0.12	47 298	122.8
5	Kopisty	II	377	42.0	39.5	9.4	345	86.9	0.12	48 373	128.8
6	Milešovka	I	350	64.5	50.5	5.2	230	63.4	0.06	14 280	40.8
6	Milešovka	II	377	62.3	51.8	5.8	295	75.4	0.05	14 695	38.9
2	Bystřany	I	385	53.5	52.0	6.9	296	74.2	0.02	19 326	50.1
2	Bystřany	II	377	51.6	47.5	9.2	348	86.4	0.06	18 655	44.4
14	Cínovec	I	410	70.1	54.3	3.3	235	57.9	0.03	20 119	49.0
4	Hamr	I	410	66.6	55.0	5.0	231	62.2	0.04	40 415	98.5
4	Hamr	II	377	61.8	55.8	7.4	325	82.9	0.04	31 593	83.8
11	Teplice	I	410	56.8	46.3	6.9	305	72.6	0.19	34 795	84.8
11	Teplice	II	377	39.4	37.3	10.0	347	88.1	0.11	27 102	71.8
12	Třebenice	I	410	59.7	52.3	6.4	288	70.2	0.02	18 820	45.9
12	Třebenice	II	377	52.3	48.1	8.7	335	85.6	0.04	13 331	35.3
1	Bořislav	I	410	50.8	40.7	5.7	267	66.4	0.02	22 510	54.9
1	Bořislav	II	377	47.7	43.0	8.5	335	85.9	0.05	20 542	54.4
15	Výsluní	I	385	68.2	56.5	4.4	241	61.8	0.09	25 917	67.3
13	Újezd	I	385	53.9	44.7	6.6	281	73.2	0.09	30 042	78.0
13	Újezd	II	377	50.7	45.7	9.1	339	85.3	0.06	23 361	61.9
9	Pětipsy	I	350	45.7	43.8	7.9	273	78.5	0.05	15 042	42.2
9	Pětipsy	II	377	48.5	44.9	8.7	335	85.1	0.04	11 078	29.3
7	Měděnec	I	350	69.5	54.2	4.8	231	67.1	0.08	31 304	89.4
7	Měděnec	II	377	63.5	52.8	5.7	295	72.9	0.09	27 869	73.9
3	Dubí	I	410	66.7	58.2	5.6	271	65.8	0.05	23 670	57.7
3	Dubí	II	377	54.5	53.5	7.5	332	83.7	0.06	17 076	45.2
Frýdlant Region:											
1	Andělka	I	380	58.8	49.3	7.3	271	76.1	0.01	43 136	50.8
4	Nové Město	I	380	59.7	57.6	5.6	272	72.1	0.01	34 934	41.1
3	Hejnice	I	380	54.2	47.4	7.0	283	75.2	0.02	34 311	40.4

the external environment is not yet efficiently impeded by the layer or corrosion products.

Other authors [*3–5*] utilize the power function for describing the time-dependent course of the corrosion of metals, steel in particular. The parameters of the function depend on the material properties of the metals and the aggressivity of the atmosphere and offer the possibility to characterize them to a considerable extent or, at least, to compare them.

In our work we employed both approaches [*6*], and the results of the regression analysis are briefly treated in the present contribution. Our systematically pursued aim, however, is to attain a solution to the problem by utilizing ideas about the process of atmospheric corrosion, and we endeavor to use them in the creation of a model suitable for mathematical treatment.

The principal point in a successful treatment is the suggestion of the characteristics of climate and air pollution which would be representative for judging the corrosion aggressivity of atmospheres and would be, as far as possible, directly treatable from published data and usable in formulas for the prognosis of a long-term corrosion process. We have suggested and numerically expressed such characteristics which inform about the frequency of the occurrence or the duration of the individual values that are important to the corrosion. Some simply treatable characteristics are numerically expressed in Table 1 and further listed in Table 2. The optimization of the characteristics is at present carried out mathematically. The grouping of these data permits us to judge the ratio of the duration of moistening of the corroding surface, the concentration of stimulating ions, the ratio of the time of existence of temperatures favorable for the course of the corrosion process, and the average temperature in these periods. These suggested characteristics permit us to set out from both the published data on long-term action of the climate and from measurements performed in various special micro- and cryptoclimates.

TABLE 2—*Symbols used for climatic factors and their characteristics.*

V	Humidity
T	Temperature
Z	Pollution
V_1	Numerosity of occurrence of 80 percent and higher relative humidity, per cent
V_2	Numerosity of occurrence of 80 percent and higher relative humidity, percent; however, for reading at temperatures exceeding 0°C (32°F) only
T_1	Average air temperature, °C
T_2	Number of days with daily average temperature above 0°C
T_3	Numerosity of occurrence of temperatures above 0°C, percent
T_4	Number of days with temperature above 0°C when measured in the morning term
Z_1	Average pollution with SO_2 in mg SO_2/m^3
Z_2	Cumulative dose of pollution determined by the absorption method in mg SO_2/m^2
Z_3	Average daily dose of pollution, mg $SO_2/m^2/day$

In the actual elaborating stage, we consider t = 0°C (32°F) to be the limit temperature at which corrosion processes start in the surface electrolyte layer, although we are aware of the fact that the effective boundary lies below the ice point and is dependent upon the nature of the surface electrolyte. However, this boundary is variable and no relations for its determination are known; therefore, we have chosen a simpler though less precise procedure.

For a rapid judging of the corrosion aggressivity of the locality, we have suggested combined characteristics which are a certain simple index of the aggressivity of the medium (Table 3). This index is the product of the degree of the influence of moisture and the overall or average value of air pollution whereby it comprises the dominant corrosion factors. The numerically expressed index of corrosion aggressivity formerly published by Oden [7] (product of the significance of the weighted frequencies of the occurrence of moistures and temperatures) was distinctly more loosely related to the resultant corrosion factor.

TABLE 3—*Combined characteristics.*

No.	Station Name	Program	Time of Exposure, days	Characteristic Data				
				V_1Z_1	V_2Z_1	V_1Z_2	V_2Z_2	V_2Z_3
North-Bohemian Region:								
10	Práhly	I	350	3.1	2.5	12 690	10.286	2938
10	Práhly	II	377	0.4	0.3	10 377	8 861	2348
5	Kopisty	I	385	6.4	5.2	25 060	20 660	5366
5	Kopisty	II	377	5.0	4.7	20 400	19 186	5087
6	Milešovka	I	350	3.9	3.1	955	7 260	2076
6	Milešovka	II	377	3.1	2.6	9 154	7 612	2015
2	Bystřany	I	385	1.1	1.0	10 339	10 049	2605
2	Bystřany	II	377	3.1	2.9	9 625	8 861	2346
4	Hamr	I	410	2.7	2.2	26 916	22 470	5476
4	Hamr	II	377	2.5	2.2	19 524	17 628	4676
3	Dubí	I	410	3.3	2.9	15 787	13 775	3358
3	Dubí	II	377	3.3	3.2	9 306	9 118	2413
12	Třebenice	I	410	1.2	1.1	11 235	9 842	2400
12	Třebenice	II	377	2.1	1.9	6 972	6 412	1697
1	Bořislav	I	410	...	...	11 435	9 161	2234
1	Bořislav	II	377	2.4	2.1	9 798	8 883	2339
15	Výsluní	I	385	6.1	5.1	17 675	14 643	3802
13	Újezd	I	385	4.8	4.0	16 192	13 428	3486
13	Újezd	II	377	3.0	2.7	11 844	10 675	2828
9	Pětipsy	I	350	2.4	2.2	6 874	6 588	1879
9	Pětipsy	II	377	1.9	1.8	5 372	4 974	1315
7	Měděnec	I	350	5.6	4.0	21 756	18 531	5292
7	Měděnec	II	377	5.7	4.8	17 696	14 714	3901
Frýdlant Region:								
1	Andělka	I	380	0.6	0.5	12 526	10 524	2766
4	Nové Město	I	380	0.6	0.5	10 149	9 696	2551
3	Hejnice	I	380	0.1	1.0	9 633	8 424	2213

Both trends indicated herein set out from theoretical laboratory tests as well as from widely conceived field tests. The program reported in this paper comprises more than 150 exposure situations of principal metals, and it is thus sufficiently representative.

Tests

The corrosion tests were performed on single-purpose corrosion stations according to the method given in the National Standard ČSN 03 8110. This method is in accordance with usual practice. The distribution of the stations is shown in Figs. 1 and 5. The tests were carried out as five-year (1st program) and two-year (2nd program) tests with sampling after 3, 6, and 12 months, and 2, 3, and 5 years. The first testing program was started in autumn, the second one in spring. Principal technical metals were tested: iron (nonalloyed structural low-carbon steel), zinc (99.8 percent), copper (99.9 percent), and aluminum (99.95 percent).

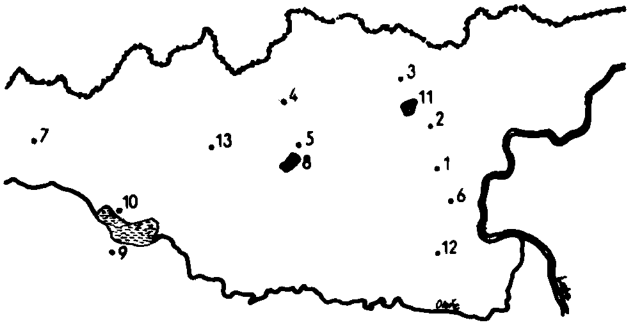

FIG. 1*a*—*Diagram of North-Bohemian model region.*

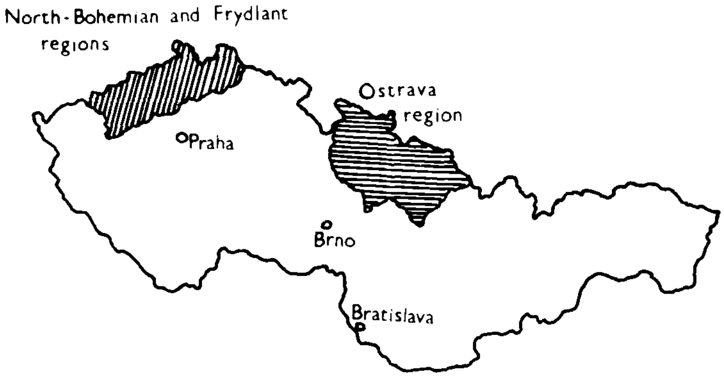

FIG. 1*b*—*Layout diagram of model regions in the territory of the Czechoslovak Socialist Republic.*

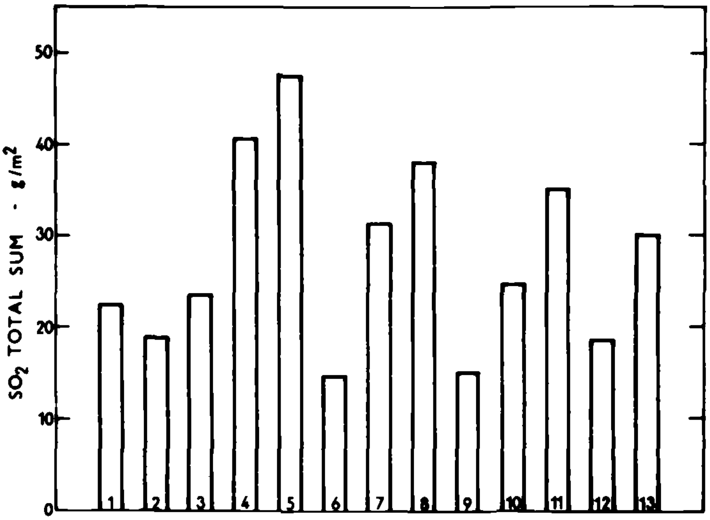

FIG. 2—*Total value of pollution with* SO_2 *during one year's exposure, determined by the absorption method (North-Bohemian model region, 1st testing program).*

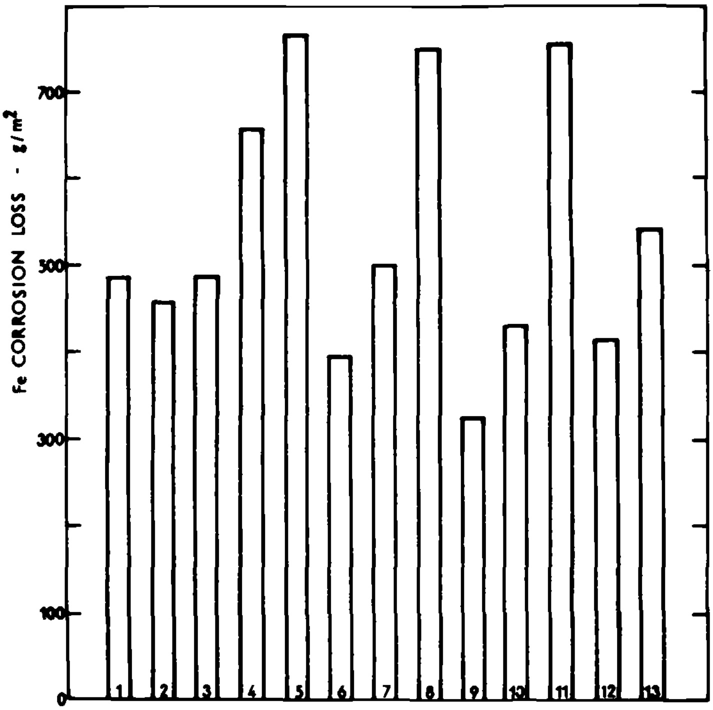

FIG. 3—*Iron corrosion loss after one year's exposure (North-Bohemian model region, 1st testing program).*

In the course of the tests, the relative humidity and the temperature were measured (in intervals of 7, 14, and 21 h) as well as the content of SO_2 in the atmosphere. Moreover, the precipitations were observed, and the cumulative doses of SO_2 and chlorides, absorbed on alkaline porous plates, were determined (modified Liesegang method). The weight losses due to corrosion were evaluated after the pickling of the samples in the respective solutions by means of the method given in the National Standard ČSN 03 8102.

The experimental materials are extraordinarily comprehensive; therefore, we give only the results of the tests after one year's exposure (Table 4). Of the group of more than 20 numerically expressed methods of processing climatic data into characteristics of moisture, temperature, and air pollution, we present only selected simple forms (Tables 1 and 3). The results of the first test program for one year's exposure are shown in Figs. 2–4 and 6–8.

Analysis of the Results

We shall limit the discussions on the results proper of the corrosion tests, and instead shall aim at proposing the methods of evaluating these results.

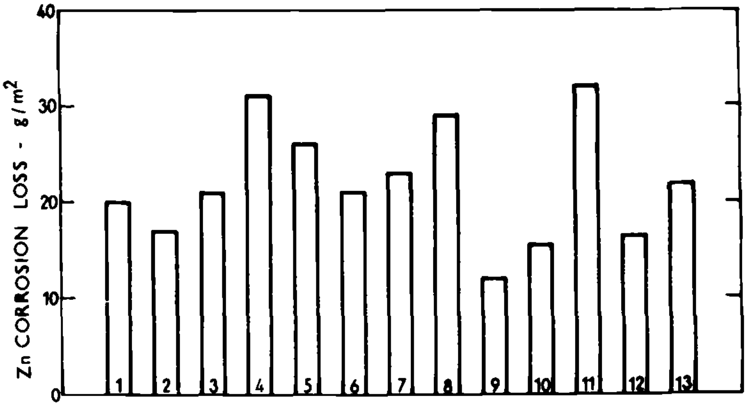

FIG. 4—*Zinc corrosion loss after one year's exposure (North-Bohemian model region, 1st testing program).*

FIG. 5—*Diagram of Frýdlant model region.*

TABLE 4—*Weight losses and corrosion rates of major technical metals.*

Station				Corrosion							
			Time of Exposure,	Loss, g/m²				Rate, g/m²			
No.	Name	Program	days	Fe	Zn	Cu	Al	Fe	Zn	Cu	Al
North-Bohemian Region:											
10	Práhly	I	350	434.0	15.5	24.9	0.96	1.23	0.04	0.07	...
10	Práhly	II	377	379.6	15.5	...	...	1.00	0.041	...	...
5	Kopisty	I	385	764.0	26.2	63.0	1.74	1.48	0.068	0.173	0.0045
5	Kopisty	II	377	633.4	24.3	...	...	1.68	0.064	...	...
6	Milešovka	I	350	394.0	20.7	19.5	1.08	1.11	0.055	0.052	0.0021
6	Milešovka	II	370	585.0	21.1	...	...	1.80	0.056	...	...
2	Bystřany	I	385	454.0	17.2	30.4	0.98	1.18	0.050	0.075	0.0027
2	Bystřany	II	377	469.8	15.2	...	...	1.25	0.051	...	...
14	Cínovec	I	410	526.2	27.3	24.4	1.99	1.28	0.066	0.054	0.0050
4	Hamr	I	410	657.0	31.5	32.5	1.60	1.60	0.077	0.079	0.0059
4	Hamr	II	377	468.1	19.8	...	...	1.24	0.52	...	...
3	Dubí	I	410	486.0	20.9	28.0	2.52	1.19	0.051	0.068	0.0061
3	Dubí	II	377	442.2	15.3	...	...	1.17	0.040	...	...

12	Třebenice	I	410	416.3	16.4	24.0	0.58	1.01	0.04	0.059	0.0014
12	Třebenice	II	377	359.1	7.3	...	...	0.95	0.010	...	...
1	Bořislav	I	410	485.0	19.7	26.6	2.56	1.18	0.047	0.067	0.0096
1	Bořislav	II	377	428.4	14.7	...	...	1.13	0.039	...	...
15	Výsluní	I	385	444.0	14.1	21.3	1.49	1.15	0.049	0.053	0.0039
13	Újezd	I	385	347.0	22.3	35.1	1.68	1.42	0.060	0.092	0.0043
13	Újezd	II	377	454.0	18.5	...	...	1.20	0.049	...	...
9	Pětipsy	I	350	326.6	12.1	20.6	0.47	0.95	0.035	0.059	0.0014
9	Pětipsy	II	377	411.3	12.7	...	...	1.09	0.034	...	...
7	Měděnec	I	350	448.0	23.1	22.8	1.55	1.42	0.086	0.065	0.0044
7	Měděnec	II	377	423.3	18.2	...	...	1.12	0.048	...	...
11	Teplice	I	410	757.0	32.4	22.9	2.84	1.84	0.081	0.073	0.0064
11	Teplice	II	377	593.5	18.3	...	...	1.57	0.048	...	...
8	Most	I	410	749.0	28.7	41.5	2.14	1.77	0.070	0.100	0.0053
8	Most	II	377	605.4	17.1	...	...	1.60	0.045	...	...
Frýdlant Region:											
1	Andělka	I	380	477.7	23.1	15.3	1.20	1.07	0.052	0.041	0.0040
4	Nové Město	I	380	360.6	17.1	14.4	1.19	0.41	0.046	0.037	0.0030
3	Hejnice	I	380	422.0	23.6	13.7	1.22	1.00	0.070	0.036	0.0040
2	Frýdlant	I	380	403.0	14.7	15.7	1.52	1.18	0.060	0.042	0.0040

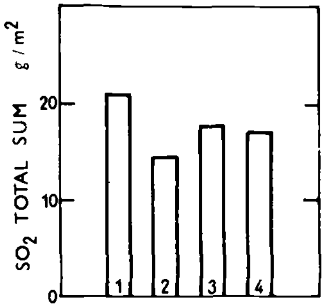

FIG. 6—*Total value of pollution with SO_2 during one year's exposure, determined by the absorption method (Frýdlant model region, 1st testing program).*

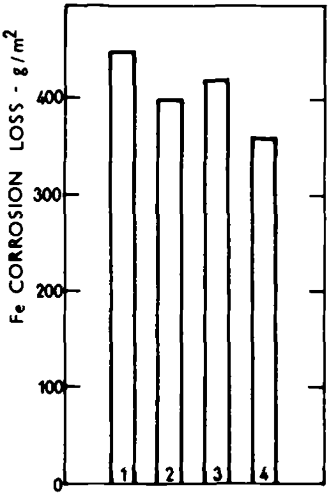

FIG. 7—*Iron corrosion loss after one year's exposure (Frýdlant model region, 1st testing program).*

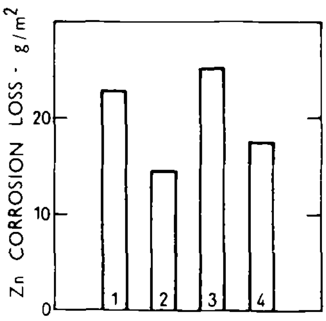

FIG. 8—*Zinc corrosion loss after one year's exposure (Frýdlant model region, 1st testing program).*

The one year's exposure in the first program has resulted in an altogether higher corrosion loss than one year's exposure in the second program. The main reason for it is evidently the fact that the exposure in the first program started in the winter season, although the values of the humidity characteristics, too, proved greater in the first case.

The correlation analysis of results of the short-term corrosion tests has proved clearly that the weight of the pollution factor is of great importance.

The comparison of values of the humidity, pollution, and temperature characteristics with the consequences of their effects—with the corrosion loss—has proved that it is necessary to understand the environmental effects in their coexistence and to also take into consideration the aspects of the corrosion mechanism of single metals sorts, although the effect of pollution is prevailing.

Thus, for example, there exist apparent discrepancies between the value of the zinc and iron corrosion loss and the value of the pollution (Localities 4 and 5 and 6 and 9 in the North-Bohemian region). A higher value of Z and T_1 characteristics in the case of the iron corrosion in Locality 5 at the increased humidity (V_1) must necessarily result in a high corrosion attack; the conditions are favorable for the chemical mechanism of the corrosion effect. Contrarily, the zinc corrosion is not dependent upon temperature within the studied interval of average temperatures. However, the very high value of the V_1 characteristic in Locality 4 is very significant. Similar results have been found also upon comparing Localities 6 and 9. Higher precipitation and condensation (due to a wooded summit) have been found, too, in Locality 6.

These examples prove that it is impossible to draw conclusions as to the locality corrosiveness from a single, though highly significant, characteristic. Better information for the estimate can be obtained from the combined characteristics we suggested, especially from V_1Z_2 and V_2Z_2. As a matter of fact, it is possible to place the locality with the corrosiveness class appertaining here, which is sufficient in the majority of technical cases. The use of further suggested regression functions will then permit the binding together of the effects of the basic climatic corrosion factors in a relatively simple way.

For a further comparison of the results of the corrosion tests, we take the Pètipsy locality, situated at the border of the North-Bohemian industrial agglomeration. The Kopisty, Most, Teplice and Hamr localities show considerably greater corrosion aggressivity than other sites examined. This is because these towns are either close to the sources of industrial emissions or are easily affected by air pollution due to their specific geographic location (Hamr).

The localities are classified according to the level of air pollution with SO_2; that is, by comparison of the ascertained cumulative value of SO_2 with the critical value. By critical we mean the values suggested by Barton

[*8*], which for the usual steels express the pollution when the corrosion process passes to a considerable extent into the mechanism in the active state (6 to 10 g SO_2/m^2/year). The critical value of air pollution for nonferrous metals (18 to 20 g SO_2/m^2/year for zinc and copper) is the value at which the destruction process of the layer of corrosion products in the passive state becomes kinetically significant (Table 5). The corrosiveness classes then delimit the values of the critical pollution (Class I), of its multiple (Class II), of its quadruple (Class III) and of a higher pollution (Class IV).

TABLE 5—*Relation of degree of pollution to critical value for iron, zinc, and copper.*

	Iron		Zinc and Copper	
Station	*a*	*b*	*a*	*b*
Kopisty	4.7	IV	2.36	III
Teplice	3.4	III	1.73	II
Most	3.8	III	1.90	II
Hamr	4.0	IV	2.02	III
Újezd	3.0	III	1.50	II
Měděnec	3.1	III	1.56	II
Dubí	2.3	III	1.15	II
Bořislav	2.2	III	1.12	II
Bystřany	1.9	II	0.95	I
Výsluní	2.5	III	1.29	II
Práhly	2.4	III	1.23	II
Třebenice	1.8	II	0.94	I
Milešovka	1.4	II	0.71	I
Pětipsy	1.5	II	0.75	I

a = Relation to critical value of pollution.
b = Class of aggressivity according to degree of pollution.

The results are at present in the stage of complex mathematical processing which after completion will be the subject of further papers. We present here only partial conclusions.

On the basis of the results of tests of three years of the described program and of tests of five to eight years on eight types of steels in three main atmospheric test stations of the National Research Institute for Protection of Materials, differing in their aggressivity, we analyzed the dependence of corrosion on time with the use of the power function ($K = at^b$), the expanded power function ($K = at^{b+ct}$), and the power function passing into a linear and hyperbolic function [$K = a + bt - (ac/t + c)$]. The best correlation was attained for the hyperbolic function, as shown in Table 6. It can be assumed that the hyperbolic function has most closely approximated the law of the time-dependent course of the corrosion process. The equalization was successful also for the nonferrous metals, zinc,

TABLE 6—*Average coefficients of correlation.*

Steel No.	Power Function Passing into Straight Line	Power Function with Variable Exponent	Hyperbolic Function
1	0.04707	0.01639	0.02292
2	0.03441	0.01891	0.00936
3	0.05877	0.05148	0.02607
4	0.01567	0.02372	0.00965
5	0.06696	0.01529	0.02745
6	0.06644	0.04472	0.01601
7	0.06663	0.02249	0.01601
8	0.06715	0.04092	0.02898

copper, and aluminum, even when equalization by a straight line was sufficient. The possibility of equalization by means of an exponential function is dealt with in the following text.

Moreover, we have endeavored to find a multifold regression function, which can be generally written as

$$K = f(t,T,V,Z) \tag{2}$$

For the individual partial dependencies we represented the functions which best correspond to practical experience. With the use of these partial functions and with regard to the fact that the hyperbolic function has proved to be most suitable for the time-dependent course of atmospheric corrosion of metals, we suggested the complex regression function

$$K(t,T,V,Z) = \alpha_1\alpha_2{}^T\cdot\alpha_3{}^Z\cdot V^{\alpha_4\alpha_5^2}[1 - \alpha_6(t + \alpha_7)^{-1} + \alpha_8 t] \tag{3}$$

The calculation of the parameters of this function in logarithmic form, however, did not lead to results that permitted a real solution.

Therefore, we carried out a regression analysis for the standardized time $t = 300$ and 600 days; the functions were again suggested according to experimentally determined partial dependencies.

The regression analysis was performed with the use of various forms of the characteristics for moisture, temperature, and air pollution, so that it was at the same time an optimization of the characteristics employed.

The principal criterion for judging the suitability of ten selected functions and combinations of characteristics was the comparison of the coefficients of correlation with the critical values F for α(percent) = 0.01; 0.025; 0.05; and 0.1.

The most favorable function was expressed in the form

$$K = \alpha_0 V^{\alpha 1}\cdot e^{\alpha_2 T+\alpha_3 Z} \tag{4}$$

Of the characteristics included in the processing, the following were found to be most suitable:

1. Frequency of occurrence of relative humidities exceeding 80 percent (V_1).

2. Number of days with a temperature above 0°C (32°F) as measured in the morning (T_4).
3. Average temperature (T_1).
4. Pollution with SO_2 in units mg SO_2/m^2 per day (Z_3).

The average difference between the theoretical and the empirical results was 5 percent; the coefficient of correlation amounted to 0.07726.

At the same time we also started our work on the development of a cybernetic model of atmospheric corrosion of metals, which we deal with in a separate section.

Mathematical Model of Atmospheric Corrosion of Metals

The procedures so far employed for determining the time-dependent course of the corrosion are limited to the selection of a certain function (usually a polynomial or hyperbolic dependence on time) whose coefficients are determined by a regression analysis. In the numerous suggestions, even including the exponential function of time, the following principal shortcomings of this procedure are evident:

1. The selection of the regression function is quite random, in most cases only according to the introduced type of regression, although only a correct selection is decisive for a successful analysis. It is self-evident that, of ten incorrectly selected curves, always at least one best approximates the measured values, even if this "optimum" approximation is unusable.
2. The coefficients determinable by regression analysis are in the case of random selection not directly connected with the principle of the corrosion phenomenon. For instance, the coefficients of hyperbolic regression are complicated functions of independent variables.

From this fact it is clear that the basis of a modern approach to a mathematical prediction of a long-term course of atmospheric corrosion cannot be simplified functions of elementary or truly geometrical character. Decisive for the selection of the regression function are first of all the nature of the kinetics of the process and the utilization of all theoretically and experimentally ascertainable parameters of the corrosion phenomenon. Such a demand leads to the formulation of a cybernetic model whose principle we indicate here in a simplified form.

It is known that the corrosion process taking place discontinuously in periods t_i according to the relation

$$K(t^*) = \sum_{i=0}^{m} v_{si}(t_{i+1} - t_i) \tag{5}$$

at the medium corrosion rate

$$v_{si} = \frac{1}{t_{i+1} - t_i} \int_{t_i}^{t_{i+1}} V_k(t)\, dt$$

exhibits—apart from few exceptions—a decreasing rate with increasing time, even at unchanged action of all existing atmospheric influences. The general variability of this rate, however, is not a function of time but of the growing layer of corrosion products and its "decelerating" or even accelerating action on the corrosion process. This fact is of major importance for the existence of a cybernetic feedback model, whose extraordinary flexibility permits us to formulate the regression functions of quite a new type with parameters directly connected with the kinetics of the corrosion.

The rate of the corrosion $V_k(t)$ is in general a function of atmospheric or even other influences, $a_1(t) = a_{H_2O}(t)$; $a_2(t) = a_{SO_4^{2-}}(t)$; $a_3(t) = T(t)$, etc., and for sufficiently short intervals (t_i, t_{i+1}) it can be expressed as a linear combination with the coefficients $1/r_{ij}$ in the form

$$V_{si} = \sum_{j=1}^{n} \frac{1}{r_{ij}} a_{ij}(t) \tag{6}$$

which with regard to the general relation for the corrosion $K(t)$

$$V_k(t) = \frac{d}{dt}[K(t) + K_0]$$

and on introduction of the dimensionless quantities

$$\frac{K(t^*)}{K_0} = X(t^*), \frac{a_{ij}(t)}{a_0} = y_{ij}(t)$$

leads to the form

$$X(t^*) = \sum_{i=0}^{m} \sum_{j=1}^{n} \frac{1}{T_{ij}} \int_{ti}^{ti+1} y_{ij}(t)\, dt \tag{7}$$

This clearly indicates the astatic nature of the phenomenon of the corrosion with the integration time constant, $T_{ij} = a_0/(r_{ij}K_0)$, variable in the intervals t_i. At the same time, however, $y_{ij}(t)$ also varies even at constant values of the atmospheric influences. This means that various influences m correspond to the same value of pollution or moisture of the atmosphere according to the time of exposure of the material. To the measured values we must then ascribe a whole group of numerical quantities depending on whether the action on the material is at the beginning or in the further course of the corrosion process. This involves the principal shortcoming, which cannot be eliminated only by a true mathematical or even an empirical selection of the elementary regression function.

For the cybernetic model we first define a truly astatic object, which has n inputs y_i, that is, atmospheric influences $a_j(t)$-$y_i(t)$, and only one output, the corrosion effect $x_1(t)$. We regard the system as being continuous within the time interval $t_{i+1} - t_i$. This limitation is not necessary, however, and the transition to a continuous system or continuous along the intervals does not cause any difficulties. The system is described by the equation

$$x_1(s) = y(s)P_1(s) \tag{8a}$$

where

$$y_1(s) = [y_1(s), y_2(s) \ldots, y_n(s)]$$

and

$$P_1(s) = \left[\frac{1}{sT_{11}}, \frac{1}{sT_{21}} \ldots, \frac{1}{sT_{n1}}\right]^T$$

The transfers $1/sT_{j1}$ express the ratio of the Laplace transforms of the components of the output corrosion $x_{1j}s$ to the individual input quantities $y_j(s)$. Their superposition

$$\sum_{j=1}^{n} x_{1j}(s) = x_1(s) = \sum_{j=1}^{n} y_j(s)\frac{1}{sT_{j1}} \tag{8b}$$

is the expanded form of Eq 8*a*.

We regard the object defined in this way as the model of an isolated corrosion process (for example, on a pure metal) at constant values of the inputs $y_j(s)$, and it may be exceptionally suitable for materials whose corrosion proceeds even for a long time as a linear function of time t.

Into this isolated model we now introduce the retroactive influence on the corrosion rate from its instantaneous value $x_1(t)$ in such a way that the arising corrosion layer weakens or strengthens the influence of the external constituents of the atmospheric pollution $a_j(t)$ or $y_j(t)$. This can be schematically represented by Fig. 9, where the transfers of the retroactive action $R = c_{11}(s), c_{12}(s) \ldots c_{1n}(s)$ are transforms of the linear relations between the corrosion layer and the "deceleration" of the effect of the individual constituents of the atmospheric influence (Fig. 9). In the simplest case, the elements c_{1j} of the vector **R** will be constants. Even in this way it is possible to attain a very good flexibility of the resultant exponential course, whose Laplace transform is

$$x_1(s) = y(s)P_1(s)\,[1 + \mathbf{R}(s)\cdot P_1(s)]^{-1} \tag{9a}$$

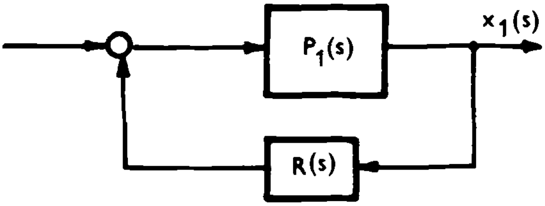

FIG. 9—*Schematical representation of reverse-coupling effects of corrosion product layer.*

This can be given in expanded form as follows:

$$x_1(s) = \frac{\sum_{j=1}^{n} y_j(s)\cdot\frac{1}{sT_{j1}}}{1\sum_{j=1}^{n}\frac{c_{1j}(s)}{sT_{j1}}} = \frac{\sum_{j=1}^{n} y_j(s)\prod_{\substack{k=1\\k\neq j}}^{n} T_{k1}}{s\prod_{k=1}^{n} T_{k1} + \sum_{j=1}^{n} c_{1j}(s)\prod_{\substack{k=1\\k\neq j}}^{n} T_{k1}} \tag{9b}$$

The respective differential equations are obviously of the first order with values of T constant in relation to time, whose magnitude, analogously as a new stabilized state, is connected with the selection of the transfers $c_{1j}(s)$. The initial slope of the course $x_1(t)$ is given by the selection of the time constants of the astatism T_{j1}. For constant magnitudes of c_{1j}, the resultant form is

$$x_1(s) = \frac{\sum_{j=1}^{n} y_j(s)\cdot T_j^{n-1}}{sT_n^{\,n} + T_{n-1}^{\,n-1}} = \frac{\sum_{j=1}^{n} y_j(s)\cdot K_j}{sT_0 + 1} \tag{9c}$$

where

$$T_0 = \frac{\prod_{k=1}^{n} T_{k1}}{\sum_{j=1}^{n} c_{1j}\prod_{\substack{k=1\\k\neq j}}^{n} T_{k1}}$$

The feedbacks of $c_{1j}(s)$, considered in Eq 9 as being negative throughout, may in certain cases have a position sign (rising rate of corrosion), and then express exponentially increasing courses.

The indicated model describes the course of the corrosion, $x_1(t)$, up to the attainment of a new stabilized state, that is, practically a complete stoppage of the corrosion by its own protective effect. This, however, is in contradiction to experiences according to which, after expiration of a certain time or after attainment of a certain corrosion layer, a constant rate $(d/at)\ x_1(t) = V_{k0} = \text{const}$ (Fig. 10) is assumed.

We respect this fact in the resultant course $x_1(t)$ in such a way that at the instant t_{1k} the output signal $x_1(s)\mathbf{R}(s)$ becomes constant and independent of the further growth of the corrosion layer. From this instant we have again an isolated model with constant reduction of the external influences y. Since for constant components of y_{jk} of the vector of y holds

$$\frac{d}{dt}\,x_1(t) = \sum_{j=1}^{n} \mathrm{y}_{jk}\cdot K_j(1 - e^{-t/T_0}) = V_{k0} \tag{10}$$

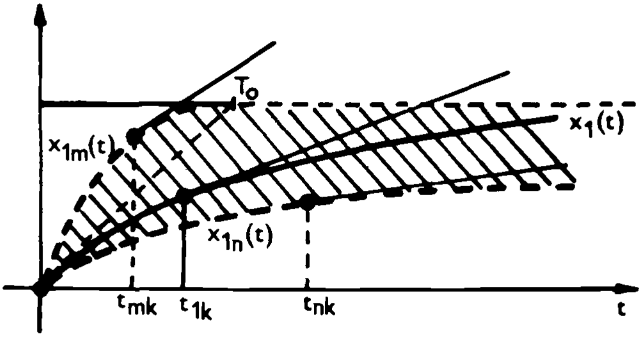

FIG. 10—*Representation of time dependence of corrosion directed to a stationary condition.*

there will be for $t = t_{1k}$

$$t_{1k} = T_0 \cdot \ln \frac{1}{V_{k0}} \sum_{j=1}^{n} y_{jk} K_j$$

The determination of the position of the critical point from the ascertainment of the constant rate of the corrosion does not cause any difficulties even for an arbitrary input course; this consideration is obviously no proof of the existence of this break. More thorough analyses, however, lead to considerably more complicated courses of this time prediction; for example, composite exponential curves with various time constants and several points of inflection. This is in particular the case if we introduce the more general transfers $c_{1j}(s)$. Figure 10 also clearly shows a distinct increase of the flexibility of the function $x_1(t)$ by a greater selection of the time constants of the astatism of an isolated system as a functon of time; for example, $T_{j1}(t) = T_{j0} + b_{j1}(t)$. The pencil of choosable exponential curves (Fig. 10) then fills up the entire region between the extremum courses $x_{1m}(t)$ and $x_{1n}(t)$.

These considerations demonstrate the crucial significance of the determination of the retroactive influence on the effects of $y_j(s)$ by means of the transfers of $c_{1j}(s)$ for most of the various materials and all aggressive actions. In the transfers of $c_{1j}(s)$ all influences of the internal kinetics of the corrosion are expressed, and their determination follows from both theoretical and experimental investigation. The suggested model shown in Fig. 9 corresponds to the cybernetic conception of n-fold single-parameter regulation. In the later stage of research it is necessary, however, to assume the use of a more complicated model, where the output of the isolated model is not the total increase of the corrosion, $x_1(t)$, but is given by the individual components of this increase; that is, the vector $\mathbf{x}(s) = [x_1(s), x_2(s) \ldots, x_n(s)]$ and each of these components can be influenced by all aggressive actions simultaneously or even by only one component of $y_j(s)$. The principle of this superposition has so far not been decided upon, and also the internal parasitic couplings of the isolated system $P(s)$ must be determined. The cybernetic model has in this general form the diagram shown in Fig. 11

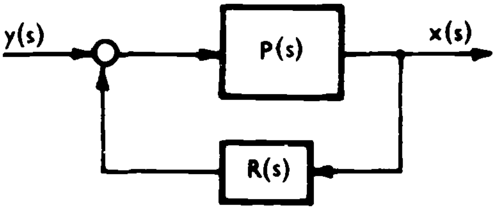

FIG. 11—*General form of atmospheric corrosion cybernetic model.*

where

$$\mathbf{P} = \left[\frac{1}{sT_{jk}}\right]_{(n,n)} \qquad \mathbf{R}(s) = [c_{ij}(s)]_{(n,n)}$$

$$\mathbf{y}(s) = [y_1(s)]_{(1,n)} \qquad \mathbf{x}(s) = [x_k(s)]_{(1,n)}$$

The numerical processing of these relations is feasible only by means of computers. Considerably simpler is the case where $c_{ij}(s)$ are constants and the matrix of $P(s)$ is diagonal. The analyses given in this section can now be summarized.

The cybernetic model of the corrosion process consists of the system of the isolated object $P(s)$, the external action of stimulating factors $y(s)$, and the feedback action $R(s)$, which expresses the "decelerating" protective effect of the corrosion layer. These components of the logic follow from the principle of the corrosion process. The introduction of this conception renders the external effects independent, and their correction according to the time of exposure of the material is dispensed with. The model is formulated in general for an arbitrary number of aggressive effects, and it can be arbitrarily extended even for any number of components of the corrosion itself. It also permits us to decide, on a solid basis, upon the existence of a two- or multiphase corrosion process, points of inflection, and its smooth or broken course for all materials under examination.

The theoretical proposition of a cybernetic model of the atmospheric corrosion process has arisen on the basis of an intellectual analysis of the physical-chemical substance of the process, and of a mathematical analysis of the corrosion time curves at different levels and combinations of external factors, for which the corrosion test results given herein have been used.

Actually, we are filling the theoretical model with concrete relations for the effects of stimulation factors and for the reverse-coupling effects, utilizing the results of field and laboratory tests made by us as well as the data from the literature. The proposed procedure represents also a way of obtaining a reliable prediction of atmospheric corrosion for longer periods.

Conclusion

For another model region Ostrava, a center of heavy industry and extensive coal mining, we selected different procedure. We were concerned with a corrosional-economic investigation of the corrosive effect and of the damage caused on typical metallic structures (steel bridges, gasholders, hoisting towers, etc.) in localities with gradated aggressivity. For these localities we also expressed numerically the characteristics of the climate and the air pollution, and we calculated the combined characteristics of aggressivity. After the analysis of the results, corrosion tests were performed only as a supplement. Further regions will be treated predominantly on the basis of the numerically expressed characteristics.

In connection with the study of the aggressivity in the network of test stations, it is necessary, however, to bear in mind that the possibility of generalization of the results is limited. Besides quantities varying more or less continuously and offering the conditions for being utilized in meso- or microclimatic maps, there are further influences which cannot be treated in this way. Critical values of air pollution are attained throughout in small localities, and the degree and components of the pollution are locally quite variable. Even the first group of influences can be generally expressed only as a group of characteristics of the external medium, the actual

FIG. 12—*Atmospheric station, Bystřany.*

conditions on the corroding surface then depend on the properties of the product and its location. For deriving these relations there exist at present only general technical criteria rather than mathematical relations. For this reason, we do not regard as appropriate mapping the corrosion aggressivity of large areas as suggested, for example, by Rychtera [*9*]. Already better suited is the procedure according to Golubyev [*10*] and Mikhailovski and Shuvakhina [*11*], who from long-term investigation of the climate calculated the probable times of the moistening of metal surfaces, on the basis of which they divided the territory of the USSR into individual districts. The corrosion aggressivity is judged according to the time of moistening read from the map and the actual value of air pollution.

In our project of cartographic treatment of the corrosion aggressivity in Czechoslovakia, on which work has already been started, we assume the numerical expression of the complete group of characteristics of the climate from hourly measurements of moisture and temperature, as well as from data on the precipitation during a representative period of time. The mapping will be performed with the use of computers according to the coexistence of the selected values of the individual characteristics or their surpassing of a significant level. The pollution will be pointed out only informationally (especially affected regions, significant sources); actual data must be obtained by direct measurement.

FIG. 13—*Atmospheric station, Hamr.*

The selected complete group of characteristics also permits expressing the corrosion aggressivity for further important materials such as plastics, insulation materials, and inorganic nonmetallic materials.

However, for deriving the degree of corrosion aggressivity in a technical sense, and for the entire group of working media (also including cryptoclimates), a rather general technical classification of the corrosion aggressivity of the atmospheres is of significance, and this classification must be realized before mapping. Our work (tests in model regions, tests in various factories, results of theoretical and laboratory work) is directed at a novelization of the existing Czechoslovak National Standard [*12*]. And of the international recommendation [*13*] in this respect, we aim to include in the classification all principal constructional materials of technical products, and to define the individual degrees of aggressivity by actual values of the characteristics of the climate.

Acknowledgment

The authors express their thanks to V. Marek, V. Patč, and to Mrs. J. Vlková for technical realization of the test programs, to Mr. Hekš, for the mathematical treatment, and to K. Barton̆ for his cooperation during this work.

References

[*1*] Guttmann, K. and Sereda, P. J. in *Metal Corrosion in the Atmosphere, ASTM STP 435*, American Society for Testing and Materials, 1968, p. 326.
[*2*] Haynie, F. H. and Upham, J. P. in *Materials Protection and Performance*, Vol. 9, No. 8, 1970, p. 35.
[*3*] Schwenk, W. and Ternes, H., *Stahl und Eisen*, Vol. 88, No. 7, 1968, p. 318.
[*4*] Sakate, J. and Moroishi, T., 5th World Congress on Metal Corrosion, Tokyo, May 1973
[*5*] Wallner, F. et al., *Berg- und Hüttenmännische Monatshefte*, Vol. 115, No. 9, 1970, p. 304.
[*6*] Knotková, D., Barton̆, K., and Spanilý, V., Research Report of the National Institute for Protection of Materials 140/71.
[*7*] Oden, L., Liljenvall, Lecture, International Meteorological Institute, Stockholm, Sweden, 1964.
[*8*] Barton̆, K., private communication.
[*9*] Rychtera, M., "Deterioration of Electrical Equipment," Czechoslovak Academy of Sciences, Academia, Prague, Czechoslovakia, 1970.
[*10*] Golubyev, I. A., 3rd International Congress on Metal Corrosion, Moscow, 1966.
[*11*] Mikhailovski, J. and Shuvakhina, L., *Zashchita Metallov*, Vol. 7, No. 51, 1971, p. 534.
[*12*] ČSN 03 8203.
[*13*] RS 1238/68, Recommendation of the Council of Mutual Economic Assistance.

W. H. Ailor[1]

Seven-Year Exposure at Point Reyes, California

REFERENCE: Ailor, W. H., "**Seven-Year Exposure at Point Reyes, California,**" *Corrosion in Natural Environments, ASTM STP 558,* American Society for Testing and Materials, 1974, pp. 75–81.

ABSTRACT: This report is concerned with the data obtained from the seven-year Point Reyes, California removals (second exposure). These exposed panels included 39 alloys of eight basis metals of the 1957 program.

Previous reports concerning this program may be found in the Committee B-3 reports in the *ASTM Proceedings* for 1959, 1961, and 1962 and in the Committee G-1 report (1966 *Proceedings*).

A number of test panels were lost due to the work of vandals at the Point Reyes test site during the fall of 1962. A fence subsequently erected should protect panels still exposed for future years. Replacements for seven- and twenty-year panels for most alloys were exposed on 12 June 1964. The seven-year panels were removed by task group member T. J. Summerson on 6 June 1971 after a total of 2550 exposure days. The twenty-year test panels remain on the racks for subsequent removal.

KEY WORDS: corrosion, corrosion tests, atmospheric tests, metal corrosion, pitting, corrosion rates, aluminum, lead, magnesium, nickel, copper, molybdenum, titanium, zinc

Alloys

The 1957 program[2] contains 77 alloys on test at four ASTM sites and three additional aluminum alloys on test at five locations in England. Of these alloys, 39 were of necessity reexposed at Point Reyes, California. The number of alloys in each metal category for this exposure and the task group member responsible for testing are given in Table 1.

---

[1] Research scientist, Metallurgical Research Division, Reynolds Metals Company, Richmond, Va. 23218.

[2] ASTM B-3/VI. Report of Subcommittee G01.04 on Atmospheric Corrosion (formerly Committee B-3, Subcommittee VI): S. W. Dean, chairman; W. H. Ailor, task group chairman.

TABLE 1—*Task group assignments.*

Metal	Number of Alloys	Testing Supervisor
Aluminum	7	W. H. Ailor William King V. E. Carter T. J. Summerson
Copper	10	C. J. Barton E. J. Duffy L. C. Kenausis D. Tomalin
Lead	2	O. E. Olsen
Magnesium	4	S. L. Couling
Molybdenum	1	W. H. Ailor
Nickel	5	D. van Rooyen
Titanium	8	H. B. Bomberger R. G. Broadwell L. C. Covington
Zinc	2	S. R. Dunbar

Test Program

Atmospheric Exposure

Test Location—Site C, Point Reyes, California (West Coast Marine). This site is described in a Report of the Advisory Committee on Corrosion (*ASTM Proceedings*, Vol. 59, 1959).

Test Periods—Data from the seven-year exposure (triplicate panels) are reported in Table 2. The 20-year panels are scheduled for removal in 1984.

Test Panels—8 by 4 by 0.05 in.

Identification—Panels were marked, as noted in the original report,[3] by alloy number (arbitrarily assigned to each alloy in the program), site location code letter, and panel specimen number.

Laboratory Tests Prior to Exposure

Chemical analyses were made on all 39 test alloys and reported in the Appendix to the B-3 Annual Report for 1959.

Thickness measurements were made to the nearest 0.001 in.

Length and width measurements were made to the nearest 0.01 in.

Weighing all alloys was to the nearest 0.001 g.

Tension tests were made on six specimens, three each from two panels (see Table 2).

---

[3] Appendix to B-3 Report, *ASTM Proceedings*, Vol. 59, 1959.

Evaluation of Corrosion Damage

Cleaning of all exposed panels was accomplished by techniques outlined in the 1962 Report.

Weighing of the cleaned panels was to the nearest 0.01 g, except for the aluminum and magnesium panels, which were weighed to the nearest 0.001 g.

Tension tests were made on six specimens, three each from duplicate storage panels and two each from triplicate exposure panels after cleaning and weighing (see Table 2).

Pit depth determinations were made on the center section of each exposed panel after removal of tension specimens. Either a dial depth gage or a calibrated focus microscope was used for making these determinations.

Visual examinations of the test panels before removal were made by T. J. Summerson. These results are shown in Table 3.

Exposure Period

The exposure period for the Point Reyes seven-year panels was 2550 days (from 12 June 1964 to 6 June 1971).

Participating Companies

The following companies furnished the laboratory services, manpower, and equipment required for making the evaluation tests on the after-exposure and control panels:

Aluminum Company of America
The Anaconda-American Brass Company
Bridgeport Brass Company
British Non-Ferrous Metals Research Association
Chase Brass and Copper Company
The Dow Chemical Company
The International Nickel Company
Kaiser Aluminum and Chemical Corporation
Kawecki Chemical Company
National Lead Company
The New Jersey Zinc Company
Reactive Metals Inc.
Reynolds Metals Company
Scovill Manufacturing Company
Titanium Metals Corporation of America

The assistance of the personnel and companies supplying equipment and manpower to perform this work is appreciated.

TABLE 2—*Seven-year data, Point Reyes, California, reexposure—Site C, 2550 days.*

Alloy Code	Commercial Designation	Density, g per cm^3	Panel Numbers	Weight Change, mg per dm^2	Corrosion Rate		Pit Depth					Ultimate Strength, ksi		Loss in Strength by Corrosion, %	Elongation in 2 in. %		Loss in Elongation by Corrosion, %
					mg per dm^2 per day	mils per year	4 Deepest			Maximum		Control	Exposed		Control	Exposed	
							Sky	Ground	Avg	Sky	Ground						
ALUMINUM ALLOYS																	
10	1188-H14	2.70	37-42	10.3017	0.0040	0.0021	0.5	0.9	0.7	0.8	1.7	11.7	11.9	0	12.0	13.2	0
11	1135-H14	2.70	37-42	22.2585	0.0084	0.0045	1.0	1.6	1.3	1.4	1.8	16.4	16.8	0	11.8	10.5	11.1
12	3004-H34	2.70	37-42	17.1087	0.0066	0.0035	2.5	2.9	2.7	3.1	3.6	36.6	36.4	0.6	9.0	8.7	3.3
13	4043-H14	2.70	37-42	21.5685	0.0082	0.0044	1.8	1.8	1.8	3.5	5.1	22.8	22.4	1.8	10.7	10.2	4.7
14	X5454-0	2.68	37-42	14.9722	0.0057	0.0030	2.0	4.4	3.2	2.5	7.7	37.3	39.1	0	20.8	19.8	4.8
86	Alc 7079-T6	2.80	37-42	21.5591	0.0085	0.0044	1.6	2.4	2.0	1.9	2.5	73.1	72.1	1.4	10.9	11.3	0
87	1199-H18	2.70	37-42	7.82	0.0030	0.0016	1.5	2.2	1.9	1.8	2.6	16.7	13.3	20.2	4.8	5.2	0
MAGNESIUM ALLOYS																	
43	HK31A-H24	1.79	37-42	2130	0.833	0.627	33.3	11.6	22.5	*a*	18.0	36.4	27.5	24.4	9.4	1.4	85.2
44	HM21XA-T8	1.78	37-42	2232	0.876	0.704	30.3	11.7	21.0	38.0	27.0	35.3	26.8	24.1	5.8	1.1	81.0
45	ZE10XA-H24	1.76	37-42	2368	0.928	0.746	29.1	13.4	21.2	38.0	21.0	39.1	29.2	25.4	13.4	1.5	88.8
46	ZH11X1-H24	1.77	37-38 41-42	2290	0.899	0.723	50.5	23.0	36.8	*b*	39.0	38.8	24.7	36.3	16.5	0.4	97.5
LEAD ALLOYS																	
40	Chemical lead	11.34	37-42	400.3	0.157	0.020	1.3	0.7	1.0	3.5	1.1	2.3	2.3	0	52.4	49.3	5.9
41	6% antimonial lead	10.88	37-42	347.3	0.136	0.018	0.8	0.8	0.8	3.0	1.4	3.7	3.8	0	56.9	50.8	10.7
MOLYBDENUM																	
47	Molybdenum	10.2	37-42	1178	0.4620	6.5	1.6	0.9	1.3	2.6	2.0	102.2	97.2	4.9	15.2	22.3	0
NICKEL ALLOYS																	
48	"A" nickel	8.85	37-42	57.329	0.0224	0.0036	~1	~1	~1	~1	~1	62.5	61.9	1.0	44.0	39.1	11.2
49	Incoloy	8.00	37-42	13.204	0.0051	0.0009	~1	~1	~1	~1	~1	85.0	84.7	0.4	44.2	40.6	8.1

50	Inconel	8.54	37-42	13.447	0.0052	0.0009	~1	~1	~1	~1	~1	90.8	92.7	8.9	42.5	40.3	5.2
51	Monel	8.80	37-42	84.139	0.0342	0.0056	~1	~1	~1	~1	~1	75.0	74.7	0.4	39.5	37.1	6.1
52	Ni-O-Nel	8.00	37-42	10.116	0.0040	0.0006	~1	~1	~1	~1	~1	89.5	89.7	0	48.0	46.1	4.0
	TITANIUM ALLOYS																
53	6Al-4V titanium	4.42	37-42	0.07	nil	nil	nil	nil	nil	nil	nil	133.0	134.3	0	9.9	9.6	3.0
54	8 Mn titanium	4.76	37-42	0.07	nil	nil	nil	nil	nil	nil	nil	145.8	146.8	0	17.2	17.4	1.1
55	2.5Al-16V titanium	4.65	37-42	0.42	nil	nil	nil	nil	nil	nil	nil	171.3	171.3	0	6.1	6.0	1.7
56	821	4.40	37-42	0.07	nil	nil	nil	nil	nil	nil	nil	125.8	129.4	0	16.7	16.1	3.6
57	75A	4.54	37-42	0	nil	nil	nil	nil	nil	nil	nil	94.8	93.5	1.4	23.6	27.0	0
58	140A	4.65	37-42	0.37	nil	nil	nil	nil	nil	nil	nil	133.6	132.2	1.1	17.4	20.7	0
59	5Al-2.5Sn titanium	4.46	37-42	0	nil	nil	nil	nil	nil	nil	nil	124.8	123.1	1.4	15.4	18.9	0
60	4Al-3Mo-1V titanium	4.54	37-42	0.467	nil	nil	nil	nil	nil	nil	nil	131.8	131.1	0.5	12.1	13.7	0
	ZINC ALLOYS																
61	High grade zinc	7.13	37-42	282.7	0.111	0.022	1.2	1.2	1.2	2.7	1.7	19.0	19.1	0	86.3	65.0	24.7
62	1 Cu zinc	7.18	37-42	324.0	0.127	0.026	2.4	0.9	1.7	3.2	1.4	23.4	23.4	0	66.0	53.0	19.7
	COPPER ALLOYS																
67	5 Sn phosphor bronze	8.90	37-42	694.1	0.23	0.03	nil	nil	nil	nil	nil	[c]	47.6	...	[c]	52.0	...
68	Tin brass	8.78	37-42	281.1	0.11	0.02	nil	nil	nil	nil	nil	[c]	44.8	...	[c]	55.1	...
69	2Si-7Al bronze	7.78	37-42	90.1	0.033	0.01	nil	nil	nil	nil	nil	[c]	74.0	...	[c]	46.7	...
76	No. 60	8.90	37-42	343.4	0.137	0.02	nil	nil	nil	nil	nil	33.9	32.7	3.5	43.5	43.3	0.5
77	No. 95	8.90	37-42	254.8	0.104	0.013	0.3	0.2	0.3	0.5	0.2	39.5	37.3	5.6	39.5	[d]	...
78	No. 180	8.90	37-42	261.4	0.136	0.017	0.3	0.2	0.3	0.3	0.2	[c]	45.8	...	[c]	[d]	...
80	No. 212	8.41	47-42	723.9	0.257	0.047	0.3	0.4	0.4	0.5	0.5	57.3	57.1	0.4	40.6	41.2	...
81	Beraloy A	8.26	37-42	308.9	0.121	0.021	0.2	0.2	0.2	0.3	0.3	[c]	74.0	...	[c]	[d]	...
82	Beraloy D	8.26	37-42	308.8	0.121	0.021	0.3	0.3	0.3	0.4	0.4	[c]	67.6	...	[c]	[d]	...
83	Beraloy C	8.75	37-42	550.4	0.136	0.035	0.2	0.2	0.2	0.4	0.2	[c]	49.4	...	[c]	[d]	...

Note—[a] = one perforation.
[b] = five perforations.
[c] = no control values.
[d] = no after-exposure values.

TABLE 3—*Visual examination of panels at Point Reyes, California*[a]

Alloy No.	Appearance of Specimen Surfaces	
	Top Side	Bottom Side
10	Light gray, light etch	white corrosion products and deposits
11	Light gray, light etch	white corrosion products and deposits
12	Light gray, light etch	white corrosion products and deposits
13	Light gray, light etch	white corrosion products and deposits
14	Light gray, light etch	white corrosion products and deposits
40	White-gray film	darker in color
41	White-bluish film	darker in color
43	Gray-white, random deep pitting	gray color
44	Tan-white, random deep pitting	gray color
45	White-yellow film, general pitting	gray color
46	Gray-black, scattered deep pits	gray color
47	Black smut	blue iridescent
48	Dull gold-bronze	bright gold-bronze
49	Metallic gray, mottled stain	
50	Metallic gray, mottled stain	
51	Slight green tint	
52	Slight tarnish	
53	Black spots	no effect
54	Slight dull metallic	no effect
55	Orange-red spots	no effect
56	Metallic	no effect
57	Metallic	
58	Metallic, light-gray stain	
59	Metallic	
60	Metallic, matte finish	
61	Sagging in center-white corrosion	
62	Sagging in center-white corrosion	
67	Red-brown color	red-brown color
68	Magenta-brown color	
69	Orange-brown color	
76	Brown-red, trace of patina	same as top
77	Brown-red, trace of patina	same as top
78	Brown-red, trace of patina	same as top
80	Charcoal color	charcoal color, scale present
81	Violet brown trace of patina	
82	Violet brown, trace of patina	
83	Violet brown, trace of patina	
86	Light etch, dull gray	slight buildup of corrosion product
87	Aluminum colored, random white-gray deposits	aluminum colored, heavier white-gray corrosion products

Comments

As a result of creep, Series 40 (panels 37–38, 39–40, 41–42, 61–62, and 63–64—five panels) all touch the stainless steel frames. Contact is made at the edges, usually intermediate between the porcelain insulators and frequently at the top corners of the panel. The same is true for panels of the 41 alloy series. They droop toward the stainless steel frame at the top and along the edges, sagging in the middle, but touching usually only at point contact. Alloy 61 series sags a bit in the middle, but does not touch the stainless steel frames. On frame 4–10 there are three AZ-1 panels all identified as C-13-14, 15-16, and

(*continued*)

TABLE 3—*Continued.*

17-18. These panels sag and touch the stainless steel frames at the top corners, except for panel 15-16, which sags without touching.

A few miscellaneous observations follow. Panel 41-C-37-38 was exposed upside down so the number side, contrary to the usual condition, was down rather than up. The three panels 37-42 for Series 43 are badly corroded at the edges where insulators contacted the panels.

Only two of the three panels of the reexposed 7-year Series 45 alloys were found. All of these show very deep etch-pitting on the surface. The skyward surface is a mud color, over a dark slate gray. Backside is gray.

Panel 39-40 in Series 46 is missing. The two remaining panels look as if they may have come loose and been replaced on the rack.

---

[a] Inspection made on 6 June 1971.

R. S. Herman[1] *and A. P. Castillo*[1]

Short-Term Atmospheric Corrosion of Various Copper-Base Alloys—Two- and Four-Year Results

REFERENCE: Herman, R. S. and Castillo, A. P., "**Short-Term Atmospheric Corrosion of Various Copper-Base Alloys—Two- and Four-Year Results,**" *Corrosion in Natural Environments, ASTM STP 558,* American Society for Testing and Materials, 1974, pp. 82–96.

ABSTRACT: Corrosion data pertaining to a variety of copper-base alloys after two- and four-year exposure to natural environments at New Haven, Connecticut, Brooklyn, New York, and Daytona Beach, Florida are presented. High zinc alloys, cartridge brass alloy B36 (260) and nickel silver alloy B122 (770) experienced substantial decreases in mechanical properties due to "plug type" dezincification and pitting. In addition, the rate of attack on high zinc containing alloys was environment specific. Alloy (619), a copper-aluminum-iron alloy, displayed substantial increases in mechanical properties with time. This is attributed to a long-term low-temperature order-disorder mechanism. The degree of patination was alloy, time, and environment specific. To avoid ambiguity, it is suggested that instantaneous corrosion rate rather than changes in absolute weight loss be used as the criterion for duration of atmospheric testing of copper-base alloys.

KEY WORDS: corrosion, atmospheric corrosion tests, copper-containing alloys, patination, patina coatings, alloy environment specificity

An important phase of alloy development is determination of definitive engineering corrosion information in a wide range of environmental conditions. In determining the corrosion resistance of new alloys, it is important to compare the performance of the newer alloy with that of existing alloys. Accordingly, Olin Corporation, Metals Research Laboratory, maintains several atmospheric test sites to determine the long-range corrosion performance of selected standard and new alloys in a variety of natural environments.

In atmospheric corrosion, moisture is generally the main controlling variable [*1*].[2] The effect of pollutants such as hydrogen sulfide and sulphur

---

[1] Senior research engineer and corrosion research engineer, respectively, Metals Research Laboratories, Olin Corp., New Haven, Conn. 06504.

[2] The italic numbers in brackets refer to the list of references appended to this paper.

dioxide is much more pronounced in moist than in dry air. In large industrial cities, considerable amounts of solid particulate matter are carried in the atmosphere and may be deposited on specimen surfaces. These deposits may accelerate corrosion and cause localized corrosion through the formation of concentration cells or the retention of moisture on the metal surface.

The time at which patination begins to appear on a copper alloy is variable and is environment specific. In outdoor exposure, copper quickly tarnishes, especially in the presence of sulfur compounds. The tarnish first formed is usually brown in color and gradually turns black. After a few years, the characteristic green patina starts to appear. The green color is usually attributed to basic copper sulfate, but copper chlorides and carbonates are often present [*2*].

Typical services to which long-term corrosion experience in natural environments is directly applicable in evaluating suitability of copper-base alloys are in the architectural, electrical, and industrial areas.

In 1964, three atmospheric test sites were put into operation. These are located at New Haven, Connecticut; Brooklyn, New York; and Daytona Beach, Florida. The New Haven site represents an industrial environment. The specimens are situated on the roof of a one-story building. The Brooklyn site represents an industrial-marine environment. The specimen racks are situated on the roof of a six-story building in Brooklyn approximately 1400 ft (420 m) east of the East River. The East River is an estuary of varying salinity. The Daytona Beach site represents a marine environment. Specimen racks are situated on the ground and 150 ft (46 m) from the mean high-tide water mark.

Selected copper-base alloys were placed in test. Alloy (619) was included to provide new alloy corrosion data and to correlate its corrosion performance with respect to an order-disorder mechanism associated with this material [*3*]. The original design of the experiment called for a total exposure of eight years, with interim specimen withdrawals at two and four years. The data presented are not the final long-term corrosion rate, but in many applications the metal will not be in service long enough to achieve a final corrosion rate. Designers and engineers require short-term data. This report covers the results of two- and four-year exposure at the New Haven, Brooklyn, and Daytona Beach sites. Weight loss, change in mechanical properties and degree of patination were initially considered as ways of comparing corrosion resistance. Table 1 provides a list of alloys evaluated in the program, their nominal compositions, and commercial designations with equivalent ASTM and CDA (Copper Development Association) designations. When reference is made to an alloy using the ASTM designation or where an ASTM designation does not exist, the equivalent CDA alloy designation will appear in parenthesis.

TABLE 1—*Alloys evaluated, their nominal compositions and commercial designations.*

ASTM Designation	Commercial Designation	Nominal Composition	CDA Designation
B152	electrolytic tough pitch	99.9Cu	110
B465	HSM[a]	2.1 to 2.6Fe, 0.03P, 0.05 to 0.20Zn	194
B36	red brass	15Zn	230
B36	cartridge brass	30Zn	260
...	Lubronze	12Zn, 1Sn	422
B103	phosphor bronze, 5%	5Sn, 0.2P	510
...	Alronze[a]	9.5Al, 4Fe	619
...	...	1.1Fe, 1.6Al	689
B122	nickel silver 55-18	27Zn, 18Ni	770

[a] Registered trademark of Olin Corporation.

Experimental Procedure

Material "as received" from the mill was cut into panels 4 in. (0.10 m) by 8 in. (0.20 m), with the long edge in the rolling direction. The "as received" material thickness ranged from 0.030 in. (0.76 mm) to 0.040 in. (1.00 mm). With the exception of one lot of copper alloy (619), which was annealed, all material was received in hard temper. Chemical analysis of each alloy was determined (Table 2). Initial longitudinal mechanical properties of the alloys to be evaluated were determined (Table 3). An identifying code was stamped on each specimen. The panels were degreased and cleaned in sulfuric acid as outlined in ASTM Recommended Practice for Preparing and Cleaning Corrosion Test Specimens (G 1-67). The test panels were measured to the nearest 0.01 cm and weighed to the nearest milligram. Control specimens of each alloy were retained in the laboratory to provide a periodic check of mechanical properties. These provide a base line from which to evaluate any loss in these properties as a result of

TABLE 2—*Actual chemical composition of copper-base alloys evaluated.*

ASTM (CDA) Alloy Designation	Chemical Composition, weight %						
	Cu	Fe	Sn	Al	P	Zn	Other
B152 (110)	99.9	...	...	...	...	...	...
B465 (194)	97.5	2.2	...	...	0.03	0.05–0.20	...
B36 (230)	85.2	...	...	...	...	remainder	...
B36 (260)	69.6	...	...	...	...	remainder	...
(422)	86.4	...	0.98	...	...	12.5	0.02Pb
B103 (510)	95.0	...	4.7	...	0.14	...	0.02Pb
(619)[a]	86.2	3.8	...	9.8	...	...	...
(619)	86.3	3.8	...	9.8	...	...	...
(689)	65.8	1.1	...	1.4	...	remainder	0.02Mn
B122 (770)	56.4	0.05	...	...	...	25.3	17.6Ni, 0.12Mn

[a] Annealed.

TABLE 3—*Initial longitudinal mechanical properties of alloys evaluated.*[a]

Copper Alloy ASTM (CDA) Code	Longitudinal Mechanical Properties		
	0.2% Offset Yield Strength, ksi (MN/m^2)	Ultimate Tensile Strength, ksi (MN/m^2)	Elongation, in 2 in. (0.08 m), %
B152 (110)	46.3 (319)	48.1 (322)	5.0
B465 (194)	63.3 (436)	67.6 (466)	5.8
B36 (230)	57.5 (396)	62.0 (427)	5.8
B36 (260)	67.6 (466)	75.2 (518)	7.9
(422)	66.8 (460)	71.5 (493)	5.3
B103 (510)	77.5 (534)	81.6 (563)	9.7
(619)[b]	52.2 (360)	97.1 (670)	33.2
(619)	104.4 (720)	137.2 (946)	6.2
(689)	90.8 (626)	103.9 (716)	2.7
B122 (770)	89.1 (614)	98.4 (678)	7.0

[a] Hard temper.
[b] Annealed.

corrosion. Quadruplicate panels of each alloy were placed in test for each time period at each site. Specimens were placed in aluminum frame exposure racks, in turn bolted to an aluminum test stand on site. The specimens are held in place by edge contact with four neoprene grommets which electrically insulate them from the mounting hardware, preventing galvanic effects and providing some measure of susceptibility to crevice attack. Figure 1 is a schematic of a panel as mounted. Figure 2 is a photo-

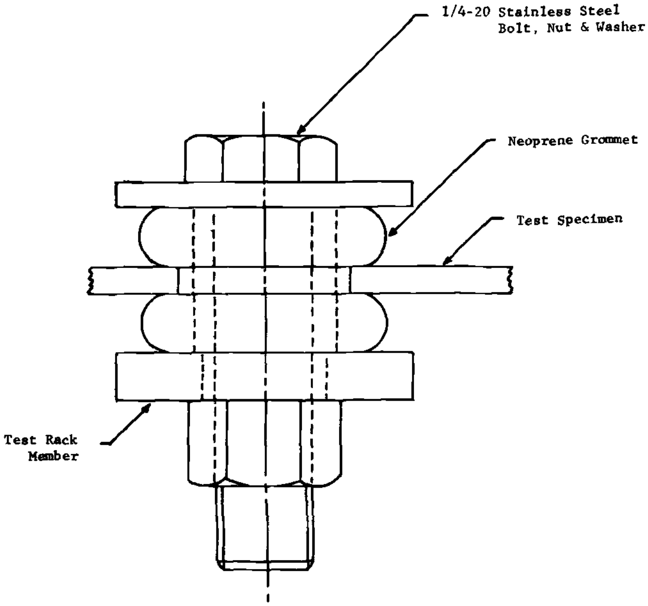

FIG. 1—*Specimen mounting method.*

FIG. 2—*Atmospheric corrosion racks, stands, and panels at the Brooklyn, N.Y. test site.*

graph of the Brooklyn, New York site showing specimens, racks, and stands. At Brooklyn and New Haven, panels face in a south-easterly direction, and at Daytona Beach in an easterly direction. Specimens are mounted at an angle of 45 deg from horizontal. Upon removal from test, panels were evaluated "as received" for any unusual effects or evidence of localized corrosion. The corrosion products were removed from two of the four samples of each alloy by immersion for 10 s in 10 volume percent sulfuric acid and scrubbing with a nylon bristle brush. Weight losses were determined from these cleaned panels. Following weight loss determinations inspection for localized corrosion was conducted on the cleaned panels. Specimens were then machined into tensile specimens and longitudinal mechanical properties determined. Longitudinal mechanical properties of control panels of the same alloy, which had been retained in the laboratory, were determined as well. The remaining pair of exposed and uncleaned specimens was cut into small coupons and encapsulated in plastic to permanently preserve the corrosion products and allow direct inspection of the appearance of the as-corroded specimens.

Results

Table 4 lists weight loss versus time data and indicates the degree of alloy-environment specificity. Nickel-silver alloy B122 (770) experienced the highest weight loss of all alloys tested both at Brooklyn and New Haven. Comparative performance was reversed at Daytona Beach, where this

TABLE 4—*Atmospheric corrosion program: weight loss versus time (mg/cm²), two- and four-year results at three locations.*

ASTM Designation	CDA Alloy	New Haven		Brooklyn		Daytona Beach	
		2 Years	4 Years	2 Years	4 Years	2 Years	4 Years
B152	(110)	1.84	3.80	3.46	6.83	4.58	8.36
		2.03	3.71	3.44	6.49	4.53	7.65
B465	(194)	1.72	3.83	3.03	6.27	3.46	5.47
		1.65	3.73	3.20	6.42	3.42	5.38
B36	(230)	1.55	3.75	3.37	(d)	1.45	2.32
		1.60	3.73	3.15	...	1.45	2.28
B36	(260)	2.18	4.53	4.36	7.39	.68	1.14
		2.30	4.58	4.34	7.90	.65	1.16
...	(422)	1.77	4.19	3.63	7.29	2.30	3.51
		1.77	4.21	3.49	7.70	2.40	3.56
B103	(510)	2.01	4.55	3.51	7.48	7.02	9.88
		2.08	4.72	3.54	7.26	6.68	9.49
...	(619)[b]	1.41[a]	2.22	3.66[a]	4.75	(d)	(d)
		1.47[a]	2.24	3.46[a]	4.62	...	...
...	(619)[c]	1.84[a]	2.41	4.07[a]	4.95	1.04	1.81
		1.79[a]	2.36	4.02[a]	5.09	1.09	1.76
...	(689)	1.74	3.71	4.24	7.73	0.85	1.33
		1.72	3.75	4.38	7.26	0.82	1.40
B122	(770)	2.42	4.60	4.53	8.62	0.65	1.36
		2.30	4.89	4.55	...	0.56	...

[a] Three-year data.
[b] Annealed temper.
[c] Hard temper.
[d] No weight loss data available.

alloy ranks amongst the lowest in weight loss. Another example of environmental specificity is cartridge-brass alloy B36 (260). At both New Haven and Brooklyn weight loss was high, whereas at Daytona Beach its ranking was among the lowest. However, electrolytic copper alloy B152 (110) was subject to high weight loss at Daytona Beach and Brooklyn and lower weight loss at New Haven.

The weight losses of several other alloys as a function of environment are worthy of attention. After four years, tin-brass alloy (422) and phosphor-bronze B103 (510) were found to behave similarly at Brooklyn, while at New Haven alloy B103 (510) displays an 18 percent greater weight loss than alloy (422). At Daytona, the difference between the two is considerably more marked, with alloy B103 (510) having a weight loss 170 percent greater than alloy (422). In all cases, copper-iron alloy B465 (194) has a lower weight loss than alloy B152 (110). At New Haven and Brooklyn the difference was 6 percent; at Daytona it was 34 percent.

Within the limits of experimental error, cartridge-brass alloy B36 (260) and nickel-silver alloy B122 (770) show significant loss in mechanical properties after four year's exposure (Table 5). As shown in Table 5, alloy B36 (260) suffered a 31.6 percent decrease in percent elongation at Brooklyn and 20 and 29 percent reductions respectively at New Haven and

DAYTONA BEACH, FLORIDA

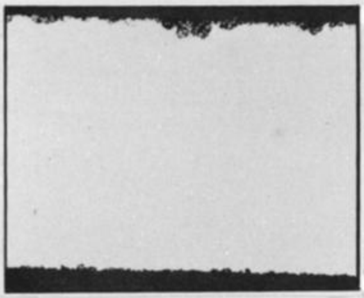

NEW HAVEN, CONNECTICUT

BROOKLYN, NEW YORK

FIG. 3—*As-polished metallographic sections of ASTM alloy B36 (260) after four years of atmospheric exposure at three locations, revealing plug-type dezincification* (×40).

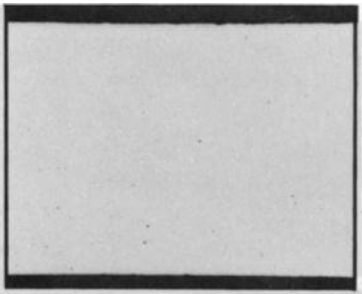

DAYTONA BEACH, FLORIDA

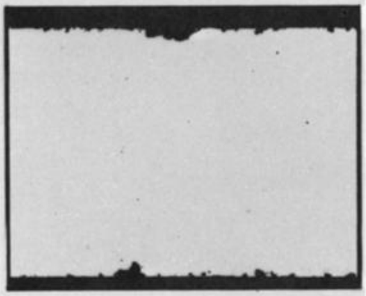

NEW HAVEN, CONNECTICUT

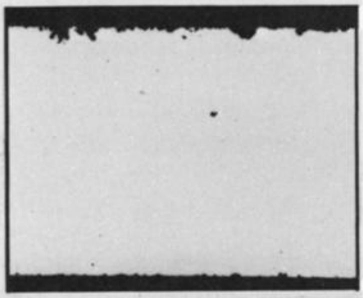

BROOKLYN, NEW YORK

FIG. 4—*As-polished metallographic sections of ASTM alloy B122 (770) after four years of exposure at three locations, revealing pitting* (×40).

Daytona Beach. The 0.2 percent offset yield and ultimate tensile strengths were reduced by 6.6 and 5.7 percent respectively for alloy B36 (260) at Brooklyn. At New Haven and Daytona Beach the yield and ultimate strengths decreased less than five percent.

Nickel-silver alloy B122 (770) in New Haven shows the largest percent decrease in percent elongation, 70 percent. Elongation decreased by 64 percent at Brooklyn, but only one percent at Daytona Beach. The 0.2 percent yield and ultimate strengths were reduced by 5.7 and 9.4 percent at New Haven and by less than five percent at Brooklyn and Daytona Beach. Percent elongation is quite sensitive to localized corrosion. Yield and ultimate tensile strength are less sensitive.

Specimens of alloys B36 (260) and B122 (770) were examined metallographically. Dezincification was found in cartridge-brass alloy B36 (260) and in nickel-silver B122 (770) at all sites. Dezincification was accompanied by pitting two to three mils deep in the case of B122 (770) at New Haven and Brooklyn (Figs. 3–6). No evidence of localized attack was found on alloy B122 (770) at Daytona Beach. Examination of all test panels after cleaning disclosed no evidence of localized crevice effects at the holding grommets after four years of exposure at any location.

Electrolytic copper alloy B152 (110) showed no signs of patina at Daytona Beach, yet in Brooklyn a slight patina was evident after only two years,

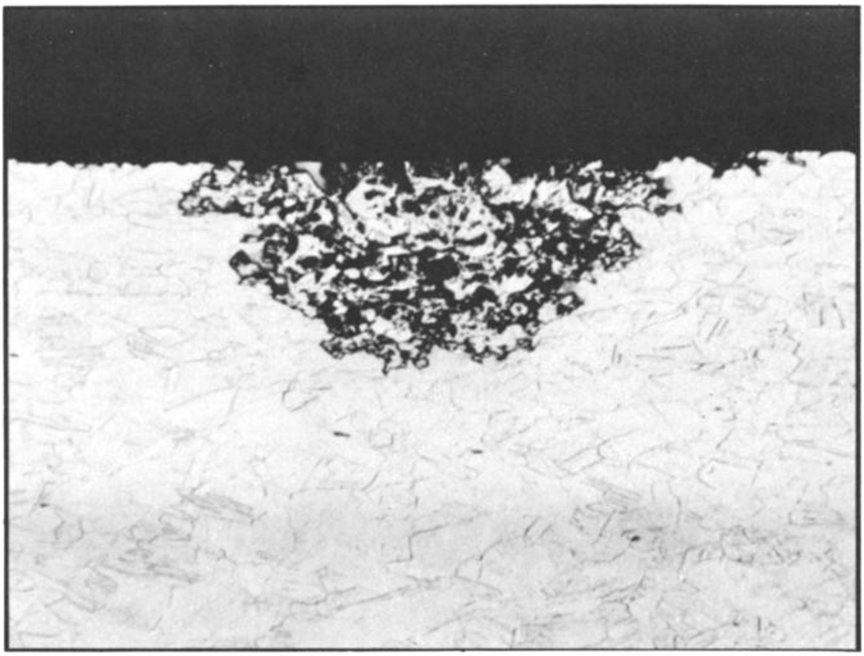

FIG. 5—*Plug-type dezincification of ASTM alloy B36 (260)—four years of exposure at Brooklyn, N. Y.* (×600).

TABLE 5—*Mechanical properties of alloys in atmospheric corrosion program after two and four years of exposure, including initial and control data.*

Copper Alloy ASTM (CDA) Code	Location[a]	Longitudinal Mechanical Properties								
		0.2% Offset Yield Strength, ksi (MN/m^2)			Ultimate Tensile Strength, ksi (MN/m^2)			Elongation in 2 in. (0.08 m), %		
		Initial	2 Years	4 Years	Initial	2 Years	4 Years	Initial	2 Years	4 Years
B152 (110)	MRL	46.3 (319)	...	...	48.1 (322)	...	...	5.0	...	...
	MRL (C)	...	46.7 (322)	...	...	48.5 (334)	...	...	4.5	...
	NH	...	46.2 (318)	45.1 (311)	...	48.0 (331)	46.9 (323)	...	5.1	5.0
	BR	...	46.1 (318)	45.5 (314)	...	47.9 (330)	47.4 (327)	...	4.9	5.0
	DB	...	46.0 (317)	45.1 (311)	...	47.7 (329)	46.9 (323)	...	5.0	5.4
B465 (194)	MRL	63.3 (436)	...	...	67.6 (466)	...	...	5.8	...	...
	MRL (C)	...	64.4 (444)	...	...	67.6 (466)	...	...	5.0	...
	NH	...	63.8 (440)	61.5 (424)	...	66.9 (461)	64.7 (446)	...	5.3	4.2
	BR	...	63.0 (434)	61.5 (424)	...	66.6 (459)	64.7 (446)	...	5.3	4.2
	DB	...	63.2 (436)	61.6 (425)	...	66.6 (459)	64.5 (445)	...	4.9	4.0
B36 (230)	MRL	57.5 (396)	...	...	62.0 (427)	...	...	5.8	...	...
	MRL (C)	...	59.1 (407)	...	...	63.3 (437)	...	...	7.0	...
	NH	...	59.1 (407)	58.2 (401)	...	63.1 (435)	62.3 (430)	...	6.0	5.6
	BR	...	59.0 (406)	58.5 (403)	...	63.1 (435)	62.3 (430)	...	5.9	5.8
	DB	...	59.3 (409)	58.7 (405)	...	63.2 (436)	62.5 (431)	...	6.1	5.6
B36 (260)	MRL	67.6 (466)	...	...	75.2 (518)	...	...	7.9	...	...
	MRL (C)	...	71.2 (491)	...	...	78.8 (543)	...	...	8.1	...
	NH	...	69.4 (478)	65.5 (452)	...	76.5 (527)	72.9 (503)	...	7.1	6.3
	BR	...	68.4 (472)	63.1 (435)	...	76.5 (527)	70.9 (489)	...	5.8	5.4
	DB	...	67.9 (468)	68.0 (469)	...	75.7 (522)	75.2 (518)	...	7.2	5.6
(422)	MRL	66.8 (460)	...	...	71.5 (493)	...	...	5.3	...	...
	MRL	...	71.9 (496)	...	...	75.3 (519)	...	...	5.0	...
	NH	...	72.4 (499)	68.7 (474)	...	76.1 (525)	72.2 (498)	...	5.0	4.5
	BR	...	72.1 (497)	68.3 (471)	...	75.5 (520)	72.2 (498)	...	5.2	4.8
	DB	...	71.6 (494)	68.3 (471)	...	75.5 (520)	72.4 (499)	...	4.9	4.9

B103 (510)	MRL	77.5 (534)	...	...	81.6 (563)	...	...	9.7	...	...
	MRL (C)	...	83.2 (574)	...	...	85.3 (588)	...	...	9.9	...
	NH	...	83.3 (574)	80.5 (555)	...	85.2 (587)	82.6 (570)	...	9.5	9.2
	BR	...	81.4 (561)	80.1 (552)	...	83.2 (574)	82.0 (565)	...	10.1	10.1
	DB	...	83.5 (576)	80.8 (557)	...	85.2 (587)	82.7 (570)	...	9.6	9.5
(619)[b]	MRL	52.2 (360)	...	...	97.1 (670)	...	...	33.2	...	...
	MRL (C)	...	54.2 (374)	...	...	99.6 (687)	...	...	31.2	...
	NH	...	52.3 (361)	54.4 (375)	...	98.0 (677)	98.4 (678)	...	31.4	31.0
	BR	...	55.1 (380)	53.4 (368)	...	98.3 (678)	97.1 (670)	...	30.8	31.5
	DB[c]	...	...	...	...	...	...	...	...	...
(619)	MRL	104.4 (720)	...	...	137.2 (946)	...	...	6.2	...	...
	MRL (C)	...	112.2 (774)	...	...	143.4 (989)	...	...	2.7	...
	NH	...	111.4 (786)	108.5 (748)	...	142.8 (985)	141.0 (972)	...	3.0	2.8
	BR	...	113.3 (781)	110.3 (761)	...	141.2 (974)	140.6 (969)	...	2.3	2.8
	DB	...	112.0 (772)	110.8 (764)	...	142.3 (981)	140.6 (969)	...	2.8	2.3
(689)	MRL	90.8 (626)	...	...	103.9 (716)	...	...	2.7	...	...
	MRL (C)	...	97.9 (675)	...	...	108.7 (749)	...	...	1.9	...
	NH	...	96.8 (667)	92.1 (635)	...	107.6 (742)	103.2 (712)	...	1.8	1.8
	BR	...	95.1 (656)	91.9 (634)	...	106.2 (732)	102.3 (705)	...	1.9	1.9
	DB	...	96.4 (665)	93.8 (647)	...	107.1 (738)	104.1 (718)	...	1.9	3.6
B122 (770)	MRL	89.1 (614)	...	...	98.4 (678)	...	...	7.0	...	...
	MRL (C)	...	91.3 (630)	...	...	99.1 (683)	...	...	7.0	...
	NH	...	92.8 (640)	84.0 (579)	...	100.1 (690)	89.2 (615)	...	5.5	2.1
	BR	...	89.2 (615)	86.8 (598)	...	96.1 (663)	93.1 (642)	...	4.4	2.5
	DB	...	93.4 (644)	92.7 (639)	...	101.2 (698)	100.3 (692)	...	7.0	6.9

(C) Retained control specimen.

[a] NH = New Haven, Conn.; BR = Brooklyn, New York; DB = Daytona Beach, Fla.; MRL = Metals Research Laboratories.

[b] Annealed.

[c] Not tested.

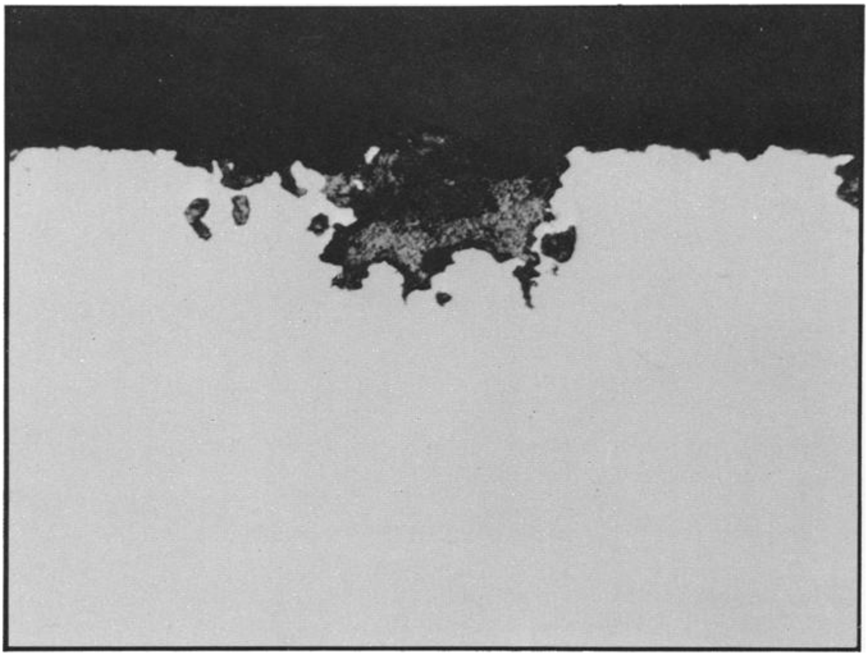

FIG. 6—*Dezincification of ASTM alloy B122 (770)—four years of exposure at Brooklyn, N. Y. (×600).*

becoming more marked after four years. In New Haven, alloy B152 (110) showed the first evidence of patina only after four years' exposure. Red-brass alloy B36 (230), tin-brass alloy (422), and phosphor-bronze alloy B103 (510) showed signs of patina formation after four years at Brooklyn and to a lesser extent at Daytona. No signs of patina were evident on these alloys in New Haven. Finally, nickel-silver B122 (770) showed patina formation increasing with time at Daytona Beach only (Table 6).

Discussion

Based on weight loss only, Brooklyn and New Haven appear to rank the majority of alloys investigated the same (Table 4). Relative rankings are considerably different at Daytona Beach. Phosphor-bronze alloy B103 (510) had the highest weight loss in four years at Daytona Beach and nickel-silver alloy B122 (770) the lowest. In all cases at Daytona Beach, the weight losses showed a decreasing trend with time. Brooklyn appears to be behaving more as an industrial site than as a marine site. The chloride present in the atmosphere may not be sufficient to affect the corrosion performance of the alloy mix tested after four years in test.

Alloys B36 (260) and B122 (770) underwent significant losses in mechanical properties, and since they are high-zinc-content alloys a metallo-

TABLE 6—*Degree of patination of copper-base alloys as a function of time at New Haven, Brooklyn, and Daytona Beach. Color of oxides on surface exposed to direct sunlight and elements.*

ASTM (CDA) Alloy Designation	New Haven		Brooklyn		Daytona Beach	
	2 Years	4 Years	2 Years	4 Years	2 Years	4 Years
B152 (110)	red-brown	green-brown[b]	brown	green-brown[c]	red-brown	red-brown-green[a]
B465 (194)	...	brown	brown	brown	brown	red-brown-green[a]
B36 (230)	brown	brown-yellow spots	brown-green[a]	green-brown spots[c]	brown-green[a]	brown-green spots[a]
B36 (260)	dark brown	dark brown	dark brown	dark brown	gold	gold-brown
(422)	red-brown	brown-yellow spots	brown-green[a]	green-brown spots[c]	brown	brown-green[a]
B103 (510)	red-brown	brown-green spots[a]	brown	green-brown spots[c]	red-brown	red-brown-green[b]
(619)	red-brown[d]	light brown	dark brown[d]	light brown	red-brown-green[a]	...
(689)	brown	light brown	dark brown	yellow-brown spots	light brown	green-light brown[b]
(770)	dark brown	brown	dark brown	brown-yellow spots	green-light brown[b]	green[c]

[a] Spots of patina formation.

[b] Small degree of uniform patination.

[c] Moderate degree of uniform pantination.

[d] Three years.

graphic examination was made to verify the possibility of dezincification as the cause of loss in properties. As shown in Figs. 3 through 6, dezincification was evident. Its extent was environment specific. The mode of dezincification of alloy B36 (260) is of the classical plug type (Fig. 5). The dezincification "plugs" are of an intermittent nature, approximately two to three mils deep at Daytona Beach (Fig. 3), whereas at Brooklyn and New Haven it appears that the plug type of attack is practically continuous over the entire surface (that is, bordering on "layer type") (Fig. 3). Figure 3 also shows, particularly at New Haven and to a lesser extent at Brooklyn, that there is a marked difference in degree of attack between the two exposed faces of the panel. At Daytona Beach, however, this effect does not seem to be evident in the case of alloy B36 (260). Nickel-silver alloy B122 (770) also displays dezincification, as shown in Fig. 6. The "plugs" had silver coloration instead of the classical copper color. No doubt this is due to the nickel in the alloy. Some pitting was also observed in this alloy at Brooklyn and New Haven (Fig. 4). It is striking that this material is relatively free of attack at Daytona Beach contrasted with the marked susceptibility to pitting at Brooklyn and New Haven (Fig. 4). No major decreases in mechanical properties were observed in the remainder of the alloy mix.

The alloy containing the largest aluminum content (619) appears to perform best in the industrial atmospheres. Those alloys containing zinc at high levels, B36 (260) and B122 (770) perform poorly. Intermediate zinc levels give intermediate performance. Tin additions have little effect. Alloy B465 (194) does not perform much differently from alloy B152 (110) in industrial atmospheres. The addition of small amounts of iron to copper appears to have little effect on corrosion performance.

Aluminum as an alloying element also seems to be beneficial in the chloride-containing nonpolluted atmosphere (Daytona Beach). On the basis of weight loss only, zinc also appears to be beneficial either as a singular alloying addition B36 (230 and 260) or coupled with aluminum (689) or nickel B122 (770) in this atmosphere. However, as previously discussed, susceptibility to dezincification as in the case of B36 (260) must also be considered. The addition of nickel to copper and zinc in nickel-silver alloy B122 (770) does improve corrosion resistance in a marine environment. Tin as an addition in phosphor-bronze alloy B103 (510) and tin-brass alloy (422) generally appears to be detrimental. The iron-containing alloy B465 (194) is performing better than alloy B512 (110) in this environment.

In general, four years' exposure was insufficient to develop the complete characteristic green patina on any alloy. Many alloys still possessed the brown or black coloration typical of copper alloys after only a few years of exposure. Table 6 provides a comparison of the various alloys and color of oxide formed as a function of time at all locations.

Based on four-year data, longer exposure times will be given to the atmospheric exposure panels in order to allow steady-state conditions to be reached. A current long-term ASTM test program for copper-base alloys is, in fact, designed for 20-year exposure, with interim withdrawals at two and seven years already completed. Analysis of the seven-year data by Thompson [*4*] leads to the conclusion that the large variation in corrosion rate with time dictates greatly extending test duration. Thompson also found that all copper-base alloys tested in an East Coast marine environment (Kure Beach, North Carolina) displayed decreasing corrosion rates with time after seven years, and 13 out of 18 alloys showed similar decreases at an industrial site (Newark, New Jersey). In his summary, Thompson states, "A seven year exposure is too short to give any real indication of what the ultimate corrosion rate will be when the terminal film has formed. Other tests have shown the corrosion rate is decreasing at the end of 20 years."

Uhlig [*5*], however, concludes on examination of earlier 20-year exposure data on copper by ASTM that, "Within experimental error of such determination, the rate for a 20 year period is about the same as for a ten year period." The length of time an experiment of this type should run would optimally be determined by analyzing the first derivatives of weight loss versus time curves, and terminating the test when decreasing corrosion rates reach or very nearly approximate steady state. Further, test duration would be tempered by economic constraints as well as by the desire to gain early utility of test data.

The discrepancies noted, on some cases in which mechanical properties of control specimens at two years show greater strength than properties determined initially, are interesting. Aluminum-bronze alloy (619) (only in the hard temper), aluminum-brass alloy (689), and nickel-silver alloy B122 (770) show substantial increases. The answer lies in consideration of the (619) results, which show increases in mechanical properties only in the cold-worked material. Some recent work [*3*] has shown that many low stacking fault energy materials exhibit order-disorder behavior. Ordering of these materials produces large increases in strength if cold work is present. In ordering alloys, disorder will occur on cold-rolling. The kinetics of reordering at room temperature are known to be extremely slow. However, after two years, significant reordering had occurred at ambient temperature, resulting in increased mechanical properties. Alloys containing aluminum would be expected to give the highest increases (which indeed they do).

Finally, atmospheric environments, particularly the industrial types, are continually changing. Ecological controls in competition with the rate of pollutant increase may be a significant factor in atmospheric corrosion of copper-base alloys. Whether or not there will be a net change in atmospheric pollutants in the future is, of course, a moot point; nevertheless, the importance of an ongoing program in atmospheric corrosion studies of commercial alloys is apparent.

Conclusions

At this time, the industrial and industrial-marine sites appear to rank the alloys tested in the same order, although corrosion rates are not the same. The marine environment ranks the alloy mix differently. A certain degree of alloy environment specificity with respect to weight loss versus time data has been observed with alloys B36 (260), B122 (770), and (689). Significant changes in the percent elongation of alloys B36 (260) and B122 (770) led to further metallographic investigation that revealed plug-type dezincification of B36 (260) at all locations and pitting coupled with plug-type dezincification of B122 (770) at the industrial and industrial-marine sites, respectively. Lack of localized corrosion of this alloy in the marine environment suggests strongly that nickel, as an alloying element, is beneficial with respect to corrosion resistance of a copper-zinc system in marine atmospheres.

The rate of patination on the formation of a protective corrosion product film is a function of alloy, environment, and time. Finally, the duration of this atmospheric study has been increased to 20 years with interim withdrawal dates of two, four, and twelve years.

Acknowledgments

The authors wish to thank the Brass Group of Olin Corporation for permission to publish the results. The experimental work of Charles Halliwell and verbal discussions with J. M. Popplewell are also gratefully acknowledged.

References

[*1*] Vernon, W. H. J., *Transactions of the Faraday Society*, 1927, Vol. 23, pp. 113, 162; 1931, Vol. 27, pp. 255, 264.

[*2*] LaQue, F. L. and Copson, H. R., *Corrosion Resistance of Metals and Alloys*, Reinhold, New York, 1963.

[*3*] Popplewell, J. M. and Crane, J., "Order-Strengthening in Cu-Al Alloys," *Metallurgical Transactions*, Vol. 2, Dec. 1971.

[*4*] Thompson, D. H. in *Metal Corrosion in the Atmosphere*, *ASTM STP 435*, American Society for Testing and Materials, 1968, pp. 129–140.

[*5*] Uhlig, H. H., *Corrosion and Corrosion Control*, Wiley, New York, 1963.

L. C. Covington[1]

Technical Note: An Evaluation of Titanium Panels After Seven Years' Exposure in a Marine Atmosphere

---

REFERENCE: Covington, L. C., "**Technical Note: An Evaluation of Titanium Panels After Seven Years' Exposure in a Marine Atmosphere,**" *Corrosion in Natural Environments, ASTM STP 558,* American Society for Testing and Materials, 1974, pp. 97–98.

ABSTRACT: An evaluation was made of test panels of four titanium alloys that were exposed to a marine atmosphere for seven years at Point Reyes, California as part of the ASTM B-3V1 1957 test program. No evidence of corrosion or significant change in physical properties was found. It was concluded that titanium is virtually immune to corrosion under most atmospheric exposure conditions.

KEY WORDS: titanium, corrosion, marine atmospheres

Since 1951 when titanium first became available as a commercial material it has been observed that it appears to be immune to corrosion in most atmospheric environments.

In 1957, ASTM began an atmospheric exposure testing program involving 77 alloys of 9 basis metals. One of these basis metals was titanium. Four alloys, Ti-75A, Ti-140A, Ti-5Al-2.5Sn, and Ti-4Al-3Mo-1V were supplied by the Titanium Metals Corporation of America (TIMET) for this program. Exposures were made at four test sites: Site A, Kure Beach, N. C. (East Coast marine); Site B, New York area (Newark, New Jersey) (industrial); site C, Point Reyes, California (West Coast marine); and Site D, State College (University Park), Pennsylvania (rural).

Test periods were for 2, 7, and 20 years. Panels 4 by 8-in. were exposed at the four locations the latter part of 1958 and early 1959. Specimens for the two-year exposure were removed at the end of this period and examined for evidence of corrosion and changes in physical properties. The titanium alloys showed no evidence of corrosion or any significant change in physical properties.

---

[1] Senior research engineer, Titanium Metals Corporation of America, Henderson, Nev. 89015.

The seven-year exposure panels were removed in 1965 from Sites A, B, and D and examined. Again the titanium specimens showed no evidence of corrosion or change in physical properties. These results were reported at the ASTM meeting in 1966.

Site C was vandalized during the summer of 1962 and approximately half the specimens were lost. Additional 4 by 8-in. panels were exposed at the Point Reyes, California marine site as part of the ASTM B-3VI 1957 test program for 7- and 20-year test periods on 12 June 1964.

The panels were removed 6 June 1971 after a total exposure of 2550 days. No significant difference was found in any of the dimensions or weight of any of the panels after exposure. Examination with a low-power microscope failed to reveal any evidence of pitting or localized attack.

Tension tests on specimens cut from the exposed panels indicated some room temperature relaxation or recovery had occurred during the years since the control specimens were tested. In general there had been a slight decline in ultimate tensile strength and a gain in elongation.

These results confirm the results obtained from the other test sites and indicate that titanium is virtually immune to corrosion under most atmospheric exposure conditions.

Acknowledgment

We wish to point out that the initial testing and preparation of the specimens was performed by M. L. Greenlee of TIMET. The exposures were carried out by ASTM Committee G-1. The final tension and elongation tests were performed by W. M. Parris of TIMET.

D. O. Sprowls,[1] *T. J. Summerson,*[2] *and F. E. Loftin*[3]

Exfoliation Corrosion Testing of 7075 and 7178 Aluminum Alloys—Interim Report on Atmospheric Exposure Tests*

REFERENCE: Sprowls, D. O., Summerson, T. J., and Loftin, F. E., "**Exfoliation Corrosion Testing of 7075 and 7178 Aluminum Alloys—Interim Report on Atmospheric Exposure Tests,**" *Corrosion in Natural Environments, ASTM STP 558,* American Society for Testing and Materials, 1974, pp. 99–113.

ABSTRACT: Atmospheric exposures of 18 to 39 months have been completed at seacoast and inland industrial locations to determine the resistance to exfoliation corrosion of specially heat-treated test panels of high-strength aluminum alloys. Two seacoast locations, one at Point Judith, Rhode Island, and another at Daytona Beach, Florida, were selected, together with an industrial location near Chicago, Illinois, to represent the relatively severe atmospheric conditions to which aluminum alloy aircraft structures are subjected in service. The purpose of these tests was to demonstrate the relationship of the performances in the accelerated exfoliation corrosion tests previously evaluated by this task group with those in relatively aggressive natural environments.

The exfoliation performance is being evaluated on test panels heat treated to produce three different metallurgical structures that would be expected to provide a high, low, and medium resistance to exfoliation of both a 7075 alloy extrusion and a 7178 alloy rolled plate. Results obtained thus far are gratifying in that the atmospheric exposures are ranking the test materials in the same relative order as the new ASTM Standard Method of Test for Exfoliation Corrosion Susceptibility in 7XXX Series Copper Containing Aluminum Alloys (G 34-72, EXCO test). That is, the materials that showed either a high or a low resistance to exfoliation in the EXCO test also showed the same performance in the seacoast atmosphere, and that which showed an intermediate resistance in the EXCO test showed more spotty and a slower rate of exfoliation in the atmospheric exposures.

Exfoliation of the most susceptible items initiated more rapidly (within five months) at the seacoast, but the exfoliation tended to be more uniform at the industrial site. Other factors such as the climatic conditions at the seacoast, location, and exposure position of the test panels are considered.

---

* Report of an ASTM G01.05.02 interlaboratory testing program in cooperation with the Aluminum Association.

[1] Head, Stress Corrosion Section of Chemical Metallurgy Division, Alcoa Laboratories, Alcoa Center, Pa. 15069.

[2] Head, Corrosion Section, Kaiser Aluminum & Chemical Corporation Center for Technology, Pleasanton, Calif. 94566.

[3] Research Engineer, Metallurgical Research Division, Reynolds Metals Company, Richmond, Va. 23218.

KEY WORDS: corrosion, exfoliation corrosion, atmospheric corrosion, accelerated tests, aluminum-zinc-magnesium-copper alloys, exfoliation-resistant tempers

The development of heat treatments to impart high resistance to exfoliation corrosion to 7075 and 7178 aluminum alloy products has led to the need for a laboratory test method to differentiate between susceptible and resistant materials. Such tests are indispensable to both research and quality-control engineers.

A previous report of this task group[4] summarized the results of an interlaboratory testing program to compare several accelerated exfoliation corrosion test methods. It was concluded that the EXCO immersion test was the best laboratory test method for the copper-bearing 7XXX series aluminum alloys, and a standard procedure was prepared by the task group, approved by ASTM Committee G 01 and the Aluminum Association and assigned ASTM Designation G 34-72. (EXCO test.)[5] This test has been recognized by U. S. Government agencies responsible for issuing specifications for 7075-T76 and 7178-T76 alloy products, and such specifications are gradually being revised to substitute the EXCO test for the salt-spray test previously stipulated.

During the interlaboratory evaluation of the accelerated corrosion tests, exposures also were started at three different outdoor atmospheric weathering stations. The purpose of these tests was to demonstrate the relationship of the performances in the accelerated exfoliation tests previously evaluated with the resistance to exfoliation in relatively aggressive natural environments. Two seacoast locations and an inland industrial location were selected to represent the relatively severe atmospheric conditions to which aluminum alloy aircraft structures may be subjected in service. This interim report presents the test results after 18 to 39 months in the outdoor environments.

Test Materials

Test panels were machined from commercial products heat treated to produce three different metallurgical conditions. Artificial aging treatments were selected to provide a high resistance to exfoliation and two degrees of susceptibility. The "high resistance" materials are representative of commercial T76 temper products but the "low resistance" items were not intended to represent any standard commercial tempers. Machined test panels from a 1½ by 6-in. extruded rectangle of 7075 alloy were supplied by Martin-Marietta Corporation and from ⅜-in.-thick plate of 7178 alloy by Alcoa Laboratories. The heat treatments used for these materials, the mechanical properties, and electrical conductivities are given in Table 1.

---

[4] Ketcham, S. J. and Jeffrey, P. W. in *Localized Corrosion—Cause of Metal Failure, ASTM STP 516*, American Society for Testing and Materials, 1972, p. 273.

[5] ASTM Standard Method of Test, G 34-72, 1973, p. 1.

TABLE 1—*Description of test materials.*

				Avg Tensile Properties			Avg Conductivity, % IACS	
Alloy	Product	Intended Resistance to Exfoliation	Precipitation Heat Treatment	Tensile Strength, ksi	Yield Strength, ksi	% El.	T/10	T/2
7075	½ x 6 in. extruded bar	low	24 h 250°F (121°C) + 8 h 310°F (154°C)	86.4	78.1	11	35.0	35.1
7075	½ x 6 in. extruded bar	medium (low, Lot 2)	24 h 250°F + 2 h 310°F	87.5	79.0	14	33.4	33.8
7075 (T76511)	½ x 6 in. extruded bar	high	24 h 250°F + 20 h 325°F (163°C)	79.6	70.6	14	39.2	39.4
7178	⅜-in. plate	low	3 h 250°F + 4 h 325°F	88.4	80.8	10	34.9	35.4
7178	⅜-in. plate	medium (low, Lot 2)	3 h 250°F + 8 h 325°F	85.6	76.8	11	36.4	37.1
7178 (T7651)	⅜-in plate	high	3 h 250°F + 18 h 325°F	79.8	69.7	10	38.8	39.4

Chemical Compositions

	Si	Fe	Cu	Mn	Mg	Cr	Zn	Ti
7075	0.15	0.22	1.47	0.03	2.41	0.20	5.65	0.03
7178	0.10	0.26	1.89	0.03	2.74	0.18	7.25	0.03

Solution Heat Treatment

Both products were manufactured, solution heat treated, quenched in cold water and stretched in commercial production mills by standard practices. The 7075 alloy extrusion also was aged 24 h at 250°F (121°C) in the mill and then divided and given the three special second-step aging treatments in laboratory equipment. Both steps of the precipitation treatment given the 7178 alloy plate were applied in laboratory equipment.

Experimental Procedure

Stepped panels were machined from the materials, as shown in Fig. 1, to obtain test surfaces at the generally specified T/10 plane (10 percent of the thickness machined from one side) and at the T/2 plane (midthickness) that frequently exhibits the lowest resistance to exfoliation. Panels were exposed in the as-machined condition, with only a solvent cleaning to remove machining lubricant, fingerprints, etc.

The procedure for the EXCO laboratory test is given in ASTM Method G 34-72, and a description follows of the three atmospheric exposure stations and the method of exposure of the test panels.

Seacoast Weathering Station at Point Judith, Rhode Island

The Alcoa seacoast weathering station is near Point Judith lighthouse on the tip of a small peninsula at the entrance to Narraganset Bay, about 30 miles south of Providence, Rhode Island. The area is sparsely populated with no appreciable industrial influences. The exposure racks, inclined at a 45-deg angle, are located about 300 ft from and facing the Atlantic Ocean to the south. Prevailing winds are from offshore, usually from the southwest, with an average velocity of about 17 mph. The beach is stony and the sea is often rough so that generally there is considerable salt mist in the

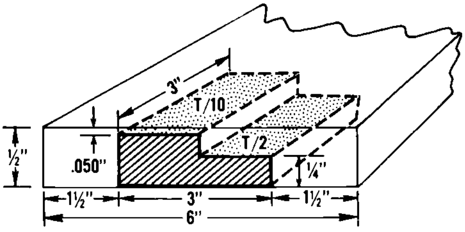

7075 ALLOY EXTRUDED ½"×6" BAR

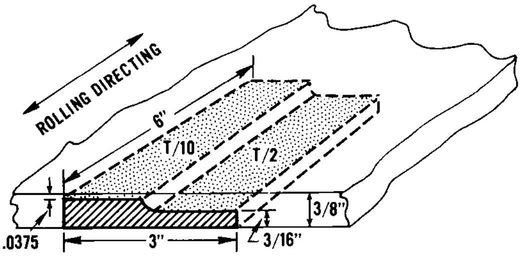

7178 ALLOY ROLLED 3/8" PLATE

FIG. 1—*Location of exfoliation test panels.*

air; fogs are frequent. Mean air temperatures are 29°F (−2°C) in the winter and 72°F (22°C) in the summer with an average relative humidity of 73 percent. The average rainfall is 41 in. per year, with rain falling about 125 days per year. These weather data were recorded at a U. S. Weather Service station on Block Island located ten miles due south of Point Judith.

The test panels of 7178 alloy were exposed in July 1970, with the machined surfaces inclined skyward at a 45-deg angle. (Duplicate sets of 7075 alloy panels were exposed in June 1971, with the machined surfaces facing skyward in one set and facing earthward in the other set.) Test panels were bolted to open frames so that both surfaces of the panels were freely exposed to the atmosphere. The test panels were mounted about 8 ft above the ground.

Seacoast Weathering Station at Daytona Beach, Florida

Test panels were exposed under contract from Kaiser Aluminum at the Daytona Beach marine atmospheric site, which is owned by Battelle Memorial Institute (this test site has been used in other ASTM calibration test programs under the auspices of ASTM G01.04). The area is sparsely populated with no industrial influences; fog is infrequent. Pipe frame racks, inclined at a 45-deg angle, are located about 500 ft from the sandy beach, facing the Atlantic Ocean to the east. Prevailing winds are from offshore, usually from the southeast with an average velocity of 8 mph. Mean air temperatures are 62°F (17°C) in the winter and 80°F (27°C) in the summer with an average relative humidity of 74 percent; average rainfall is about 50 in. per year. These weather data were recorded at a U. S. Weather Service station at the Daytona Beach Airport, located 10 miles inland.

The test panels were attached to large painted wooden boards with porcelain insulators and screws. The boards were attached to the pipe frame racks so that the machined surfaces faced earthward at a distance of about 3 ft above the ground. The test surfaces were thus shielded from direct exposure to the offshore breezes and to rainfall. Exposure dates were August 1970, for the 7178 alloy panels and February 1971, for those of 7075 alloy.

Inland Industrial Weathering Station at Brookfield, Illinois

A third set of test panels was exposed at the Reynolds Metals Company industrial atmospheric site at their McCook Plant in Brookfield, Illinois, near Chicago. The test site is located 500 ft east of the McCook Plant, and within a one-mile radius of other industrial operations including chemical and petroleum processing plants and a limestone quarry. Also, residential developments surround the plant site and there is considerable automobile traffic in the area. While fogs are infrequent, visibility is often restricted by air pollution, a condition that is worst during the heating season (mid-September to June) but which continues throughout the year. Prevailing winds are from the west and southwest with an average velocity of about 10 mph. Exposure racks face south and are inclined 30 deg to the horizontal. Mean air temperatures are 32°F (0°C) in the winter and 72°F (22°C) in the summer with an average relative humidity of 66 percent. While the relative humidity in the a.m. is relatively constant throughout the year at 70 to 80 percent, in the p.m. it decreases from 60 to 70 percent in winter to 50 to 60 percent in summer months. The average rainfall is 33 in. per year, with rain falling in about 120 days per year. These weather data were recorded at a U. S. Weather Service station located at Chicago's Midway Airport, four miles east of the test site.

The test specimens were attached to panels of polyvinyl chloride (PVC) sheet that were in turn mounted on the rack so that the machined test surfaces faced earthward, about 4 ft above the ground. Test panels of both alloys were initially exposed in October 1970.

Results and Discussion

The results of the exfoliation tests were evaluated by periodic visual examination and photographs of the test panels. The examinations were generally performed on-site, but in some instances test panels were returned to the laboratories for photographing.

TABLE 2—*Comparison of exfoliation ratings in EXCO test with exposure times until exfoliation observed in atmospheric exposures.*

Test Material[a]	EXCO Rating[b]	Time Until First Exfoliation, months		
		Brookfield	Point Judith	Daytona
7075, low resistance 1, T/10	E-D	5 to 13	0 to 5	3 to 6
7178, low resistance 1, T/2	E-D	5 to 13	0 to 11[c]	3 to 15
7075, low resistance 2, T/10	E-D	5 to 13	0 to 5	12 to 15
7075, low resistance 1, T/2	E-D	5 to 13	0 to 5	OK22
7075, low resistance 2, T/2	E-C/D	5 to 13	0 to 5	OK22
7178, low resistance 2, T/2	E-C/D	5 to 13	11 to 20[c]	15 to 22
7178, low resistance 1, T/10	E-C/D	5 to 13	OK30[c]	OK38
7178, low resistance 2, T/10	E-B/D	OK39	OK30[c]	OK38
7178, high resistance, T/2	P/P(B)	OK39	OK30[c]	OK38
7075, high resistance, T/10	P/P(B)	OK39	OK18	OK32
7075, high resistance, T/2	P/P(B)	OK39	OK18	OK32
7178, high resistance, T/10	P	OK39	OK30[c]	OK38

[a] Combinations of test material and test surface were listed from top to bottom in order of decreasing exfoliation tendencies in the EXCO test.

[b] Typical ratings per G 34-72 converted from the visual ratings reported for the nine participating laboratories in the round-robin test program (see footnote 4 of paper).

[c] These times are for panel test surfaces exposed skyward, facing prevailing breeze from the ocean; all other times, for test surfaces exposed earthward, facing away from the ocean and prevailing breezes.

Table 2 gives the exfoliation ratings in the EXCO test and the approximate times until the first evidence of exfoliation was noted in the atmospheric exposures; combinations of test material and test surface were listed from top to bottom in order of decreasing exfoliation tendencies in the EXCO test. Figures 2–7 show photographs of representative test panels comparing their appearance after atmospheric exposure with that in the EXCO test.

It is gratifying that the performances in the EXCO test closely paralleled the performances in the atmospheric exposures. There was a range of performances noted in the EXCO test results from one laboratory to the next

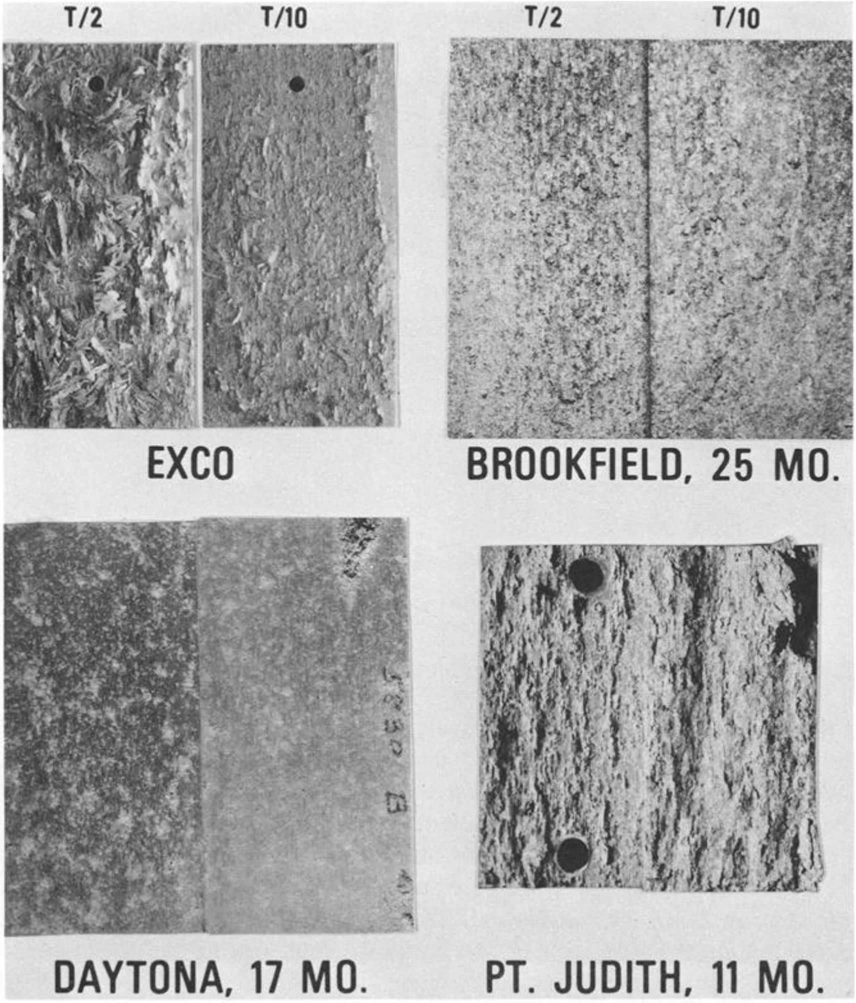

FIG. 2—*7075 low-resistance Lot 1.*

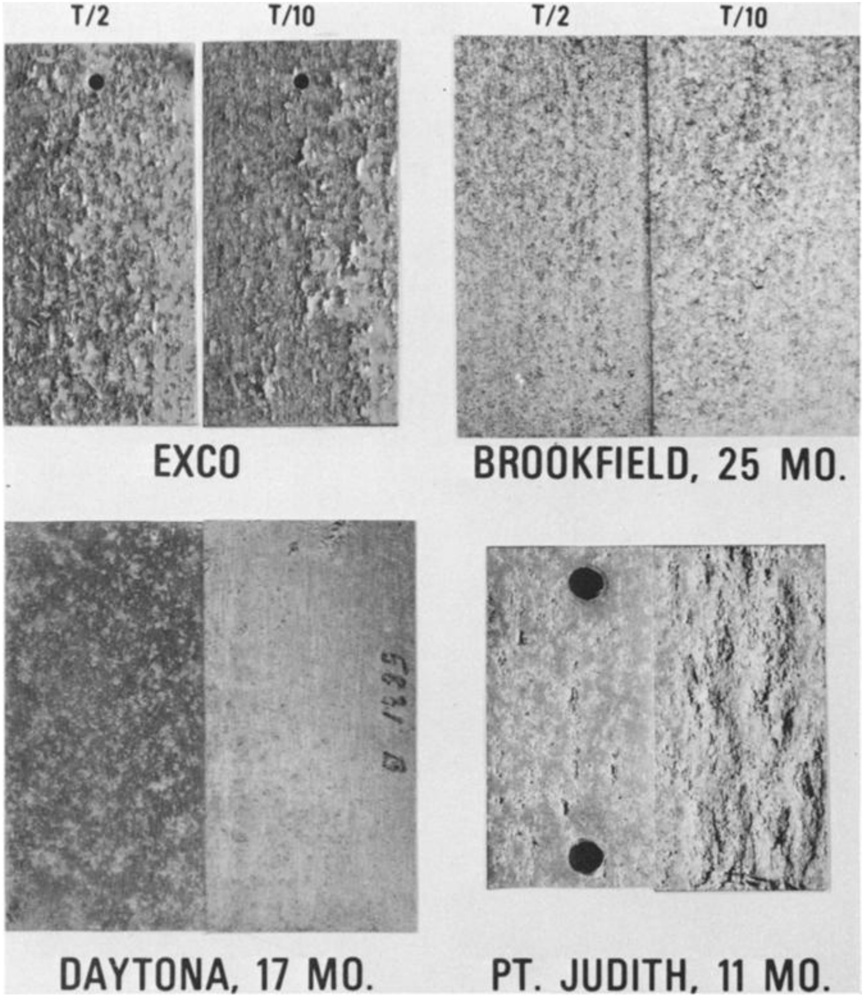

FIG. 3—*7075 low-resistance Lot 2.*

(for example, E-C/D, etc.); however, the range was small and no doubt stems mainly from the problem in making judgments based on the visual rating standards. Test surfaces that exfoliated most severely in the EXCO test have exfoliated severely at one or more of the atmospheric test sites, and those that did not exfoliate in the EXCO test have not exfoliated in the atmospheric exposures. There was one test surface (T/10 of 7178 alloy low-resistance Lot 2) that did exfoliate in the EXCO test and has not yet exfoliated in the atmosphere. Continued exposures to the atmosphere probably will eliminate this discrepancy. All things considered, there is good concurrence between performance in the EXCO test and in aggressive outdoor atmospheric environments.

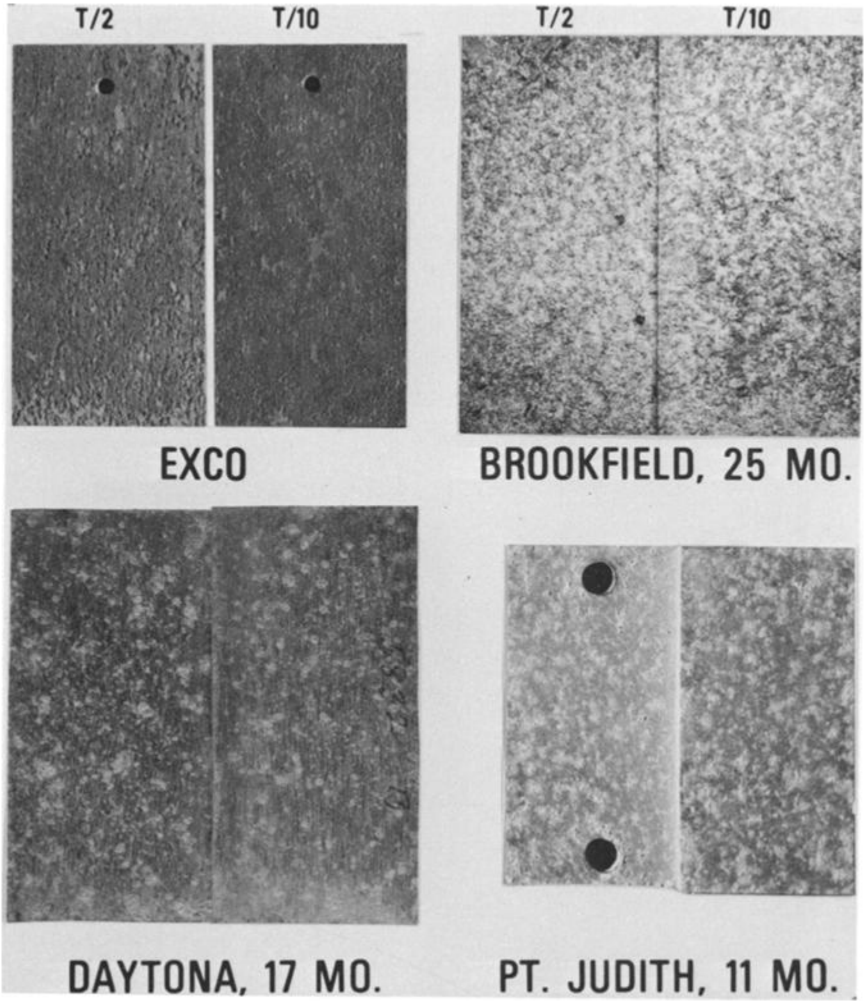

FIG. 4—*7075 high resistance.*

It is unfortunate that most of the conditions tested represent materials with relatively low or relatively high resistance to exfoliation, and there were no materials with just a slight degree of susceptibility to exfoliation in the EXCO test. However, another paper in this volume does contain such comparisons.[6]

Most of the test panels in this investigation were exposed with the machined test surfaces facing earthward to obtain more corrosive conditions. Previous testing experience has shown that exfoliation corrosion forms more quickly and progresses more rapidly on sheltered surfaces

---

[6] Lifka, B. W. and Sprowls, D. O. in *Corrosion in Natural Environments, ASTM STP 558*, American Society for Testing and Materials, 1974, pp. 306–333.

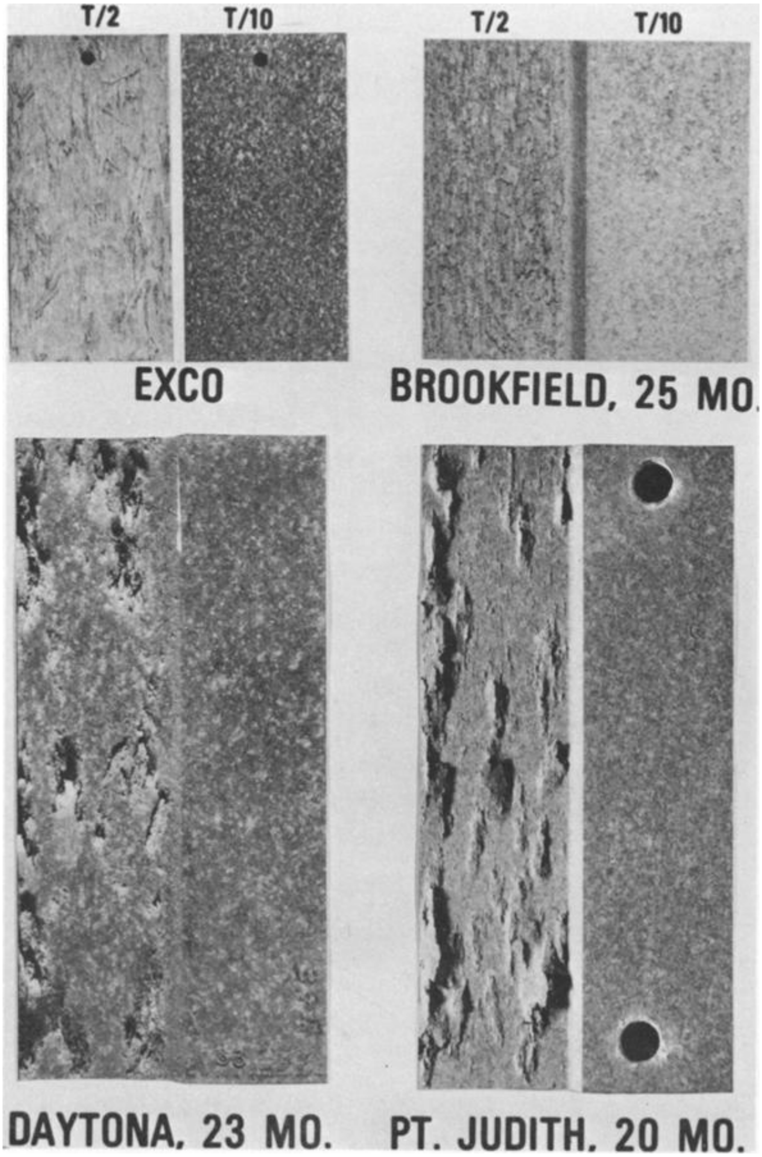

FIG. 5—*7178 low-resistance Lot 1.*

because they tend to remain damp longer with condensed moisture and are not washed by rainfall. An example of this is shown in Fig. 8 with test specimens of the 7075 alloy extrusion, for which duplicate sets of specimens were exposed at Point Judith, one set facing skyward and the other set facing earthward.

The exfoliation tendencies shown in Figs. 2–8 varied with both the climatic and exposure conditions. It is recognized that the corrosivity of

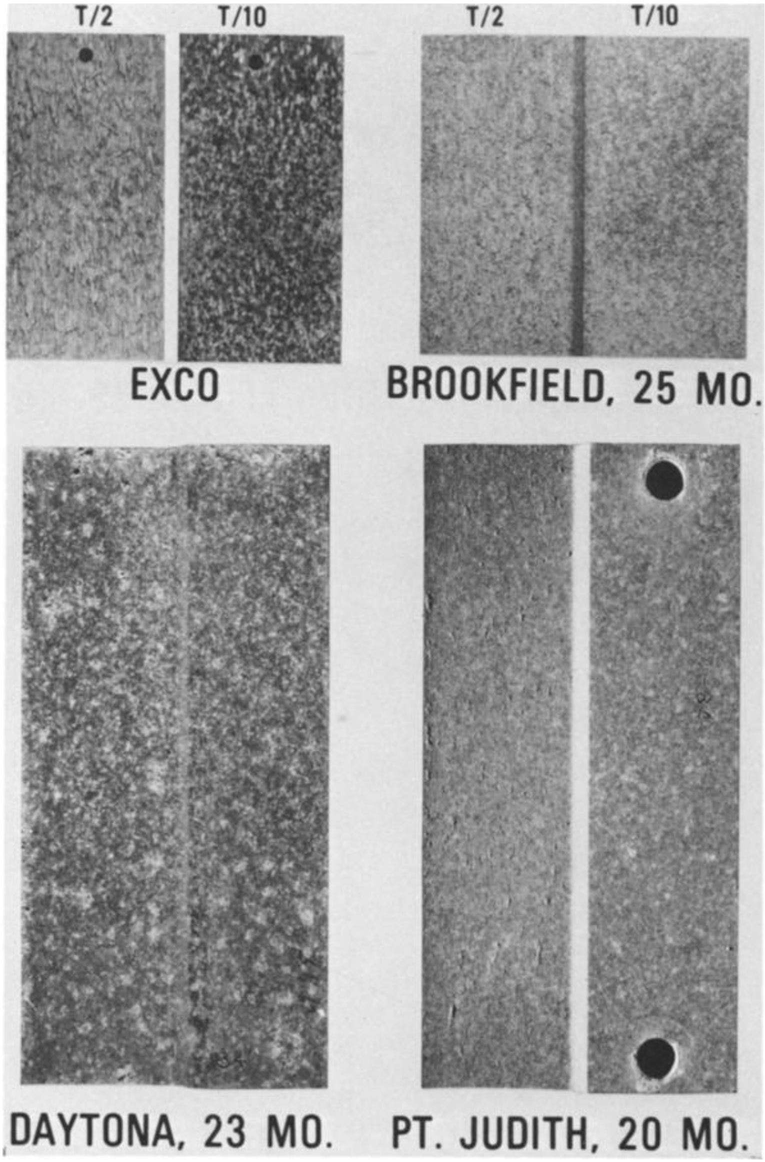

FIG. 6—*7178 low-resistance Lot 2.*

an atmosphere is controlled by factors relating to the moisture on a corroding surface and by atmospheric pollutants such as chlorides and oxides of sulfur and nitrogen. Moreover, it was shown by Carter and Campbell[7] that the weather conditions during the initial period of exposure, particu-

---

[7] Carter, V. E. and Campbell, H. S. in *Metal Corrosion in the Atmosphere, ASTM STP 435*, American Society for Testing and Materials, 1968, p. 39.

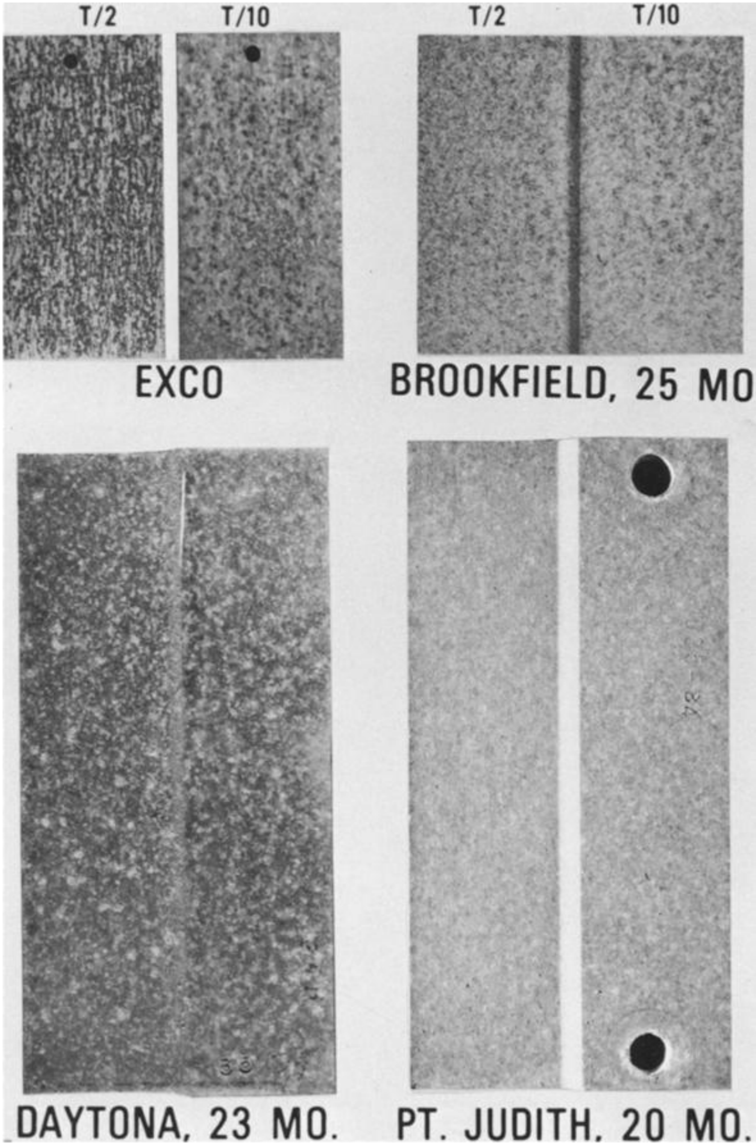

FIG. 7—*7178 high resistance.*

larly as they affect the time of wetness, will have a critical influence on the pattern of corrosion that develops on aluminum. Thus, comparisons between the exposure sites are complicated by the initial exposure dates being in different seasons of the year, and not all test panels being exposed with the test surfaces facing earthward. Nevertheless, some interesting comparisons can be made.

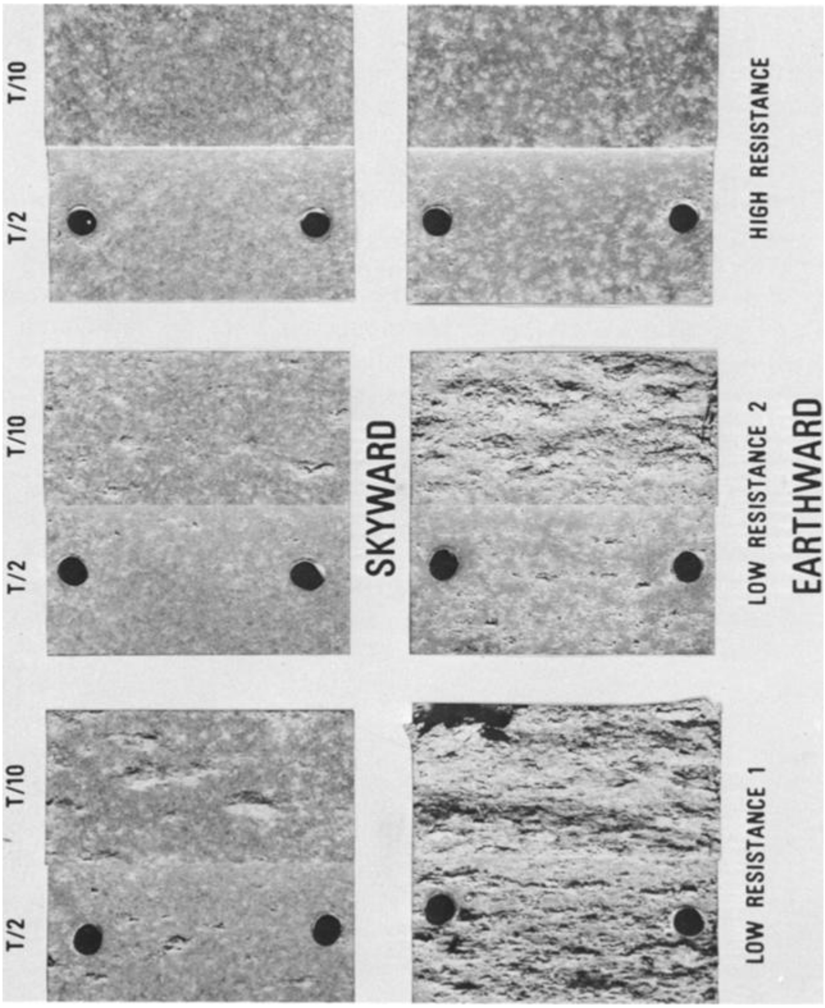

FIG. 8—*7075 extrusion—Point Judith, 11 months.*

At the two seacoast locations, the exfoliation tendencies were greater at the Point Judith test site than at Daytona Beach. This trend is especially apparent with the 7075 alloy specimens, as shown in Figs. 2 and 3, and by the times until first exfoliation, summarized in Table 2. The trend is noticeable also with the 7178 alloy panels (Figs. 5 and 6) even though the panels at Point Judith were facing skyward instead of earthward. The greater exfoliation and general corrosion at Point Judith probably can be attributed to the stronger marine influence resulting from more salt spray produced on the stony beach, a shorter distance from the shoreline to the exposure racks, and longer periods of wetness during cold and foggy weather. The test panels at Daytona also were sheltered from sea breezes by the relatively large wood panels to which they were attached.

More surprising than the difference in the performances at the two seacoast locations is the rapidity at which exfoliation commenced at the inland industrial test site at Brookfield, Illinois (see Table 2). Corrosion of these test panels probably was stimulated by the fact that the initial seven months of exposure was during the heating season, when the air polluton is worst, and the panels would remain wet for a high percentage of the time. There were relatively thick accumulations of corrosion product and deposits from the atmosphere on panels exposed at Brookfield, as can be seeen in Figs. 4 and 7. A relatively uniform distribution of corrosion is typical in industrial environments and is associated with the deposits of particulate matter that cling to the metal surface. This condition also resulted in the more uniform pattern of exfoliation corrosion evident in Figs. 5 and 6. However, the condition of the 7075 alloy panels, Figs. 2 and 3, after only 11 months at Point Judith indicates that the rate of progress of the exfoliation was much higher at that site than at Brookfield or Daytona Beach.

Summary

The times to initiate exfoliation in the atmospheric tests coupled with the severity of attack in the 1½ to 3-year exposures to date rank the test materials in the same order as the ratings in the ASTM G 34-72 EXCO laboratory corrosion test. Test surfaces that exfoliated severely in the EXCO test have exfoliated severely in the atmosphere, and those that did not exfoliate in the EXCO test have not yet exfoliated in the atmospheric tests (Table 2). In one instance (T/10 surface of 7178 alloy low-resistance Lot 2) exfoliation occurred in the EXCO test but has not yet occurred in the atmosphere; continued exposures to the atmosphere probably will eliminate this discrepancy. These 1½ to 3-year atmospheric exposures, supplemented by the longer-term (4 to 11 years) exposure data at Point Judith reported by Lifka and Sprowls (see footnote 6), indicate the validity of the EXCO test for predicting the resistance to exfoliation of 7075 and

7178 type alloy products in seacoast and industrial atmospheric environments.

Tendencies for exfoliation corrosion in the atmosphere are promoted by the same conditions that aggravate weathering corrosion, namely, strong marine influences and industrial pollution. Exfoliation is stimulated by climatic and exposure conditions that cause the metal surfaces to become damp frequently and to dry slowly.

Status

The exposures will be extended to at least four or five years with semiannual inspections to note the progress of exfoliation of the various test panels and to observe the initiation of exfoliation of additional specimens.

Acknowledgments

The authors gratefully acknowledge the participation and contributions of the following collaborators in the interlaboratory testing program: H. L. Craig, University of Miami; S. G. Epstein, The Aluminum Association; J. H. Gehrke, Martin Marietta Aluminum; G. W. Kelly, LTV Aero Corporation; B. W. Lfika, Alcoa Laboratories; A. W. Morris, McDonnell-Douglas Corporation; B. R. Pathak, Alcan Research and Development, Ltd.; and I. S. Shaffer, Naval Air Development Center.

Seawater Environments

W. H. Ailor[1]

Ten-Year Seawater Tests on Aluminum

REFERENCE: Ailor, W. H., "**Ten-Year Seawater Tests on Aluminum,**" *Corrosion in Natural Environments*, *ASTM STP 558*, American Society for Testing and Materials, 1974, pp. 117–134.

ABSTRACT: Seven aluminum alloys and panels of high-purity aluminum were exposed for ten years in seawater at Wrightsville Beach, N. C. Replicate 4 by 12-in. panels of each material were exposed in half-tide immersion and full immersion. Removals in triplicate were made at the end of one-, two-, five-, and ten-year exposures.

Other than the 1199 aluminum (99.99 percent purity), seven aluminum-magnesium alloys (5000 series) were tested. Panels were degreased prior to exposure and were cleaned ultrasonically after exposure in a chromic-phosphoric acid solution. After depth of pitting was measured, tension specimens were cut from each panel, and the mechanical properties determined.

Panels were heavily fouled with barnacles and other marine growth for all exposure periods. The fouling had little apparent effect on the pitting depth of the aluminum in tidal immersion, but generated heavy etching on some alloys during the 5 to 10 year exposure interval.

Little change in tensile properties after ten years' exposure was noted for any of the test alloys. Tensile losses reported for several alloys after full immersion include: 5086-0 (3.7 percent), 5154-H38 (5.1 percent), and 5457-H34 (5.2 percent). The high-purity 1199 and alloys 5154-H38, 5456-0, and 5456-H321 showed losses of 16 to 27 percent in elongation while the change in elongation for the 5086-0 was a decrease of about 6 percent.

Confirming other work, we found the corrosion rates to be greater for the full seawater immersion than for the tidal immersion. The lowest ten-year corrosion rate in the half-tide location was 0.014 mpy (mils per year) and the 5456-0, and the highest rate for the aluminum-magnesium 5000 series was 0.051 mpy for the 5456-H321 alloy. In full-immersion tests, the lowest rate was 0.064. For comparison, the rates for the 1199 alloy were 0.036 mpy in tidal and 0.061 mpy in full immersion. Corrosion weight losses and depth of pitting had reduced rates of growth over the interval between five years and ten years. Maximum depth of pitting for an alloy was generally at least four times the magnitude of the average of the twenty deepest pits.

The deepest pit found for any alloy after ten years was 72.0 mils for 5456-H321 in half-tide immersion and 131.0 mils for the same alloy (0 temper) in full immersion. Least apparent pitting depths occurred on alloys 5154-H38, 5457-H34, 5086-0 and high-purity 1199 where heavy etching tended to hide pits on the ten-year full-immersion panels.

KEY WORDS: aluminum alloys, corrosion, seawater corrosion, fouling, pitting, mechanical properties, tests, evaluation, intergranular corrosion, tidal immersion

[1] Research engineer, Reynolds Metals Company, Metallurgical Research Division, Richmond, Va. 23218.

The literature has many references detailing the applications for aluminum and its alloys in seawater. Brenner et al [*1*],[2] and Faller [*3*], examined a German naval vessel containing bare, anodized and painted aluminum and submerged in seawater for a period of seven years. Clad Duralumin-type sheet (anodized and painted) showed almost no corrosion. Painted aluminum-silicon alloy castings and bare 1150 alloy sheet were in good condition. Only sections and rivets fabricated from Al-7Mg alloy had severe pitting and intergranular attack.

Studies by Basil and Rausch [*2*] indicated a life of at least ten years for 3003 pipe (wall thickness 0.133 in.) carrying seawaters at a velocity of 10 fps. The maximum pitting depth after 42 months was 0.04 in. In clad 3003 pipe, pits were confined to the cladding thickness (0.016 to 0.019 in.) with no core penetration. No intergranular attack developed in any of the three test alloys (3003, alclad 3003 and 5052).

Tests designed to measure the corrosivity of 2024 and 6061 aluminum alloys embedded in wooden hull materials exposed in seawater were reported in 1957 [*4*]. Various coatings and sealants were investigated. Other test results on aluminum in harbor waters have been published by Brouillette [*5*], Dalrymple [*6*], and Rogers [*7*]. Successful use of aluminum wire to protect electric cables for as long as 29 years has been noted [*8,9*]. Navy work reported the effect of seawater on extruded 7075 fatigue life and corrosion [*10*], and Campbell [*11*] discussed the uses of aluminum in marine applications. Alloy 6061-T6 has been successfully used for the hulls of torpedoes [*12*].

Work by Lagutina et al [*13*] showed that natural seawater immersion for one year was five to six times more aggressive toward aluminum and other metals than artificial seawater used in laboratory tests. Biological action and water movement were given as the reasons for this increased activity.

Corrosion behavior of aluminum and its alloys in hydrospace (deepsea environments) has been well documented in recent years [*14–22,41*].

Exposures in seawater for as long as five years have confirmed the excellent corrosion characteristics of the aluminum-magnesium alloys in both bare and welded conditions [*23–26,29,31,34,35,42*].

Corrosion potentials of many aluminum alloys in surface seawater have been measured by a number of investigators [*27,30,32,37,39*].

Hailstone [*36*] tested 13 sand-cast and die-cast aluminum alloys, with and without coating protection, for as long as 20 years in seawater.

The desirability of fabricating rivets from aluminum alloys having less than 3.5 percent magnesium was reported by Hall [*38*], and Lagutina and Shevchenko [*40*] studied the effects of seasonal variations on seawater corrosion.

---

[2] The italic numbers in brackets refer to the list of references appended to this paper.

An earlier report [31] discussed the results of five-year removals of aluminum alloys from tidal and full-immersion tests at Wrightsville Beach, N. C. This paper gives the ten-year data for these materials.

Procedure

Triplicate 4 by 12-in. panels of seven aluminum alloys and of one high-purity aluminum were cleaned in acetone, measured, and weighed prior to exposure at both the tidal-immersion (half tide) and full-immersion locations in coastal seawater. The length of each panel was taken in the sheet rolling direction. The panels were exposed on 26 October 1961 at the Francis L. LaQue Corrosion Laboratory of the International Nickel Company, Inc., Wrightsville Beach, N. C.

After removal from test, specimens were scraped to remove fouling and then cleaned for 10 min in an ultrasonically agitated solution of 2 percent chromic acid and 5 percent phosphoric acid (by weight) at 180°F (82°C), followed by a 3-min dip in 70 percent nitric acid, photographed, weighed, and measurements made for depth of pitting by use of a calibrated focus microscope. Triplicate panels of each alloy were removed after one-, two-, five-, and ten-year exposure periods. Mechanical properties were determined by the procedure specified in ASTM Method for Tension Testing of Metallic Materials (E 8-66) from tensile strips cut from the test panels as shown in Fig. 1. Corrosion rates were calculated from weight losses for

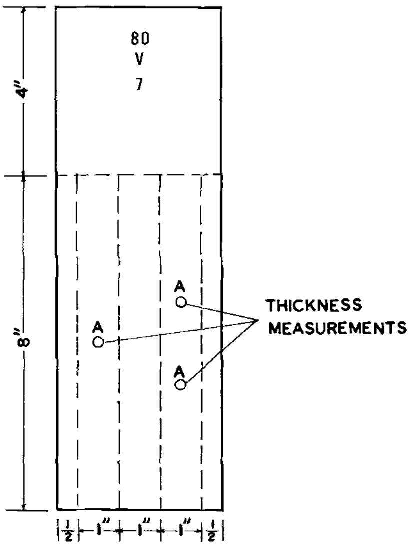

EXPOSURE PANEL, INDICATING LOCATION OF TENSION TEST BARS AND MARKING CODE. THE CODE INDICATES: ALLOY NUMBER AT TOP, TEST LOCATION LETTER, AND SPECIMEN NUMBER. POINTS DESIGNATED "A" ARE THE POINTS AT WHICH THICKNESS MEASUREMENTS ARE MADE.

FIG. 1—*Plan for cutting tension specimens.*

TABLE 1—*Chemical compositions.*

Alloy[a]	Gage[b]	Values in Weight Percent (balance is aluminum)								
		Cu	Fe	Si	Mn	Mg	Zn	Cr	Ti	Ni
5154-H38	0.050	0.02	0.16	0.11	<0.02	3.05	<0.02	0.23	<0.01	<0.02
5454-H34	0.188	0.03	0.22	0.13	0.71	2.75	0.02	0.12	<0.02	<0.02
5457-H34	0.040	0.03	0.07	0.05	0.21	0.85	...	...	0.02	...
5086-0	0.080	0.06	0.28	0.13	0.33	3.94	0.10	0.15	<0.02	<0.02
5083-0	0.250	0.06	0.31	0.17	0.71	4.78	0.08	0.14	0.03	...
5456-0	0.240	0.12	0.26	0.14	0.78	5.35	0.07	0.14	0.03	0.01
5456-H321	0.245	0.13	0.25	0.14	0.80	5.49	0.07	0.14	0.03	0.01
1199	0.050	0.0025	0.0045	0.0025	...	...	...	...	...	...

[a] The Aluminum Association Aluminum Standards and Data.

[b] Inches.

each exposure period. All data computations were done on an IBM 1410 computer, using a procedure previously described (*ASTM STP 435*, 1968, pp. 43–60).

The chemical analyses of the test alloys are given in Table 1, and the original and after-exposure mechanical properties in Table 2. The solution potentials for the test alloys given in Table 3 were measured by three test

TABLE 2—*Mechanical property changes due to corrosion.*

Alloy	Maximum Pit Depth, mils	Tensile Strength[a]		Yield Strength[a]		Elongation[a] in 2 in.	
		1000 psi	Change, %	1000 psi	Change, %	%	Change, %
Half-Tide Exposure (Wrightsville Beach, N. C.)—10 Years							
1199	39.0	11.9		11.6		10.9	
		12.2	+2.5	12.0	+3.5	13.5	+23.8
5083-0	38.0	46.8		20.8		20.5	
		47.5	+1.5	20.3	−2.4	19.1	−6.8
5086-0	27.0	40.4		17.6		23.3	
		39.3	−2.7	17.7	+0.6	22.5	−3.4
5154-H38	19.5	46.7		39.1		8.4	
		45.7	−2.1	38.9	−0.5	8.1	−3.6
5454-H34	15.5	44.0		33.8		11.0	
		43.7	−0.7	33.6	−0.6	11.9	+8.2
5456-0	68.5	50.7		21.0		22.2	
		50.5	−0.4	21.0	0	17.5	−20.3
5456-H321	72.0	57.2		38.7		13.6	
		54.5	−4.5	37.2	−3.9	10.1	−25.4
5457-H34	22.0	28.5		24.0		7.8	
		27.3	−4.2	23.2	−3.3	7.7	−1.3
Full-Immersion Exposure (Wrightsville Beach, N. C.)—10 Years							
1199	...[b]	11.9		11.6		10.9	
		11.9	0	11.8	+1.8	9.2	−15.6
5083-0	24.0	46.8		20.8		20.5	
		46.9	+0.2	20.5	−1.5	20.6	+0.5
5086-0	...[b]	40.4		17.6		23.3	
		38.9	−3.7	17.5	−0.6	21.8	−6.0
5154-H38	...[b]	46.7		39.1		8.4	
		44.3	−5.1	37.9	−3.1	6.4	−23.8
5454-H34	20.0	44.0		33.8		11.0	
		43.8	−0.5	33.7	−0.3	11.8	+7.3
5456-0	131.0	50.7		21.0		22.2	
		49.2	−3.0	21.1	+0.5	16.3	−26.5
5456-H321	44.0	57.2		38.7		13.6	
		56.6	−1.1	37.6	−2.9	11.3	−16.9
5457-H34	...[b]	28.5		24.0		7.8	
		27.0	−5.2	22.9	−4.6	6.5	−16.7

[a] Control properties listed first. After-exposure values below for each alloy.

[b] Panels heavily etched and unsuitable for pit measurement.

TABLE 3—*Solution potentials, V.*

Alloy	Salt Peroxide[a]	Synthetic Seawater[b]	Flowing Seawater[c]
1199	−1.20	−0.91	−1.42
5083-0	−0.89	−0.91	−0.88
5086-0	−0.82	−0.78	−0.93
5456-0	−0.83	−0.82	−0.76
5154-H38	−0.84	−0.88	...
5454-H34	−0.86	−0.88	...
5456-H321	−0.84	−0.86	−0.90
5457-H34	−0.85	−0.91	...

[a] 1N NaCl + 0.3% H_2O_2 versus 0.1N calomel electrode; value given is after 2 h in solution at 30.0°C ± 0.5 deg.

[b] "Sea salt" (ASTM Specification D 1141-52) dissolved in deionized water (41.953 g/liter). Value given is an average of five determinations made on each of five consecutive days (4th to 8th day) at 30.0°C ± 0.5 deg.

[c] Flowing seawater at 238 cm/s (7.8 ft/s) at 21°C (70°F)—values are averages for last ten days of 45-day test.

techniques: (1) salt-peroxide solution, (2) synthetic seawater, and (3) flowing natural seawater.

Discussion

Corrosion Effects on Mechanical Properties

A comparison of original mechanical properties with those determined for unexposed control panels showed that the aging effects were negligible for all alloys over the ten-year test period. Essentially no change in ultimate tensile strengths was noted for the high-purity 1199 aluminum and the aluminum-magnesium alloys 5083-0, 5086-0, 5454-H34, and 5456-0 after ten years in tidal and full-immersion exposures. The aluminum-magnesium alloys 5456-H321 and 5457-H34 showed only slight decreases (4.2–5.2 percent) in strength—the full-immersion panels somewhat more than the tidal-immersion panels for the 5457-H34. The 5456-H321 alloy had a negligible loss in ultimate strength for the ten-year total-immersion samples. The 5154-H38 alloy showed a loss of 5.1 percent in tensile value after ten years in full seawater immersion. The original ultimate tensile strengths for the test alloys along with those for one-, two-, five-, and ten-year removal periods are given in Table 4.

As was true for the tensile property, little change was noted in the yield strengths (Table 2) for the 5083, 5086, 5454 alloys and for the high-purity 1199 aluminum after long-term immersions. Slight decreases were found for the 5154 panels in total immersion exposure and for the 5456 and 5457 in both tidal and full immersions. The greatest loss found for yield strength in any of the tested alloys was 4.6 percent for the ten-year immersion of 5457 alloy.

TABLE 4—*Changes in ultimate tensile strength due to corrosion.*

Alloy	Year	Ultimate Tensile Strength, 1000 psi Half Tide	Full Immersion
1199	0	11.9	11.9
	1	11.8	11.7
	2	12.1	12.1
	5	12.1	12.1
	10	12.2	11.9
5083-0	0	46.8	46.8
	1	46.9	46.5
	2	46.2	46.4
	5	46.1	45.9
	10	47.5	46.9
5086-0	0	40.4	40.4
	1	40.2	40.1
	2	40.0	40.1
	5	39.7	39.4
	10	39.3	38.9
5456-0	0	50.7	50.7
	1	50.6	50.1
	2	50.0	49.3
	5	49.4	48.9
	10	50.5	49.2
5154-H38	0	46.7	46.7
	1	46.3	46.1
	2	47.2	46.8
	5	46.2	44.1
	10	45.7	44.3
5454-H34	0	44.0	44.0
	1	43.6	43.6
	2	43.7	43.4
	5	43.2	43.2
	10	43.7	43.8
5456-H321	0	57.2	57.2
	1	46.9	56.4
	2	56.8	56.7
	5	56.2	56.5
	10	54.5	56.6
5457-H34	0	28.5	28.5
	1	28.1	27.2
	2	28.0	27.8
	5	28.2	27.8
	10	27.3	27.0

In most cases the full-immersion panels were more affected as to loss of yield strength than were the tidal panels.

No significant changes in elongation (Table 2) were noted for the 1199, 5083, 5086, and 5454 panels over the ten-year test period. Slight losses in elongation were found for the 5456 in tidal immersions and for the 5154, 5456, and 5457 in full-immersion exposure. In most cases the effect of total seawater immersion was greater for the elongation property than the effect of tidal exposure.

Corrosion Rates

Weight losses of exposed panels were used in the calculation of the corrosion rates in milligrams per square decimeter per day (mdd) and mils per year (mpy). A mil is 0.001 of an inch. These values (mpy) are recorded in Table 5 for the four removal periods.

Over the ten-year test period, the corrosion rates showed consistent drops for the one-, two, five-, and ten-year points for both tidal and full immersion exposures. After ten years, no corrosion rate greater than 0.12

TABLE 5—*Corrosion rates of test alloys.*

Alloy	Magnesium Content, %	Year	Seawater Corrosion Corrosion Rates, mpy	
			Half Tide	Full Immersion
1199	...	1	0.216	0.179
		2	0.108	0.149
		5	0.059	0.093
		10	0.036	0.061
5083-0	4.5	1	0.119	0.173
		2	0.077	0.120
		5	0.040	0.066
		10	0.036	0.059
5086-0	4.0	1	0.133	0.155
		2	0.078	0.122
		5	0.053	0.087
		10	0.035	0.057
5456-0	5.1	1	0.127	0.320
		2	0.092	0.333
		5	0.068	0.634
		10	0.014	0.116
5154-H38	3.5	1	...	0.170
		2	0.089	0.103
		5	0.050	0.084
		10	0.037	0.055
5454-H34	2.7	1	0.168	0.171
		2	0.106	0.141
		5	0.056	0.091
		10	0.041	0.059
5456-H321	5.1	1	0.122	0.219
		2	0.070	0.157
		5	0.054	0.126
		10	0.051	0.064
5457-H34	1.0	1	0.161	0.149
		2	0.101	0.123
		5	0.046	0.071
		10	0.036	0.056

mpy was found for any alloy in full immersion. Except for the 5456-0 having some intergranular attack, the next highest rate was 0.06 mpy. The highest rate in the half-tide exposure was 0.05 mpy.

The bar graph in Fig. 2 indicates the usual pattern of decreasing corrosion rates with time for all alloys in tidal exposures. Figure 3 shows the corrosion rates for all test alloys in full seawater immersion for the four removal periods. An increasing rate for the 5456-0 alloy is noted for the removal panels after one, two, and five years due to intergranular attack at the machined edges. By the tenth year the rate had dropped substantially (0.12 mpy) even though the intergranular attack was well established.

Corrosion Effects—Pitting

The maximum measured deepest pits found over the course of the ten-year exposure period are recorded in Table 6. As reported earlier [*31*] no consistent pattern of pit growth was observable over the test period. In some cases, the deepest pit occurred on the panels having the longest exposure. In many instances, particularly on the full-immersion samples, the deepest pit was found on one-, two-, or five-year panels. Explanations for this seeming anomaly can be found in the random nature of pitting and in the heavy etching of some longer-term panels—an effect tending to destroy the original zero-reference surface and thereby reduce the apparent pitting depth. The etching was probably due to chemical action beneath the attached barnacles and oysters.

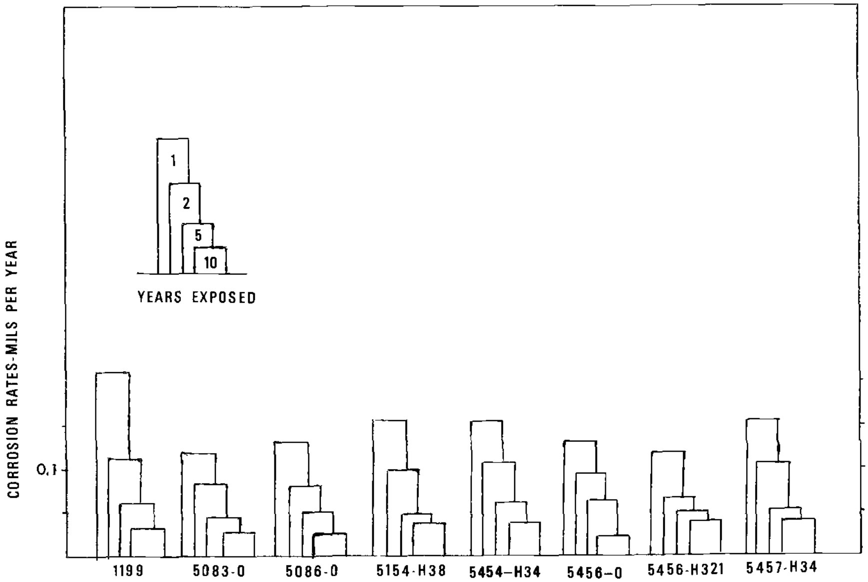

FIG. 2—*Corrosion rates for test alloys in tidal exposure.*

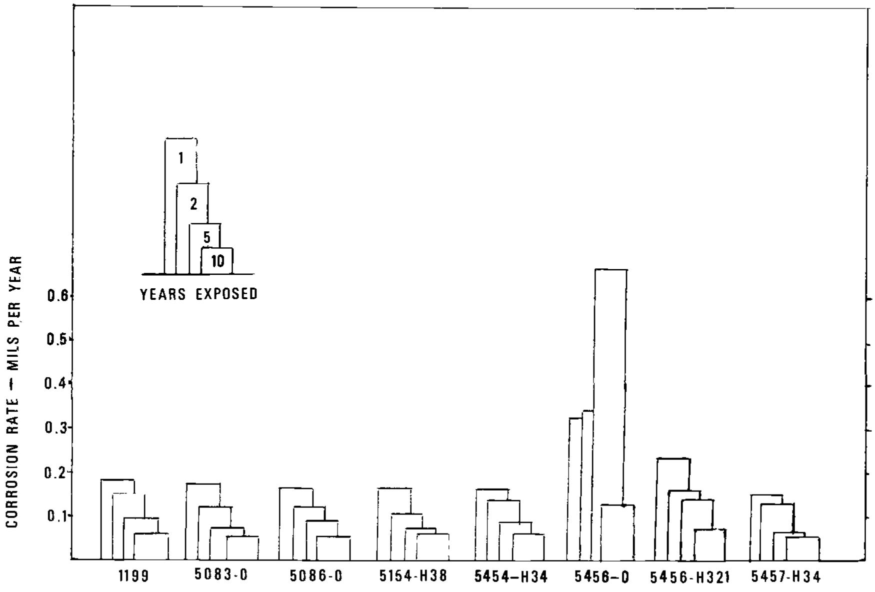

FIG. 3—*Corrosion rates for test alloys in full seawater immersion.*

The ten-year average depth of pitting attack for tidal exposure was 2.7 mils for the 1199 aluminum and 1.0 mil for the 5457 alloy (Table 7). The 5456 (0 and H321 tempers) had the deepest average pits after ten years (12.7 and 13.5 mils) and also the deepest measured pits (68.5 and 72.0 mils) for tidal exposure. The 5086 alloy had a maximum pitting depth of 27.0 mils and an average depth of 2.5 mils, while the 5083 showed a maximum pit of 38.0 mils and an average of 12.4 mils. Table 8 ranks the test alloys as to pitting resistance in tidal exposures.

TABLE 6—*Seawater immersion.*

Alloy	Maximum Pit Depths, mils Measured over 10-year Exposure Period Half Tide	Full Immersion
5154-H34	$19.5^{(10)a}$	$15.2^{(1)a}$
5454-H34	$19.9^{(5)}$	$20.0^{(10)}$
5456-H34	$22.0^{(10)}$	$12.0^{(1)}$
5086-0	$27.0^{(10)}$	$18.1^{(1)}$
5083-0	$38.0^{(10)}$	$24.0^{(10)}$
5456-0	$68.5^{(10)}$	$131.0^{(10)}$
5456-H321	$72.0^{(10)}$	$45.3^{(2)}$
1199	$39.0^{(10)}$	$12.7^{(1)}$

[a] Number in parentheses indicates exposure year for recorded pit depth.

TABLE 7—*Ten-year seawater pitting depths (mils).*

Alloy	Gage, in.	Year	Half Tide		Full Immersion	
			Max	Avg	Max	Avg
5154-H38	0.050	1	3.6	1.5	15.2	3.5
		2	5.1	2.5	7.0	3.1
		5	18.9	1.9	9.3	0.3
		10	19.5	5.0	(*a*)	(*a*)
5454-H34	0.188	1	9.4	2.2	17.6	8.3
		2	8.9	3.6	19.9	6.0
		5	19.9	1.0	7.1	3.4
		10	15.5	2.6	20.0	3.8
5457-H34	0.040	1	8.9	3.6	12.0	7.3
		2	11.4	2.3	11.7	6.2
		5	4.5	3.7	3.5	2.7
		10	22.0	1.0	(*a*)	(*a*)
5086-0	0.080	1	11.3	3.5	18.1	9.3
		2	8.9	3.9	7.5	4.5
		5	17.5	2.8	2.0	1.6
		10	27.0	2.5	1.2	(*a*)
5083-0	0.250	1	25.0	8.2	20.9	8.2
		2	8.5	4.0	18.9	5.4
		5	11.0	3.0	7.0	1.0
		10	38.0	12.4	24.0	1.0
5456-0	0.240	1	13.2	7.5	39.2	20.3
		2	25.6	8.3	60.7	19.7
		5	50.0	8.0	80.0	20.3
		10	68.5	12.7	131.0	39.9
5456-H321	0.245	1	15.2	3.9	28.8	6.2
		2	10.0	5.5	45.3	9.3
		5	33.0	11.7	37.0	7.3
		10	72.0	13.5	44.0	12.4
1199	0.050	1	5.3	0.1	12.7	2.4
		2	3.6	1.8	6.5	2.5
		5	9.1	0.1	3.2	0.1
		10	39.0	2.7	(*a*)	(*a*)

(*a*) Heavily etched—not suitable for pit measurement.

As in the tidal results, the aluminum-magnesium alloys 5457-H34, 5154-H34, 5086-0, and 5454-H34 showed excellent pitting resistance, along with the high-purity 1199, in full seawater immersion. The deepest ten-year pit found on these panels was 20.0 mils for the 5454, and the average depths were less than 3.8 mils. The excellent condition of these alloys is seen in Fig. 4. The 5456-0 alloy with a maximum depth of 131.0 mils and an average depth of 39.9 mils had the deepest pitting of any of the test alloys in total immersion. A summary Table 9 ranks the test alloys as to pitting resistance for full seawater immersions.

TABLE 8—*Pitting resistance rating*[a]*—half-tide exposure.*

Alloy	Years of Exposure				Average of Maximum Pits (4 time periods)	Average[b] (20 deepest pits)
	1	2	5	10		
5154-H38	1	2	5	2	1	5
1199	2	1	2	6	2	4
5457-H34	3	7	1	3	3	1
5454-H34	4	$3\frac{1}{2}$	6	1	4	3
5086-0	5	$3\frac{1}{2}$	4	4	5	2
5083-0	8	5	3	5	6	6
5456-H321	7	6	7	8	7	8
5456-0	6	8	8	7	8	7

[a] Number 1 is best.
[b] Ten-year values.

TABLE 9—*Pitting resistance rating*[a]*—full immersion.*

Alloy	Years of Exposure				Average of Maximum Pits (4 time periods)	Average[b] (20 deepest pits)
	1	2	5	10		
1199	2	1	2	$2\frac{1}{2}$	1	$2\frac{1}{2}$
5457-H34	1	4	3	$2\frac{1}{2}$	2	$2\frac{1}{2}$
5086-0	5	3	1	$2\frac{1}{2}$	3	$2\frac{1}{2}$
5154-H38	3	2	6	$2\frac{1}{2}$	4	$2\frac{1}{2}$
5454-H34	4	6	5	5	5	6
5083-0	6	5	4	6	6	5
5456-H321	7	7	7	7	7	7
5456-0	8	8	8	8	8	8

[a] Number 1 is best.
[b] Ten year values.

Other Corrosion Phenomena

In addition to the usual pitting-type corrosion, panels of 5456-0 and 5456-H321 showed intergranular attack at the machined edges, starting with the one-year removals in full immersion. Even after ten years, however, the attack had not caused severe lamellar-type corrosion. Figure 5 indicates the nature of the intergranular attack.

The excellent seawater resistance of welded aluminum can be seen in Fig. 6. The 5053-H113 plate was welded using 5356 alloy wire and the 5454 plate was welded using 5554 alloy wire. In these examples, no corrosion of the weld bead, panel, or heat- affected zone was found for either half-tide or full immersion after exposures of ten years.

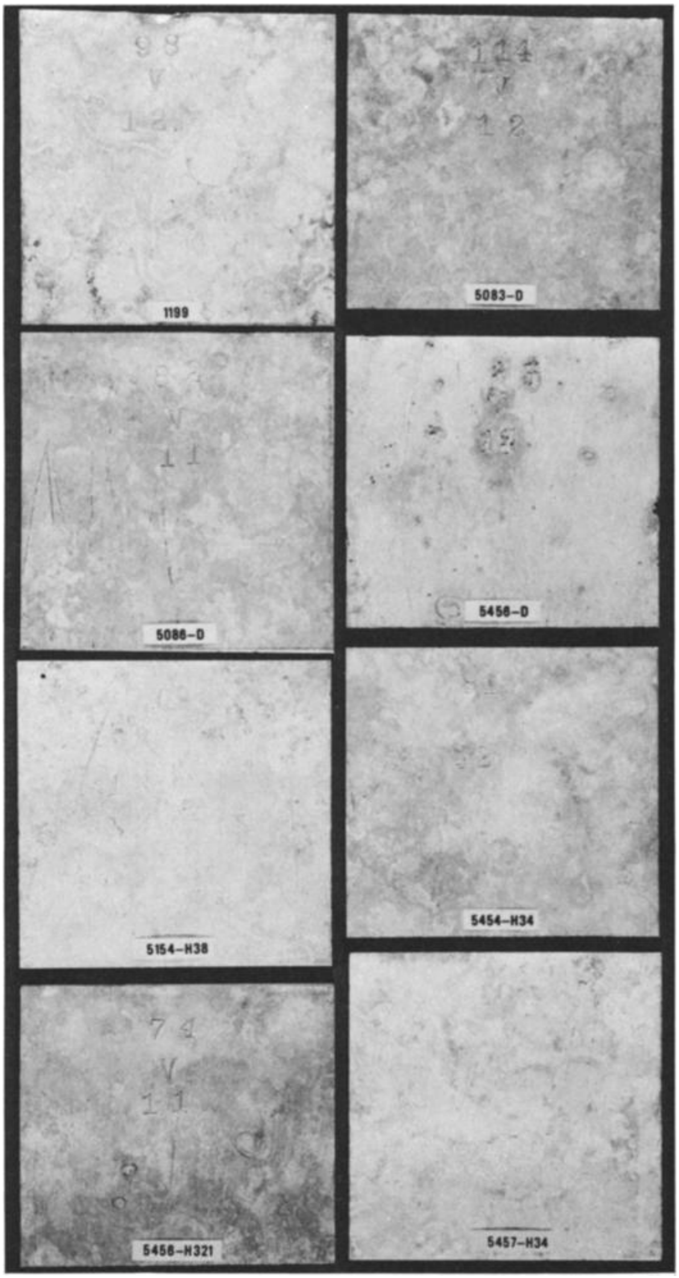

FIG. 4—*Appearance after cleaning of ten-year full seawater immersion test panels.*

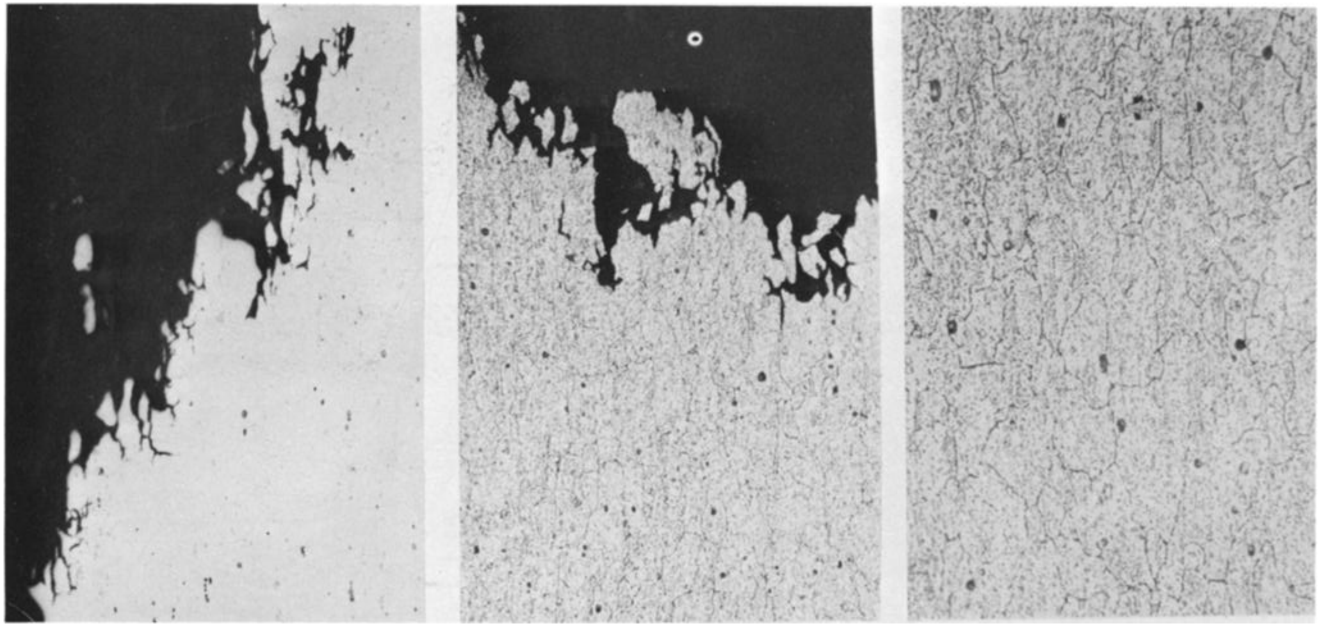

FIG. 5—*Photomicrographs of cross sections of the 5456-0 sheet showing* (left) *intergranular corrosion* (*as-polished cross section*—×*187*); (middle) *intergranular corrosion extending along grain boundaries* [*25 percent* HNO_3 *at 70°C* (*158°*F)—×*187*]; *and* (right) *relatively dense, moderately continuous grain boundary precipitate* [*25 percent* HNO_3 *at 70°C* (*158°F*)—×*375*].

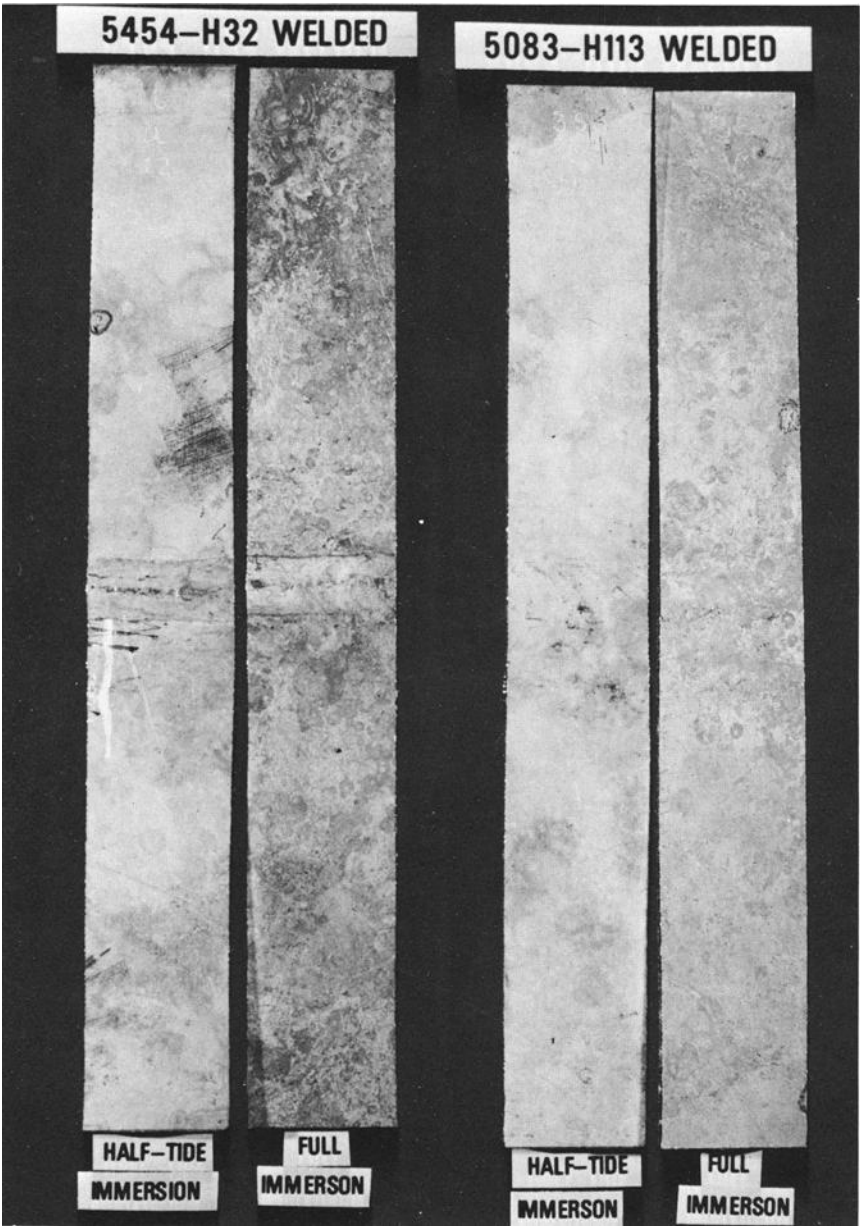

FIG. 6—*Welded ten-year seawater exposure panels after cleaning.*

Solution Potentials of Test Alloys

The results of laboratory determinations of solution potentials for the test alloys are compared with the corrosion potentials measured in seawater at the test site (Table 3). The values measured in actual seawater are sufficiently different from those values measured in commonly used laboratory solutions to indicate that laboratory values cannot reliably be used to predict behavior of aluminum in seawater. A detailed study on seawater corrosion potentials of aluminum and its alloys has been reported elsewhere [*39*]. Commonly used tables of aluminum solution potentials in salt-peroxide or synthetic seawater may or may not accurately indicate the anodic-cathodic relationships of alloys in flowing seawater. Cladding of aluminum alloys with other aluminum alloys is successful for seawater applications only as the cladding is sufficiently anodic to the base metal to ensure a potential difference in the order of −0.15 V.

Conclusions

The results of ten years' exposure of seven aluminum alloys to half-tide and total immersion in coastal weawater at Wrightsville Beach, N. C. lead to the following conclusions:

1. Corrosion of aluminum in seawater generally takes the form of pitting. Aluminum-magnesium alloys (5000 series) have excellent resistance to pitting and general corrosion attack.
2. The 5456 alloy in the annealed temper 0 and in the strain-hardened and stabilized temper H321 (quarter-hard), having 5½ percent magnesium, developed some intergranular attack and exfoliation at the edge surfaces. The intergranular attack on the 5456 alloys was much more severe for the full-immersion panels.
3. The best aluminum alloys tested from a pitting resistance standpoint in seawater were the aluminum-magnesium 5086, 5154, 5454, and 5457 alloys.
4. Deepest pits were found in the 5456 and 5083 aluminum-magnesium alloys.
5. Deepest pitting generally occurred on the full-immersion specimens.
6. The 5086, 5457, 5454, 5154, and 5083 alloys had the best resistance to general corrosion as measured by loss of weight over the exposure period.
7. Fouling had some apparent effect on the corrosion of the aluminum. The point of attachment of barnacles in some instances was the initiation point for the development of a pit and severe etching was noted in some cases beneath the barnacle.
8. Properly welded aluminum-magnesium alloys have the same excellent corrosion resistance as the parent metal.
9. The ten-year seawater exposure had little significant effect on the mechanical properties of the aluminum-magnesium alloys.

10. A decreasing corrosion rate was noted for the aluminum-magnesium alloys over the test period.

11. The importance of keeping the copper content of aluminum alloys in the order of 0.07 percent or less in surface seawater applications, as discussed in the earlier five-year report, was emphasized by these results.

Acknowledgments

The cooperation of the personnel at Francis L. LaQue Corrosion Laboratory of The International Nickel Company, Inc. at Wrightsville Beach, N. C., has been very helpful. Appreciation is also expressed to the management of the Metallurgical Research Division of Reynolds Metals Company for permitting and encouraging the publication of these results.

References

[*1*] Brenner, P., Faller, F. E., and Domes, T., *Forschungshefte fur Schiffstechnik*, Vol. 2, No. 10, July 1955, pp. 165–170; translation: Aluminum Development Association Technical Memorandum No. 300.

[*2*] Basil, J. L. and Rausch, M. W., "Sea Water Corrosion Test of Aluminum Alloy Pipe," U. S. Naval Engineering Experiment Station, Evaluation Report 040037A (5), Feb. 1955, 7 pp.

[*3*] Faller, F. E., *Aluminium*, Vol. 32, No. 3, March 1956, pp. 136–138 (in German).

[*4*] Wright, T. E., Godard, H. P., and Jenks, I. H., *Corrosion*, Vol. 13, No. 7, July 1957, pp. 481t–487t.

[*5*] Brouillette, C. V., *Corrosion*, Vol. 14, No. 8, Aug. 1958, pp. 352t–356t.

[*6*] Dalrymple, R. S., *Oil and Gas Journal*, Vol. 57, No. 38, Sept. 14, 1959, pp. 84–87.

[*7*] Rogers, T. H. in *Transactions of the Institute of Marine Engineers* (Canadian Division Supplement), No. 2, Dec. 1960, pp. 31–37.

[*8*] "Unaffected After 29 Years in Salt Water," *Electrical Journal*, Vol. 168, No. 8, Feb. 23, 1962, p. 421.

[*9*] "Aluminum Takes Sea Attack," *Iron Age*, Vol. 191, No. 6, Feb. 7, 1963, p. 15.

[*10*] Shaffer, I. S., Sebastian, J. C., Rosenfeld, M. S., and Ketcham, S. J. in *Proceedings of the Air Force Materials Laboratory Conference on Corrosion of Military and Aerospace Equipment*, Nov. 1967, pp. 692–731.

[*11*] Campbell, H. S., *Ocean Engineering*, Vol. 1, No. 4, May 1969, pp. 387–393.

[*12*] Fink, F. W., Haynie, F. H., White, E. L., Boyd, W. K., and DiBeri, G. A., "Corrosion Control of Aluminum-Hulled Torpedoes in Sea Water-Flooded Tubes, paper presented at the NACE National Conference, Philadelphia, Pa., March 1970.

[*13*] Lagutina, A. G., Danil'chenko, K. P., Shevchenko, O. F., and Barannik, V. P., *Zashchita Metallov*, Vol. 6, No. 1, Jan.–Feb. 1970, pp. 48–51 (in Russian).

[*14*] Forgeson, B. W., Waldron, L. J., et al, "Abyssal Corrosion and Its Mitigation, Part II, Results of a Pilot Text Exposure," Naval Research Laboratory Memorandum Report No. 1383 on Project SR 007-08-11, Order AD-296545 from OTS, Washington, D. C., Dec. 1962.

[*15*] Reinhart, F. M., "Corrosion of Materials in Hydrospace," AD-644 473, NCEL-TR-504; HC $3.00MF$0.65, Naval Civil Engineering Laboratory, Port Hueneme, Calif., Dec. 1966.

[*16*] Ailor, W. H., *Metallurgia*, Vol. 75, No. 449, March 1967, pp. 98–108.

[*17*] Reinhart, F. M., "Corrosion of Materials in Hydrospace," Naval Civil Engineering Laboratory paper presented at the Air Force Materials Laboratory 50th Anniversary Corrosion of Military Aerospace Equipment Technical Conference, Colorado, May 1967.

[*18*] Rynewicz, J., "Marine Corrosion Control for Deep Submergence Vehicles," *Proceedings of the Air Force Materials Laboratory Conference on Corrosion of Military and Aerospace Equipment*, Technical Report No. AFML-TR-67-329, Nov. 1967.

[*19*] Wei, Maurice W., *Corrosion*, Vol. 23, No. 9, 1967.
[*20*] Ailor, W. H., Jr., *Journal of Hydronautics*, Vol. 2, No. 1, Jan. 1968, pp. 26–33.
[*21*] Reinhart, Fred M., "Corrosion of Materials in Hydrospace. Part 5. Aluminum Alloys," Naval Civil Engineering Laboratory, Port Hueneme, Calif., Jan. 1969.
[*22*] Muraoka, J. S., "Relationship Between Marine Fouling and Corrosion Rate of Carbon Steel and Aluminum Alloy at the Surface and at 6000-Foot Depth," Report No. NCEL-TR-681, Naval Civil Engineering Laboratory, May 1970.
[*23*] Ailor, W. H. and Lindberg, R. I., *Journal of the American Society of Naval Engineers*, Vol. 73, No. 3, 1961, pp. 545–547.
[*24*] Ailor, W. H., Jr. and Reinhart, F. M., *Naval Engineers Journal*, Vol. 76, No. 3, June 1964, pp. 443–449.
[*25*] Harasimowicz, L. A. and Booth, F. F., *Metallurgia*, Vol. 69, No. 412, Feb. 1964, pp. 59–64.
[*26*] Hagiwara, Michiki, *Journal of the Japanese Institute of Light Metals*, Vol. 19, No. 4, April 1969, pp. 136–141 (in Japanese).
[*27*] Peterson, M. H. and Lennox, T. J., Jr., "Electrochemical Potentials and Corrosion Performance of Aluminum Alloys in Sea Water," paper presented at the NACE 23rd Annual Conference, Los Angeles, Calif., March 1967.
[*28*] Spirin, A. A., Akhmedov, G. M., Trifel', M. S., and Shakov, V. I., *Protection Metals*, Vol. 4, No. 5, Sept.-Oct. 1968, pp. 515–516.
[*29*] Paunel, Maria-Ana and Marcu, P., *Metallurgia*, Vol. 20, No. 11, Nov. 1968, pp. 646–650 (in Rumanian).
[*30*] Spirin, A. A., Akhmedov, G. M., Trifel', M. S., and Shakov, V. I., *Zashchita Metallov*, Vol. 4, No. 5, 1968, pp. 580–582 (in Russian).
[*31*] Ailor, W. H., Jr. in *Materials Performance and the Deep Sea, ASTM STP 455*, American Society for Testing and Materials, 1969, pp. 115–130.
[*32*] Groover, R. E., Lennox, T. J., Jr., and Peterson, M. H., "Marine Corrosion Studies: Characterization of the Corrosion Behavior and Response to Cathodic Protection of Nineteen Aluminum Alloys in Sea Water," Naval Research Laboratory, Washington, D. C., Jan. 1969, 28 pp.
[*33*] Southwell, C. R., *Corrosion Science*, Vol. 9, No. 3, March 1969, pp. 179–183.
[*34*] Hagiwara, Michiki, *Sumitomo Light Metals Technical Report*, Vol. 11, No. 3, July 1970, pp. 21–31.
[*35*] Paunel, M. and Marcu, P., *Revista Constructillor si a Materialelor de Constructii*, Vol. 21, No. 9, Sept. 1969, pp. 479–483.
[*36*] Hailstone, S. C., *Metallurgia*, Vol. 80, No. 480, Oct. 1969, pp. 136–140.
[*37*] Groover, R. E., Lennox, T. J., Jr., and Peterson, M. H., *Materials Protection*, Vol. 8, No. 11, Nov. 1969, pp. 25–30.
[*38*] Hall, B. N. in *Proceedings of the Symposium on Deterioration of Metals in Marine Environment*, 1970; Southampton University Yacht Research Report, Vol. 30, pp. 1–6.
[*39*] Ailor, W. H. in *Proceedings of the NACE 26th Conference*, Houston, Tex., 1970, pp. 200–212.
[*40*] Lagutina, A. G. and Shevchenko, O. F., *Zashchita Metallov*, Vol. 7, No. 2, Mar.-April 1971, pp. 197–200 (in Russian).
[*41*] Reinhart, F. M. and Jenkins, J. F., "Corrosion of Alloys in Hydrospace—189 Days at 5,900 Feet," Naval Civil Engineering Laboratory Technical Note N-1224, April 1972.
[*42*] Reinhart, F. M. and Jenkins, J. F., "Corrosion of Materials in Surface Seawater After 12 and 18 Months of Exposure," Naval Civil Engineering Laboratory Technical Note N-1213, Jan. 1972.

F. M. Reinhart[1]

Corrosion of Copper Alloys in Hydrospace

REFERENCE: Reinhart, F. M., "**Corrosion of Copper Alloys in Hydrospace,**" *Corrosion in Natural Environments, ASTM STP 558*, American Society for Testing and Materials, 1974, pp. 135–170.

ABSTRACT: A total of 1050 specimens of 46 different copper alloys were exposed in the Pacific Ocean at two depths, 760 and 1830 m, for periods of time varying from 123 to 1064 days in order to determine the effects of deep-ocean environments on their corrosion resistance.

Most of the copper-base alloys corroded uniformly and their corrosion rates were low, 25 μm per year or less after one year at a depth of 760 m and after two years at a depth of 1830 m. A few of the alloys containing zinc, aluminum or silicon were attacked by parting corrosion. They were not susceptible to stress corrosion cracking. Only the mechanical properties of the alloys attacked by parting corrosion were adversely affected.

The aggressiveness of the seawater and of the bottom sediments on the copper alloys was about the same, except for the copper-nickel alloys, where the bottom sediments were less aggressive.

KEY WORDS: corrosion, materials, hydrospace, copper, copper alloys, ocean environments, corrosion resistance

The U. S. Naval Civil Engineering Laboratory is conducting a research program to determine the effects of deep-ocean environments on materials. It is expected that this research will establish the best materials for use in deep-ocean construction.

A submersible test unit (STU) was designed, on which many test specimens can be mounted. The STU can be lowered to the ocean floor and left for long periods of exposure.

Thus far, exposures have been made at two deep-ocean test sites and at a surface seawater site in the Pacific Ocean. Six STU's have been exposed and recovered. Test Site I (nominal depth of 1830 m) is approximately 150 km west-southwest of Port Hueneme, California, latitude 33 deg 44 min N and longitude 120 deg 45 min W. Test Site II (nominal depth of 760 m) is 140 km west of Port Hueneme, California, latitude 34 deg 06 min N and longitude 120 deg 42 min W. A surface seawater exposure site (V) was established at Point Mugu, California, 34 deg 06 min N–119 deg 07 min W, to obtain surface immersion data for comparison purposes.

---

[1] Metallurgist, Naval Civil Engineering Laboratory, Port Hueneme, Calif. 93043.

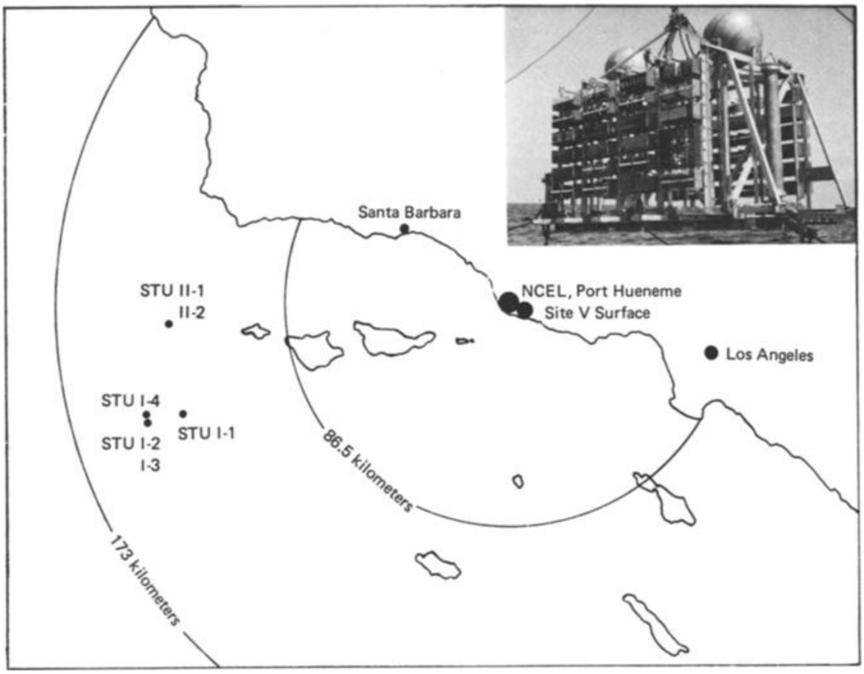

FIG. 1—*Area map showing STU sites off the Pacific Coast; STU structure in inset.*

The test sites are shown in Fig. 1 and their specific geographical locations are given in Table 1. The complete oceanographic data at these sites, obtained from NCEL cruises between 1961 and 1967, are summarized in Fig. 2. Initially, it was decided to utilize the site at the 1830 m depth. Because of the minimum oxygen concentration zone found between the 610 and 910 m depths, during the early oceanographic cruises, it was decided to establish a second exposure site (STU II-1 and II-2) at a nominal depth of 760 m. For comparative purposes, the surface water site V was established. Even though the actual depths are shown in the tables, the nominal depths of 1830 and 760 m are used throughout the text.

A summary of the characteristics of the bottom waters three meters above the bottom sediments at the two deep-ocean exposure sites and at the surface exposure site is given in Table 1.

Sources of information pertaining to the biological characteristics of the bottom sediments, biological deterioration of materials, detailed oceanographic data, and construction, emplacement, and retrieval of STU structures are given in an earlier paper [*1*].[2]

The procedures for the preparation of the specimens for exposure and for evaluating them after exposure are described in Ref *2*.

[2] The italic numbers in brackets refer to the list of references appended to this paper.

TABLE 1—*STU locations and bottom water characteristics.*

Site No.	Latitude, N	Longitude, W	Depth, m	Exposure, days	Temperature, °C	Oxygen, ml/liter	Salinity, ppt	pH	Current, knots, avg
Surface	. . .	. . .	20	. . .	14.0	5.9	33.76	8.1	variable
I-1	33 deg 46 min	120 deg 37 min	1615	1064	2.6	1.2	34.51	7.5	0.03
I-2	33 deg 44 min	120 deg 45 min	1720	751	2.3	1.3	34.51	7.6	0.03
I-3	33 deg 44 min	120 deg 45 min	1720	123	2.3	1.3	34.51	7.6	0.03
I-4	33 deg 46 min	120 deg 46 min	2070	403	2.2	1.6	34.40	7.7	0.03
II-1	34 deg 06 min	120 deg 42 min	715	197	5.0	0.4	34.36	7.5	0.06
II-2	34 deg 06 min	120 deg 42 min	720	402	5.0	0.4	34.36	7.5	0.06
V	34 deg 06 min	119 deg 07 min	2	181	15.5	5.8	33.51	8.1	variable

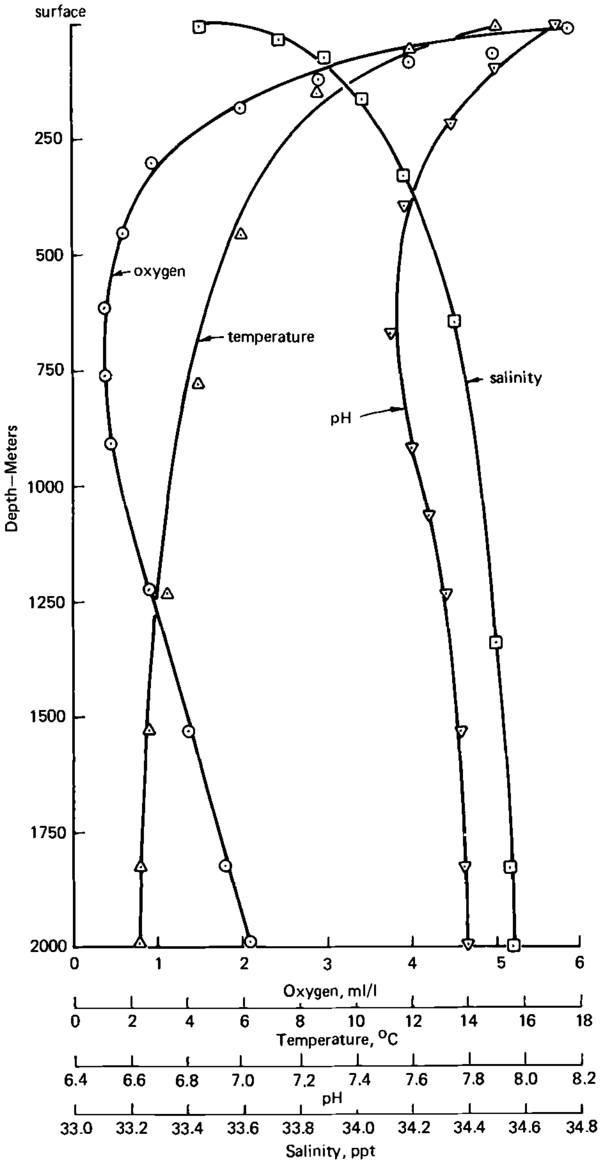

FIG. 2—*Oceanographic data at STU sites.*

Previous reports pertaining to the performance of materials in the deep-ocean environments are given in Refs *1–8*.

This report is a discussion of the results obtained of the corrosion of copper and copper alloys for the seven exposure periods shown in Table 1.

Results and Discussion

The results presented and discussed herein also include the corrosion data for copper alloys exposed on the STU structures for the International Nickel Company, Incorporated. Permission for their incorporation in this report was granted by Dr. T. P. May (ret.), former manager, Francis L. LaQue Corrosion Laboratory, Wrightsville Beach, North Carolina [*9*].

Results of other corrosion investigations on copper alloys in the deep ocean in the Atlantic [*12,13*], at the surface in the Atlantic [*14*], and at the surface in the Pacific Ocean [*15,16*] are compared with these results to furnish a picture of the behavior of copper alloys in both oceans.

Corrosion

Effect of Duration of Exposure

Copper—The chemical composition of the coppers is given in Table 2 and their corrosion rates and types of corrosion in Table 3.

TABLE 2—*Chemical composition of the coppers, percent by weight.*

Alloy	CDA No.[a]	Cu	Ni	Be	Co
Copper, O free	102	99.96	...	...	...
Be-Cu	172	97.80	0.05	1.9	0.25
Be-Cu chain[b]	825	97.50	...	2.0	0.5

[a] Copper Development Association alloy number.
[b] Cast alloy.

The excellent corrosion resistance of copper is partially due to its being a relatively noble metal. However, in many environments its satisfactory performance depends on the formation of adherent, relatively thin films of corrosion products. In seawater corrosion, resistance depends on the presence of a surface oxide film through which oxygen must diffuse in order for corrosion to continue. This oxide film adjoining the metal is cuprous oxide covered with a mixture of cupric oxychloride, cupric hydroxide, basic cupric carbonate and calcium sulfate. Since oxygen must diffuse through this film for corrosion to occur, it would be expected that under normal circumstances the corrosion rate would decrease with increase in time of exposure. The type of corrosion in seawater is usually uniform.

TABLE 3—*Corrosion rates and types of corrosion of coppers.*

Alloy, CDA No.[a]	Environment[b]	Exposure, days	Depth, m	Oxygen, ml/liter, avg	Corrosion Rate, μm/year	Types of Corrosion[c]
102	W	123	1720	1.35	39	U
102	S	123	1720	...	36	U
102	W	403	2070	1.35	32	U
102	S	403	2070	...	28	U
102	W	751	1720	1.35	22	U
102	S	751	1720	...	18	U
102	W	1064	1615	1.35	13	U
102	S	1064	1615	...	8	U
102	W	197	715	0.40	28	U
102	S	197	715	...	5	U
102	W	402	720	0.40	29	U
102	S	402	720	...	10	ET
102	W	181	1.5	5.75	40	G, P (559 μm)
102	W	366	1.5	5.75	31	G
102	W	398	1.5	5.75	28	G, P (940 μm)
102	W	540	1.5	5.75	23	G, P (559 μm)
102	W	588	1.5	5.75	23	G, P (508 μm)
172	W	402	720	0.40	15	U
172	S	402	720	...	13	U
172	W	181	1.5	5.75	3	U
172	W	364	1.5	5.75	28	U
172	W	723	1.5	5.75	20	U
172	W	763	1.5	5.75	20	U
172[d]	W	402	720	0.40	13	U[f]
172[d]	S	402	720	...	13	U[f]
172[d]	W	181	1.5	5.75	3	U[f]
172[d]	W	364	1.5	5.75	25	U[f]
172[d]	W	723	1.5	5.75	18	U[f]
172[d]	W	763	1.5	5.75	20	U[f]
172[e]	W	402	720	0.40	15	ET
172[e]	W	402	720	...	13	ET
172[e]	W	181	1.5	5.75	3	ET
172[e]	W	364	1.5	5.75	28	U
172[e]	W	723	1.5	5.75	18	U
172[e]	W	763	1.5	5.75	18	U
825[g]	W	402	720	0.40	13	U
825[g]	S	402	720	...	10	U
825[g]	W	181	1.5	5.75	25	U
825[g]	W	364	1.5	5.75	25	U
825[g]	W	723	1.5	5.75	20	U
825[g]	W	763	1.5	5.75	20	U, P (775 μm)

[a] Copper Development Association alloy numbers.

[b] W = totally exposed in seawater on sides of structure; S = exposed in base of structure so that the lower portions of the specimens were embedded in the bottom sediments.

[c] Symbols for types of corrosion: ET = etching; G = general; P = pitting; U = uniform. Numbers indicate microns; that is, 20 μm = 20 microns maximum.

[d] MIG weld.

[e] TIG weld.

[f] Uniform, weld bead etched.

[g] Cast chain.

The corrosion rates of copper in seawater, both at depth and at the surface, are shown in Fig. 3. The corrosion rate decreased with increase in duration of exposure at the 1830 m depth in the Pacific Ocean. At the 1700 m depth in the Atlantic Ocean [*12*] the corrosion rate of copper after 1050 days of exposure was practically the same as at the 1830 m depth in the Pacific Ocean. This close agreement of the corrosion rates of copper in the two oceans is not unexpected since the corrosion of copper is not appreciably affected by changes in oxygen concentration.

At depths of 1300 and 1370 m in the Atlantic Ocean [*13*] the corrosion rates were about one half the corrosion rate at 1700 m in the Atlantic Ocean and about two thirds the corrosion rate at 1830 m in the Pacific Ocean. They were more in agreement with the NCEL corrosion rates of copper at the 760 m depth in the Pacific Ocean.

For practical purposes the corrosion of copper can be considered constant and of the same magnitude after exposure for one year in seawater at the surface and at depths in both the Atlantic and Pacific Oceans. The corrosion rates ranged between 13 and 38 μm per year with an average of about 25 μm per year.

Copper partially embedded in the bottom sediments at the 1830 m depth corroded at essentially the same rate as in the seawater at this depth. The corrosion rate decreased with increasing duration of exposure. At the 760 m depth, copper corroded at a lower rate in the bottom sediment than in the sediment at the 1830 m depth as well as in the water at 760 m.

The addition of about two percent beryllium to copper did not affect the corrosion of copper after 402 days of exposure at a depth of 760 m. The beryllium-copper was in the form of wrought sheet and cast chain. Their corrosion rates were 15 and 13 μm per year, respectively, in seawater and

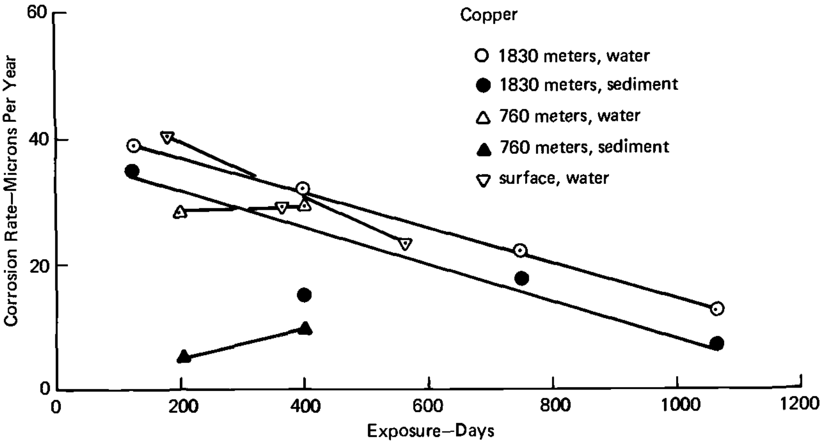

FIG. 3—*Effect of duration of exposure on the corrosion rates of copper.*

13 and 13 μm per year, respectively, in the bottom sediments, while those of copper were 15 and 5 μm per year in seawater and in the bottom sediment, respectively, Table 3. The corrosion of the wrought beryllium-copper sheet was not affected by welding either by the metal-inert gas (MIG) or tungsten-inert gas (TIG) processes.

Brasses—The chemical compositions of the copper-zinc alloys (brasses) are given in Table 4 and their corrosion rates and types of corrosion in Table 5.

Corrosion of the brasses usually occurs as uniform, pitting, crevice, parting, or stress corrosion cracking. The tendency for the brasses to corrode by parting and stress corrosion cracking varies with the zinc content; the higher the zinc content of the alloy the greater the susceptibility. Pitting and crevice corrosion are usually caused by differential aeration cells.

The corrosion rates of the majority of the brasses were so similar that the averages for the alloys not attacked by severe parting corrosion were plotted in Fig. 4 to show the effect of the duration of exposure on their corrosion rates.

Although their corrosion rates decreased slightly with duration of exposure, for all practical purposes they can be considered constant. The brasses corroded at faster rates in seawater at the surface than at depth, the rates being faster at 1830 m than at 760 m. They corroded at the same rates in the bottom sediments as in the seawater at the 1830 m depth, but at slower rates in the sediments than in the seawater at the 760 m depth.

The brasses, in general, corroded uniformly except for parting corrosion, which is discussed later.

Naval brass (CDA 464) corroded at a slower rate in seawater at the 1830 m depth in the Pacific Ocean than at a depth of 1710 m in the Atlantic

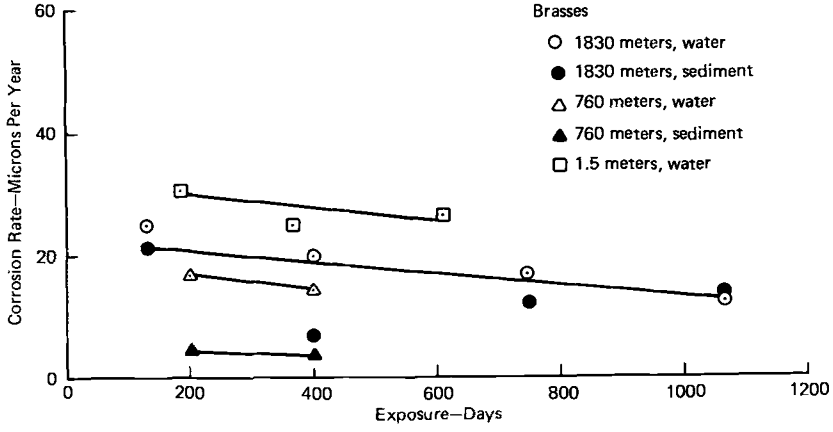

FIG. 4—*Effect of duration of exposure on the average corrosion rates of the brasses.*

TABLE 4—*Chemical composition of copper-zinc alloys (brasses), percent by weight.*

Alloy	CDA No.[a]	Cu	Zn	Sn	Ni	Al	Mn	Fe	Other
Commercial bronze	220	90.0	10.0	...	...	...	...	...	...
Red brass	230	85.0	15.0	...	...	...	...	...	...
Commercial brass	268	66.47	33.51	0.05	...	...	...	0.02	0.01Pb
Yellow brass	268	68.48	31.50	0.05	...	...	...	0.02	0.01Pb
Arsenical admiralty	443	71.19	27.77	1.00	...	...	...	0.01	0.027As
Arsenical admiralty	443	70.0	29.0	1.0	...	...	...	...	0.04As
Yellow brass	270	65.0	35.0	...	...	...	...	...	...
Muntz metal	280	60.69	39.29	...	...	...	...	0.02	...
Muntz metal	280	60.0	40.0	...	...	...	...	...	...
Naval brass	464	60.46	38.74	0.69	...	...	...	0.03	0.08Pb
Tobin bronze	...	58.94	39.07	0.89	Nil	0.10	...	1.10	0.05Pb
Ni-Mn bronze[b]	868	54.58	34.48	0.70	3.77	1.73	3.06	1.66	0.02Pb
Mn-bronze A	675	56.0	42.0	...	...	1.0	0.1	1.0	...
Al-brass	...	78.0	20.0	...	...	2.0	...	...	...
Ni-brass	...	50.0	40.0	...	8.0	...	...	2.0	...

[a] Copper Development Association alloy number.

[b] Cast alloy.

TABLE 5—*Corrosion rates and types of corrosion of copper-zinc alloys.*

Alloy, CDA No.[a]	Environment[b]	Exposure, days	Depth, m	Oxygen, ml/liter, avg	Corrosion Rate, μm/year	Types of Corrosion[c]
220	W	123	1720	1.35	15	U
220	S	123	1720	...	8	U
220	W	403	2070	1.35	15	U
220	S	403	2070	...	3	U
220	W	751	1720	1.35	15	C,230
220	S	751	1720	...	10	C,510
220	W	1064	1615	1.35	10	C,510
220	S	1064	1615	...	15	U
220	W	197	715	0.40	8	U
220	S	197	715	...	3	NU ET
220	W	402	720	0.40	5	SL DZ
220	S	402	720	...	3	SL DZ
220	W	181	1.5	5.75	28	U
220	W	366	1.5	5.75	28	P(100)
230	W	123	1720	1.35	33	U
230	S	123	1720	...	43	SL DZ
230	W	403	2070	1.35	31	SL DZ
230	S	403	2070	...	10	GBSL
230	W	751	1720	1.35	23	SL DZ
230	S	751	1720	...	18	U
230	W	1064	1615	1.35	15	SL DZ
230	S	1064	1615	...	8	G
230	W	197	715	0.40	25	U
230	S	197	715	...	3	U
230	W	402	720	0.40	18	U
230	S	402	720	...	3	ET
230	W	181	1.5	5.75	46	SL DZ
230	W	366	1.5	5.75	31	CR (150 μm)
268	W	1064	1615	1.35	20	S DZ
268	W	1064	1615	1.35	15	MO DZ
443	W	123	1720	1.35	27	U
443	S	123	1720	...	25	U
443	W	403	2070	1.35	19	U
443	S	403	2070	...	13	U,GBSL
443	W	751	1720	1.35	16	U
443	S	751	1720	...	12	U
443	W	1064	1615	1.35	13	U
443	S	1064	1615	...	13	U
443	W	197	715	0.40	20	U
443	S	197	715	...	3	U
443	W	402	720	0.40	15	U
443	S	402	720	...	6	U,ET
443	W	181	1.5	5.75	39	G
443	W	366	1.5	5.75	33	U
443	W	608	1.5	5.75	28	U,IP
270	W	123	1720	1.35	36	U
270	S	123	1720	...	33	U
270	W	403	2070	1.35	25	U

(*continued*)

TABLE 5—*Continued.*

Alloy, CDA No.[a]	Environment[b]	Exposure, days	Depth, m	Oxygen, ml/liter, avg	Corrosion Rate, µm/year	Types of Corrosion[c]
270	S	403	2070	. . .	5	GBSL
270	W	751	1720	1.35	64	SL DZ
270	S	751	1720	. . .	15	SL DZ
270	W	1064	1615	1.35	15	U
270	S	1064	1615	. . .	13	U
270	W	197	715	0.40	23	U
270	S	197	715	. . .	5	NU ET
270	W	402	720	0.40	23	U
270	S	402	720	. . .	3	ET
270	W	181	1.5	5.75	53	U
270	W	366	1.5	5.75	33	U
280	W	123	1720	1.35	47	SL DZ
280	S	123	1720	. . .	36	SL DZ
280	W	403	2070	1.35	75	S DZ
280	S	403	2070	. . .	30	SL DZ
280	W	751	1720	1.35	91	S DZ
280	S	751	1720	. . .	43	S DZ
280	W	1064	1615	1.35	58	S DZ
280	S	1064	1615	. . .	20	U
280	W	197	715	0.40	18	SL DZ;P,254 µm, 58 avg
280	S	197	715	. . .	13	SL DZ[d];P,5 µm, 3 avg
280	W	402	720	0.40	18	SL DZ
280	S	402	720	. . .	9	SL DZ
280	W	181	1.5	5.75	74	DZ
280	W	366	1.5	5.75	94	S DZ
280	W	398	1.5	5.75	79	MO DZ
280	W	540	1.5	5.75	86	DZ,IP
280	W	588	1.5	5.75	84	DZ,IP
464	W	1064	1615	1.35	25	S DZ
Tobin Bronze	W	1064	1615	1.35	23	S DZ
675	W	123	1720	1.35	74	EX DZ
675	S	123	1720	. . .	51	EX DZ
675	W	403	2070	1.35	69	S DZ
675	S	403	2070	. . .	23	S DZ
675	W	751	1720	1.35	183	S DZ
675	S	751	1720	. . .	66	V S DZ
675	W	1064	1615	1.35	51	S DZ
675	S	1064	1615	. . .	31	S DZ
675	W	197	715	0.40	31	S DZ
675	S	197	715	. . .	5	SL DZ
675	W	402	720	0.40	20	S DZ
675	S	402	720	. . .	3	SL DZ
675	W	181	1.5	5.75	122	S DZ
675	W	366	1.5	5.75	48	S DZ
868[e]	W	123	1720	1.35	13	SL DZ
868[e]	W	403	2070	1.35	10	MD DZ

(continued)

TABLE 5—*Continued.*

Alloy, CDA No.[a]	Environment[b]	Exposure, days	Depth, m	Oxygen, ml/liter, avg	Corrosion Rate, μm/year	Types of Corrosion[c]
868[e]	S	403	2070	...	13	MD DZ
868[e]	W	751	1720	1.35	28	V S DZ
868[e]	W	197	715	0.40	10	SL DZ
868[e]	S	197	715	...	10	SL DZ
868[e]	W	402	720	0.40	41	SL DZ
868[e]	S	402	720	...	74	SL DZ
868[e]	W	181	1.5	5.75	3	SL DZ
868[e]	W	364	1.5	5.75	18	DZ
868[e]	W	723	1.5	5.75	74	DZ
868[e]	W	763	1.5	5.75	76	DZ
Al-brass	W	123	1720	1.35	18	U
Al-brass	S	123	1720	...	13	U
Al-brass	W	403	2070	1.35	10	U
Al-brass	S	403	2070	...	3	GBSL
Al-brass	W	751	1720	1.35	8	U
Al-brass	S	751	1720	...	3	U
Al-brass	W	1064	1615	1.35	5	U
Al-brass	S	1064	1615	...	20	G
Al-brass	W	197	715	0.40	13	U
Al-brass	S	197	715	...	3	U
Al-brass	W	402	720	0.40	8	U
Al-brass	S	402	720	...	3	ET
Al-brass	W	181	1.5	5.75	20	G
Al-brass	W	366	1.5	5.75	10	P,102
Ni-brass	W	123	1720	1.35	33	U
Ni-brass	S	123	1720	...	28	U
Ni-brass	W	403	2070	1.35	33	U
Ni-brass	S	403	2070	...	5	GBSL
Ni-brass	W	751	1720	1.35	25	U
Ni-brass	S	751	1720	...	18	U
Ni-brass	W	1064	1615	1.35	20	U
Ni-brass	S	1064	1615	...	13	U
Ni-brass	W	197	715	0.40	20	U
Ni-brass	S	197	715	...	3	NU ET
Ni-brass	W	402	720	0.40	18	U
Ni-brass	S	402	720	...	3	ET
Ni-brass	W	181	1.5	5.75	28	U
Ni-brass	W	366	1.5	5.75	23	U

---

[a] Copper Development Association alloy number.

[b] W = totally exposed in seawater on sides of structure; S = exposed in base of structure so that the lower portions of the specimens were embedded in the bottom sediments.

[c] Symbols for types of corrosion: C = crevice; DZ = dezincification; CR = cratering; ET = etching; EX = extensive; G = general; GBSL = general below sediment line; I = incipient; MD = medium; MO = moderate; NU = nonuniform; P = pitting; S = severe; SL = slight; U = uniform; V = very. Numbers indicate microns; that is, 20 = 20 microns; 20 μm = 20 microns maximum.

[d] At spacer.

[e] Cast alloy.

Ocean [*12*]; than at the surface in the Pacific Ocean at Fort Amador, Panama Canal Zone [*16*]; and than at Port Hueneme Harbor, California [*15*]. However, after 1050 days of exposure at 1710 m in the Atlantic Ocean and 1064 days of exposure at 1830 m in the Pacific Ocean the corrosion rates of alloy 464 were essentially the same.

Bronzes—The chemical compositions of the bronzes are given in Table 6 and their corrosion rates and types of corrosion in Table 7.

The corrosion rates of all the bronzes, except the silicon bronzes, were so similar that the averages for the alloys were plotted in Fig. 5 to show the effect of the duration of exposure on their corrosion behavior. The bronzes corroded at higher rates in the surface seawater than at depth, and the rates decreased gradually with increasing time of exposure. At depths of 760 and 1830 m the corrosion rates were the same in the bottom sediments as in the seawater and were constant with increasing duration of exposure. The corrosion rates of the silicon bronzes at depth were higher than those of the other bronzes; about the same as the corrosion rates of the bronzes in surface seawater; and decreased with increasing time of exposure at the same rate as did the bronzes in surface seawater.

In general, the corrosion rates of the bronzes exposed at the surface and at depth in the Atlantic and Pacific Oceans were in good agreement.

Generally, the bronzes corroded uniformly except for some parting corrosion, which is discussed later.

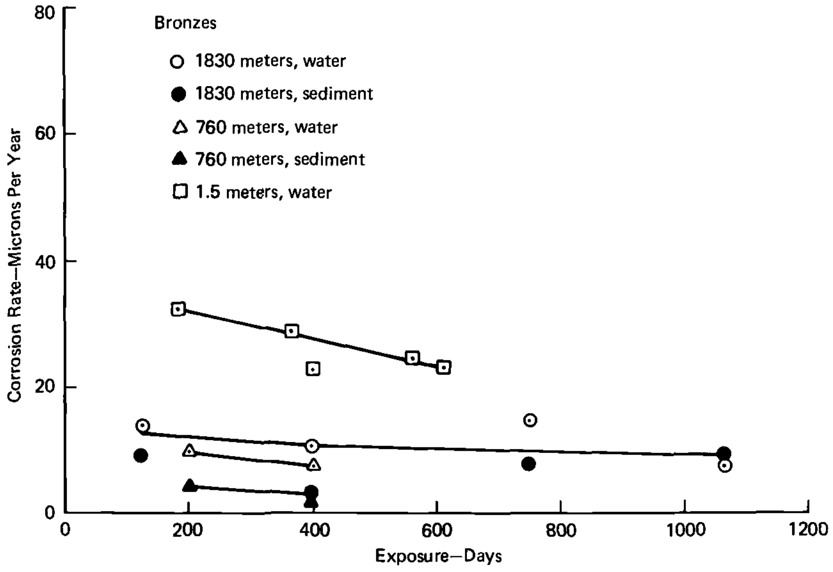

FIG. 5—*Effect of duration of exposure on the average corrosion rates of the bronzes.*

TABLE 6—*Chemical composition of copper alloys (bronzes), percent by weight.*

Alloy	CDA No.[a]	Cu	Sn	Zn	Ni	Al	Fe	Si	Other
G bronze[b]	905	88.0	2.0	10.0	...	...	...	...	...
Modified G bronze[b]	903	88.0	8.0	4.0	...	...	...	...	...
M bronze[b]	962	88.2	6.0	4.0	...	...	...	...	2.0Pb
Leaded Sn bronze[b]	836	85.0	5.0	5.0	...	...	...	...	5.0Pb
Phosphor bronzeA	510	94.64	4.94	0.10	...	...	0.05	...	0.26P
Phosphor bronze A	510	96.0	4.0	...	...	...	...	...	0.25P
Phosphor bronze A	510	95.62	4.44	0.10	...	...	0.05	...	0.06P
Phosphor bronze D	524	90.00	9.23	0.10	...	...	0.05	...	0.17P
Al-bronze	606	95.0	...	...	...	5.0	...	...	...
Al-bronze	606	95.11	...	...	...	4.76	0.05	...	...
Al-bronze D	614	90.11	...	0.15	...	6.59	3.15	...	0.02Pb
Al-bronze, 7%	614	90.0	...	...	...	7.0	3.0	...	...
Al-bronze, 10%[b]	953	89.0	...	...	...	10.0	1.0	...	...
Al-bronze, 11%[b]	954	86.0	...	...	...	10.0	4.0	...	...
Al-bronze, 13%[b]	...	83.0	...	...	...	13.0	4.0	...	...
Ni-Al bronze No. 1[b]	955	80.0	...	...	4.0	11.0	4.0	...	1.0Mn
Ni-Al bronze No. 2[b]	...	80.0	...	...	5.0	10.0	4.0	...	0.5Mn
Ni-Al bronze No. 3[b]	958	80.0	...	...	5.0	9.0	3.5	...	3.0Mn
Si-bronze, 3%	653	97.0	...	...	...	...	...	3.0	...
Si-bronze A	655	95.49	...	...	...	...	0.02	3.28	1.18Mn
Si-bronze A	655	95.0	...	...	...	...	...	3.0	1.0Mn
Ni-Vee bronze A[b]	947	88.0	5.0	2.0	5.0	...	...	...	...
Ni-Vee bronze B[b]	948	87.0	5.0	2.0	5.0	...	...	1.0	...
Ni-Vee bronze C[b]	...	80.0	5.0	5.0	5.0	...	...	5.0	...

[a] Copper Development Association alloy number.

[b] Cast alloy.

TABLE 7—*Corrosion rates and types of corrosion of bronzes.*

Alloy, CDA No.[a]	Environment[b]	Exposure, days	Depth, m	Oxygen, ml/liter, avg	Corrosion Rate, μm/year	Types of Corrosion[c]
905[d]	W	123	1720	1.35	13	U
905[d]	S	123	1720	...	8	U
905[d]	W	403	2070	1.35	18	U
905[d]	S	403	2070	...	3	GBSL
905[d]	W	751	1720	1.35	18	U
905[d]	S	751	1720	...	8	U
905[d]	W	1064	1615	1.35	8	U
905[d]	S	1064	1615	...	10	U
905[d]	W	197	715	0.40	5	U
905[d]	S	197	715	...	3	I C
905[d]	W	402	720	0.40	8	U
905[d]	S	402	720	...	3	ET
905[d]	W	181	1.5	5.75	33	G
905[d]	W	366	1.5	5.75	31	CR,229 μm
903[d]	W	123	1720	1.35	13	U
903[d]	S	123	1720	...	8	U
903[d]	W	403	2070	1.35	10	U
903[d]	S	403	2070	...	3	U
903[d]	W	751	1720	1.35	18	U
903[d]	S	751	1720	...	10	C,483 μm
903[d]	W	1064	1615	1.35	10	C,457 μm;P
903[d]	S	1064	1615	...	13	U
903[d]	W	197	715	0.40	8	U
903[d]	S	197	715	...	5	NU ET
903[d]	W	402	720	0.40	8	U
903[d]	S	402	720	...	3	ET
903[d]	W	181	1.5	5.75	33	G
903[d]	W	366	1.5	5.75	25	CR,178 μm
922[d]	W	123	1720	1.35	13	U
922[d]	S	123	1720	...	10	U
922[d]	W	403	2070	1.35	10	U
922[d]	S	403	2070	...	3	U
922[d]	W	751	1720	1.35	18	U
922[d]	S	751	1720	...	8	U
922[d]	W	1064	1615	1.35	10	U
922[d]	S	1064	1615	...	10	U
922[d]	W	197	715	0.40	10	U
922[d]	S	197	715	...	3	ET
922[d]	W	402	720	0.40	8	U
922[d]	S	402	720	...	3	ET
922[d]	W	181	1.5	5.75	41	G
922[d]	W	366	1.5	5.75	28	CR,51 μm
836[d]	W	123	1720	1.35	10	U
836[d]	S	123	1720	...	5	U
836[d]	W	403	2070	1.35	13	U
836[d]	S	403	2070	...	3	U
836[d]	W	751	1720	1.35	15	U

(*continued*)

TABLE 7—*Continued.*

Alloy, CDA No.[a]	Environment[b]	Exposure, days	Depth, m	Oxygen, ml/liter, avg	Corrosion Rate, μm/year	Types of Corrosion[c]
836[d]	S	751	1720	...	81	S G
836[d]	W	1064	1615	1.35	10	U
836[d]	S	1064	1615	...	8	U
836[d]	W	197	715	0.40	13	U
836[d]	S	197	715	...	3	NU ET
836[d]	W	402	720	0.40	13	U
836[d]	S	402	720	...	3	ET
836[d]	W	181	1.5	5.75	36	G
836[d]	W	366	1.5	5.75	33	CR,127 μm
510	W	123	1720	1.35	14	U
510	S	123	1720	...	10	U
510	W	403	2070	1.35	6	ET
510	S	403	2070	...	5	GBSL
510	W	751	1720	1.35	6	ET
510	S	751	1720	...	3	U
510	W	1064	1615	1.35	8	U
510	S	1064	1615	...	10	G
510	W	197	715	0.40	9	U
510	S	197	715	...	4	I C[e]
510	W	402	720	0.40	4	ET
510	S	402	720	...	5	EWO
510	W	181	1.5	5.75	34	P,102 μm
510	W	366	1.5	5.75	33	CR,127 μm
510	W	588	1.5	5.75	33	CR,381 μm;C,76 μm
510	W	608	1.5	5.75	28	CR,381 μm
524	W	123	1720	1.35	13	U
524	S	123	1720	...	10	U
524	W	403	2070	1.35	5	ET
524	S	403	2070	...	8	ET
524	W	751	1720	1.35	8	U
524	S	751	1720	...	10	NU
524	W	197	715	0.40	10	U
524	S	197	715	...	5	U
524	W	402	720	0.40	3	U
524	S	402	720	...	3	U
524	W	181	1.5	5.75	28	NU
524	W	398	1.5	5.75	23	P,102 μm
524	W	540	1.5	5.75	18	CR,51 μm
524	W	608	1.5	5.75	18	CR,178 μm;C,127 μm
606	W	123	1720	1.35	15	U
606	S	123	1720	...	10	U
606	W	403	2070	1.35	5	SL DA
606	S	403	2070	...	3	U
606	W	751	1720	1.35	8	SL DA
606	S	751	1720	...	5	V SL DA
606	W	1064	1615	1.35	5	CR,127
606	S	1064	1615	...	13	U

(continued)

TABLE 7—*Continued.*

Alloy, CDA No.[a]	Environment[b]	Exposure, days	Depth, m	Oxygen, ml/liter, avg	Corrosion Rate, µm/year	Types of Corrosion[c]
606	W	197	715	0.40	10	U
606	S	197	715	...	5	NU ET
606	W	402	720	0.40	5	U
606	S	402	720	...	3	ET
606	W	181	1.5	5.75	28	G
606	W	366	1.5	5.75	18	G
614	W	123	1720	1.35	14	SL DA
614	S	123	1720	...	9	U
614	W	403	2070	1.35	11	SL DA;C,305;P,305 µm, 168 avg
614	S	403	2070	...	9	SL DA;C,330;P,406 µm, 254 avg
614	W	751	1720	1.35	25	MD DA;C,178;P,305 µm, 201 avg
614	S	751	1720	...	5	V SL DA
614	W	1064	1615	1.35	5	CR,178
614	S	1064	1615	...	5	MO DA
614	W	197	715	0.40	8	U
614	S	197	715	...	4	ET
614	W	402	720	0.40	5	ET
614	S	402	720	...	4	SL DA
614	W	181	1.5	5.75	47	NU DA
614	W	366	1.5	5.75	15	G
614	W	588	1.5	5.75	23	SL DA;CR,1118 µm; C,508 µm
953[d]	W	123	1720	1.35	18	SL DA
953[d]	S	123	1720	...	15	SL DA
953[d]	W	403	2070	1.35	18	MO DA
953[d]	S	403	2070	...	3	SL DA
953[d]	W	751	1720	1.35	58	G
953[d]	S	751	1720	...	23	U SL DA
953[d]	W	1064	1615	1.35	5	U
953[d]	S	1064	1615	...	10	SL DA
953[d]	W	197	715	0.40	8	MO DA
953[d]	S	197	715	...	5	MO DA
953[d]	W	402	720	0.40	8	S DA
953[d]	S	402	720	...	3	MO DA
953[d]	W	181	1.5	5.75	53	MO DA
953[d]	W	366	1.5	5.75	33	MO DA
954[d]	W	123	1720	1.35	13	V SL DA
954[d]	S	123	1720	...	10	V SL DA
954[d]	W	403	2070	1.35	3	SL DA
954[d]	S	403	2070	...	3	SL DA
954[d]	W	751	1720	1.35	20	SL DA
954[d]	S	751	1720	...	3	V SL DA
954[d]	W	1064	1615	1.35	3	SL DA
954[d]	S	1064	1615	...	5	MO DA
954[d]	W	197	715	0.40	5	SL DA[f]

(*continued*)

TABLE 7—*Continued.*

Alloy, CDA No.[a]	Environment[b]	Exposure, days	Depth, m	Oxygen, ml/liter, avg	Corrosion Rate, μm/year	Types of Corrosion[c]
954[d]	S	197	715	...	3	SL DA[g]
954[d]	W	402	720	0.40	5	MO DA
954[d]	S	402	720	...	3	SL DA
954[d]	W	366	1.5	5.75	28	U
Al-Bz, 13%[d]	W	123	1720	1.35	13	V SL DA
Al-Bz, 13%[d]	S	123	1720	...	13	V SL DA
Al-Bz, 13%[d]	W	403	2070	1.35	15	S DA
Al-Bz, 13%[d]	S	403	2070	...	3	SL DA
Al-Bz, 13%[d]	W	751	1720	1.35	48	S DA
Al-Bz, 13%[d]	S	751	1720	...	13	MO DA
Al-Bz, 13%[d]	W	1064	1615	1.35	15	S DA
Al-Bz, 13%[d]	S	1064	1615	...	8	SL DA
Al-Bz, 13%[d]	W	197	715	0.40	10	MO DA
Al-Bz, 13%[d]	S	197	715	...	3	SL DA
Al-Bz, 13%[d]	W	402	720	0.40	8	MO DA
Al-Bz, 13%[d]	S	402	720	...	3	SL DA
Al-Bz, 13%[d]	W	181	1.5	5.75	53	S DA
Al-Bz, 13%[d]	W	366	1.5	5.75	48	S DA
955[d]	W	123	1720	1.35	10	I P
955[d]	S	123	1720	...	5	I P
955[d]	W	403	2070	1.35	8	I P
955[d]	S	403	2070	...	3	U
955[d]	W	751	1720	1.35	28	C,406;P
955[d]	S	751	1720	...	8	P,432
955[d]	W	1064	1615	1.35	3	P,203
955[d]	S	1064	1615	...	31	CR,762
955[d]	W	197	715	0.40	8	U
955[d]	S	197	715	...	3	U ET
955[d]	W	366	1.5	5.75	28	U
Ni-Al Bz, No. 2	W	123	1720	1.35	13	U
Ni-Al Bz, No. 2	S	123	1720	...	8	U
Ni-Al Bz, No. 2	W	403	2070	1.35	5	I P
Ni-Al Bz, No. 2	S	403	2070	...	3	U
Ni-Al Bz, No. 2	W	751	1720	1.35	13	SL DA
Ni-Al Bz, No. 2	S	751	1720	...	5	C,330
Ni-Al Bz, No. 2	W	1064	1615	1.35	5	C,127
Ni-Al Bz, No. 2	S	1064	1615	...	13	CR,533
Ni-Al Bz, No. 2	W	197	715	0.40	8	U
Ni-Al Bz, No. 2	S	197	715	...	3	U
Ni-Al Bz, No. 2	W	402	720	0.40	5	U
Ni-Al Bz, No. 2	S	402	720	...	3	ET
Ni-Al Bz, No. 2	W	181	1.5	5.75	25	C,203
Ni-Al Bz, No. 2	W	366	1.5	5.75	10	U
958[d]	W	123	1720	1.35	10	U
958[d]	S	123	1720	...	8	U
958[d]	W	403	2070	1.35	5	U
958[d]	S	403	2070	...	3	NU ET

(continued)

TABLE 7—*Continued.*

Alloy, CDA No.[a]	Environment[b]	Exposure, days	Depth, m	Oxygen, ml/liter, avg	Corrosion Rate, μm/year	Types of Corrosion[c]
958[d]	W	751	1720	1.35	5	I P
958[d]	S	751	1720	...	3	U
958[d]	W	1064	1615	1.35	3	P,102
958[d]	S	1064	1615	...	5	CR,254
958[d]	W	197	715	0.40	8	U
958[d]	S	197	715	...	5	U
653	W	123	1720	1.35	33	U
653	S	123	1720	...	38	U
653	W	403	2070	1.35	31	MO CO
653	S	403	2070	...	10	GBSL
653	W	751	1720	1.35	25	U
653	S	751	1720	...	18	U
653	W	1064	1615	1.35	15	MO CO
653	S	1064	1615	...	10	SL CO
653	W	197	715	0.40	28	U
653	S	197	715	...	3	NU ET
653	W	402	720	0.40	31	U
653	S	402	720	...	5	ET
653	W	181	1.5	5.75	43	U
653	W	366	1.5	5.75	28	G
655	W	123	1720	1.35	38	U
655	S	123	1720	...	42	U
655	W	403	2070	1.35	31	U
655	S	403	2070	...	25	ET;GBSL
655	W	751	1720	1.35	28	S CO
655	S	751	1720	...	23	G
655	W	1064	1615	1.35	15	SL CO
655	S	1064	1615	...	10	U
655	W	197	715	0.40	25	U
655	S	197	715	...	10	U
655	W	402	720	0.40	23	ET
655	S	402	720	...	11	ET
655	W	181	1.5	5.75	43	U
655	W	366	1.5	5.75	31	G
655	W	398	1.5	5.75	28	U
655	W	540	1.5	5.75	64	CR,762;C,381
655	W	588	1.5	5.75	23	CR,229
947[d]	W	123	1720	1.35	18	U
947[d]	S	123	1720	...	13	U
947[d]	W	403	2070	1.35	15	U
947[d]	S	403	2070	...	8	U
947[d]	W	751	1720	1.35	66	S CR[h]
947[d]	S	751	1720	...	10	U
947[d]	W	1064	1615	1.35	56	CR,508
947[d]	S	1064	1615	...	8	U
947[d]	W	197	715	0.40	15	U
947[d]	S	197	715	...	3	NU ET

(continued)

TABLE 7—*Continued.*

Alloy, CDA No.[a]	Environment[b]	Exposure, days	Depth, m	Oxygen, ml/liter, avg	Corrosion Rate, μm/year	Types of Corrosion[b]
947[d]	W	402	720	0.40	10	U
947[d]	S	402	720	...	3	ET
947[d]	W	181	1.5	5.75	51	P,178
947[d]	W	366	1.5	5.75	38	CR,254 μm
948[d]	W	123	1720	1.35	15	U
948[d]	S	123	1720	...	10	U
948[d]	W	403	2070	1.35	13	U
948[d]	S	403	2070	...	3	U
948[d]	W	751	1720	1.35	13	U
948[d]	S	751	1720	...	8	U
948[d]	W	1064	1615	1.35	8	U
948[d]	S	1064	1615	...	10	U
948[d]	W	197	715	0.40	15	U
948[d]	S	197	715	...	3	NU ET
948[d]	W	402	720	0.40	31	U
948[d]	S	402	720	...	3	ET
948[d]	W	181	1.5	5.75	48	P,102
948[d]	W	366	1.5	5.75	33	CR,152 μm
Ni-Vee Bz C[d]	W	123	1720	1.35	20	U
Ni-Vee Bz C[d]	S	123	1720	...	13	U
Ni-Vee Bz C[d]	W	403	2070	1.35	20	U
Ni-Vee Bz C[d]	S	403	2070	...	5	U
Ni-Vee Bz C[d]	W	751	1720	1.35	51	G
Ni-Vee Bz C[d]	S	751	1720	...	10	U
Ni-Vee Bz C[d]	W	1064	1615	1.35	13	U
Ni-Vee Bz C[d]	S	1064	1615	...	8	U
Ni-Vee Bz C[d]	W	197	715	0.40	20	U
Ni-Vee Bz C[d]	S	197	715	...	3	ET
Ni-Vee Bz C[d]	W	402	720	0.40	15	U
Ni-Vee Bz C[d]	S	402	720	...	3	ET
Ni-Vee Bz C[d]	W	181	1.5	5.75	46	U
Ni-Vee Bz C[d]	W	366	1.5	5.75	38	CR,127 μm

[a] Copper Development Association alloy number.

[b] W = totally exposed in seawater on sides of structure; S = exposed in base of structure so that a portion of each specimen was exposed in the bottom sediments.

[c] Symbols for types of corrosion: C = crevice; CO = coppering, a selective attack where copper appears on surface similar to dezincification; CR = cratering; DA = dealuminification; ET = etching; EWO = etched only in the water; G = general; GBSL = general below sediment line; I = incipient; MD = medium; MO = moderate; NU = nonuniform; P = pitting; S = severe; SL = slight; U = uniform; V = very. Numbers indicate microns; that is, 20 = 20 microns, 20 μm = 20 microns maximum.

[d] Cast alloy.

[e] Pitting in bottom sediment, 305 μm.

[f] At spacer.

[g] At crevice.

[h] In one small area only.

Bz = bronze.

Copper-Nickel Alloys—The chemical compositions of the copper-nickel (Cu-Ni) alloys are given in Table 8 and their corrosion rates and types of corrosion in Table 9.

The copper-nickel alloys corroded uniformly except for alloy 716.

The corrosion rates of the copper-nickel alloys 704, 706, 962, 710, 715, and 55-45 were so similar that their averages were plotted in Fig. 6. The corrosion rates in surface seawater were constant and about the same as those at the 1830 m depth. The corrosion rates in both seawater and the bottom sediments decreased with increasing duration of exposure and

TABLE 8—*Chemical composition of copper-nickel alloys, percent by weight.*

Alloy	CDA No.[a]	Cu	Ni	Fe	Mn	Zn	Pb
Cu-Ni, 95-5	704	91.98	6.25	1.24	0.53	...	...
Cu-Ni, 90-10	706	89.04	9.42	1.16	0.38	...	...
Cu-Ni, 90-10	706	89.0	10.0	1.4	0.5	...	...
Cu-Ni, 90-10	962[b]	86.0	11.0	1.4	1.3	...	...
Cu-Ni, 80-20	710	78.62	20.41	0.62	0.35	...	...
Cu-Ni, 80-20	711	80.0	20.0	0.03	0.2	...	...
Cu-Ni, 70-30	715	68.61	30.53	0.53	0.33	...	...
Cu-Ni, 70-30	715	69.0	30.0	0.6	0.4	...	...
Cu-Ni, 70-30	716	64.02	29.95	5.27	0.75	...	...
Cu-Ni, 55-45	...	54.0	45.0	0.1	1.0	...	...
Cu-Ni-Zn-Pb	...	62.0	25.0	...	...	8.0	5.0
Nickel-silver	752	65.0	18.0	...	...	17.0	...

[a] Copper Development Association alloy number.
[b] Cast alloy.

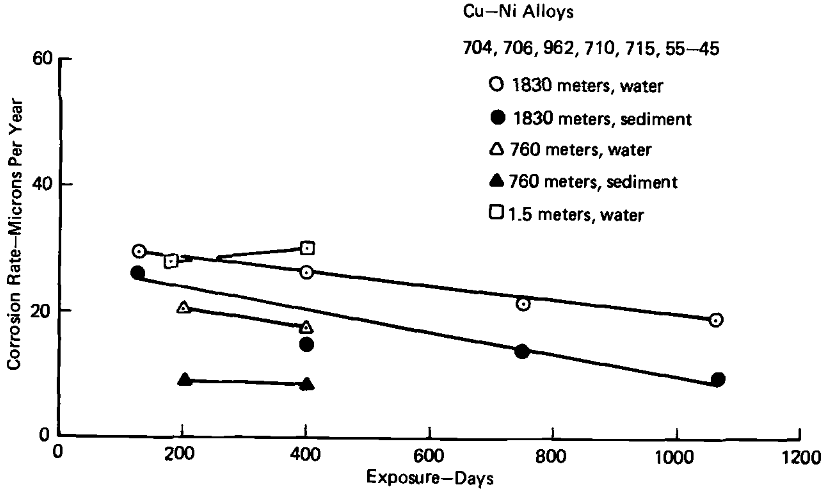

FIG. 6—*Effect of duration of exposure on the corrosion rates of copper-nickel alloys.*

TABLE 9—*Corrosion rates and types of corrosion of copper-nickel alloys.*

Alloy, CDA No.[a]	Environment[b]	Exposure, days	Depth, m	Oxygen, ml/liter, avg	Corrosion Rate, μm/year	Types of Corrosion[c]
704	W	123	1720	1.35	38	U
704	S	123	1720	...	38	U
704	W	403	2070	1.35	20	U
704	S	403	2070	...	20	U
704	W	751	1720	1.35	18	U
704	S	751	1720	...	15	U
704	W	197	715	0.40	23	U
704	S	197	715	...	15	U
704	W	402	720	0.40	23	U
704	S	402	720	...	20	U
706	W	123	1720	1.35	30	U
706	S	123	1720	...	25	U
706	W	403	2070	1.35	18	U
706	S	403	2070	...	9	U
706	W	751	1720	1.35	16	U
706	S	751	1720	...	13	U
706	W	1064	1615	1.35	18	U
706	S	1064	1615	...	5	G
706	W	197	715	0.40	20	U
706	S	197	715	...	7	U
706	W	402	720	0.40	19	U
706	S	402	720	...	7	U[d]
706	W	181	1.5	5.75	25	NU
706	W	366	1.5	5.75	15	U
706	W	608	1.5	5.75	13	U
962[e]	W	402	720	0.40	18	U
962[e]	S	402	720	...	3	ET
962[e]	W	181	1.5	5.75	28	U
962[e]	W	366	1.5	5.75	23	U
710	W	123	1720	1.35	31	U
710	S	123	1720	...	33	U
710	W	403	2070	1.35	31	ET
710	S	403	2070	...	25	ET
710	W	751	1720	1.35	20	U
710	W	197	715	0.40	18	U
710	S	197	715	...	13	U
710	W	402	720	0.40	15	U
710	S	402	720	...	13	U[f]
711	W	123	1720	1.35	48	U
711	S	123	1720	...	28	U
711	W	403	2070	1.35	38	U
711	S	403	2070	...	3	EBSL
711	W	751	1720	1.35	33	U
711	S	751	1720	...	25	U

(*continued*)

TABLE 9—*Continued.*

Alloy, CDA No.[a]	Environment[b]	Exposure, days	Depth, m	Oxygen, ml/liter, avg	Corrosion Rate, μm/year	Types of Corrosion[c]
711	W	1064	1615	1.35	25	U
711	S	1064	1615	...	13	U
711	W	197	715	0.40	28	U
711	S	197	715	...	3	SL ET
711	W	402	720	0.40	28	U
711	S	402	720	...	5	ET
711	W	181	1.5	5.75	71	G
711	W	366	1.5	5.75	48	G
715	W	123	1720	1.35	32	U
715	S	123	1720	...	21	U
715	W	403	2070	1.35	31	U
715	S	403	2070	...	16	U
715	W	751	1720	1.35	20	U
715	S	751	1720	...	18	U
715	W	1064	1615	1.35	15	U
715	S	1064	1615	...	13	G
715	W	197	715	0.40	20	U
715	S	197	715	...	3	SL ET
715	W	402	720	0.40	14	U
715	S	402	720	...	6	U
715	W	181	1.5	5.75	13	U
715	W	366	1.5	5.75	10	G
715	W	398	1.5	5.75	10	U
715	W	608	1.5	5.75	8	I P
716	W	123	1720	1.35	5	U
716	S	123	1720	...	5	U
716	W	403	2070	1.35	3	ET
716	S	403	2070	...	3	ET
716	W	751	1720	1.35	13	C,406;CO;NU P,406 μm, 216 avg
716	S	751	1720	...	5	C,356;CO;NU P,610 μm, 203 avg
716	W	197	715	0.40	3	U
716	S	197	715	...	3	U
716	W	402	720	0.40	3	U
716	S	402	720	...	3	U
716	W	181	1.5	5.75	20	I P;C,127
716	W	398	1.5	5.75	18	CR,432 μm
716	W	608	1.5	5.75	15	C,330;CR,457
Cu-Ni 55-45	W	123	1720	1.35	18	U
Cu-Ni 55-45	S	123	1720	...	18	U
Cu-Ni 55-45	W	403	2070	1.35	31	U
Cu-Ni 55-45	S	403	2070	...	3	SL ET
Cu-Ni 55-45	W	751	1720	1.35	25	U
Cu-Ni 55-45	S	751	1720	...	13	U

(continued)

TABLE 9—*Continued.*

Alloy, CDA No.[a]	Environment[b]	Exposure, days	Depth, m	Oxygen, ml/liter, avg	Corrosion Rate, μm/year	Types of Corrosion[c]
Cu-Ni 55-45	W	1064	1615	1.35	25	G
Cu-Ni 55-45	S	1064	1615	...	13	C to PR,1270;S E
Cu-Ni 55-45	W	197	715	0.40	20	U
Cu-Ni 55-45	S	197	715	...	5	I C,I P
Cu-Ni 55-45	W	402	720	0.40	18	U
Cu-Ni 55-45	S	402	720	...	3	ET
Cu-Ni 55-45	W	181	1.5	5.75	48	U
Cu-Ni 55-45	W	366	1.5	5.75	31	U
Cu-Ni-Zn-Pb	W	123	1720	1.35	23	U
Cu-Ni-Zn-Pb	S	123	1720	...	15	U
Cu-Ni-Zn-Pb	W	403	2070	1.35	20	U
Cu-Ni-Zn-Pb	S	403	2070	...	3	GBSL
Cu-Ni-Zn-Pb	W	751	1720	1.35	15	U
Cu-Ni-Zn-Pb	S	751	1720	...	13	U
Cu-Ni-Zn-Pb	W	1064	1615	1.35	13	U
Cu-Ni-Zn-Pb	S	1064	1615	...	8	U
Cu-Ni-Zn-Pb	W	197	715	0.40	13	U
Cu-Ni-Zn-Pb	S	197	715	...	3	SL ET
Cu-Ni-Zn-Pb	W	402	720	0.40	10	U
Cu-Ni-Zn-Pb	S	402	720	...	3	ET
Cu-Ni-Zn-Pb	W	181	1.5	5.75	25	U
Cu-Ni-Zn-Pb	W	366	1.5	5.75	18	U
752	W	123	1720	1.35	51	U
752	S	123	1720	...	66	U
752	W	403	2070	1.35	36	U
752	S	403	2070	...	13	GBSL
752	W	751	1720	1.35	38	U
752	S	751	1720	...	20	U
752	W	1064	1615	1.35	15	U
752	S	1064	1615	...	10	G
752	W	197	715	0.40	25	U
752	S	197	715	...	3	SL ET
752	W	402	720	0.40	25	U
752	S	402	720	...	3	ET
752	W	181	1.5	5.75	28	U
752	W	366	1.5	5.75	18	U

---

[a] Copper Development Association alloy numbers.

[b] W = totally exposed in seawater on sides of structure; S = exposed in base of structure so that a portion of each specimen was embedded in the bottom sediments.

[c] Symbols for types of corrosion: C = crevice; E = edge; ET = etching; EBSL = etched below sediment line; G = general; GBSL = general below sediment line; I = incipient; NU = nonuniform; P = pitting; S = severe; SL = slight; U = uniform. Numbers refer to microns; that is, 20 = 20 microns, 20 μm = 20 microns maximum.

[d] Much less below sediment line.

[e] Cast alloy.

[f] No visible corrosion below sediment line.

those in the bottom sediments were nearly the same as those in the seawater. Corrosion was slower at the 760 m depth than at the 1830 m depth, with the corrosion rates being practically constant with increasing duration of exposure and those in the bottom sediments slightly lower than those in the seawater.

The effect of duration of exposure on the corrosion rates of alloy 711 (80-20, 0.03Fe) is shown in Fig. 7. Comparing these curves with those in Fig. 6 shows those for seawater exposure with higher corrosion rates for alloy 711 than the averages of the other alloys. These higher corrosion rates are attributed to the low iron content of alloy 711 as compared with those for the alloys in Fig. 6. The differences in the iron contents had no apparent influence in the bottom sediments.

The effect of duration of exposure on the corrosion rates of alloy 710 (70-30, 5Fe) is shown in Fig. 8. The corrosion rates in surface seawater were higher than those at depth and decreased with increasing duration of exposure. The corrosion rates at depth were very low and the same in the bottom sediments as in the seawater at both depths for the first 400 days of exposure. Between 400 and 750 days of exposure in seawater at the 1830 m depth, the corrosion rate more than doubled. This increase is attributed to the change in the protective film on this alloy. Through 400 days of exposure at both depths the specimens were protected by a thin, hard, black, shiny film which deteriorated during longer exposure periods, causing crevice and pitting corrosion. There were copious deposits of

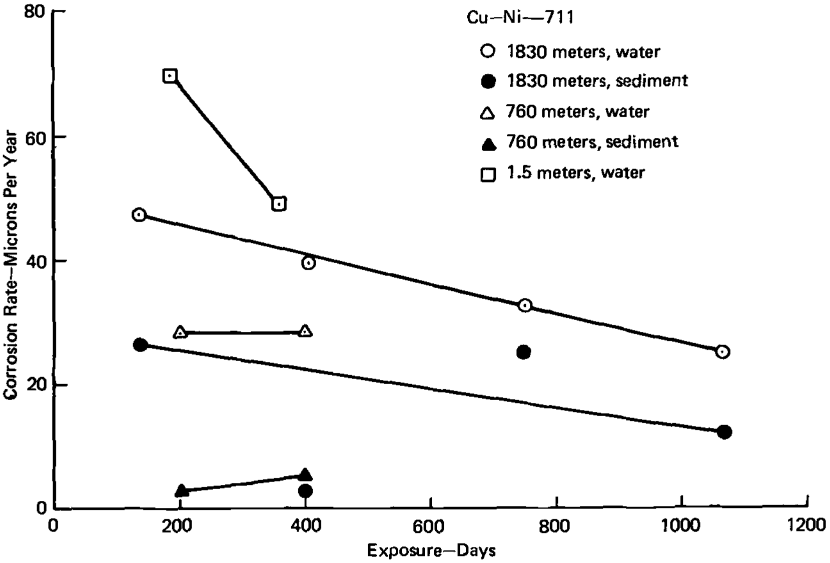

FIG. 7—*Effect of duration of exposure on the corrosion rates of copper-nickel alloy 711.*

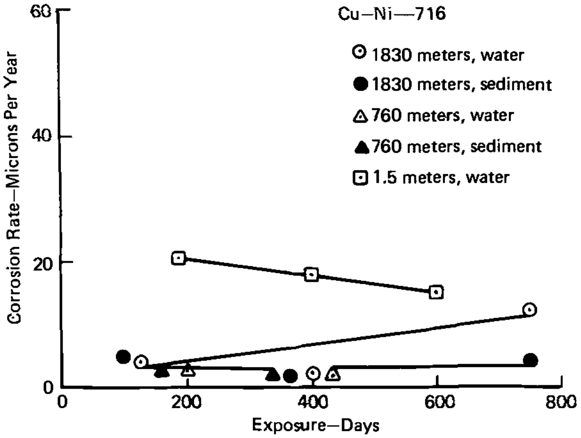

FIG. 8—*Effect of duration of exposure on the corrosion rates of copper-nickel alloy 716.*

copper on the specimens after 750 days of exposure, especially in pits and at the faying surfaces.

The curves in Fig. 8 by comparison are lower than the corresponding curves in Fig. 6.

Effect of Iron Content on Corrosion of Copper-Nickel Alloys

In the discussions of alloys 710 and 711 it was stated that the iron content of the copper-nickel alloys influenced their corrosion behavior. Curves for copper-nickel alloys with the same chemical compositions except for their iron contents are shown in Fig. 9. These curves show quite clearly that the corrosion rates decrease with increasing iron content from 0.03 to

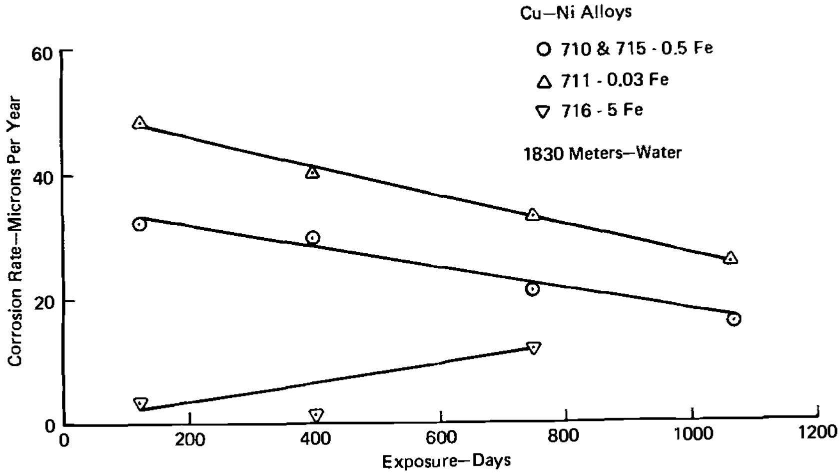

FIG. 9—*Corrosion rates of copper-nickel alloys with different iron contents.*

0.5 percent. Although the corrosion rates for the alloy with 5 percent iron were lower than those for the alloy with 0.5 percent iron for the first 400 days of exposure, its corrosion rate, thereafter, increased. If the increase continued at the same rate for longer exposure times it could have been equivalent to that of the alloy with 0.5 percent iron after about 1000 days of exposure.

The curves for the majority of the copper-base alloys in seawater at the 1830 m depth are shown in Fig. 10. The average corrosion rates decreased with increasing duration of exposure and the corrosion rates of the bronzes were lower than any of the other alloys. However, the differences in the corrosion rates of the different types of alloys were considered to be of not much practical significance; after 123 days of exposure the maximum spread in values was about 25 μm per year and after 1064 days of exposure this spread in values had decreased to 12 μm per year.

Parting Corrosion

Parting corrosion is also known as selective corrosion, dezincification, dealuminification, desiliconization, denickelification, etc. It is the selective corrosion of copper-base alloys by which the original alloy is converted into a spongy mass of copper of approximately the same size and dimensions of the original alloy but with poor mechanical properties. The most favored theory of this mechanism is that the metal corrodes as an alloy and the copper is subsequently redeposited.

Because it is not possible to remove all the corrosion products (redeposited, spongy copper) it is not possible to obtain true weight losses from which to calculate corrosion rates. Therefore, corrosion rates so obtained

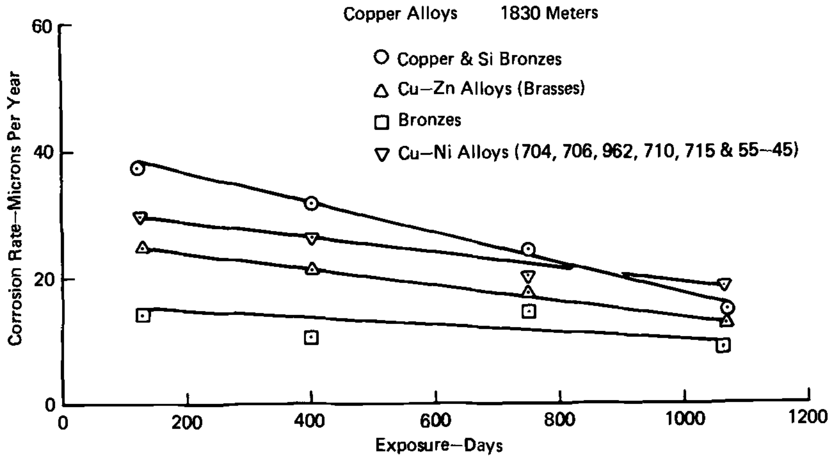

FIG. 10—*Effect of duration of exposure on the corrosion rates of copper alloys in seawater at the 1830 m depth.*

are always lower than they are actually. Hence, corrosion rates determined for alloys attacked by parting corrosion, particularly those severely attacked are not reliable for assessing the corrosion of such alloys.

Brasses—There was parting corrosion of alloys 220, 230, 268, 270, 280, Tobin Bronze, 675, and 868, varying in degree from slight to severe. The alloys most severely attacked were 280, Tobin Bronze, and 675. Twenty-eight percent of the thickness of the 3-mm-thick specimens of alloy 280 was affected by parting corrosion. Because of the extensive parting corrosion of alloys 280 and 675, corrosion rates considerably higher than those of the other brasses were found; also, they were rather erratic with respect to the duration of exposure.

Bronzes—There was parting corrosion of alloys 606, 614, 953, 954, 13 percent aluminum bronze, nickel-aluminum bronze No. 2, 653, and 655, varying in degree from slight to severe.

One specimen of wrought alloy 606, about half the specimens of wrought alloy 614, and all the specimens of cast alloys 953, 954, and 13 percent aluminum bronze were attacked by parting corrosion. The cast alloys were more severely attacked than were the wrought alloys.

Williams [*17*] has reported that parting corrosion was found on wrought aluminum bronzes containing 6.5 to 11 percent aluminum after exposure in surface seawater and that an aluminum bronze containing 6 to 8 percent aluminum and 3.5 percent iron was not attacked. In this investigation, slight parting corrosion was found on a wrought aluminum bronze (alloy 606) containing 4.76 percent aluminum and less than 0.05 percent iron, at the 1830 m depth. There was more parting corrosion on two lots of wrought aluminum bronze (alloy 614) containing about 7 percent aluminum and 3 percent iron than on alloy 606 at both the 760 and 1830 m depths. The three cast aluminum bronzes, 953 (10 percent aluminum), 954 (11 percent aluminum) and 13 percent aluminum, were the most severely attacked of all the aluminum bronzes.

Effect of Concentration of Oxygen

The effect of the concentration of oxygen in seawater on the corrosion of copper alloys is shown in Figs. 11 and 12.

The statement "effect of concentration of oxygen in seawater on the corrosion of copper alloys" is not to be construed as the effect of the sole variable "oxygen." It is not possible in tests conducted in unaltered seawater as encountered in the open ocean to separate the effect of any one variable from those of the other variables in order to study the influence of that variable alone. A study of the variables determined in seawater during these exposures has shown that the effects of the concentration of oxygen are considerably greater than any of the others, either individually

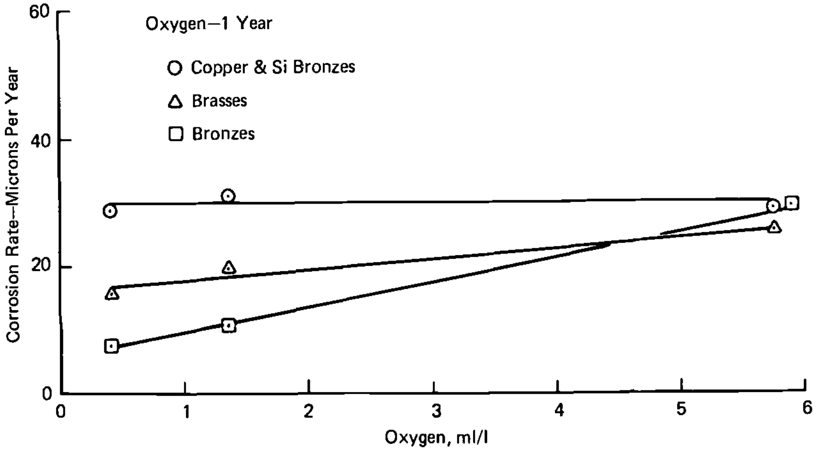

FIG. 11—*Effect of concentration of oxygen in seawater on the corrosion of copper alloys.*

or combined. These other variables, shown in Fig. 2, were temperature, pH, salinity, and depth.

Therefore, the following discussion on the effect of oxygen concentration is understood to also reflect the lesser effects of the other variables.

As shown in Fig. 11, the corrosion of copper and the silicon bronzes was not affected by changes in the concentration of oxygen in seawater within

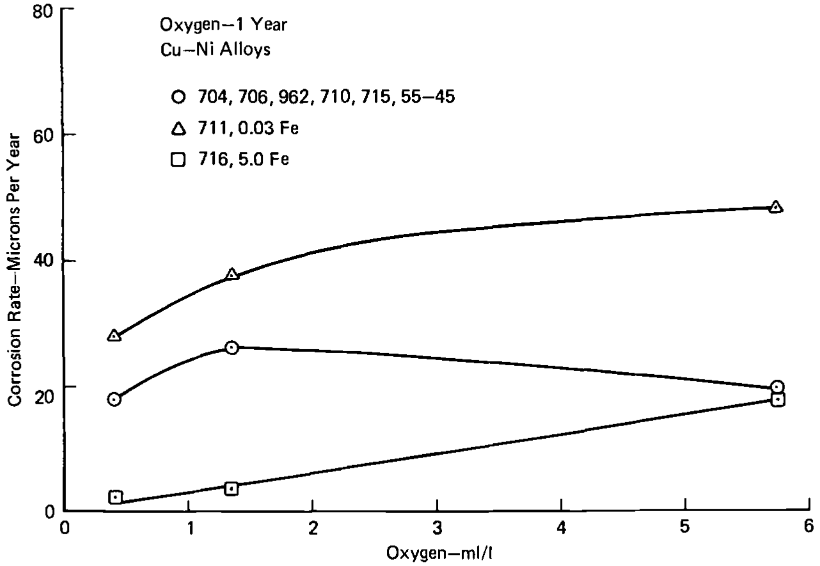

FIG. 12—*Effect of concentration of oxygen in seawater on the corrosion of copper-nickel alloys.*

the range of 0.4 to 5.75 ml of oxygen per liter of seawater. However, the average corrosion rates of the brasses increased linearly and slightly with increasing concentration of oxygen. The average corrosion rates of the bronzes also increased linearly with increasing concentration of oxygen at a greater rate than did the brasses.

The average corrosion rates of the copper-nickel alloys and alloy 711 (0.03Fe) were not directly proportional to changes in the concentration of oxygen in seawater, Fig. 12. However, the corrosion rate of alloy 716 (70-30 5Fe) increased linearly with increasing concentration of oxygen.

Effect of Depth

The effect of depth on the corrosion of copper alloys is shown in Figs. 13 and 14.

Depth does not appear to exert any significant influence on the corrosion of copper, the silicon bronzes, and the brasses as shown in Fig. 13. Although there was a decrease in the average corrosion rate for the bronzes to a depth of 760 m, this was not considered to be of any practical importance.

The curves in Fig. 14 indicate that (1) the corrosion rates of most of the copper-nickel alloys were insensitive to changes in depth; (2) the corrosion rate of alloy 752 (nickel-silver) increased slightly with depth, but not significantly; and (3) the corrosion rates of alloys 711 (80-20, 0.03Fe) and 716 (70-30 5Fe) decreased with depth to 760 m, which again, for practical purposes, is not considered significant.

Stress Corrosion

Specimens of alloys 102, 280, 443, 510, 524, 606, 655, 704, 706, 710, 715, and 716 were exposed at depths of 760 and 1830 m for periods of time up to 400 days. Specimens were exposed, mostly in triplicate, at stresses equivalent to 35, 50, and 75 percent of the yield strength of the alloy.

There were no failures caused by stress corrosion.

Corrosion Products

When it was possible, corrosion products were obtained from some of the alloys for chemical analyses. Analytical methods used were: X-ray diffraction, spectrographic, infrared spectrophotometric, and quantitative analyses.

Corrosion products removed from alloy 868 after 403 days of exposure at a depth of 1830 m were composed of cupric chloride, copper hydroxychloride, copper as metal 35.98 percent, minor amounts of aluminum, iron, silicon and sodium, chloride ions 0.91 percent, sulfate ions 11.53 percent.

Corrosion products removed from some of the aluminum bronzes were composed of copper oxychloride, cupric chloride, major elements copper

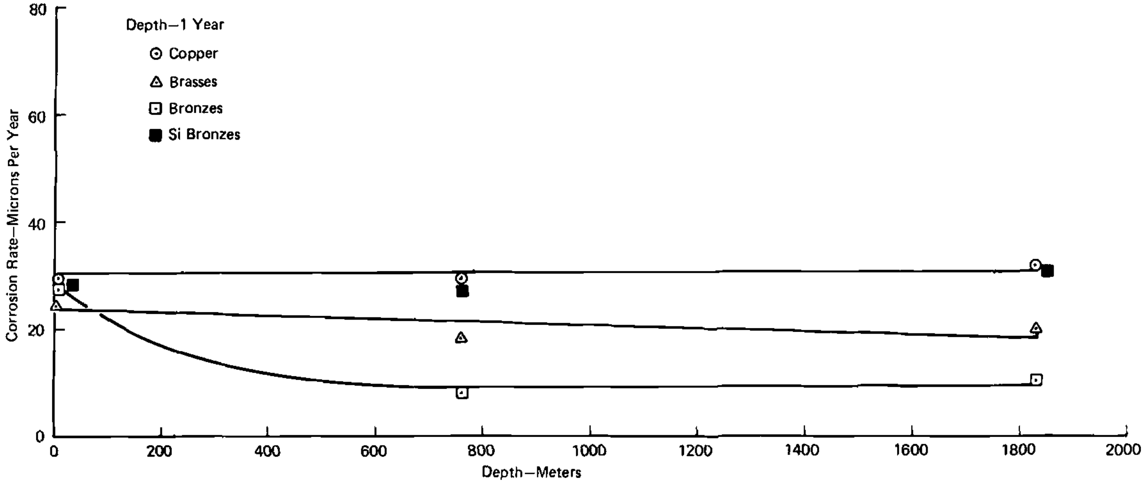

FIG. 13—*Effect of depth on the corrosion of copper alloys.*

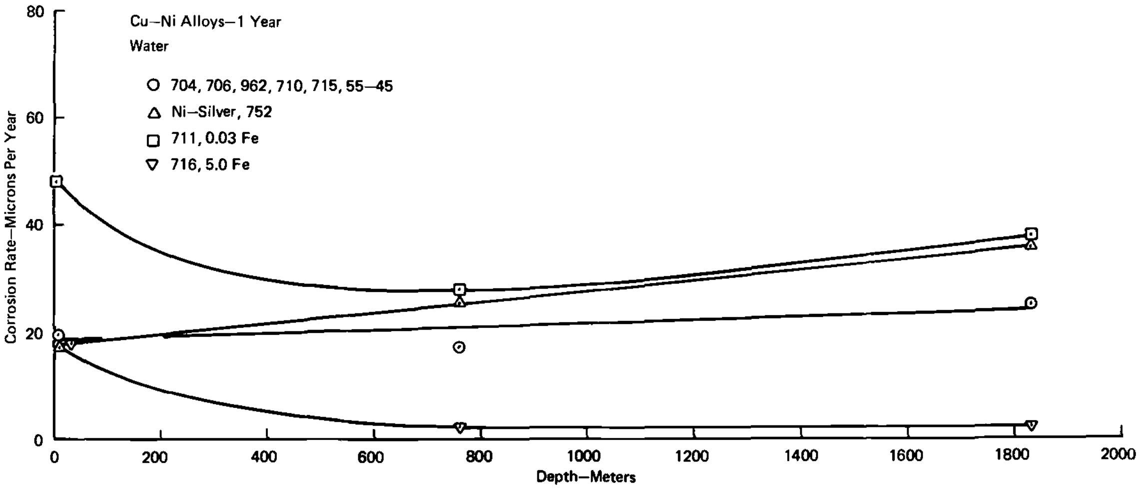

FIG. 14—*Effect of depth on the corrosion of copper-nickel alloys.*

and aluminum, minor elements iron, magnesium, calcium and silicon, chloride ion 0.9 percent, and sulfate ion 9.0 percent.

Corrosion products removed from alloy 716, exposed for 751 days at the 1830 m depth, were composed of nickel hydroxide, cupric chloride, major elements copper and nickel, minor elements iron, manganese, sodium, and traces of silicon and magnesium, chloride ion 4.77 percent, sulfate ion 0.80 percent, copper as metal 43.63 percent.

Mechanical Properties

The mechanical properties of alloys 102, 172, 280, 443, 868, 510, 524, 606, 655, 704, 706, 710, 715, and 716 were determined after exposure for 402 and 751 days at depths of 760 and 1830 m.

The mechanical properties of alloys 102, 172, 443, 510, 524, 704, 706, 710, 715, and 716 were not impaired by exposures at depth in the Pacific Ocean.

The mechanical properties of alloys 280 and 868 were impaired. In both alloys the impairment increased with time of exposure at both depths. The greatest impairment was about 30 percent for the tensile and yield strengths and percentage elongation of alloy 280 after 751 days of exposure at the 1830 m depth. Also, the greatest impairment in mechanical properties of alloy 868 occurred after 751 days of exposure at the 1830 m depth. The tensile strength was decreased about 40 percent, the yield strength by about 60 percent, and the percentage elongation by about 25 percent. The degree of impairment in both cases roughly paralleled the degree of severity of the parting corrosion.

The elongation of alloy 606 was decreased considerably (28 percent), especially after 403 and 751 days of exposure at the 1830 m depth, and is attributed to pitting and parting corrosion.

The tensile and yield strengths and percentage elongation of alloy 655 were seriously impaired after 403 days of exposure in the bottom sediment at the 1830 m depth. The percentage decreases were 25, 18, and 40 percent, respectively. This decrease in mechanical properties is attributed to the severe parting corrosion of the alloy.

Summary and Conclusions

The purpose of this investigation was to determine the effects of deep-ocean environments on the corrosion of copper and copper alloys. To accomplish this a total of 1050 specimens of 46 different alloys was exposed at nominal depths of 760 and 1830 m for periods of time varying from 123 to 1064 days.

Copper (alloy 102) and beryllium-copper (alloy 172) corroded uniformly at all depths, but alloy 102 was pitted during surface exposure in the Pacific Ocean at Point Mugu, California. The corrosion rates of copper decreased linearly with increasing duration of exposure, both in seawater and in the bottom sediments at the 1830 m depth. At the 760 m depth the corrosion rates of alloy 102 were nearly constant with time; those in the seawater were comparable with those in the seawater and in the bottom sediments at the 1830 m depth while those in the bottom sediments were lower than any of the others. Copper corroded at the same rate in surface seawater in the Pacific Ocean as at depth.

The addition of 2 percent beryllium to copper did not affect its corrosion rate. Neither MIG nor TIG welding affected the corrosion of alloy 172.

Except for alloys 280 and 868, the brasses corroded at rates which decreased linearly with increasing duration of exposure in seawater and in the bottom sediments at both depths, 760 and 1830 m, as well as in the seawater at the surface. The higher corrosion rates of alloys 280 and 868 are attributed to the severe parting corrosion. The brasses corroded at higher rates in the surface seawater than at depth.

The corrosion rates of the bronzes in surface seawater decreased linearly with increasing duration of exposure. At depths of 760 and 1830 m, the corrosion rates of the bronzes, except the silicon bronzes, were constant with increasing duration of exposure, both in seawater and in the bottom sediments. Also, these corrosion rates were comparable and for all practical purposes can be considered the same.

The corrosion rates of the copper-nickel alloys, except alloy 716, in seawater and in the bottom sediments at depths of 760 and 1830 m, and in surface seawater, decreased linearly with increasing duration of exposure. However, the corrosion rates in the bottom sediments were lower than those in seawater.

Alloy 716 corroded at slower rates than did the others and at essentially the same rates at depth both in seawater and in the bottom sediments, except for the specimens exposed in the seawater for 751 days at a depth of 1830 m. These slower corrosion rates are attributed to the hard, shiny, black, impervious film which formed on its surfaces, and which did not deteriorate until after 400 days of exposure.

All the copper-nickel alloys, except alloys 716 and 55-45, corroded uniformly. Alloy 716 was attacked by pitting and crevice corrosion after 751 days of exposure at the 1830 m depth, and alloy 55-45 was perforated by crevice corrosion after 1064 days of exposure at the 1830 m depth. The average corrosion rates of copper-nickel alloys 704, 706, 962, 710, 715, and 55-45 at the surface were the same as those in seawater at the 1830 m depth. The corrosion rates of alloys 711 and 716 in surface seawater were higher than those at depth.

In general, as the iron content of the copper-nickel alloys increased from 0.03 to 5 percent, their corrosion rates decreased.

Except for alloys 102, 653, 655, 711, and 716, the corrosion rates of the copper-base alloys increased linearly with increasing concentration of oxygen in seawater. The corrosion rates of alloys 102, 653, and 655 were insensitive to changes in the concentration of oxygen. Changes in the concentration of oxygen in seawater did not exert a uniform influence on the corrosion rates of alloys 711 and 716.

Depth did not influence the corrosion rates of the copper alloys to any significant extent.

The copper alloys were not susceptible to stress corrosion cracking in seawater, either at the surface or at depth.

Corrosion products were composed of cupric chloride, copper hydroxychloride, copper oxychloride, nickel chloride, copper, nickel, aluminum, iron, silicon, sodium, magnesium, calcium, manganese, chloride ion, and sulfate ion.

Only the mechanical properties of the alloys severely attacked by parting corrosion were adversely affected.

References

[*1*] Reinhart, F. M., "Corrosion of Materials in Hydrospace—Part I—Irons, Steels, Cast Irons and Steel Products," NCEL Technical Note N-900, U. S. Naval Civil Engineering Laboratory, Port Hueneme, Calif., July 1967.

[*2*] Reinhart, F. M., "Corrosion of Materials in Hydrospace," NCEL Technical Report R-504, U. S. Naval Civil Engineering Laboratory, Port Hueneme, Calif., Dec. 1966.

[*3*] Reinhart, F. M., "Corrosion of Materials in Hydrospcae—Part II—Nickel and Nickel Alloys," NCEL Technical Note N-915, U. S. Naval Civil Engineering Laboratory, Port Hueneme, Calif., Aug. 1967.

[*4*] Reinhart, F. M., "Corrosion of Materials in Hydrospace—Part III—Titanium and Titanium Alloys," NCEL Technical Note N-921, U. S. Naval Civil Engineering Laboratory, Port Hueneme, Calif., Sept. 1967.

[*5*] Reinhart, F. M., "Preliminary Examination of Materials Exposed on STU 1-3 in the Deep Ocean—(5,640 Feet of Depth for 123 Days)," NCEL Technical Note N-605, U. S. Naval Civil Engineering Laboratory, Port Hueneme, Calif., June 1964.

[*6*] Reinhart, F. M., "Examples of Corrosion of Materials Exposed on STU 11-1 in the Deep Ocean—(2,340 Feet of Depth for 197 Days)," NCEL Technical Note N-695, U. S. Naval Civil Engineering Laboratory, Port Hueneme, Calif., Feb. 1965.

[*7*] Reinhart, F. M., "Effect of Deep Ocean Environments on the Corrosion of Selected Alloys," NCEL Technical Note N-781, U. S. Naval Civil Engineering Laboratory, Port Hueneme, Calif., Oct. 1965.

[*8*] Reinhart, F. M., "Visual Observations of Corrosion of Materials on STUI-I after 1064 Days of Exposure at a Depth of 5300 Feet in the Pacific Ocean," NCEL Technical Note N-793, U. S. Naval Civil Engineering Laboratory, Port Hueneme, Calif., Nov. 1965.

[*9*] May, T. P., unpublished data, International Nickel Co., Inc., Wrightsville Beach, N. C.

[*10*] Wheatfall, W. L., "Metal Corrosion in Deep-Ocean Environments," MEL R&D Phase Report 429/66, U. S. Navy Marine Engineering Laboratory, Annapolis, Md., Jan. 1967.

[*11*] Crilly, J. B. and Haynes, W. S., "Corrosion Rates of Selected Alloys in the Deep Ocean," NCEL Technical Note N-859, U. S. Naval Civil Engineering Laboratory, Port Hueneme, Calif., Nov. 1966.

[*12*] Brown, B. F. et al., "Marine Corrosion Studies: Stress Corrosion Cracking, Deep Ocean Technology, Cathodic Protection and Corrosion Fatigue, Third Interim Report of Progress," Technical Memorandum 1634, U. S. Naval Research Laboratory, Washington, D. C., July 1965.

[*13*] Fischer, E. and Finger, S., "Corrosion at 4,500 Foot Depth in Tongue-of-the-Ocean," Technical Memorandum 3, Laboratory Project 9400-72, Mar. 1966; and Anastasio, A.

and Macander, A., "Retrieval, Examination and Evaluation of Materials Exposed for 199 Days on NASL Deep Sea Materials Exposure Mooring No. 1," Technical Memorandum 5, Laboratory Project 9300-6, U. S. Naval Applied Science Laboratory, Brooklyn, N. Y., July 1966.

[*14*] La Que, F. L. in *Corrosion Handbook*, 1948 ed., H. H. Uhlig, Ed., Wiley, New York, pp. 394–400.

[*15*] Brouillette, C. V., *Corrosion*, Vol. 14, No. 8, Aug. 1958, pp. 352t–356t.

[*16*] Southwell, C. R., Hummer, C. W., Jr., and Alexander, A. L., "Corrosion of Metals in Tropical Environments, Part 7—Copper and Copper Alloys—Sixteen Years' Exposure," NRL Report 6452, U. S. Naval Research Laboratory, Washington, D. C., Oct. 1966.

[*17*] Williams, W. L., *Journal of the American Society of Naval Engineers*, Vol. 63, 1957, pp. 453–461.

R. Baboian[1] *and G. S. Haynes*[1]

Galvanic Corrosion of Ferritic Stainless Steels in Seawater

REFERENCE: Baboian, R. and Haynes, G. S., "**Galvanic Corrosion of Ferritic Stainless Steels in Seawater,**" *Corrosion in Natural Environments, ASTM STP 558*, American Society for Testing and Materials, 1974, pp. 171–184.

ABSTRACT: Galvanic behavior of stainless steels in seawater is difficult to predict because of their susceptibility to localized corrosion. This susceptibility can be either enhanced or eliminated depending on the particular galvanic couple.

This paper deals with seawater corrosion of several ferritic stainless steels in galvanic couples. Methods of predicting their behavior are described based on electrochemical polarization measurements, various laboratory tests, and actual immersion in seawater.

Results of electrochemical and laboratory tests are compared with those obtained in seawater. The validity of each of the test procedures is discussed with regard to alloy development and designing materials systems.

KEY WORDS: corrosion, galvanic corrosion, polarization, pitting, crevice corrosion, seawater, ferritic stainless steels, protection potential

Galvanic effects occur when two or more metals are in electrical and electrolyte contact. To predict their behavior in galvanic couples, a galvanic series of metals can be constructed according to their potentials measured in a specific environment. Usually the corrosion rate of the more noble metal is decreased, and that of the more active metal is increased in a couple.

In addition to potential differences, polarization behavior of metals is also important in predicting galvanic effects. For example, metals which corrode uniformly when electrically isolated may undergo localized corrosion when galvanically coupled. Stainless steels which normally have a protective film over a wide range of potentials are susceptible to pitting and crevice corrosion in chloride-containing solutions. Galvanic couples of these alloys with other metals can either inhibit or induce localized corrosion.

---

[1] Manager and project engineer, respectively, Materials and Electrical Products Group, Product Research Department, Corrosion Laboratory, Texas Instruments Incorporated, Attleboro, Mass. 02703.

In a previous paper [*1*],[2] techniques were described to accurately predict the corrosion behavior of stainless steels in galvanic couples. By choosing a galvanic couple with a mixed potential in the proper potential region, protection of the stainless steel from localized corrosion occurred.

This paper describes methods of predicting the occurrence of galvanic corrosion of several ferritic stainless steels in seawater and how electrochemical techniques can be used to develop new alloys. The ultimate goal is to develop economic stainless steels which are compatible with the more noble metals such as copper in seawater.

Theory

Electrode Kinetics

Materials which contain several different metals and alloys are susceptible to galvanic corrosion. The difference in electrochemical potential between two or more dissimilar metals in electrical and electrolyte contact causes electron flow between them. Attack of the more noble metal or metals is usually decreased, and corrosion of the more active metal is usually increased. A galvanic series of metals can be constructed according to their potential measured in a particular environment. However, the information concerning a galvanic couple obtained from such a series is of limited value because the series is affected strongly by environmental factors such as type of electrolyte, temperature, and agitation. In addition, under the influence of galvanic coupling, appreciable polarization of the metals may occur, producing a protective film on the metal surface or causing breakdown of an already existing protective film. This effect is commonly observed with stainless steel. Thus, an overall characterization of each metal in the galvanic couple is necessary to evaluate the behavior of the metals in a particular corrosive environment.

Galvanic corrosion of metals can be treated by application of the mixed potential theory first described by Wagner and Traud [*2*]. The theory is based on two simple hypotheses: (1) any electrochemical reaction can be divided into two or more oxidation or reduction reactions, and (2) there can be no net accumulation of electrical charge during an electrochemical reaction.

Under the simplest circumstance, metallic corrosion would involve only two reactions—oxidation and reduction. The corrosion of iron in sulfuric acid (H_2SO_4) involves the anodic dissolution of iron and the evolution of hydrogen. This is demonstrated by the polarization curves for iron in 0.52 N H_2SO_4 in Fig. 1 [*3*]. The first hypothesis of the mixed potential theory is satisfied if one considers that each reaction has its own reversible potential and polarization parameters. The second hypothesis, that the total rate of oxidation equals the total rate of reduction, is only

---

[2] The italic numbers in brackets refer to the list of references appended to this paper.

satisfied at the intersection E_{corr}, the corrosion or "mixed" potential. At this point the rate of iron dissolution is equal to the rate of hydrogen evolution. The potential is so displaced from the equilibrium potential that the reverse reactions occur at a negligible rate and do not influence the corrosion rate.

In Fig. 1, the data indicate that iron will corrode at a rate of about 0.5 mA/cm^2 and will exhibit a potential of about −0.52 V versus the saturated calomel electrode (SCE).

Galvanic Couples

When two different corroding metals are coupled electrically in the same electrolyte, both metals are polarized so that each corrodes at a new rate. In Fig. 2 the corrosion potentials and polarization parameters for un-

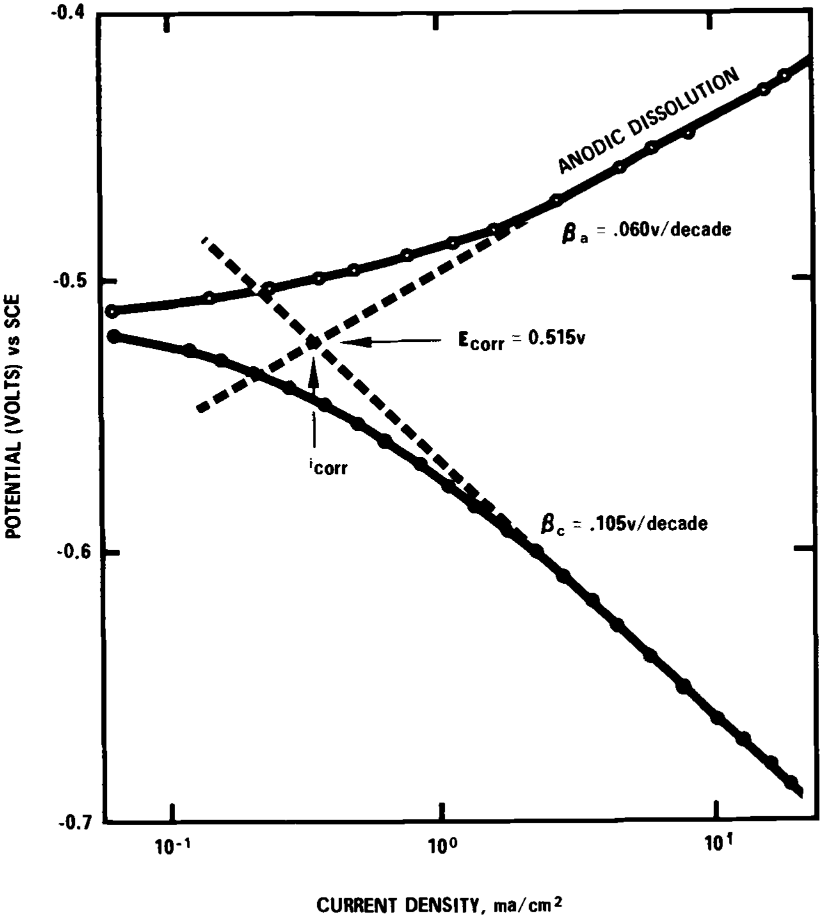

FIG. 1—*Polarization behavior of iron in 0.52 N sulfuric acid.*

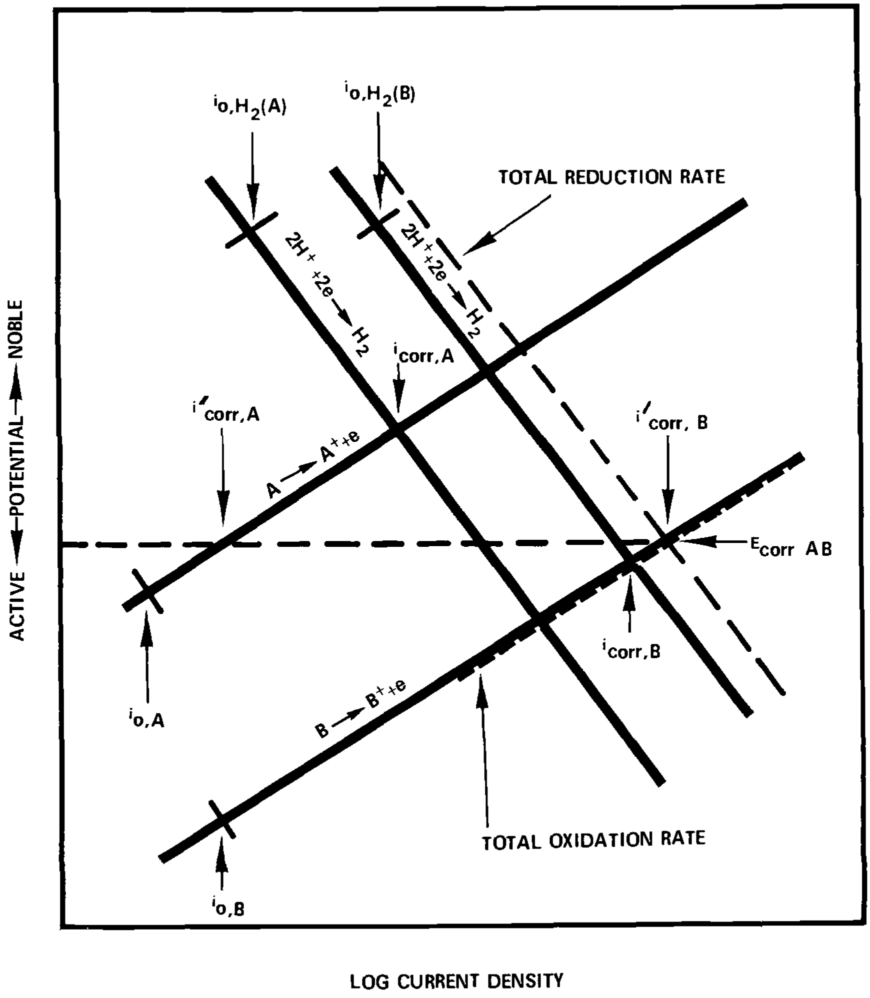

FIG. 2—*Mixed potential behavior of galvanically coupled metals.*

coupled Metals A and B are shown. Metal A is more noble than Metal B in that the equilibrium potential is less negative. When the mixed potential theory is applied to the individual reactions ($A/A+$, $H_2/H+$, $B/B+$, $H_2/H+$) the uncoupled corrosion rates are $i_{corr,A}$ for Metal A and $i_{corr,B}$ for Metal B. When equal areas of Metals A and B are coupled, the resultant mixed potential of the system $E_{corr,AB}$ is at the intersection where the total oxidation rate equals the total reduction rate. The rate of oxidation of the individual coupled metals is such that Metal A corrodes at a reduced rate $i'_{corr,A}$ and Metal B corrodes at an increased rate $i'_{corr,B}$.

The information required to predict the corrosion behavior of galvanically coupled Metals A and B is shown in Fig. 2. In addition to the anodic polarization curves for Metals A and B, it is necessary to measure the mixed potential of the galvanic couple ($E_{\text{corr},AB}$) under actual environmental conditions because the nature of the cathodic reactions can have a marked influence on the mixed potential.

Galvanic behavior of stainless steels is difficult to predict because of the passive behavior exhibited by these alloys over a wide range of potentials. In addition, pitting and crevice corrosion due to the localized breakdown of the passive film occur in aqueous chloride solutions.

Polarization techniques and critical breakdown potentials, E_c, have been widely used as a measure of the pitting susceptibility of alloys in chloride solutions [*4–8*]. However, E_c values are not useful for predicting the galvanic behavior of stainless steels. Measurement of critical protection potentials, E_p, is more valuable for this purpose [*1,7,9*].

Polarization behavior of stainless steel in sodium chloride solution is represented in Fig. 3. The solid line represents anodic potentiodynamic polarization from active to noble potentials. The dashed line represents reverse polarization back to more active potentials.

Polarization above the critical breakdown potential, E_c, results in a marked increase in current density due to initiation of pitting. Reverse

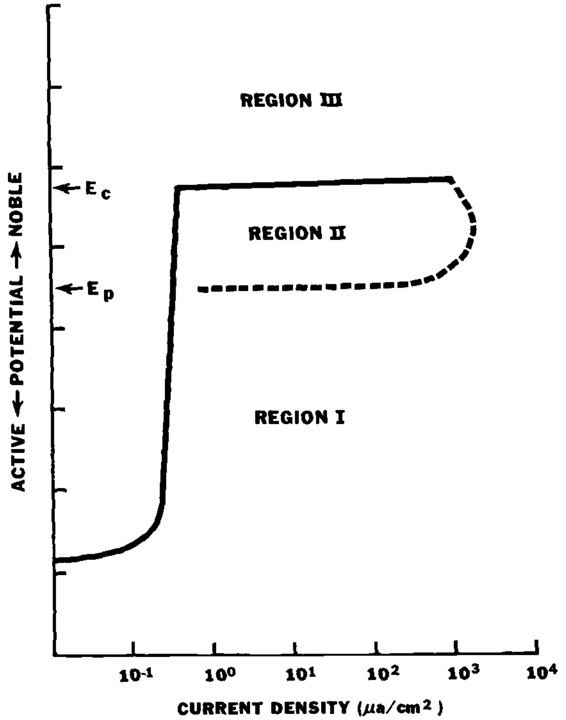

FIG. 3—*Schematic potentiodynamic polarization curve for stainless steel in 5NaCl at room temperature.*

polarization below E_c does not reduce the current density appreciably, indicating that propagation of existing pits and crevice corrosion occurs. At the critical protection potential, E_p, the current density approaches zero. Below E_p propagation of existing pits and crevice corrosion does not occur.

The corrosion behavior of stainless steels can be thus separated into three potential regions: Region I, where protection from pit propagation and crevice corrosion is observed; Region II, where propagation of existing pits and crevice corrosion occurs; and Region III, where initiation of pitting and crevice corrosion occurs. This behavior is observed in oxygen-containing and oxygen-free electrolytes, as shown previously [*1*].

Experimental

Polarization Measurements

The potentiodynamic method (continuous potential scan and current recording) described previously was used in this work [*10–13*]. The current from the potentiostat to the auxiliary electrode is measured as a potential across a precision resistor which is selected to provide the required logarithmic converter input voltage. The filtered output from the logarithmic converter is plotted on the *X*-axis, and the working electrode potential versus the saturated calomel electrode is plotted simultaneously on the *Y*-axis. In the laboratory, potentials were scanned at a rate of 0.6 V/h while in seawater the scan rate was 2.0 V/h.

Laboratory polarization measurements were made using a cell similar to that described previously [*10,14*].

The chemical compositions of the ferritic stainless steels used in this study are listed in Table 1. The 409, 430, and 434 stainless steels are widely used commercially available materials. Alloys 260 and 261 are high-purity ferritic stainless steels produced by induction melting and casting in vacuum.

Disk-shaped specimens for polarization measurements were punched from sheet material in the mill-annealed condition. The specimen surface was polished with 600-grit silicon carbide paper, followed by ultrasonic cleaning in detergent solution, and finally rinsed with distilled water. The specimen was mounted in the type of holder described previously by Myers et al [*15*]. In use, the specimen holder exposed only Teflon, and 1 cm^2 of specimen to the electrolyte. This design avoids solution contamination and crevice effects, while allowing the use of flat metal specimens.

For laboratory measurements in 5 percent NaCl solution at a pH of 7 and 30°C (86°F), solutions were prepared by dissolving reagent grade NaCl in distilled water and neutralizing with hydrochloric acid or sodium hydroxide. Air was passed through a fritted gas bubbler to continuously

TABLE 1—*Composition of ferritic stainless steels.*

Alloy	Cr	C	N_2	Mo	Ni	Mn	Si	S	P	Ti	Fe
409SS	10.5 to 11.75	0.08	. . .	. . .	0.05 max	1.00 max	1.00 max	0.045 max	0.045 max	6XC or 0.75 max	balance
430SS	16.5	0.05	. . .	0.03	0.27	0.4	0.49	0.009	0.013	. . .	balance
434SS	16.5	0.07	0.03	1.0	0.3	0.3	0.3	. . .	. . .	. . .	balance
Alloy 260	25.7	0.0035	0.012	<0.01	0.09	<0.01	0.28	0.0085	0.009	. . .	balance
Alloy 261	26.3	0.0020	0.013	1.07	0.14	<0.01	0.27	0.0070	0.010	. . .	balance

aerate the solution. Seawater polarization measurements were made similarly to laboratory measurements except that they were made in a 5-ft by 3-ft by 10-in. water table containing fresh seawater at 30°C (86°F) continuously pumped from Duxbury Harbor.

Immersion Tests

Laboratory immersion tests were conducted in the NaCl solution prepared as described in the foregoing. Measurements were made in air-saturated solutions using a constant temperature bath to maintain the solution temperature at 30°C ± 0.1°C (86°F).

Rectangular strip (2.5 by 5.0 cm) specimens of metals in the mill-annealed condition were ground flat and polished through 600-grit silicon carbide paper. Specimens for galvanic coupling were then centrally drilled and connected with 10-32 nylon nuts and bolts. Nylon nuts and bolts were also placed on monolithic specimens to create similar crevices on all specimens.

Periodically the mixed potential (versus the SCE) of each specimen was measured with a digital voltmeter-electrometer combination, and the values reported in this study are the stabilized (to within ±10 mV) ones. Weight loss measurements were made after ultrasonic cleaning in detergent and distilled water.

Seawater immersion tests were conducted at Battelle's William F. Clapp Laboratories site located in Duxbury, Massachusetts in a 12 by 6-ft aquarium with a depth of 4 ft. Seawater from Duxbury Harbor was continuously pumped into the aquarium and the water table, with the water level being maintained by an overflow.

Specimens were either pressure roll bonded to form bimetal strip or coupled with nylon nuts and bolts. Total immersion specimens were fastened to plexiglass racks with nylon nuts and bolts and exposed in the aquarium. Specimens exposed in this manner contained crevices similar to the laboratory immersion tests.

Replicate specimens were partially immersed by fastening them with nylon nuts and bolts to a wooden rack which was placed 2 in. above the waterline in the water table. All specimens were exposed in areas where flow rates were negligible.

Periodically the mixed potential (versus the SCE) of the partially immersed specimens was measured with a digital voltmeter-electrometer combination, and the stabilized potentials (to within ±10 mV) are reported in this study.

Results

Results of potentiodynamic polarization of the ferritic stainless steels in air-saturated 5 percent NaCl solution are shown in Fig. 4. Notice that

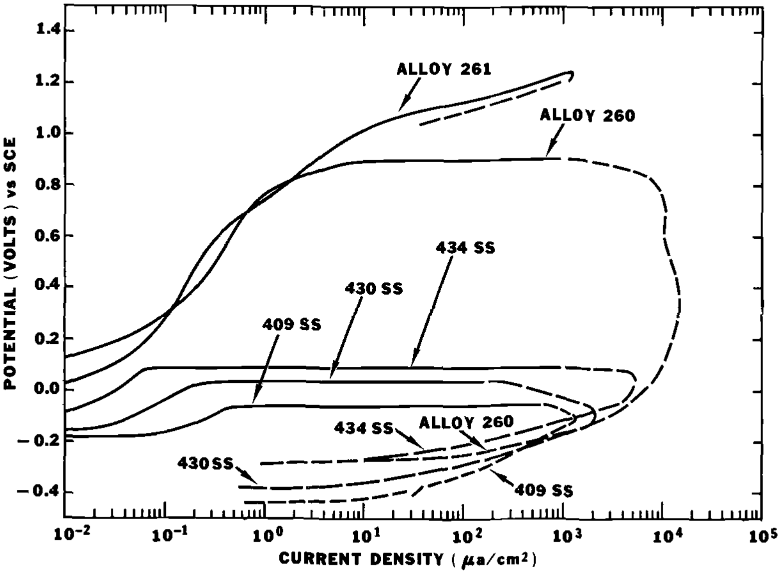

FIG. 4—*Potentiodynamic polarization curves for ferritic stainless steels in air-saturated 5 percent NaCl solution at 30°C (86°F) (0.6 V/h scan rate).*

the critical breakdown potentials (E_c) are in the order 409, 430, and 434 stainless steels, and alloys 260 and 261. The shapes of the curves are similar to that shown in Fig. 3. The critical protection potentials (E_p) are also in the same order.

Data on the corrosion behavior of the electrically isolated metals and their mixed potentials in 5 percent aerated NaCl solutions are listed in Table 2. As indicated in Table 2 and Fig. 5, all of the stainless steel alloys

TABLE 2—*Laboratory immersion of ferritic stainless steels in 5 NaCl.*

Alloy Type	Initiation of Localized Corrosion (days)	Mixed Potential (V versus SCE)	Weight Loss/Year (mg) 1 × 2 in. Coupons
409	2		596
409/Cu	2	−0.278	730
430	2		156
430/Cu	2	−0.280	34
434	2		168
434/Cu	2	−0.260	338
Alloy 260	7		13
Alloy 260/Cu	361	−0.272	0.4
Alloy 261	18		0.2
Alloy 261/Cu	(361)	−0.280	0

Note: Data in parenthesis indicate no localized corrosion.

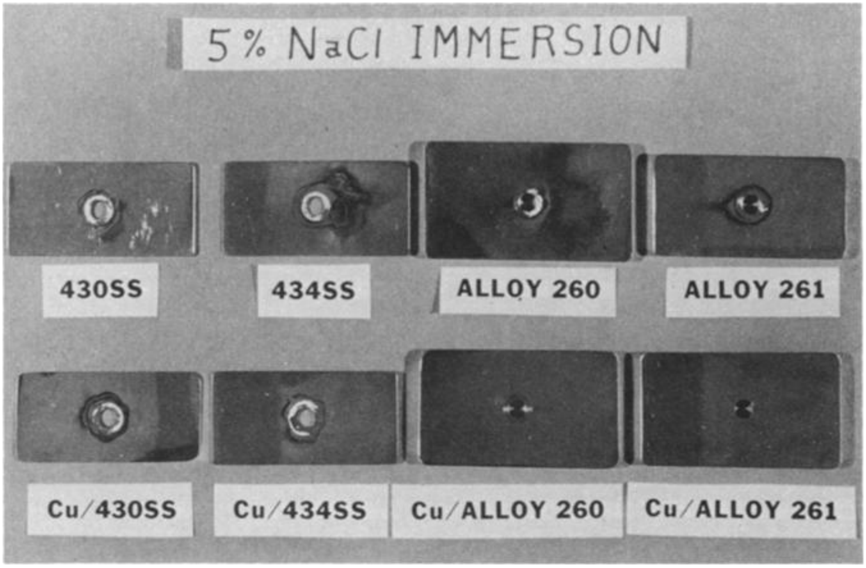

FIG. 5—*Photograph of ferritic stainless steel (cleaned) after total immersion in air-saturated 5 percent NaCl solution at 30°C (86°F).*

undergo localized (crevice) corrosion in this solution. The crevice corrosion of alloy 261, however, is minimal as indicated by the extremely small weight loss.

The corrosion behavior of the stainless steel alloys coupled to copper is also shown in Fig. 5. The data in Table 2 and Fig. 5 show that only 409, 430, and 434 stainless steels undergo crevice corrosion (although there was a very small weight loss for alloy 260).

Potentiodynamic polarization curves for the ferritic stainless steels in seawater are shown in Fig. 6. The critical breakdown potentials (E_c) and the critical protection potentials (E_p) are in the order 409, 430, and 434 stainless steels, and alloys 260 and 261. This is the same order of E_c and E_p for the alloys in 5 percent NaCl.

The appearance of the stainless steel after one-year exposure in seawater can be observed in Fig. 7. Data on the corrosion behavior of the alloys and their mixed potentials in seawater are listed in Table 3.

All of the alloys except alloy 261 undergo crevice corrosion in seawater in the freely corroding electrically isolated condition and when coupled to copper. The appearance of galvanically coupled specimens after cleaning is observed in Fig. 8.

Discussion

The localized corrosion behavior of the stainless steel alloys can be explained by referring to the polarization curves in Figs. 4 and 6 and the

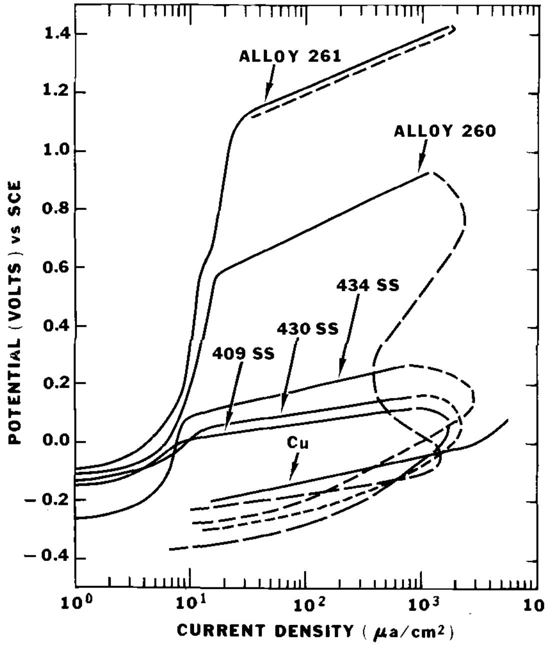

FIG. 6—*Potentiodynamic polarization curves for ferritic stainless steels in seawater at 30°C (86°F) (2.0 V/h scan rate).*

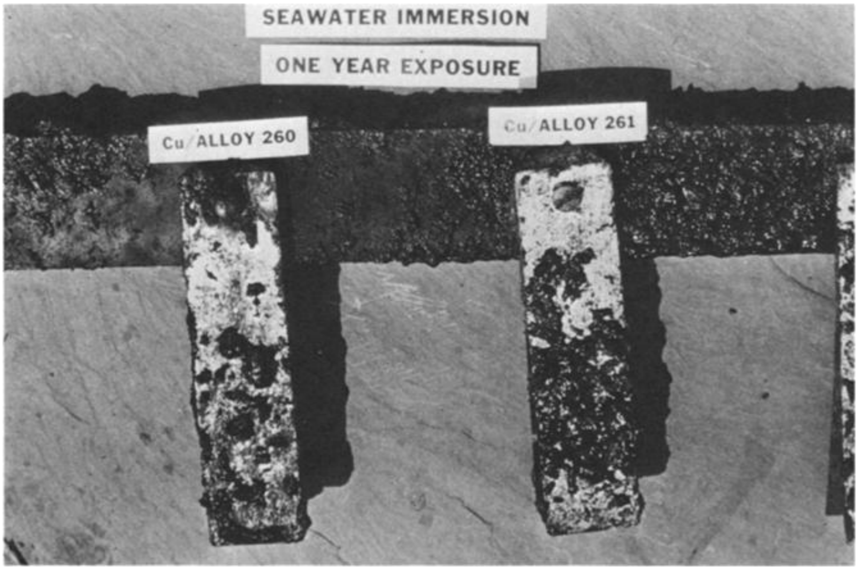

FIG. 7—*Photograph of ferritic stainless steels showing surface appearance of specimens after immersion in Duxbury Bay (Massachusetts) seawater.*

TABLE 3—*Seawater immersion of ferritic stainless steels.*

Alloy Type	Occurrence of Localized Corrosion (1-year exposure)	Mixed Potential (V versus SCE)
409	+	
409/Cu	+	−0.242
430	+	
430/Cu	+	−0.127
434	+	
434/Cu	+	−0.120
Alloy 260	+	
Alloy 260/Cu	+	−0.101
Alloy 261	−	
Alloy 261/Cu	−	−0.090

mixed potentials in Tables 2 and 3. In aerated 5 percent NaCl, alloys 260 and 261 behave similarly when galvanically coupled to copper. The mixed potentials for these alloys (when coupled to copper) lie within Region I, and, therefore, crevice corrosion is not expected. The mixed potentials for 409, 430, and 434 stainless steels coupled to copper all lie within Region II, where crevice corrosion is observed.

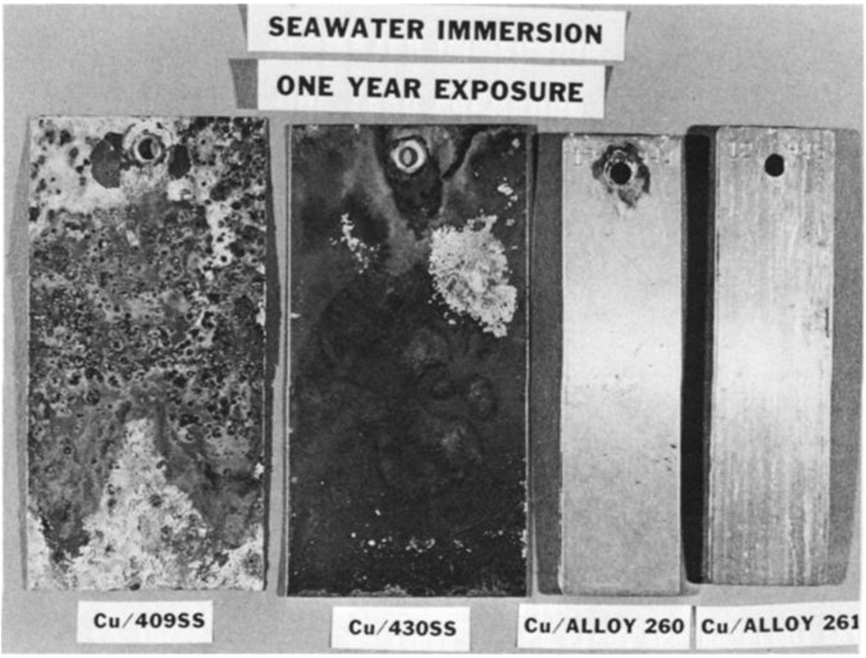

FIG. 8—*Photograph of ferritic stainless steels (cleaned) after total immersion in seawater for one year.*

In the freely corroding, electrically isolated condition in 5 percent NaCl, all of the alloys undergo crevice corrosion since their mixed potentials are not regulated within the protected region.

In seawater, the mixed potentials for the alloys coupled to copper (Table 3) lie within Region II with the exception of alloy 261, which is within Region I. As expected, only alloy 261 coupled to copper is free from crevice corrosion.

The difference in behavior of alloy 260 coupled to copper in aerated 5 percent NaCl and seawater can be explained by referring to the polarization curves in Figs. 4 and 6 and their mixed potentials in Tables 2 and 3.

The mixed potential for alloy 260 coupled to copper is less electronegative in seawater than for that in 5 percent NaCl by almost 200 mV. Clearly, that mixed potential lies within Region II of the polarization curve in seawater and crevice corrosion is expected for this system.

Conclusions

Although the galvanic series of metals can be useful in predicting galvanic behavior of metals, use of the mixed potential theory and polarization of metals can lead to more precise information.

Galvanic behavior of stainless steels is explained best by referring to the polarization behavior of these metals. Above E_c, the critical breakdown potential, pit initiation and crevice corrosion occur. This behavior occurs when stainless steels are galvanically polarized above E_c. Between E_p, the critical protection potential, and E_c, propagation of existing pits and crevices occurs. Below E_p, protection from pitting and crevice corrosion is observed.

As described previously [1], stainless steels can be protected from pitting and crevice corrosion in chloride solutions by choosing galvanic couples with mixed potentials below E_p (Region I).

In this paper, techniques are described to correlate the behavior of several ferritic stainless steels in electrochemical studies with immersion studies.

Results show that it is not sufficient to raise only E_c, the critical breakdown potential, in order to improve corrosion resistance in galvanic couples (compare the results of alloy 260 with 434 stainless steel). By proper alloying, E_p, the critical protection potential, can be raised to more positive potentials so that in galvanic couples with the more noble metals (such as with copper), protection from crevice corrosion occurs as indicated by the results with alloy 261.

References

[1] Baboian, R. in *Localized Corrosion—Cause of Metal Failure, ASTM STP 516,* American Society for Testing and Materials, 1972, pp. 145–163.

[2] Wagner, C. and Traud, W., *Zeitschrift für Electrochemie,* Vol. 44, 1938, p. 391.

[3] Makrides, A. C., *Journal of the Electrochemical Society*, Vol. 107, 1960, p. 869.
[4] Brennert, S., *Journal of the Iron and Steel Institute*, Vol. 135, 1937, p. 101.
[5] Hospadaruk, V. and Petrocelli, J. V., *Journal of the Electrochemical Society*, Vol. 113, 1966, p. 878.
[6] Horvath, J. and Uhlig, H. H., *Journal of the Electrochemical Society*, Vol. 115, 1968, p. 791.
[7] Pourbaix, M., Klimzack-Mathieiu, L., Mertens, C., Meunier, J., Vanleugenhaghe, C., DeNuncky, L., Laverys, J., Neelemans, L., and Warzee, M., *Corrosion Science*, Vol. 3, 1963, p. 239.
[8] Defranoux, J. M., *Corrosion Science*, Vol. 3, 1963, p. 75.
[9] Pourbaix, M., *Corrosion*, Vol. 26, 1970, p. 431.
[10] Greene, N. D., "Experimental Electrode Kinetics," Rensselaer Polytechnic Institute, Troy, N. Y., 1965.
[11] Littlewood, R., *Corrosion Science*, Vol. 3, 1963, p. 99.
[12] France, W. D. and Lietz, R. W., *Corrosion*, Vol. 24, 1968, p. 298.
[13] Baboian, R., "Corrosion Resistant, High Strength Clad Metal System for Hydraulic Brake Line Tubing," Paper 720290 presented at SAE Automotive Engineering Congress, Detroit, Jan. 1972.
[14] ASTM G 5-69, Recommended Practice for a Standard Reference Method for Making Potentiostatic and Potentiodynamic Anodic Polarization Measurements, American Society for Testing and Materials, 1969.
[15] Myers, J. R., Gruewler, F. G., and Smulczenski, L. A., *Corrosion*, Vol. 24, 1968, p. 352.

J. S. Di Gregorio[1] *and J. P. Fraser*[1]

Corrosion Tests in the Gulf Floor

REFERENCE: Di Gregorio, J. S. and Fraser, J. P., "**Corrosion Tests in the Gulf Floor,**" *Corrosion in Natural Environments, ASTM STP 558*, American Society for Testing and Materials, 1974, pp. 185–208.

ABSTRACT: Because of the importance of good corrosion control to the safe operation of offshore pipelines, a test program was started in 1966 to study the behavior of pipeline materials in and near the ocean bottom in waters of pipeline depth (50 to 500 ft). This program has included the study of the corrosion of pipeline steels in and near the ocean bottom, the cathodic protection required to control this corrosion, and the performance of coating, paint, and anode systems in and near bottom sediments of the Gulf of Mexico.

Results to date have shown that the corrosion of separate, buried steel panels and the cathodic protection current densities required to control this corrosion are less than in the ocean immediately above the mudline. The corrosion rate of unprotected steel panels exposed to seawater above the mud is as high as 11 mpy (mils per year) depending on the time and location of exposure. Unprotected panels below the mudline, however, corrode at rates of 1 to 3 mpy. Pitting corrosion of these panels is also more intense in the water above the mud than buried in the mud. The current density required to reduce the corrosion rate of these panels to less than 1 mpy is in excess of 3.2 mA/ft^2 above the mudline; below the mudline a current density of 0.6 to 2.5 mA/ft^2 is required to reduce the corrosion rate to the same level. The current density required to control corrosion decreases with increasing depth of burial below the mudline. The corrosion rates of electrically connected pipe lengths partially buried in the mud are independent of position relative to the mudline. A large amount of calcareous deposit was formed on zinc metal when it was made electrically negative for 10.5 months in seawater.

KEY WORDS: corrosion, cathodic protection, offshore, ocean bottom, marine pipelines, current density, materials behavior

Compared with the amount of research on corrosion in shallow seawater, there has been relatively little research on corrosion in the deep sea. The greatest amount of information available in the open literature is that provided by the U. S. Navy, covering studies performed by the U. S. Naval Civil Engineering Laboratory (NCEL) and the U. S. Naval Research Laboratory (NRL). Starting in 1959, NCEL has studied the behavior of metals, alloys, and nonmetallic materials in the Pacific Ocean at depths down to 6800 ft for periods of up to three years [*1*].[2] In the Atlantic Ocean,

---

[1] Chemist and supervisor, respectively, Shell Development Company, Pipeline Research and Development Laboratory, Houston, Tex. 77035.

[2] The italic numbers in brackets refer to the list of references appended to this paper.

NRL in cooperation with the Woods Hole Oceanographic Institute [*2*] has studied the behavior of materials in the Tongue of the Ocean off Bermuda (3000 to 15 000 ft). A few other studies of corrosion in the deep sea have been made by the Bell Laboratories [*3*], Reynolds Metals Company [*4*], United States Rubber Company [*5*] and other industrial groups and government agencies interested in the behavior of materials in the deep sea.

Although many thousands of specimens of hundreds of materials have been exposed in deep-sea water in the studies just mentioned, only a small part of these studies has been concerned with the corrosion of materials used for oil and gas production and transportation equipment, such as pipelines. For example, no information is available on the effects of the deep-sea environment on pipeline coating materials. Coatings such as thin film epoxies and asphalt mastics, which for years have been widely used on marine pipelines in shallow waters, are untested in the deep sea. Likewise sacrificial anode materials, such as zinc and magnesium, which have a long history of service on offshore pipelines in shallow waters, have not been sufficiently tested in deep waters. In addition, and most importantly, very little information [*1*] has been developed on corrosion of metals completely buried in the ocean bottom sediments or partially buried, partially exposed in these sediments.

Factors which control the corrosion rate in marine environments (oxygen concentration, pH, temperature, salinity, water velocity, etc.) all vary with water depth [*6,7*]. In considering all of these factors and how they affect corrosion rates, it is convenient to distinguish specific zones; namely, the atmosphere above the sea, the splash zone, the tidal zone, the shallow sea, the deep sea, and the ocean bottom sediment. The corrosion rate of steel varies from zone to zone, but in general the rate is highest in the splash zone area, where metal is continually washed with seawater of high oxygen content. In the shallow sea, corrosion rates are usually lower than in the splash zone because of lower temperature and decreased oxygen availability (that is, because oxygen must diffuse down from the water surface and through a relatively thick layer adjacent to the metal surface). In the deep sea, corrosion may actually be greater than at intermediate water depths because of increasing oxygen content; however, the increase in corrosion should not be drastic due to the low temperatures and high salinity of deep water. Less fouling is observed in deeper water because fewer organisms are present at very great depths. In the mud of the ocean bottom, where pipelines operate, steel corrosion rates are generally lower than in the other zones, but are not negligible.

Oxygen Variation with Depth [*6,7*]

The mechanism of corrosion in deep-sea water differs little from the mechanism of corrosion in more shallow areas. In each case corrosion depends on several factors, such as oxygen content, pH, temperature, biological activity, water velocity, and salinity. However, differences in the rates of corrosion between shallow and deep waters have been observed. These differences can be attributed to variations in the aforementioned factors with water depth. From a corrosion point of view, the most important difference between shallow and deep water is the oxygen content. At the surface of the ocean where seawater is in contact with the atmosphere and the water is frequently agitated, the water is at or near oxygen saturation. At greater and greater depths, down to about 2500 ft, the oxygen content of the oceans decreases due to consumption by plants and animals living in the sea. These living organisms, which require sunlight and warm temperatures in addition to oxygen, are usually found in the upper level of the ocean with highest concentrations in the upper two hundred feet. Below about 2500 ft, the numbers of these organisms is very low owing to the absence of sunlight and the very low temperatures (0 to 10°C) (32–50°F) of deep-ocean water. Because less oxygen is consumed, the oxygen content of deep water begins to increase in some oceans (for example, the Pacific and the Indian Oceans) at depths below about 2500 ft. The oxygen versus water depth curve exhibits a minimum at this depth. Other factors can influence the increasing oxygen content of deeper water. For example, cold water from the melting polar ice caps flows near the bottom of some oceans, such as the Atlantic. This water is normally well-aerated. In fact, in very deep water (>3500 ft) the oxygen content may be greater than at the surface of the sea [7]. Further complicating an already complex problem is the fact that deep water in different parts of the world differs in oxygen content. This is because the total numbers of plants and animals living in the different oceans of the world vary. For example the concentration of organic matter (plants and animals) living in the Atlantic is less than in the Pacific and thus the oxygen demand of organisms in the Atlantic Ocean is less than in the Pacific Ocean. Furthermore the oxygen content of the deep Atlantic is higher than in the deep Pacific due to the southward flow of cold water, saturated with oxygen, through the funnel of the North Atlantic. The flow through the Bering Strait into the Pacific is negligible. As a result, beginning at the surface of the water in the Atlantic and continuing down to greater and greater depths, the oxygen content remains fairly constant with just a small decrease observed.

Thus the oceans of the world appear to be "layered" rather than homogeneous and these various layers are distinguished by different oxygen contents. This layered effect could be quite important in the design and operation of equipment for use in deep waters. For example continuous sections of exposed metal which pass through several sea zones (suspended flowlines, risers, and mooring cables) also pass through areas of varying oxygen concentration. Corrosion behavior in these cases could be typical of corrosion in oxygen concentration cells—more corrosion in the zones with less oxygen present and less corrosion in the zones with more oxygen present. The continuous section of exposed metal would thus be subjected to localized attack at certain locations along its length. Attack of this type could be locally more severe than general corrosion over the entire length of the section. Coatings and cathodic protection should minimize this problem, but detailed studies of coating behavior, including coating fatigue, and cathodic protection efficiency and the service life of sacrificial anodes in deep water are needed before design specifications can be formulated.

From the foregoing description, especially that on variations in oxygen concentration with water depth and geographical location, it is clear that corrosion in different parts of the world's oceans will differ.

Our primary concern is with corrosion of submarine pipelines. Corrosion leaks on a submarine pipeline are unacceptable owing to the high cost of repair. These pipelines are made of steel and are usually coated for corrosion protection. Submarine pipelines have been installed in water depths up to about 500 ft. In shallow waters (less than 200 ft water depth), pipelines are normally buried in the ocean bottom, the only parts which protrude being the risers to production platforms. In water depths greater than 200 ft, pipelines are not deliberately buried and usually rest partly below and partly above the mudline. Owing to the high content of organic matter in ocean bottom sediments, they are expected to be chemically reducing. Thus, those portions of a pipeline which are buried in the mud will be shielded from oxygen. If totally buried, corrosion on a pipeline would be expected to be very slow. However, if a pipeline is only partly buried or is resting on the ocean floor, corrosion on the buried parts may be accelerated by being galvanically coupled to those portions which are not buried.

Owing the the scarcity of data in the open literature on the behavior of materials in and near the ocean bottom in waters of intermediate depth, our laboratory initiated a test program in 1966 to assess more fully the corrosion problems to which submarine pipelines are exposed.

Corrosion Tests in the Gulf of Mexico

This study is being carried out in the ocean rather than in laboratory simulation because seawater differs from simple salt solutions both in kind and intensity of attack. Our offshore tests have included the study of the corrosion of pipeline steels in and near the ocean bottom, the cathodic protection required to control this corrosion, and the performance of materials in ocean bottom sediments. As part of this study two separate, long-term tests have been installed in the mud environment of the Gulf of Mexico in moderately deep water. The first of these tests was installed in July 1966 in 70 ft of water adjacent to Shell's Platform "A" of the Buccaneer Field located about 30 miles south-southeast of Galveston, Texas. This test lasted for about four years. The second test was installed in September 1967 in 275 ft of water in the West Delta Block 134 Field located about 30 miles southwest of the Mississippi River Delta. This test was terminated after 10.5 months' exposure. In July 1971 a third test was installed in 110 ft of water in the Vermilion Block 190 Field. This test is currently in progress. We report here results obtained from the first two tests only. Figure 1 shows the location of these three tests in the Gulf of Mexico. By installing the tests in different locations in the Gulf, the effects of different water depths, temperatures, oxygen concentrations, ocean sediment compositions, etc. can be compared.

Soil Description

Figure 2 shows the boring log to 40-ft penetration at the three test sites.

The soil at the Buccaneer test site consits of gray, clayey sand with shell fragments to a depth of about two feet. From two to seven feet the soil is generally firm gray clay with silt pockets.

The soil at the West Delta site consists of very soft, gray clay with shell fragments to a depth of about four feet. Below four feet the soil is generally very soft, gray clay.

The soil at the Vermilion test site consists of very soft, gray clay down to about ten feet with traces of wood, sandy clay seams, and sand pockets down to about 20 ft.

Specimens

The specimens tested in the Buccaneer and West Delta tests included weight loss, cathodically protected, and coated specimens. A limited number of stressed corrosion test specimens have been included to explore the possibilities of stress corrosion cracking of steels in the ocean bottom environment. Finally, the test racks themselves and steel cables used to secure the test racks were made part of the corrosion test program. The specimens used are shown in the Appendix.

Exposure Conditions

Specimens were exposed both above and below the mudline. In the Buccaneer test, the test panels were installed by divers in holes jetted into the ocean floor. A typical test assembly used in the Buccaneer tests is shown in Fig. 3. The test specimen arrangement is shown in Fig. 4. In the West Delta tests, enough weight was provided in the support rack to ensure penetration into the ocean bottom sediments under its own weight. The test rack prior to installation is shown in Fig. 5.

Instrumentation

For the Buccaneer test, measurements of potential of the cathodically protected panels were made periodially from the surface using a silver/

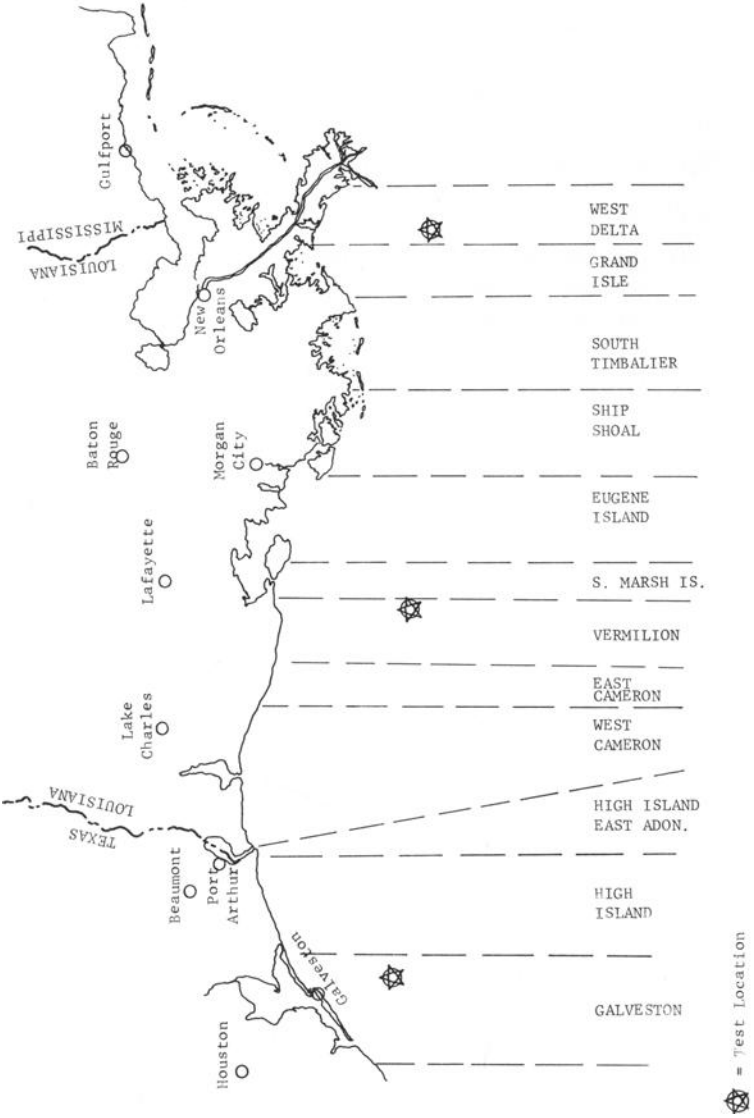

FIG. 1—*Sites for the three corrosion tests conducted in the Gulf.*

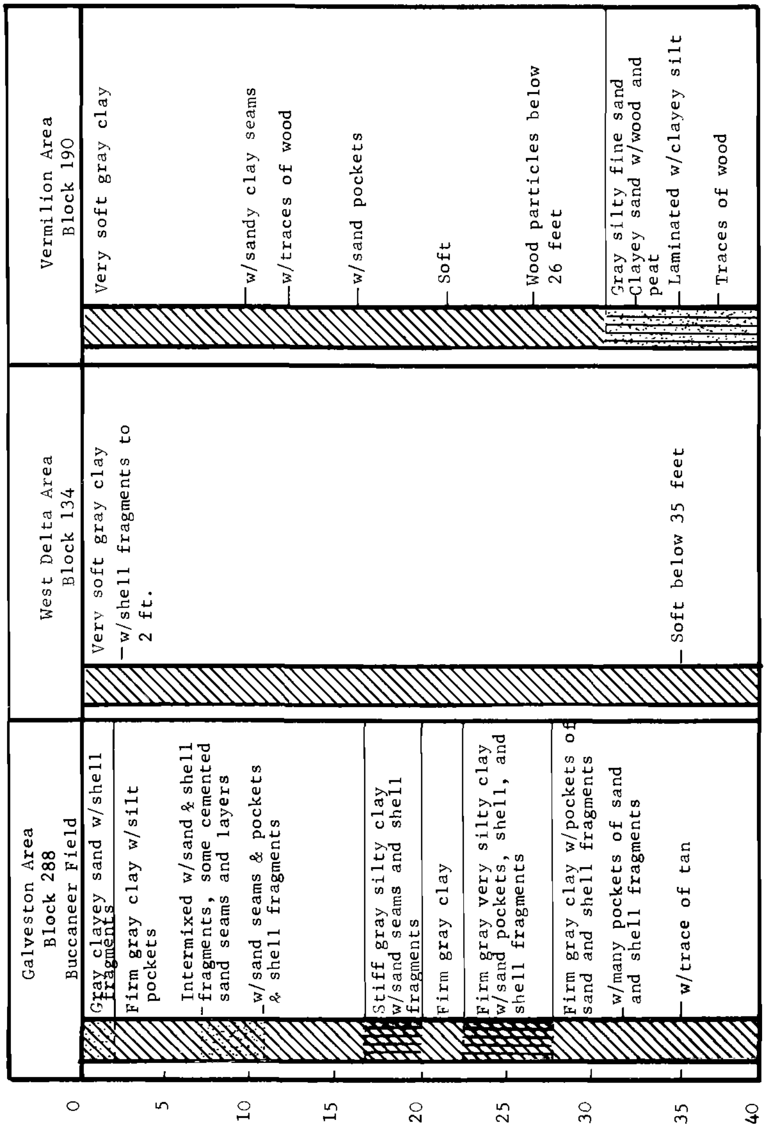

FIG. 2—*Log of boring to 40-ft penetration in Galveston Block 288, West Delta Block 134, and Vermilion Block 190.*

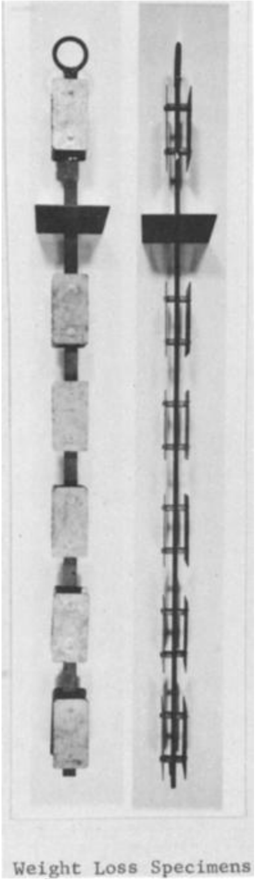

FIG. 3—*Test racks to study corrosion in ocean bottom sediments in Buccaneer Field.*

silver chloride reference electrode and a high-resistance voltmeter. Water temperature, pH, and oxygen content were measured occasionally during the test.

For the West Delta test, it was impractical to measure potentials because the specimens were not accessible during the test period. However, the water temperature, pH, and oxygen content were measured and recorded using specially designed instrumentation.

The pH meter consisted of an antimony-antimony oxide half cell versus a copper-copper sulfate half cell, a solid-state operational amplifier, a microampere recorder, and a 24 V dc battery power supply. The reduction potential (+0.316 V) of the copper-copper sulfate half cell is essentially independent of the temperature and pH of the surrounding water. The reduction potential of the antimony-antimony oxide half cell varies with

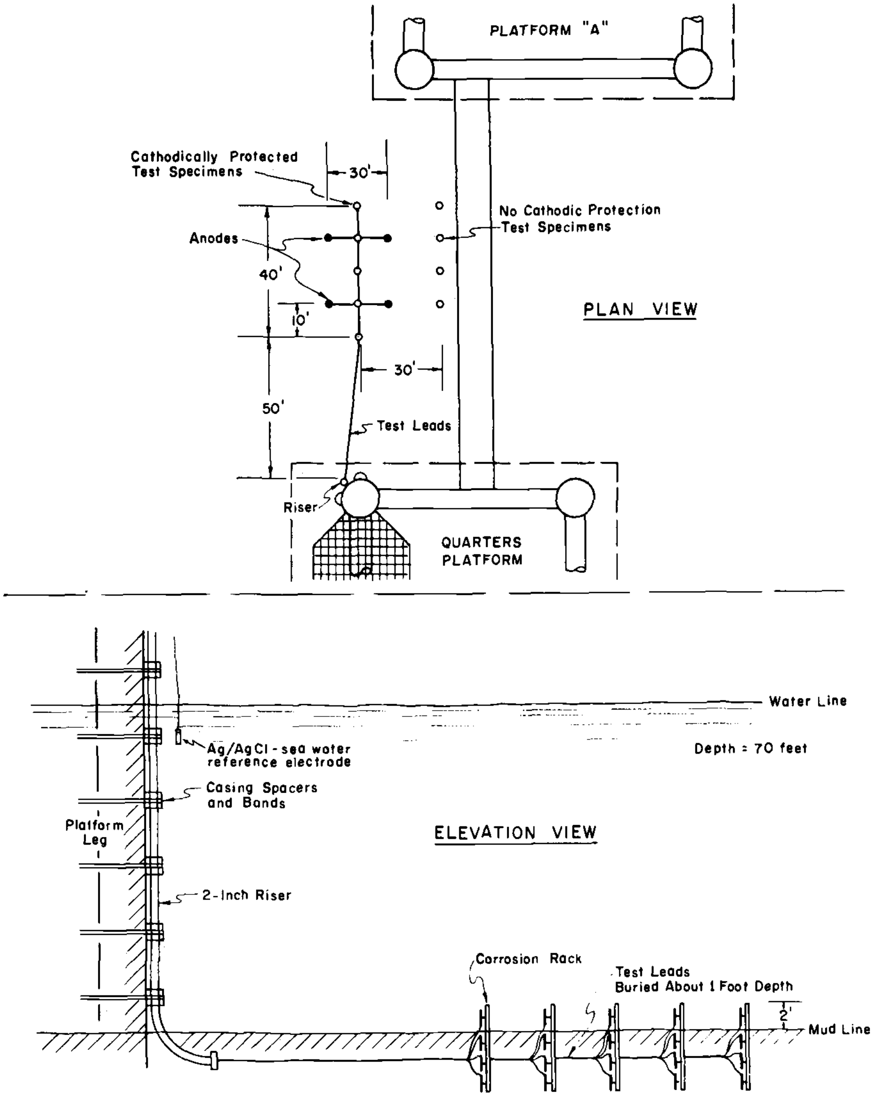

FIG. 4—*Corrosion test specimen arrangement at Platform "A", Buccaneer Field.*

temperature and pH of the surrounding water. At about 25°C (77°F) the potential varies from about +0.20 V at pH = 1 to about −0.41 V at pH = 12. The pH circuit was designed to record pH values between 4 and 9. The pH meter was calibrated using standard solutions.

The oxygen meter consisted of a modified, commercially available oxygen probe, a current-splitting circuit, a microampere recorder, and a 24 V dc power supply. (The probe was a cell which had a lead anode, a gold

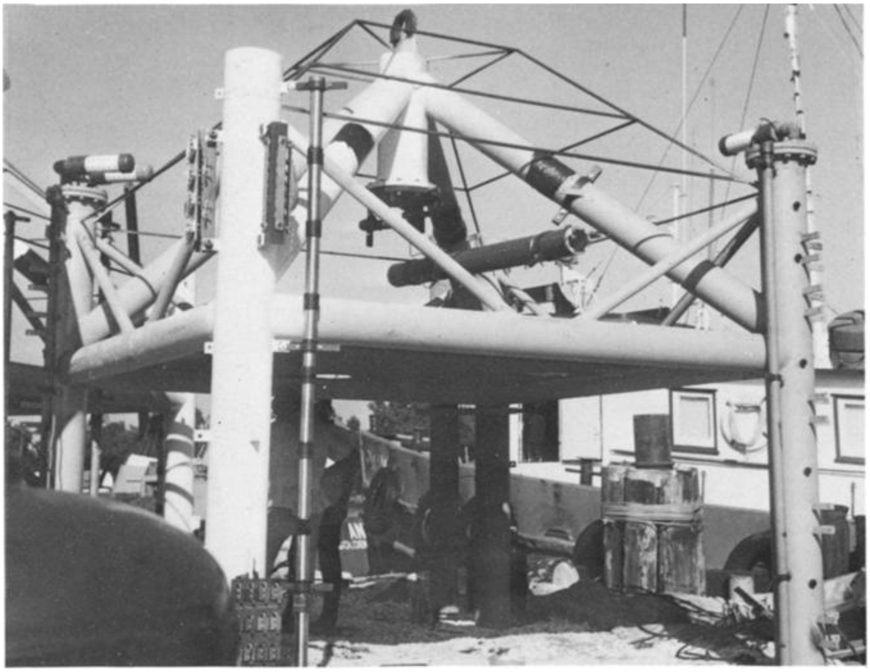

FIG. 5—*Deepwater corrosion test rack just prior to launching in West Delta Block 134 Field.*

cathode, and caustic electrolyte; the cathode was covered with an oxygen-permeable plastic membrane.) The cell potential or current output or both are a function of the amount of oxygen arriving at the cathode which in turn is a function of the oxygen content of the surrounding medium. The oxygen meter circuit was designed to record oxygen contents from 0 to about 10 ppm.

The temperature sensing probe was a full bridge with two temperature-sensitive thermistors acting as two legs. The output was recorded by a microampere recorder. The circuit was designed to record temperatures between 40 and 90°F (4 and 32°C).

The recorders, batteries, etc. were housed in a pressure vessel. The instruments operated continuously for the first 11 h and then switched to an operation which measured and recorded pH, temperature, and oxygen content 30 sec of each hour. A timer controlled the cycle time. The instrument package used in the West Delta test is shown in Fig. 6.

Exposure Times

All of the cathodically protected and stressed specimens and all but one of the weight-loss tests were removed from the Buccaneer test area for

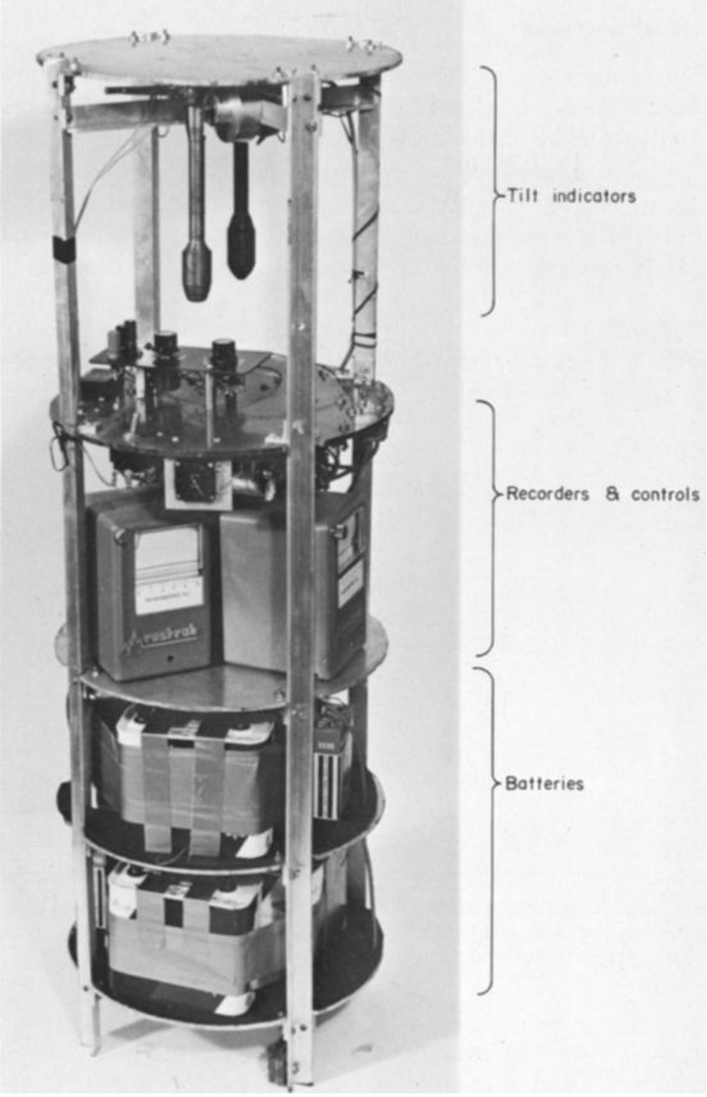

FIG. 6—*Instrumentation for test rack in West Delta 134 Field.*

inspection and analysis within 205 days. The remaining test was removed after 1471 days.

The test rack from the West Delta test was recovered after 10.5 months on the bottom.

The Vermilion test currently in progress will be terminated in the summer of 1974.

Unprotected Specimens

The corrosion rates of the unprotected panels in the Buccaneer test as a function of position relative to the mudline are given in Table 1. In all cases, the corrosion of the steel panels buried in the ocean bottom sediments was less severe than the corrosion in the ocean immediately above the bottom. In addition, the corrosion of panels buried in the mud was fairly uniform and independent of burial depth below one foot. Figure 7 shows the panels exposed for 1471 days (after cleaning).

TABLE 1—*Weight-loss corrosion rates for unprotected samples in Buccaneer Field.*

Depth Relative to Mud, ft	Corrosion Rate, mpy[a]		
	108 Days	205 Days	1471 Days
+1	9,9	6,6,7,7 (39,21,62,64)	3,3 (31,31)[b]
−1	3,4	3,3,3,3 (25,34,9,7)	2,2 (31,31)[b]
−2	3,4	2,3,7,3 (14,7,9,-)	1,1 (12,8)
−3	3,4	2,2,2,3	1,1 (9,7)
−4	3,3	4,3,3,3 (12,20,20,18)	1,1 (10,9)
−5	3,2	4,4,2,3 (37,12,14,-)	1,1 (12,10)

[a] Corrosion rates are based on weight loss and exposure time. Numbers in parentheses indicate penetration rates estimated from maximum pit depth and exposure time.

[b] Complete penetration through ⅛-in. panel.

In all cases the corrosion rate after 1471 days in test was less severe than the initial corrosion rate observed after only 108 or 205 days in test. A decrease in rate as a function of time exposed was seen for the panels located one foot above the mudline. This is attributed to (1) accumulation of corrosion products and (2) the large amount of marine growth found on the panels located one foot above the mud. In each case a protective coating was formed on the panels above the mud which reduced the corrosion rate from that originally observed. The panels located above the mud were found to be completely covered with a hard coating of various sessile and semimotile organisms after 1471 days in the seawater environment. Figure 8 shows the panels exposed one foot above the mudline for 1471 days (before cleaning). Practically no marine growths were found on

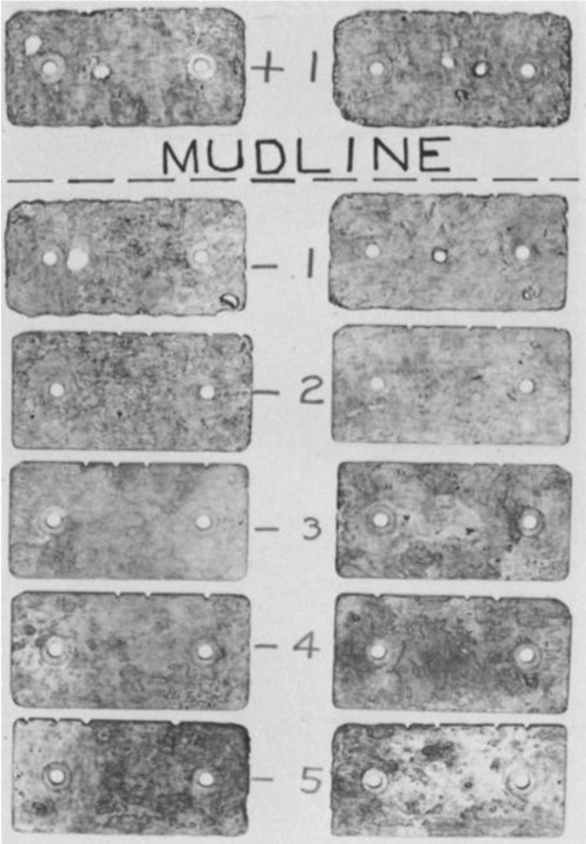

FIG. 7—*Unprotected panels exposed for 1471 days in the Buccaneer Field—after cleaning. Numbers indicate distance in feet from mudline.*

the panels located below the mudline. These panels were covered instead with gray, clayey sand, silt, and shell fragments. As shown in Table 1 for the panels buried in the mud, the initially small corrosion rates also decreased as a function of time. In these cases, however, the decrease was presumably caused only by the slow buildup of corrosion products.

After 1471 days in test, pitting corrosion was most intense at one foot above and one foot below the mudline. In these cases several pits had completely penetrated each test panel (125-mils penetration). Pitting corrosion was less severe and more uniform at two, three, four, and five feet below the mudline. Maximum pit depths in these cases were on the order of 40 to 50 mils.

Figure 9 shows all the test panels exposed in the West Delta test for 10.5 months (after removal of marine growth and deposits). Corrosion rates

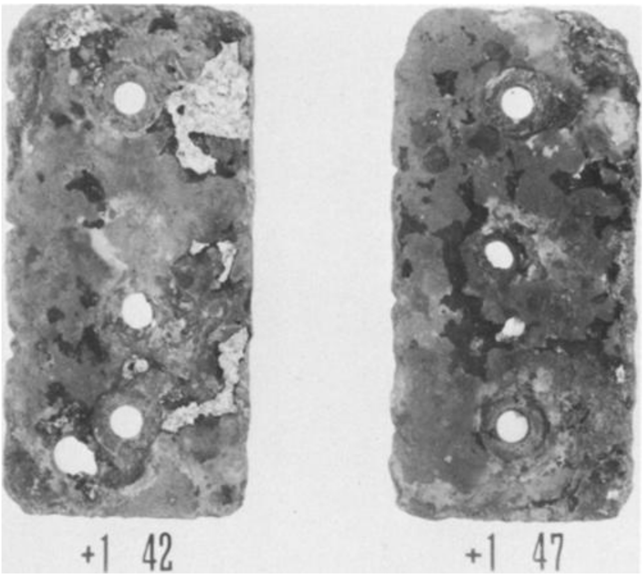

FIG. 8—*Marine growth on unprotected panels exposed 1 ft above the mudline for 1471 days in the Buccaneer test—before cleaning.*

in mils per year and corrosion pit depths for the unprotected and cathodically protected panels are given in Table 2. As was the case in the Buccaneer test, the corrosion of unprotected steel panels buried in the ocean bottom sediments was less severe than the corrosion in the water immediately above the bottom. Unprotected specimens located in the water above the

TABLE 2—*Weight-loss corrosion rates for samples in West Delta test—10.5 months exposure.*

Depth Relative to Mud, ft	Corrosion Rate, mpy[a] at Current Density mA/ft^2, of 0.0	0.6	1.2	2.2	3.2
+3	11 (35)	...	7 (40)	9 (35)	6 (9)
+2	10 (35)	...	8 (13)	9 (60)	6 (23)
0	11 (47)	10 (28)	4 (35)	7 (14)	...
−2	3 (6)	0.8	0.1	0.2	...
−4	Lost	Lost	0.8	0.1	...

[a] Corrosion rates are based on weight loss and exposure time. Numbers in parentheses indicate penetration rates calculated from maximum pit depth and exposure time.

Temperature of water: low 58°F (14°C), average 64°F (18°C), high 70°F (21°C).
Oxygen content of water: average 4.5 ppm
pH of water: 8.0 ± 0.2
pH of mud: 8.5 ± 0.2

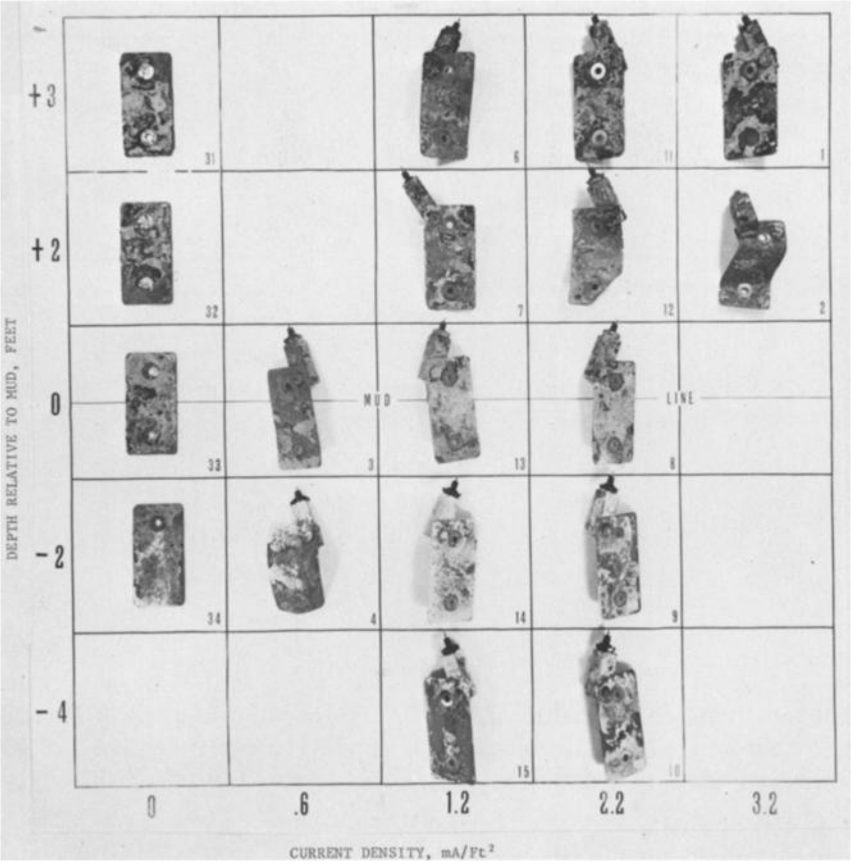

FIG. 9—*Test panels exposed in West Delta Block 134 Field for 10.5 months—after cleaning.*

mudline and at the mud/water interface corroded at a rate of 10 to 11 mpy (mils per year). The corrosion of an unprotected panel located two feet below the mudline was significantly less, 3 mpy. Pitting corrosion of unprotected panels was most intense in the vicinity of the mud/water interface and in the water above the mud. At two feet below the mud, pitting corrosion of an unprotected panel was less severe.

Cathodically Protected Specimens

In both the Buccaneer and the West Delta tests, current densities were controlled rather than potentials, owing to the complex equipment which would have been required to control potentials. From the Buccaneer tests, the current required to polarize steel from the freely corroding potential

TABLE 3—*Weeks required to polarize to −0.85 V ($Cu/CuSO_4$)—Buccaneer test.*

Current density, mA/ft^2	1.6	2.4	3.6	5.5	8.2
Depth relative to mudline, ft:					
+1	>17	>29	>29	15.5	4.5
−1	>17	>29	<1	<1	<1
−3	>17	<1	<1	<1	<1
−5	>17	<1	<1	<1	<1

Note: Tests were of limited duration. The symbol (>) indicates maximum duration of test in weeks.

(−0.75 V to −0.81 V to $Cu/CuSO_4$) to the accepted protective potential of −0.85 V to a saturated $Cu/CuSO_4$ electrode is:

Depth relative to mudline, ft	Current density required to polarize to −0.85 V to $Cu/CuSO_4$, mA/ft^2
+1	4.2
−1	2.5
−3	1.7
−5	1.7

The time required to produce this level of polarization is given in Table 3.

Weight-loss corrosion rates versus applied current density for the Buccaneer tests are given in Table 4. These data indicate the following:

1. The corrosion rate of bare steel based on 205 days' exposure in 70-ft water depth at this location was about 6 to 7 mpy.
2. The corrosion rate of bare steel below the mudline was about 3 mpy and appeared to be independent of depth of burial in the range from 1 to 5 ft below the mudline.
3. The weight-loss corrosion rate of cathodically protected steel decreased with increasing burial depth.
4. A current density of 3.6 mA/ft^2 reduced the corrosion rate of steel buried in the mud to less than 0.2 mpy regardless of the depth of burial. The current densities required to reduce the corrosion rate to less than 1 mpy at various depths of burial are shown below:

Depth relative to mudline, ft	Current density required to reduce corrosion rate to less than 1 mpy, mA/ft^2
+1	5
−1	2.5
−3	1.5
−5	1.5

TABLE 4—*Weight loss-corrosion rates in the Gulf Floor—Buccaneer test.*

	Corrosion Rate, mpy[a]							
Current density, mA/ft²	1.6[b]	2.4	3.6	5.5	8.2	None[b]	None	None
Depth relative to mudline, ft:								
+1	8	5 (30)	4	0.3	0.8	9,9	6,6 (39,21)	7,7 (62,64)
−1	2	1	0.2	0.1	0.3	3,4	3,3 (25,34)	3,3 (9,7)
−2	...	...	...	...	...	3,4	2,3 (14,7)	7,3 (9)
−3	1[c]	0.07	0.1	0.07	0.09	3,4	2,2	2,3
−4	...	...	...	...	...	3,3	4,3 (12,20)	3,3 (20,18)
−5	0.5[c]	0.1	1[d]	0.6[d]	0.09	3,2[c]	4,4 (37.12)	2,3 (14)

[a] Based on 205-day exposure time. Numbers in parentheses indicate penetration rates estimated from maximum pit depth and exposure time.

[b] Based on 108-day test period.

[c] Corrosion was somwehat localized and only occurred on a portion of these specimens. However, the rate of penetration in each case was less than twice the corrosion rate shown.

[d] Partially shorted to support rack.

There appeared to be a slight tendency for corrosion to become more localized with increasing depth of burial in the mud.

Table 4 gives weight-loss corrosion rates for panels exposed in the West Delta test. Specimens located in the water or at the mud/water interface and protected by current densities of 1.2, 2.2, 3.2 mA/ft² corroded at a smaller rate than unprotected panels in the same location. These data show that the current density required to reduce the corrosion rate to less than 1 mpy above the mud or at the interface is in excess of 3.2 mA/ft². However, below the mud a current density of only 0.6 mA/ft² reduces the corrosion rate to less than 1 mpy. In addition, at a constant current density the corrosion rate of cathodically protected steel decreases with increasing burial depth.

The results obtained on protected and unprotected panels after 10.5 months in the West Delta test are in good agreement with the results of similar studies after 7 months in the Buccaneer test. In both cases the corrosion of unprotected steel panels buried in the ocean bottom was less severe than the corrosion in the water immediately above the bottom. The corrosion rate of unprotected steel based on 7 months' exposure to seawater above the mud in the Buccaneer test was 6 to 7 mpy while after 10.5 months' exposure to seawater in the West Delta test unprotected panels showed a corrosion rate of 10 to 11 mpy. The corrosion rate of unprotected steel below the mudline was about 3 mpy in both the Buccaneer and West Delta tests. In the absence of cathodic protection, pitting corrosion was slightly less severe in the West Delta test than in the Buccaneer test. In both tests the weight-loss corrosion rate of cathodically protected steel decreased with increasing burial depth. In both the Buccaneer and West Delta tests the current density required to reduce the corrosion rate to less than 1 mpy was in excess of 3.2 mA/ft^2 above the mudline. Below the mud a current density of 0.6 mA/ft^2 in the West Delta test and 1.5 to 2.5 mA/ft^2 in the Buccaneer test was required to reduce the corrosion rate to less than 1 mpy. Slight differences between the results obtained in the Buccaneer test and those obtained in the West Delta test can be attrib-

A. CALCAREOUS DEPOSITS

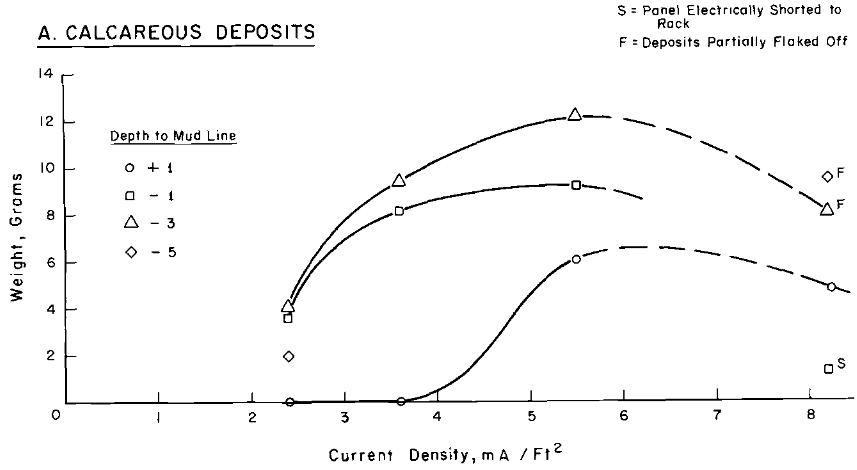

B. MARINE GROWTH 1-FOOT ABOVE MUD LINE

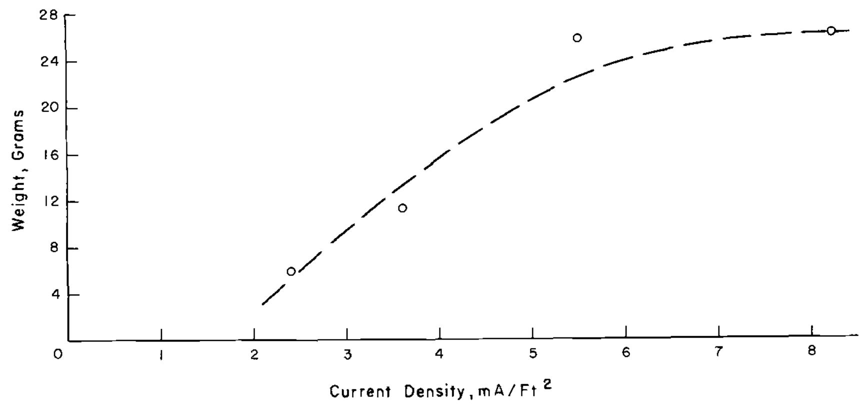

FIG. 10—*Effect of current density on deposition of marine growth and calcareous deposits, 7 months' exposure—Buccaneer test.*

uted to differences in water depth, oxygen concentration, exposure time, marine growth, and bottom composition between the two test sites.

Effect of Current Density on Calcareous Deposit Formation

Amount of Deposits—The alkaline environment created by cathodic protection causes calcium carbonates and magnesium hydroxide (calcareous deposits) to be precipitated on the steel surface. As shown in Fig. 10, in the Buccaneer test increasing current density increases the amount of calcareous deposits, reaching a maximum at a current density of about 5 to 6 mA/ft^2. At higher current density, the amount of calcareous deposit appeared to decrease, owing to flaking off of a portion of the deposits, perhaps because of hydrogen evolution. About 8.2 mA/ft^2 resulted in considerable flaking off of calcareous deposits. Small amounts of flaking were also observed on the specimen protected with a current density of 5.5 mA/ft^2.

Deposit Composition—X-ray analysis of the crystalline portions of calcareous deposits scraped from cathodically protected specimens from the Buccaneer test showed their composition to be principally aragonite and calcite (both forms of $CaCO_3$), brucite ($MgO \cdot H_2O$), and sand (quartz and feldspar). As shown in Fig. 11, the percentage of brucite in the deposits

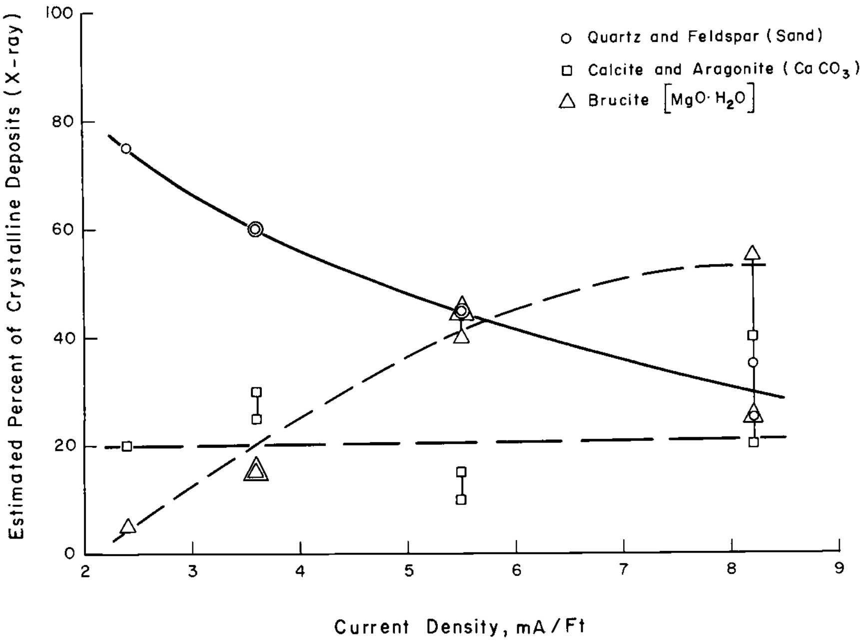

FIG. 11—*Effect of current density on relative composition of calcareous deposits on panels below mudline—Buccaneer test.*

increased with increasing current density while the amount of sand decreased. The amount of calcium carbonates appeared to be unchanged. The decrease in sand content is thought to be an apparent effect brought about by increasing the amount of brucite deposited between sand grains. However, a portion of the decrease is also due to actual displacement of the occluded sand when deposits flaked off at higher current densities. The calcareous deposits reformed behind these flaked-off deposits contained very little sand.

Microscopic Examination of Calcareous Deposits—When current densities of 2.4 and 5.5 mA/ft^2 were applied for seven months to steel panels three feet below the mudline, calcareous deposition was only partially complete on the 2.4-mA/ft^2 panel. However, the metal was being protected (corrosion rate <0.2 mpy) and was still bright. The panel with 5.5 mA/ft^2 developed a complete calcareous deposit layer. These calcareous deposits consisted of occluded sand grains surrounded by calcium carbonate and magnesium hydroxide. Deposits on an 8.2-mA/ft^2 specimen analyzed by X-ray contained 85 percent brucite, 10 percent aragonite, and 5 percent quartz.

Pipe Nipples

The corrosion rates of eight, electrically connected, unprotected nipples of pipe, exposed vertically such that the top half of the pipe nipple assembly was in the water while the bottom half was in the mud, were similar and independent of position relative to the mudline. Specimens located either above or below the mud or at the water/mud interface corroded at a rate of 4 to 5 mpy. Pitting corrosion for the eight lengths was also similar at all locations. Pitting corrosion rates of about 15 mpy were found with no apparent differences between those pipe sections located in the mud, in the water, or both.

The fact that a "continuous" pipe specimen corrodes uniformly while "separate" panels corrode at varying rates, depending on position relative to the mudline, may be explained as follows: on "separate" panels all of the oxygen which is reduced on the specimen surface causes corrosion only on that surface. However, on a "continuous" specimen, some of the oxygen which arrives at the top of the specimen above the mud can cause corrosion below the mud.

In general, marine growth on both the panels and pipe nipples exposed at West Delta was not extensive, probably owing to the relatively short duration of the test (10.5 months) and to the depth of the water at the test site (275 ft). As mentioned earlier, a large amount of marine growth was found on the panels above the mudline in the Buccaneer test after four years' exposure at a depth of 70 ft.

Other Tests

In addition to the corrosion and cathodic protection tests described in the foregoing, a series of tests on the behavior of various paints, coatings, cables and other materials was determined in the West Delta and Buccaneer tests. The results of these tests are summarized as follows:

Coating Systems (*Pipe Sections*)—A thin-film epoxy coating disbonded in an area extending ⅛ in. in all directions from controlled holidays introduced as holes and slits. The coating was subject to mechanical damage. There was no detectable difference between performance in the mud as compared with performance in the water.

Extruded polyethylene, asphalt, and coal tar coating systems held up well and were in excellent condition at the end of the test period. No disbonding or undercutting occurred at the unprotected ends or at the controlled holidays introduced as holes and slits.

A concrete coating protected steel pipe quite well, although water wicked in between coating and pipe an average of two inches from the unprotected ends and beyond intentionally damaged areas. The corrosion which occurred in the disbonded area was general with no evidence of pitting.

Coating Systems (*Rack*)—The results of the evaluations of the paint systems used on the rack itself led to ranking the paint systems as follows:

1. Inorganic zinc primers, epoxy top coat.
2. Zinc-rich epoxy primers, epoxy top coat.

Coating Systems (*Cables*)—The results of the evaluation of the three test cables used during the West Delta test are as follows:

1. Polyurethane-coated ½-in. 3 × 19 wire rope (minimum breaking strength 25 700 lb): None of the wires in the rope were broken either during installation or recovery of the test rack; no deterioration or corrosion of the cable was evident.

2. Galvanized ¾-in. 3 × 19 wire rope sling (minimum breaking strength 57 800 lb): none of the wires in the rope were broken either during installation or recovery of the test rack; approximately 20 percent of the galvanized cable was covered with light rust.

3. Aluminum-coated ⅝-in. 6 × 19 preformed improved plow wire rope (minimum breaking strength 33 400 lb): None of the wires in the rope were broken either during installation or recovery of the test rack; heavy rust completely covered the exposed cable.

Stressed Specimens—None of the stressed (mild and stainless steel) test specimens (stressed by bending into a U-shape and bolting the ends together) exposed in the West Delta test were found to contain stress corrosion cracks. It should be noted, however, that more severe stressing (that is, use of notches or fatigue cracks as stress raisers) could possibly produce stress corrosion cracking.

Anode Metal Specimens—A large amount of calcareous deposit ($\sim\frac{1}{2}$ in. thick) was formed on zinc metal when the zinc was electrically connected to a magnesium strip during the 10.5-month test. This deposit consisted mainly of brucite (93 percent) with smaller amounts of aragonite (4 percent), halite (2 percent), and calcite (1 percent). The corrosion product from the magnesium oxidation consisted entirely of brucite. In the galvanic series of metals in seawater, zinc is more noble than magnesium. Thus, when zinc metal is electrically connected to magnesium, the zinc becomes cathodic (negative) to the magnesium. On offshore pipelines zinc anode bracelets are used in a sacrificial system in conjunction with an impressed current system. When the impressed current system is in use, the zinc bracelets are made cathodic (negative) to the impressed current anode. As shown in our test in West Delta, when zinc is made negative, calcareous deposits can form.

Conclusions

Results obtained to date from corrosion tests in the Gulf floor are summarized as follows:

1. The corrosion rates of unprotected steel panels buried in ocean bottom sediments are less than in the ocean immediately above the mudline.
2. Both above and below the mudline, the general corrosion rates of unprotected panels decrease with time. This is attributed to the accumulation of corrosion products or marine growth or both on the panels.
3. Pitting corrosion of unprotected panels is most intense in the area extending from above the mudline to about one foot below the mudline. This is the region in which offshore pipelines are exposed.
4. The corrosion rates of cathodically protected steel panels decrease with increasing burial depth.
5. (*a*) Above the mudline the continuous current density required to reduce the corrosion rate of protected panels to less than 1 mpy is in excess of 3.2 mA/ft^2; (*b*) below the mudline a current density of 0.6 to 2.5 mA/ft^2 (depending on location in the Gulf and duration of test) reduces the corrosion rates of protected panels to less than 1 mpy.

The current density commonly used on pipelines in seawater is initially about 5 mA/ft^2. After the formation of a calcareous coating on the steel, this current density is decreased to about 3 mA/ft^2. Onshore pipelines require 1 to 3 mA/ft^2 of bare metal for complete cathodic protection.

6. The corrosion rates of unprotected lengths of pipe joined together are similar (4 to 5 mpy) and independent of position relative to the mudline.
7. A large amount of calcareous deposit (mainly brucite) is formed on zinc metal when it is made electrically negative for 10.5 months in seawater.

APPENDIX

Specimens Used

Unprotected Weight Loss Specimens

Panels—⅛ by 4 by 8-in. AISI C-1018 cold-finished, ground, steel panels mounted with 8-in. dimension vertical. Teflon insulation is used to isolate panels from support rack. Each panel has two drilled holes on longitudinal centerline for support.

Pipe Nipples—Eight weighed 1-ft lengths of 2-in. Grade B pipe, machined to a smooth, bright finish, connected by metal screw collars to form an electrically continuous pipe. The resulting assembly is mounted in vertical position but electrically insulated from support rack.

Cathodically Protected Weight Loss Specimens

These panels are identical to the ones just mentioned except that an insulated wire conductor was fastened to a steel block attached to one corner of each panel.

In the Buccaneer tests, current to all test panels was provided from a dc power supply, with the current to each specimen regulated by means of a one-turn 25 000-Ω potentiometer; current to each panel was measured by the IR drop across a 1000-Ω (1 percent tolerance) shunt.

In the West Delta test, current to each test panel was provided by a stack of mercury-cell batteries through precision resistors to limit the current flow. Total current to each panel was measured by coulometric integration devices.

Stressed Specimens

Buccaneer Test—Longitudinal specimens cut from a section of 8⅝-in.-outside diameter by 0.250-in. wall thickness Grade X-52 pipe with a girth weld in the middle of the test section. The specimens were stressed by bending into a U-shape and bolting the ends together with a steel bolt.

West Delta Test—Stressed ASTM B-7 bolts with and without cathodic protection (provided by zinc block).

Anode Materials

Two metallic specimens used extensively as sacrificial anodes in cathodic protection, one of magnesium and the other of zinc, were electrically connected and mounted on each rack to evaluate the effect of making zinc cathodic prior to its use as a sacrificial anode on a steel pipeline.

Cables—(West Delta Test Only)

The following three cables were used in the corrosion study:

1. Polyurethane-coated ½-in. 3 × 19 wire rope used to tether the corrosion rack to Platform A (primary recovery system).
2. Galvanized ¾-in. 3 × 19 wire rope sling used to connect Cable A to the leg of the platform.
3. Aluminum coated ⅝-in. 6 × 19 improved plow wire rope used to connect the corrosion rack to a pyramidal anchor (backup recovery system).

Coating Systems

Pipe Sections—Ten-foot lengths of 2-in. Grade B pipe were coated with the following systems in accordance with standard application practices.

1. Thin-film epoxy, 10 to 12 mils, no primer.
2. Extruded polyethylene.
3. Asphalt.
4. Coal tar.

In addition, a 10-ft length of 6-in. Grade B pipe was sandblasted to a gray finish and then a 1-in. thick standard concrete coating was applied. Pipe samples were suspended from the rack in a vertical position, which placed the bottom 5 ft in the mud and left the remainder extending into the water above the mudline. Two intentional holidays (⅛ and ¼-in. diameter) were drilled through each coating to the pipe surface before installation in the Gulf.

Rack—Each of the 10-ft-long, 10-in.-diameter pipes which acted as the four corner legs of the corrosion test rack was coated with a separate protective coating system. These systems have been used extensively throughout the industry.

The metal surface was first sandblasted to a white metal finish and then the protective systems given in Table 5 were applied in accordance with the manufacturer's recommendations.

TABLE 5—*Protective systems.*

Leg No.	Primer Coat	Thickness Primer Coat, mils	Top Coat	Total Thickness of System, mils
1.	Post cure inorganic zinc	4	epoxy	24
2.	Self-curing inorganic zinc	3	epoxy	24
3.	Zinc-rich epoxy	6	epoxy	20
4.	Zinc-rich epoxy	2½	epoxy	18

References

[*1*] Reinhart, F. M. and Jenkins, J. F., "Corrosion of Alloys in Hydrospace—189 Days at 5900 Feet," NCEL TN-1224, April 1972.

[*2*] Beaubien, L. A. et al, "Behavior of Materials in a Subsurface Ocean Environment," NRL Memorandum Report No. 7447, July 1972.

[*3*] Hazard, P. M., *Bell Laboratories Record*, Vol. 39, No. 3, 1961, p. 92.

[*4*] Ailor, W. H., *Journal of Hydronautics*, Vol. 2, No. 1, 1968, p. 26.

[*5*] Glowacki, A. S., "Protective Coatings for Deep Submergence Vessels," U. S. Rubber Co. Quarterly Report No. 5, June 1965.

[*6*] Fink, F. W. and Boyd, W. K., "The Corrosion of Metals in Marine Environments," Defense Metals Information Center Report No. 245, May 1970.

[*7*] International Nickel Company, *Guidelines for Selection of Marine Materials*, Published by INCO, 1966.

J. F. Rynewicz[1]

Evaluation of Paint Coatings Tested in the Deep Atlantic and Pacific Oceans

REFERENCE: Rynewicz, J. F., "**Evaluation of Paint Coatings Tested in the Deep Atlantic and Pacific Oceans,**" *Corrosion in Natural Environments*, *ASTM STP 558*, American Society for Testing and Materials, 1974, pp. 209–235.

ABSTRACT: Seven different paint coating systems were tested on structural steels, high-strength stainless steels, and aluminum alloys. The Pacific specimens were placed on the bottom in 5900 ft of water for six months while the Atlantic specimens were on the bottom at 4050 ft for more than four years.

The epoxy paint system provided good to excellent corrosion protection at both test locations.

The inorganic zinc coating provided adequate protection to the steel specimens for six months in the Pacific Ocean, but would have to be at least 0.010 to 0.020 in. thick to be effective for up to one year.

The two stainless steels Almar 362 and Carpenter 455 were highly susceptible to crevice corrosion when not coated. Uncoated specimens suffered from crevice attack in the same manner as types 302, 303, and 304 stainless steel.

The cathodic protection achieved by the inorganic zinc coating on steel specimens indicates that cathodic protection is a practical method of corrosion control in the deep ocean.

KEY WORDS: corrosion, epoxy coatings, inorganic coatings, crevice corrosion, cathodic protection, zinc coatings, paints

In April 1968, Lockheed Missiles & Space Company, Inc. (LMSC) placed 54 corrosion test specimens on the Naval Applied Science Laboratory's (NASL) Deep Ocean Material Array, which at that time was about to be installed on the bottom of the Atlantic Ocean in an area identified as the Tongue of the Ocean (TOTO). The test site was at the coordinates 23 deg 52 min N and 76 deg 46.6 min W as shown in Fig. 1. The array was recovered and specimens removed in August 1972 after 52 months exposure at the 4050 ft depth.

The purpose of these corrosion tests was to evaluate the effectiveness of protective coatings on structural steels and aluminum alloys in the deep ocean and to determine the corrosion resistance of two recently developed (at that time) high-strength heat-treatable stainless steels. The results of

---

[1] Lockheed Missiles & Space Company, Inc., Ocean Systems—Naval Architecture & Marine Engineering, Sunnyvale, Calif. 94088.

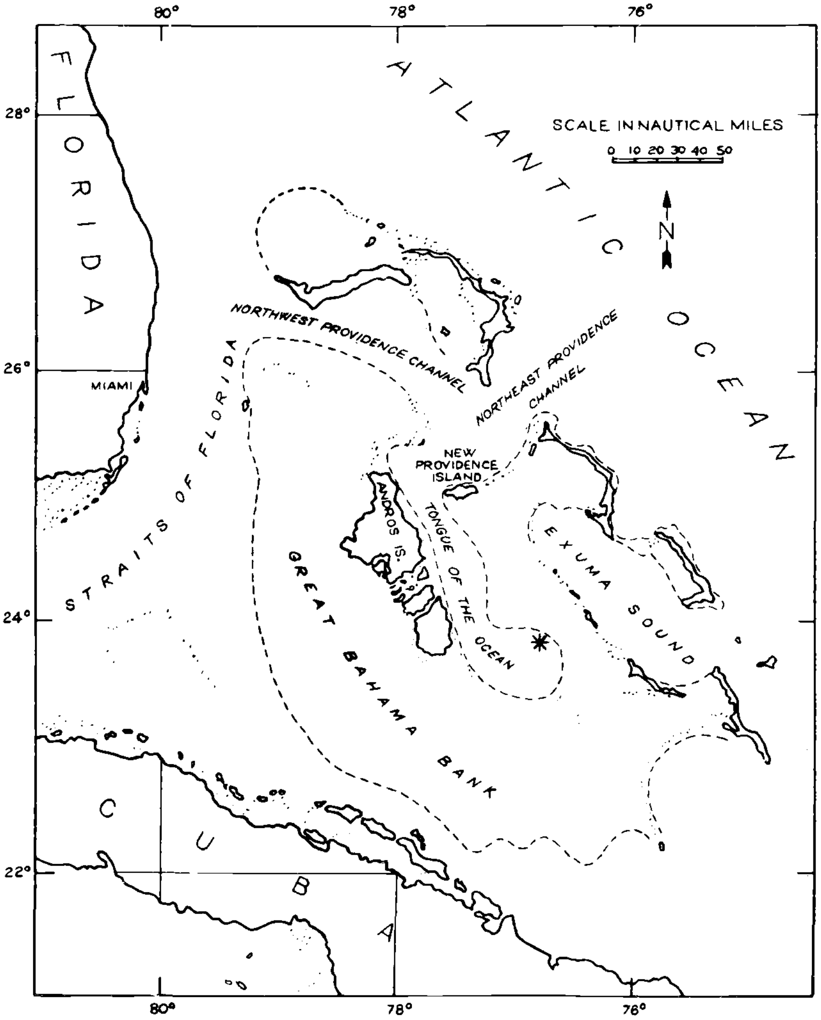

FIG. 1—*Location of exposure site in the Tongue-of-the-Ocean.*

these tests would be used by the LMSC Offshore Petroleum and Deep Ocean Mining Programs, which would be placing structures in the deep ocean.

During the same time period, the Naval Civil Engineering Laboratory (NCEL) was also placing a Deep Ocean Material Array in the Pacific. Eighty-seven specimens of the same alloys protected with the same paint systems as the NASL array specimens were mounted on the NCEL array and placed on the bottom at the 5900 ft depth in the Pacific during August 1968. The test location was 33 deg 51 min N and 120 deg 35 min W, which is approximately 75 miles west of Port Hueneme, California. This array was recovered in February 1969 after 189 days of exposure.

Description of Test Specimens

Protective coatings were tested on the structural steels, stainless steels, and aluminum alloy specimens placed in the deep Atlantic and Pacific Oceans. Stainless steel specimens were also exposed in the uncoated condition. The two specimen sizes used were 1 by 6 in. and 6 by 12 in. for the stress corrosion tests and 6 by 12 in. for the general and localized corrosion tests. The specimen thicknesses were 0.040 to 0.190 in. for the stainless steels, 0.190 and 0.250 in. for the structural steels, and 0.060 to 0.250 in. for the aluminum alloys. Table 1 provides the chemical composition of the test alloys and Table 2 lists the mechanical properties of the test specimens. The specimens tested in the Atlantic and Pacific are listed in Tables 3 and 4.

Preparation and Painting of Specimens

Surface preparation prior to paint coating of the specimens was as follows:

Structural Steels	Stainless Steels	Aluminum Alloys
1. Solvent clean	1. Solvent clean	1. Solvent clean
2. White metal sandblast	2. Passivate	2. Wire brush
3. Solvent clean		3. Solvent clean

Seven different paint coatings were used to protect the alloys listed in Tables 3 and 4. Table 5 describes the paint systems and identifies the manufacturer. All of the paint systems were epoxy or had epoxy topcoats except one, which was a two-coat inorganic zinc-rich system.

The structural steel specimens were all protected by paint coatings except for two, which had hard-facing weld deposits. Control, or unpainted, specimens of the structural steel alloys were not tested since corrosion tests in the deep ocean of low-alloy structural steels had already been performed by NCEL.[2,3]

Welding and Heat Treatment of Specimens

The structural steel stress corrosion specimens (1 by 6 in.) were produced by manual welding operations with low-hydrogen flux-coated electrodes. Electrode-type E7018 was used for the ASTM-A-242 (Cor-Ten) and

---

[2] Reinhart, Fred M., "Corrosion of Materials in Hydrospace," Naval Civil Engineering Laboratory Technical Report R-504, Dec. 1966.

[3] Reinhart, Fred M., "Corrosion of Materials in Hydrospace, Part I, Irons, Steels; Cast Irons and Steel Products," Naval Civil Engineering Laboratory Technical Note N-900, July 1967.

TABLE 1—*Chemical composition of test specimens.*

				Structural Steel Alloys						
	C	Mn	Ni	Cr	S	P	Mo	Si	Fe	Cu
ASTM-A-572	0.23	1.35	...	...	0.04	0.05	...	0.30	balance	...
ASTM-A-242	0.12	0.4	0.65	0.7	0.05	0.1	...	0.35	balance	0.35
ASTM-A-514	0.15	0.2	0.9	0.5	0.04	0.03	0.5	0.25	balance	0.35
				Stainless Steel Alloys						
	C	Mo	P	S	Si	Cr	Ni	Ti	Cu	Fe
ALMAR 362	0.027	0.22	0.017	0.012	0.12	14.65	6.82	0.85	...	balance
CUSTOM 455	0.03	0.50	...	...	...	12	9	1.0	2.25	balance
	Cu	Cr	Si	Mg	Zn	Al				
6061-T4	0.3	0.25	0.5	1.0	...	balance				
7075-T73	1.6	0.25	...	2.5	5.5	balance				

TABLE 2—*Mechanical properties of test specimens.*

	Ultimate Tensile Strength, ksi	Yield Tensile Strength, ksi	Elongation (2-in. gage length)
Steel alloys:			
ASTM-A-572 (Ex-Ten)	60	42	20
ASTM-A-242 (Cor-Ten)	70	50	18
ASTM-A-514 (T-1)	115	100	18
Aluminum alloys:			
6061-T4	30	16	16
7075-T73	67	56	8
Stainless steel alloys:			
Almar 362			
H950 Temper	170	156	11
H1050 Temper	150	140	14
Caprenter 444			
H950 Temper	252	248	11
H1050 Temper	200	180	16

TABLE 3—*Specimens exposed in the Atlantic.*

	6 by 12 in.		1 by 6 in.[b]	
	Uncoated	Coated	Uncoated	Coated
ASTM-A-514	2	4	...	6
ASTM-A-242	...	4	...	6
ASTM-A-572	...	4	...	6
Almar 362				
H950[a]	1	2	1	2
H1050[a]	2	3	...	...
Carpenter 455				
H950[a]	...	1	1	2
H1050[a]	...	1	1	2
6061-T4	...	3	...	...
Total	5	22	3	24

[a] H950 and H1050 is the heat-treatment identification. Heat-treatment was 1500°F (816°C) for 1 h, water quench, aged at 950°F (510°C) or 1050°F (566°C) for 4 h and air cooled.

[b] Four point loaded bent-beam stress corrosion specimens.

ASTM-A-572 (Ex-Ten) steels and E12018 was used for the ASTM-A-514 (T-1) steel. The larger 6 by 12-in. structural steel specimens were not welded (base metal only).

The weld hard-faced specimens were produced by welding three $\frac{1}{4}$ by 4 by 6-in. pieces of ASTM-A-514 structural steel together with two full-penetration weld joints. The welding electrode used to join this steel was E-12018, which is a flux-coated electrode of low hydrogen content. A

TABLE 4—*Specimens exposed in the Pacific.*

	6 by 12 in.		1 by 6 in.[b]	
	Uncoated	Coated	Uncoated	Coated
ASTM-A-514	...	3	...	5
ASTM-A-242	...	3	...	4
ASTM-A-572	...	3	...	5
Almar 362				
H950[a]	4	5	4	6
H1050[a]	3	4	5	7
Carpenter 455				
H950[a]	2	3	2	...
H1050[a]	2	3	2	1
6061-T4	...	7	...	...
7075-T73	...	4	...	...
Total	11	35	13	28

[a] H950 and H1050 is the heat-treatment identification. Heat-treatment was 1500°F (816°C) for 1 h, water quench, aged at 950°F (510°C) or 1050°F (566°C) for 4 h and air cooled.

[b] Four point loaded bent beam stress corrosion specimens.

TABLE 5—*Paint coating systems.*

System No.	Type	Thickness, mil	Manufacturer	Manufacturer's Identification
1	Inorganic zinc	6/8	Zinc-Lock	Zinc-Lock 351
2	Inorganic zinc	10/12	Zinc-Lock	Zinc-Lock 351
	Wash primer		...	MIL-C-8514
	Epoxy topcoat		Zinc-Lock	Oxirane A-1105
3	Inorganic zinc	10/12	Zinc-Lock	Zinc-Lock 351
	Wash primer		...	MIL-C-8514
	Epoxy topcoat		A. H. Brown	A-1105
4	Epoxy coal tar primer	16/20	Carboline	Carbomastic 3
	Epoxy coal tar topcoat			Carbomastic 5
5	Epoxy coal tar primer	16/20	Carboline	Carbomastic 3
	Epoxy coal tar topcoat			Carbomastic 12
6	Wash primer	12/16	...	MIL-C-8514
	Red lead epoxy primer		A. H. Brown	A-1109
	Epoxy topcoat		A. H. Brown	A-1105
7	Wash primer	12/16	...	MIL-C-8514
	Epoxy primer		Magna	3-4-44/10C-137
	Epoxy topcoat		A. H. Brown	A-1105

single layer of weld hard-facing metal approximately 1 by 5 in. was then deposited on both sides 2 in. from each end to balance the stresses induced during welding operations. Stoodite 2134 electrodes and Stoodite coated tube electrodes were used at each end respectively. The composition of the flux-coated weld hard-facing electrodes is given in Table 6.

TABLE 6—*Nominal composition of weld hard-facing electrodes.*

Stoodite 2134	Stoodite Coated Tube Electrode
Alloy Content 44%	Alloy Content 39%
Chromium	Chromium
Molybdenum	Manganese
Manganese	Silicon
Silicon	Molybdenum
Nickel	Zirconium
Vanadium	Carbon
Carbon	Iron base
Iron base	

One of the hard-faced specimens was protected by zinc anodes bolted at each end of the specimen. The area ratio, steel to zinc, was approximately 18 to 1. Figure 2 is a sketch of the weld hard-faced specimens prior to testing; these hardfaced specimens were tested only in the Atlantic Ocean.

The stainless steel base metal specimens of Almar 362 and Carpenter 455 were solution heat-treated, water quenched and aged at two different temperatures, 950°F (510°C) and 1050°F (566°C), for 4 h.

Weldments of the stainless steels were produced by the gas tungsten arc process without the addition of filler metal. Welding was done after

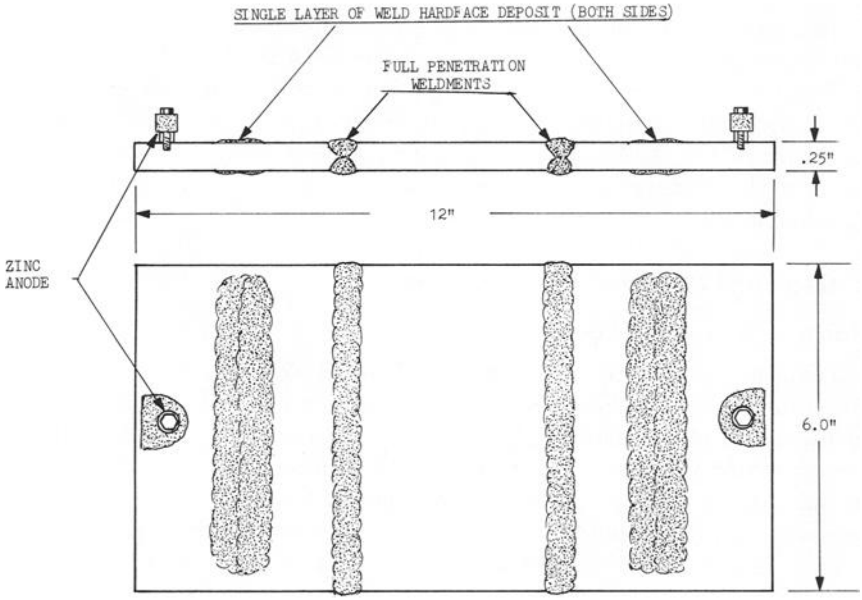

FIG. 2—*ASTM-A-514 structural steel corrosion specimen partially clad with hard-facing by weld deposits.*

solution treatment and before aging. Base metal and weldment stress corrosion specimens of the stainless steel alloys were exposed in the painted and unpainted conditions. There was no welding or heat treatment of the aluminum alloy specimens. These alloys (7075-T73 and 6061-T4) were taken from plate product that had been heat-treated by the producer.

Description of Test Sites

The Atlantic and Pacific test site locations and conditions were as follows:

	Atlantic	Pacific
Location	23 deg 52.12 min N 76 deg 46.60 min W	33 deg 51 min N 120 deg 35 min W
Depth, ft	4050	5900
Temperature, °C	4.56	2.3
Oxygen, ml/l	5.70	1.6
Salinity, ppt	34.98	34.6
Current, knots	0.5	0.03
pH	...	7.4

Description of Test Fixtures

The 6 by 12-in. specimens were held between four polyethylene rods that had machined grooves every 2 in. along the rods for holding the specimens at their mid-width and mid-length points. Figure 3 shows one of the two racks that held 6 by 12-in. specimens on the NASL Array.

The 1 by 6-in. stress corrosion specimens were bent over two glass-reinforced plastic mandrels by torquing bolts at each end of the specimens as shown in Fig. 4. The specimens were insulated from the fixture by the use of a phenolic sleeve and washer insert. All specimens were stressed to 75 percent of their respective yield strength.

Evaluation of Recovered Test Specimens

Atlantic—6 by 12-in. Coated Specimens

The 6 by 12-in. specimens that were painted were found to be in good condition except for those coated with System 1 (Table 5), which consisted of two coats of inorganic zinc-rich primer approximately 0.006 in. thick. Panels coated with this system were found to have a few small rust stains in the case of the stainless specimens such as Specimen 28 (Fig. 5), and extensive rusting in the case of the structural steel Specimens C-1 and T-2 (Figs. 6 and 7). Panels coated with Systems 2 and 3 (Table 5) had blisters on 50 to 100 percent of their surfaces with as many as 30 blisters per square inch (Figs. 8 and 9). There were small amounts of zinc corrosion products in the blisters, indicating that seawater had penetrated the epoxy topcoats.

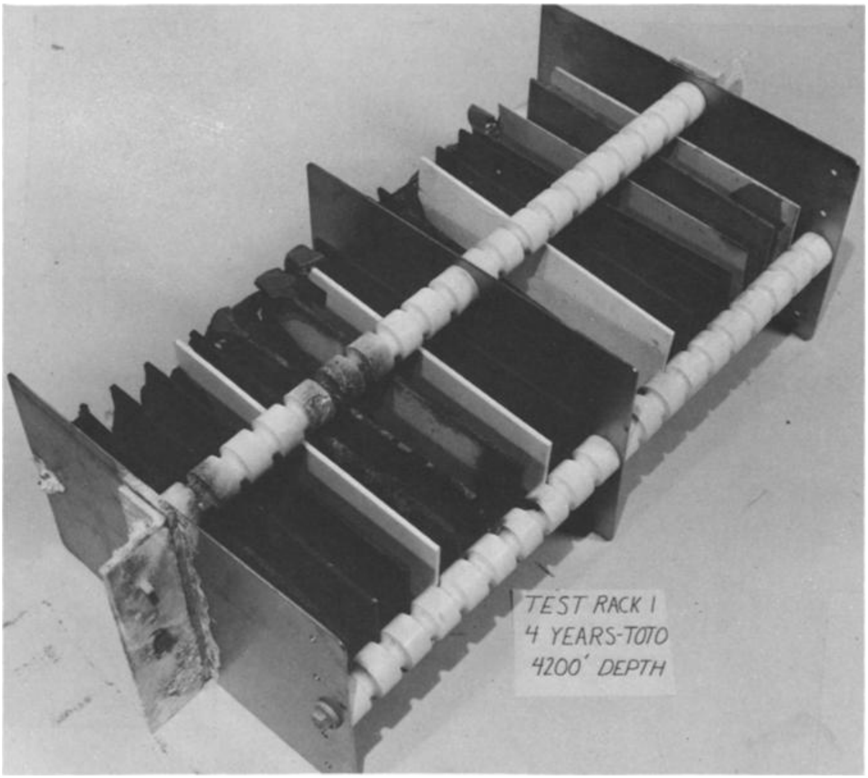

FIG. 3—*Holding fixture for 6 by 12-in. corrosion specimens that were in the Atlantic Ocean (TOTO).*

Panels coated with paint Systems 4, 5, 6, and 7 had very few failure indications. The structural steel panels painted with these systems had a maximum of six indications of tiny (0.010-in.) rust stains and most specimens had no rust indications. The stainless steel and aluminum specimens painted with System 6 had no corrosion failures. Figure 10 shows a specimen typical of those coated with Systems 4 and 5. Figure 11 shows a specimen typical of System 6.

Atlantic—6 by 12-in. Uncoated Specimens

There were three 6 by 12-in. stainless steel specimens exposed without protective coatings and each had crevice corrosion attack. Figures 12–15 show the crevice corrosion that occurred under adhesive tape and at the edge of a panel where it was in contact with the groove in the plastic holding rod. The deepest attack is shown in Fig. 15, with "tunneling" to a depth of 0.12 in. and a length of over 4 in. along the 6 in. width of the specimen edge.

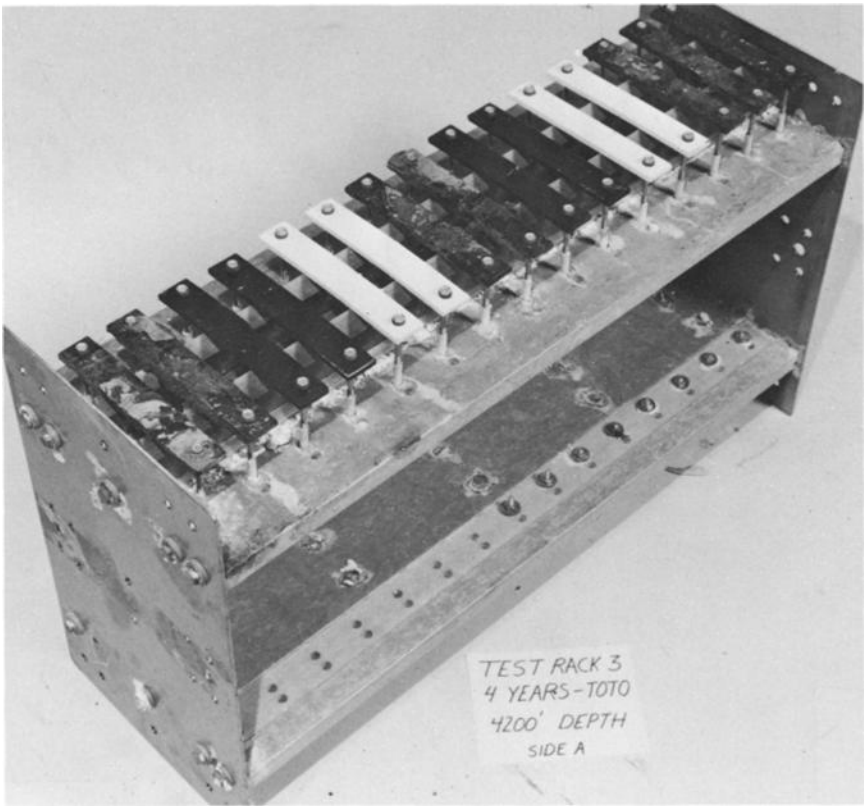

FIG. 4—*Test fixture for 1 by 6-in. stress corrosion specimens that were in the Atlantic Ocean* (*TOTO*).

The ASTM-A-514 structural steel specimens with weld hard-facing were corroded in a somewhat uniform fashion. The specimen without zinc anodes had a thickness variation of 0.211 to 0.254 in. (0.043 in.) while the weld hard-faced specimen with zinc anodes had a thickness variation of 0.226 to 0.253 in. (0.027 in.). The original nominal plate thickness was 0.250 in.

The zinc anodes were completely depleted on the protected specimens (original test plan was for two years' exposure). The zinc anodes reduced the corrosion rate to a maximum of 6.25 mpy (mil per year). Figure 16 displays the thickness variations due to corrosion for each specimen.

Figures 17 and 18 are photographs of the weld hard-faced specimens after removal of corrosion products. It is apparent that even without cathodic protection the weld hard-facing deposits did not cause excessive galvanic corrosion of the structural steel. This is undoubtedly due to the area ratio (6 to 1) favoring the structural steel.

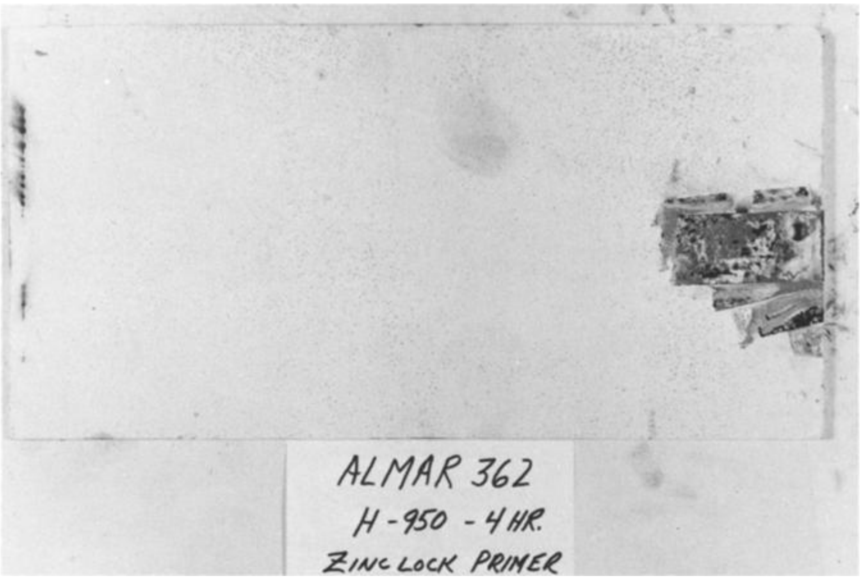

FIG. 5—*Maraging stainless steel Almar 362, condition N950, coated with inorganic zinc-rich primer. Shallow pitting and crevice corrosion has started on left edge and right center of plate.*

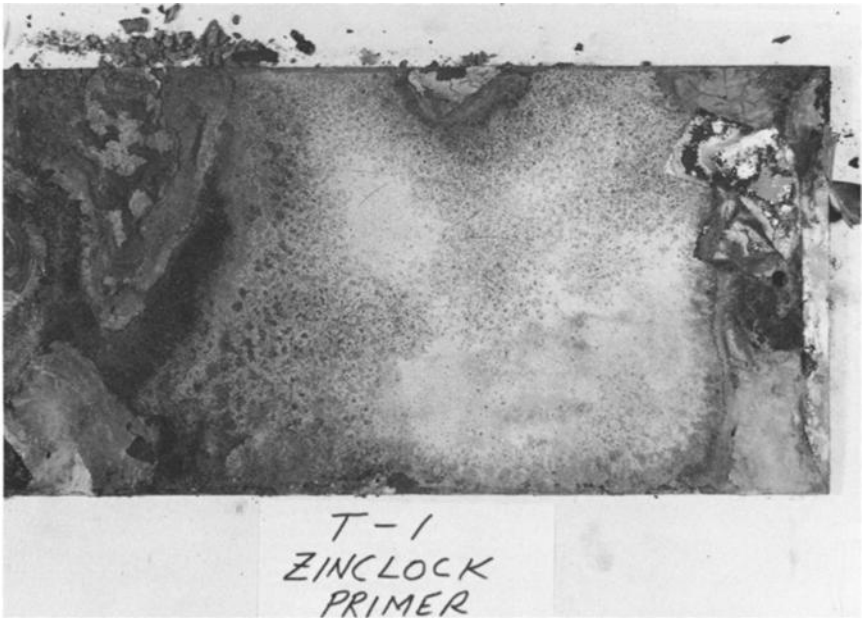

FIG. 6—*ASTM-A-514 structural steel specimen coated with inorganic zinc-rich primer. Coating essentially depleted with subsequent corrosion of specimen.*

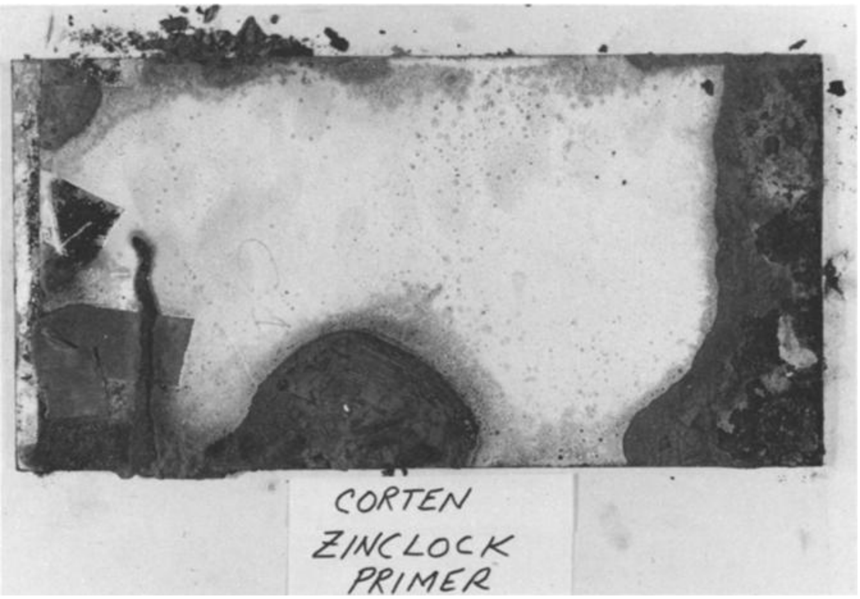

FIG. 7—*ASTM-A-242 structural steel specimen coated with inorganic zinc-rich primer. Coating no longer providing cathodic protection since extensive corrosion attack occurred.*

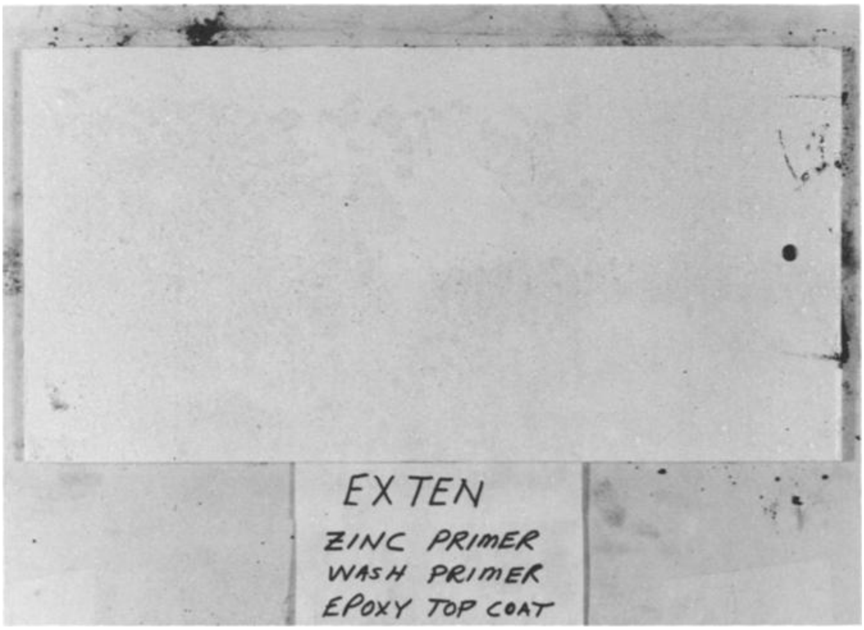

FIG. 8—*Typical blistering of specimens coated with Systems 2 and 3 (Table 5).*

FIG. 9—*Closeup of typical blistering that occurred on specimens coated with Systems 2 and 3 (Table 5).*

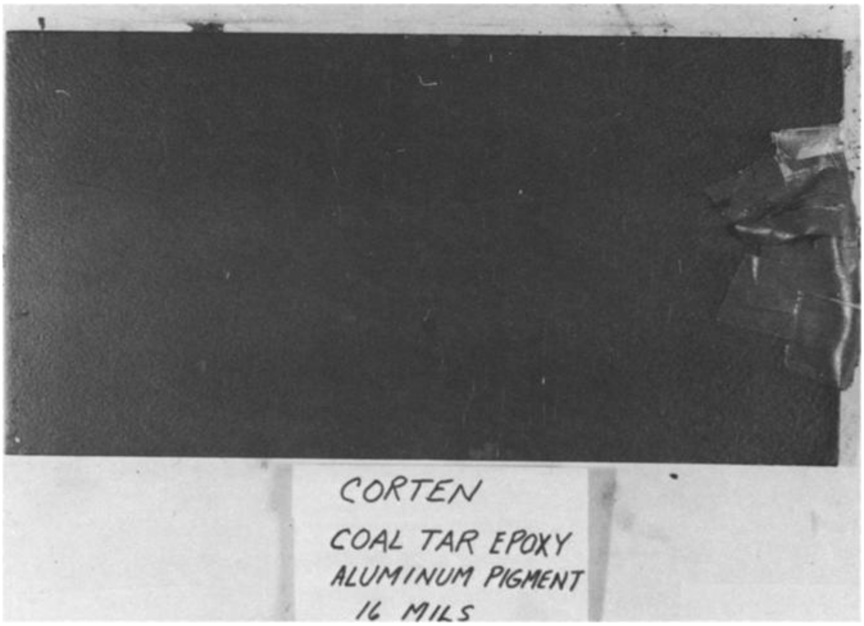

FIG. 10—*ASTM-A-242 structural steel specimen coated with System 4 (epoxy coal tar) This system provided excellent protection to all alloys tested.*

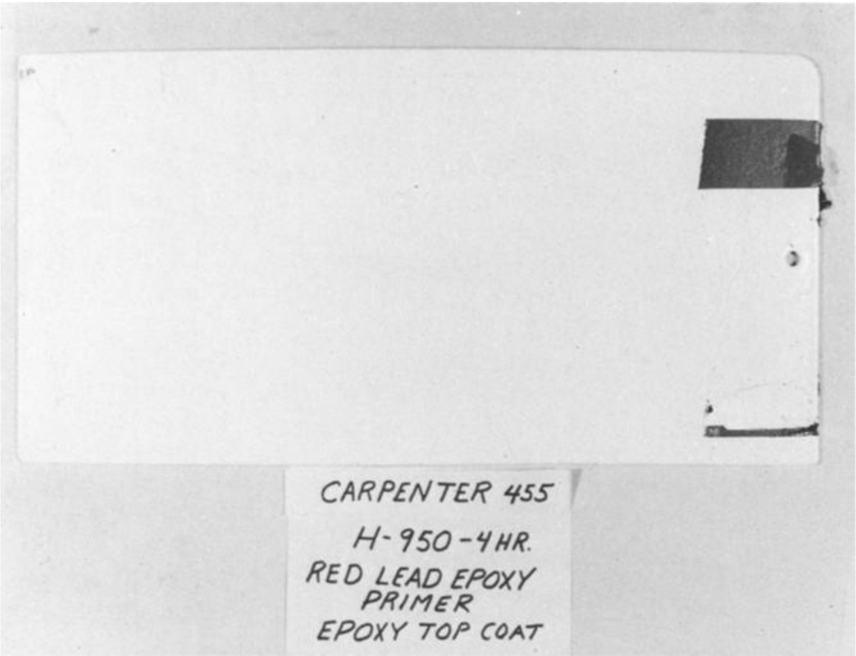

FIG. 11—*Stainless steel specimen coated with System 6. The coating was unchanged by the four-years' exposure time.*

FIG. 12—*Crevice corrosion (top left) that occurred under adhesive tape on Carpenter 455 stainless steel specimens.*

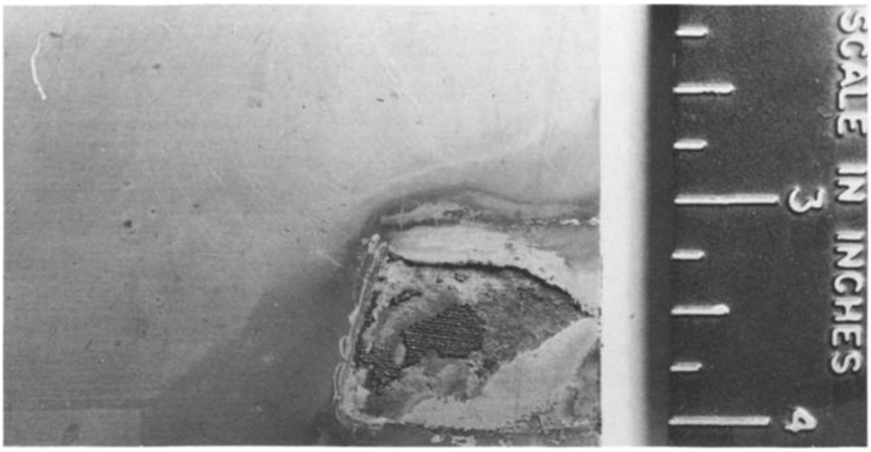

FIG. 13—*Closeup of crevice corrosion in Fig. 12. Depth of attack is 0.021 in.*

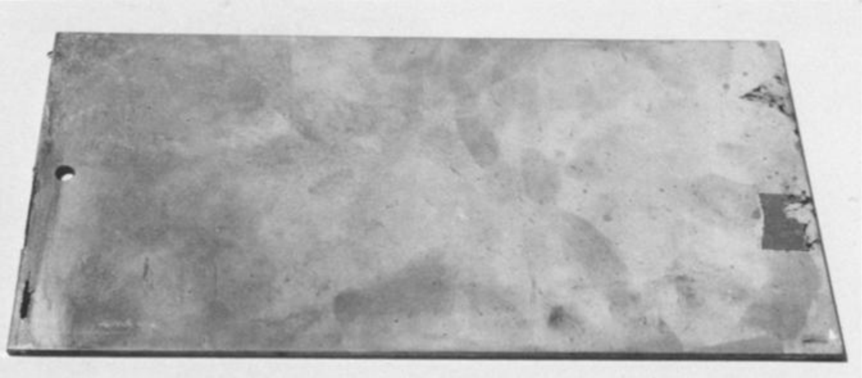

FIG. 14—*Almar 362 stainless steel specimen 0.16 in. thick without protective coating. Crevice/tunneling corrosion occurred on left edge.*

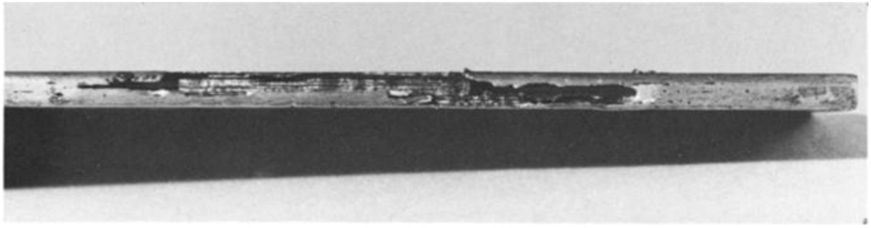

FIG. 15—*Closeup of crevice/tunneling corrosion of specimen in Fig. 14. Depth of attack is 0.12 in. and extends over 4 in. of 6 in. width of specimen.*

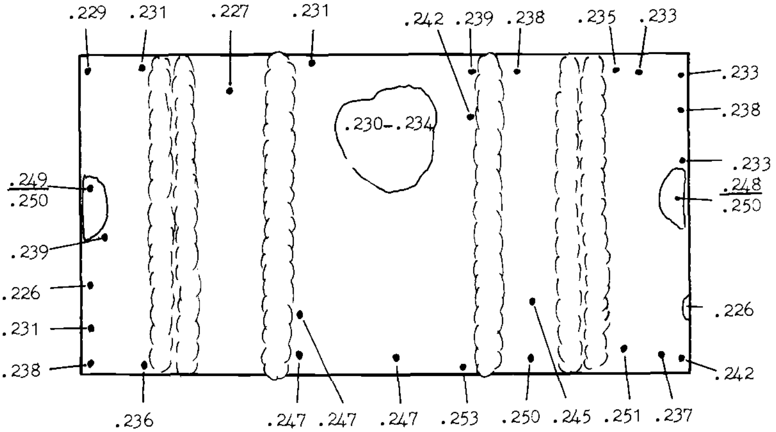

WITH ZINC ANODES

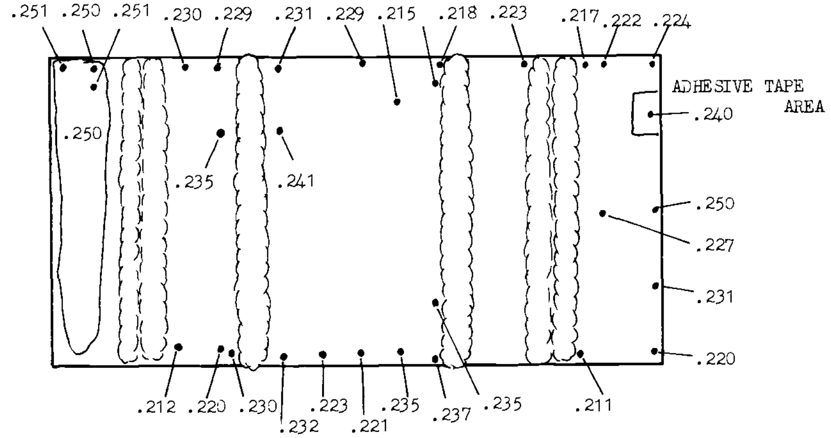

WITHOUT ZINC ANODES

FIG. 16—*Thickness measurements on weld hard-faced specimens after removal of corrosion products.*

Atlantic—1 by 6-in. Stress Corrosion Specimens

There were no occurrences of cracking of the stress corrosion specimens. The coatings protecting the structural steel weldments performed the same as they did on the 6 by 12-in. panels. Coating System 1 was completely depleted, resulting in extensive rusting of the structural steels (see Fig. 19). Coating System 3 had numerous small blisters with faint rust stains on the compression side of the specimen while on the tension side only a few rust stains occurred at the bolt holes (see Fig. 20). Coating Systems 4 and 5

FIG. 17—*Welded ASTM-A-514 (T-1) structural steel specimen with weld thard-face deposits. Although corrosion attack appears relatively uniform, the thickness variation was 0.043 in.*

provided complete protection to the structural steels as seen in Figs. 21 and 22.

The inorganic zinc-rich primer coating (System 1) on the stainless steel specimens was depleted, and on one specimen pitting had initiated at the edge of a weld (Fig. 23) but no cracking had occurred.

Pacific—6 by 12-in. Coated Specimens

The performance of the coatings on the specimens in the Pacific for six months was similar to that observed on the specimens exposed for four years in the Atlantic. The best coating systems were again the all-epoxy systems (4, 5, 6, and 7) with the poorer coating systems being 1 and 3.

FIG. 18—*Welded cathodically protected (zinc anodes) ASTM-A-514 (T-1) structural steel specimen with two 1 by 5-in. weld hard-face deposits to extreme left and right. Corrosion attack resulted in 0.027-in. thickness variation.*

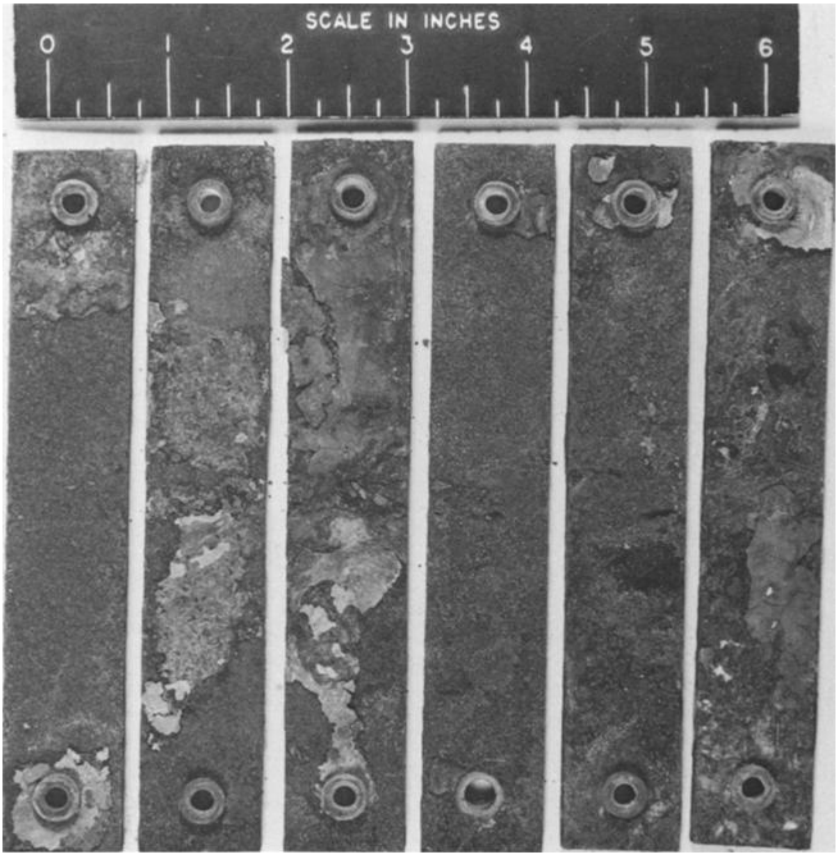

FIG. 19—*Inorganic zinc-rich, primer coat, structural steel, stress corrosion specimens showing complete depletion of coating with subsequent extensive corrosion attack.*

The inorganic zinc-rich primer (System 1) was completely depleted and small rust stains had started at a few locations on the structural steel and stainless steel specimens. The inorganic zinc primer system was no longer protecting the 6061-T4 aluminum specimen, and pitting intensity was approximately one pit per square inch (see Fig. 24).

Coating System 2 was applied only to the stainless steel specimens, which it completely protected.

Coating System 3 was completely ineffective in protecting aluminum alloy 7075-T73. This was due to the poor adhesion of the first coat, which was the inorganic zinc-rich primer. Figure 25 shows the extensive pitting and edge corrosion that occurred under coating System 3 on the 7075-T73 specimen. The depth of corrosion attack was a maximum of 0.07 in. at the specimen edges. The pitting depth ranged from less than 0.005 to 0.070 in.

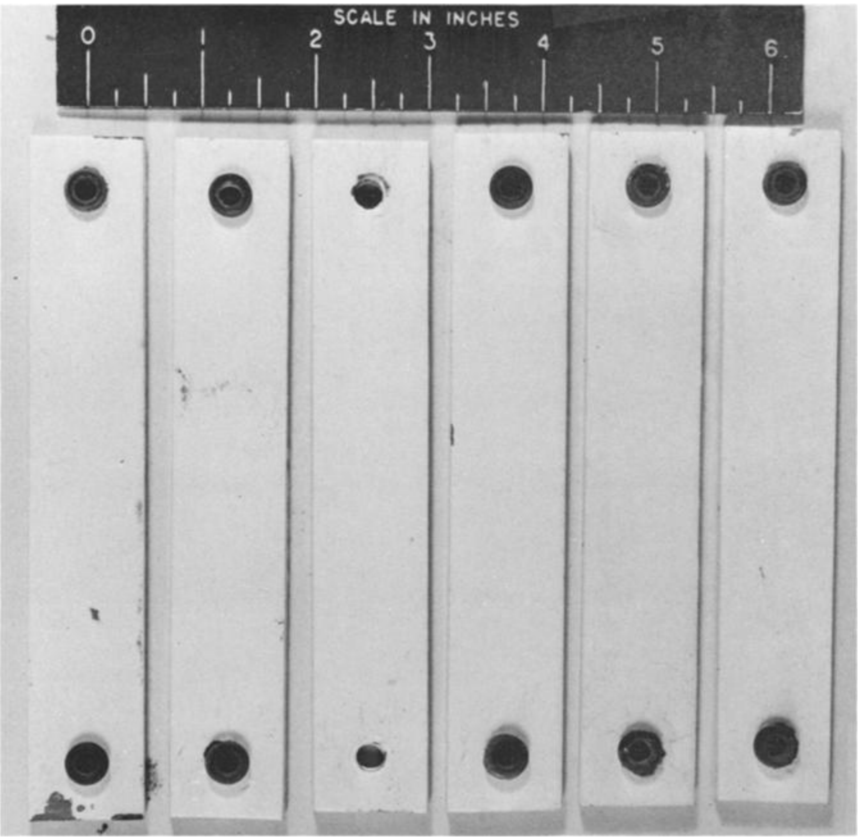

FIG. 20—*Inorganic zinc-rich primer with epoxy topcoat (System 3) provided relatively good protection to stressed structural steels.*

Pacific—6 by 12-in. Uncoated Specimens

There was a total of 11 bare 6 by 12-in. stainless steel specimens. Seven were base metal specimens and four were specimens with a 3-in.-diameter circular weld, produced without filler metal addition to induce high residual stresses that approached the yield stress.

Five of the seven base metal specimens were Almar 362 specimens, which developed a few rust spots <0.002 in. deep. One of the two Carpenter 455 condition H1050 base metal specimens had crevice corrosion 0.100 in. deep at an edge where it was in contact with the plastic rod holder.

The circular weld specimens had light rust deposits at the crater where the weld was terminated, except that one Almar 362 specimen was perforated (0.050 in.) due to pitting/crevice corrosion at the crater termination of the weldment. Figures 26 and 27 show this pitting/crevice corrosion area. There was no evidence of cracking in the corroded areas.

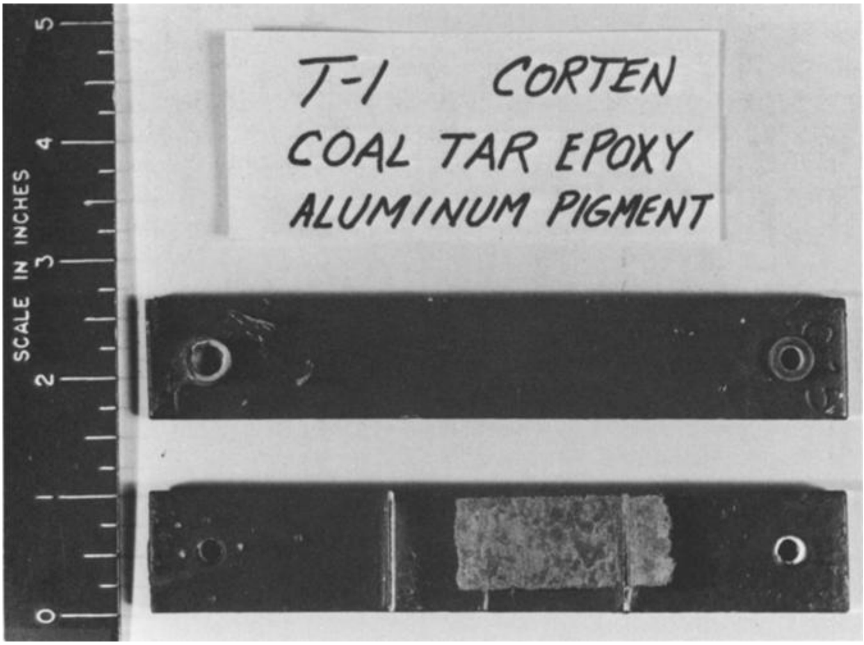

FIG. 21—*Epoxy coal tar with aluminum pigment (System 4) provided complete protection to welded structural steel stress corrosion specimens.*

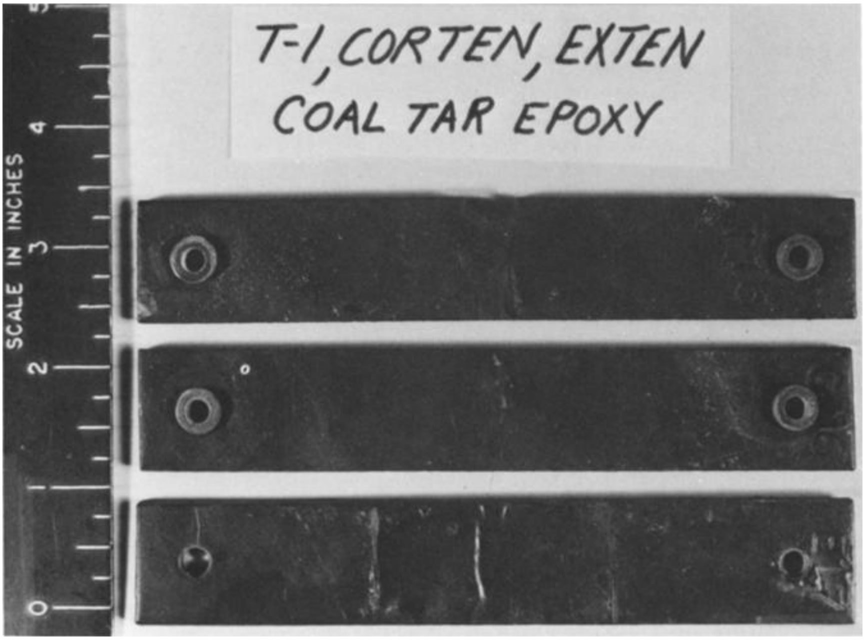

FIG. 22—*Epoxy coal tar (System 5) provided complete protection for welded structural steel stress corrosion specimens.*

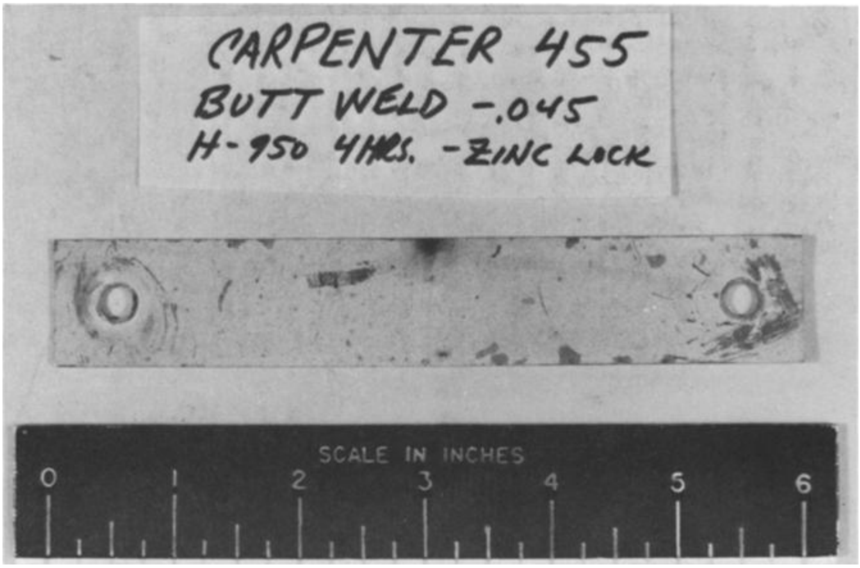

FIG. 23—*Carpenter 455 H950 condition stress corrosion specimen coated with inorganic zinc-rich primer. Corrosion has initiated at edge of the weld zone but there was no evidence of cracking.*

Pacific—1 by 6-in. Coated Stress Corrosion Specimens

There were no stress corrosion failures of the coated structural steel specimens. The structural steel specimens coated with System 1 (inorganic zinc-rich primer) had begun to develop small rust stains at random locations, indicating that the coating was depleted. The stainless steel specimens

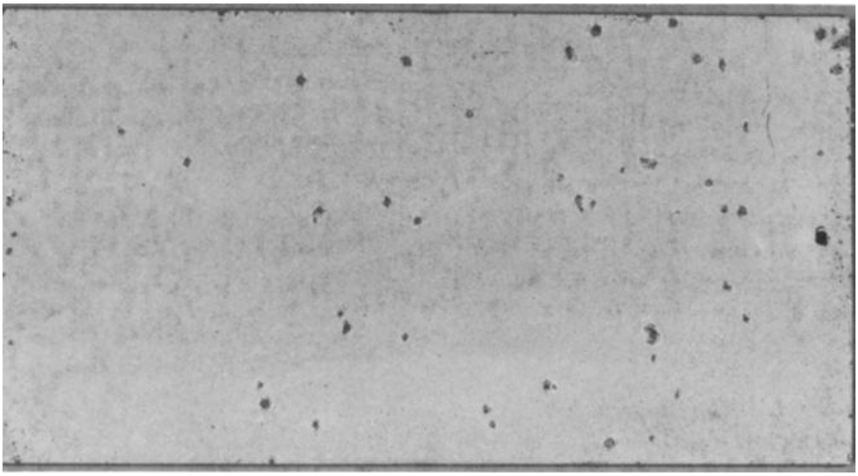

FIG. 24—*Specimen 50—aluminum alloy 6061-T4 coated with Zinc-Lock. Coating depleted and pitting corrosion started after six months in the Pacific.*

FIG. 25—*Specimen 248—aluminum alloy 7075-T73 coated with zinc-rich primer (Zinc-Lock), wash primer, and epoxy topcoat. Coating system did not adhere, resulting in extensive pitting corrosion.*

coated with System 1 had only a few minor rust stains at the bolt-holes on four of the 12 specimens, except for one specimen (Carpenter 455-H1050) that had a crack which initiated at the bolt-hole and extended through the thickness and to the edge of the specimen. The structural steel and stainless steel specimens coated with Systems 4, 5, 6, or 7 were in good condition with only minor rust stains at a few bolt-holes.

FIG. 26—*Specimen 21—maraging stainless steel (Almar 362) heat-treated to H1050 condition, welded without filler metal. Pitting and crevice corrosion has perforated 0.050 sheet at weld edge of sheet.*

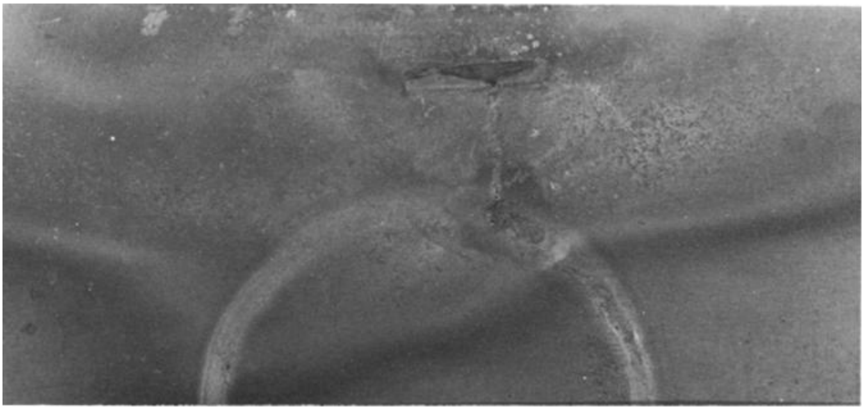

FIG. 27—*Closeup view of crevice and pitting corrosion on Specimen 21 in Fig. 26.*

Pacific—1 by 6-in. Uncoated Stress Corrosion Specimens

There were fourteen Almar 362 and three Carpenter 455 stainless steel specimens exposed without protective coatings. All of these specimens were stressed to 75 percent of their yield strength. None of the specimens exhibited any evidence of cracking even though crevice corrosion occurred at the bolt-hole and at the interface with the fiber glass mandrel.

The most severe crevice corrosion occurred at the bolt-holes. The maximum depth of attack was 0.070 in. on the three Almar 362 specimens (two of H950 temper and one of H1050 temper) of 0.160 in. thickness. Another Almar 362 specimen of 0.050 in. thickness had crevice corrosion to a depth of 0.035 in.

The three Carpenter 455 specimens had incipient (less than 0.002 in.) crevice corrosion at the interface with the fiber glass mandrel.

Comparison of Test Site Results

The performance of the seven different coating systems and the uncoated stainless steel specimens is summarized in Tables 7, 8, and 9. Discussion of the comparison of test site results is in the following sections.

Coatings

System 1—The inorganic zinc-rich primer coating (System 1) at a 0.006 in. thickness provided marginal protection to the structural steel, stainless steel, and aluminum specimens exposed for six months in the Pacific. It is apparent that this coating at the 0.006 in. thickness would not provide one year's protection since rust staining and incipient pitting had already started on a number of specimens.

TABLE 7—*Coating performance—Atlantic tests.*

	System Number						
	1	2	3	4	5	6	7
Structural steels:							
ASTM-A-572	*e*	...	*c*	*b*	*b*	...	...
ASTM-A-242							
ASTM-A-514							
Stainless steel:							
Almar 362	*c*	*c*	...	...	...	*a*	*a*
Carpenter 455							
Aluminum alloys:							
6061-T4	...	...	...	...	...	*d*	*a*

a = Excellent—no defects.
b = Very good—very infrequent small defects.
c = Good—few small corrosion indications.
d = Fair—numerous small corrosion indications.
e = Poor—extensive corrosion attack.

The same coating of the same thickness was quite inadequate for the longer four-year Atlantic tests. (It should be noted that the original plan was for a two-year test in the Atlantic.)

System 2—Coating System 2 used only on the two stainless steels and aluminum alloy 6061 provided complete protection for the Pacific specimens. Although the Atlantic stainless steel specimens coated with System 2

TABLE 8—*Coating performance—Pacific tests.*

	System Number						
	1	2	3	4	5	6	7
Structural steel:							
Ex-Ten	*d*	...	...	*b*	*b*	...	*a*
Cor-Ten							
T-1							
Stainless steel:							
Almar 362	*c*	*a*	...	...	...	*a*	*a*
Carpenter 455							
Aluminum alloys:							
6061-T4	*d*	*a*	...	...	...	*a*	*a*
7075-T73	*d*	...	*e*	...	...	*a*	*a*

a = Excellent—no defects.
b = Very good—very infrequent pinhole.
c = Good—few small corrosion indications.
d = Fair—numerous small corrosion indications.
e = Poor—extensive corrosion attack.

TABLE 9—*Performance of bare stainless steels.*

	Atlantic—4 Years	Pacific—6 Months
Almar 362:		
6 by 12 in.	incipient pitting of 0.002 in. depth to severe crevice attack of 0.125 in. depth	incipient pitting of 0.002 in.
6 by 12 in.—stressed	...	incipient pitting of 0.002 to 0.050 in. depth (perforation)
1 by 6 in.—stressed	...	no cracking—crevice from 0.002 to 0.03 in. deep
Carpenter 455:		
6 by 12 in.	crevice corrosion to 0.040 in. deep	incipient pitting of 0.002 to crevice corrosion 0.10 in. deep
6 by 12 in.—stress	...	incipient pitting of 0.002 to 0.005 in.
1 by 6 in.—stressed	...	one of three specimens cracked at bolt-hole

had numerous small blisters, there was no occurrence of rust staining. The blisters contained a gray powdery substance similar to zinc oxide and it is therefore assumed that the blisters in the paint were due to seawater entry through a pinhole in the epoxy topcoat. The seawater entrapped between the epoxy topcoat and zinc-rich primer resulted in local conversion of the zinc to zinc oxide.

System 3—Coating System 3 was used only on the Atlantic specimens, except for two Pacific aluminum alloy 7075-T73 specimens. The Atlantic specimens (structural steels) had minor rust stains at the edges of bolt-holes in the stress corrosion specimens (see Fig. 20) and numerous small blisters (0.06 in.) on the compression side of these specimens. Although these coating failures did not result in corrosion attack of any significance, it must be assumed that additional exposure time (that is, another year) would have resulted in significant deterioration of the coating system. The Pacific aluminum alloy 7075 specimens had extensive pitting and edge corrosion attack (see Fig. 25) due to complete lack of adhesion of the zinc-rich primer coat. This problem may have been due to improper specimen surface preparation and/or application and curing of the primer coat.

Systems 4 and 5—Coating Systems 4 and 5, epoxy coal tars, were applied to structural steel specimens in the Atlantic and Pacific tests. In both cases performance was very good. Defects in the coating systems were at holes or edges and were few in number (a maximum of six per specimen). All defects were of the small pinhole type that did not show any evidence of corrosion undercutting of the coating.

Coating System 4 had been previously tested in surface waters for three years and the deep ocean for one year as reported by Drisko and Brouillette.[4] Its performance was found to be excellent in surface waters and good in the deep ocean.

Systems 6 and 7—Coating System 6 was applied to the Carpenter 455 stainless steel and aluminum alloy 6061 specimens tested in the Atlantic. Coating 7 was applied to ASTM-A-572 structural steel, the two stainless steels, and to the aluminum alloy 6061 specimens tested in the Pacific and the stainless steels and aluminum alloy 6061 in the Atlantic. There were no coating defects found on any of these specimens tested in both oceans. Since there were 14 specimens coated with Systems 6 and 7, it was evident that these systems provided excellent, reliable protection.

Uncoated—The uncoated stainless steel specimens had pitting and crevice corrosion that ranged from less than 0.005 to 0.12 in. in depth. The shorter-term Pacific tests (six months) had maximum crevice attack to a depth of 0.10 in. at the edges of the 6 by 12-in. specimens (where the specimen touched the holder rod) and 0.07 in. deep at the bolt-holes of the stress corrosion specimens. The Atlantic specimens which were exposed more than four years had maximum crevice attack and tunneling to a depth of 0.12-in. at the edge of the 6 by 12-in. specimens.

The difference between the Pacific and Atlantic specimens in maximum crevice corrosion was only 0.020 in. (0.10 versus 0.12 in.). This indicates that the Pacific site with its very low oxygen content initiates loss of passivity (at local crevices) much more rapidly than the higher-oxygen-content test site in the Atlantic.

Conclusion

The coating systems tested will provide corrosion protection in the deep Atlantic or Pacific Oceans for six months to at least four years depending on the system selected. A short-term (three to six months) deep-ocean exposure of a low-alloy steel structure could be adequately protected by any of the seven coating systems tested. The ability of the inorganic zinc-rich primer to reduce the amount of corrosion of the low-alloy steels through sacrificial action indicates that cathodic protection (via sacrificial zinc anodes) would be an effective protection method for deep-ocean structures. The epoxy coating systems (4 through 7) provided very good to excellent protection for more than four years. It is the author's opinion that these coating systems will provide a minimum of five years of corrosion protection to structural steels, stainless steels, and aluminum alloys in the deep ocean.

---

[4] Drisko, R. W. and Brouillette, C. V., "Comparing Coatings in Shallow and Deep Ocean Environments," *Materials Protection*, April 1966.

The two high-strength stainless steels, Almar 362 and Carpenter 455, were found to be similar to the 300 series austentic stainless steels (that is, Types 302, 303, and 304) and the hardenable martensitic stainless steels such as 17-4 PH and PH 15-7 Mo in that they are highly susceptible to pitting and crevice corrosion.

Of the 26 stress corrosion specimens of the two stainless steels, only one cracked (Carpenter 455 H1050). It appears that both stainless alloys are relatively resistant to stress corrosion cracking even in the presence of notches such as pitting and crevice corrosion. Figure 26 shows a 6 by 12-in. specimen with a 3-in. circular weld produced without the addition of filler metal to induce high residual stresses. The crevice corrosion which occurred was an obvious stress raiser, but did not cause cracking as has been observed in similar PH 15-7 Mo, 17-4 PH, and 17-7 stainless steel corrosion specimens.

Although the foregoing results do indicate that Almar 362 and Carpenter 455 have relatively good resistance to stress corrosion cracking, it must be recognized that these tests represent only a few material heats and heat-treatments and a specific environment and test configuration.

The original objectives of this program of evaluating coating systems for deep-ocean structures were achieved in that the corrosion protection effectiveness of seven different coating systems on three structural materials was demonstrated. In addition, seawater corrosion data on two previously untested high-strength stainless steels were developed.

Laboratory and Statistical Techniques

V. Kučera[1] *and E. Mattsson*[1]

Electrochemical Technique for Determination of the Instantaneous Rate of Atmospheric Corrosion

---

REFERENCE: Kučera, V. and Mattsson, E., "**Electrochemical Technique for Determination of the Instantaneous Rate of Atmospheric Corrosion,**" *Corrosion in Natural Environments, ASTM STP 558*, American Society for Testing and Materials, 1974, pp. 239–260.

ABSTRACT: The aim of this investigation was to develop a technique and equipment for the measurement of the instantaneous rate of atmospheric corrosion of metals. An electrochemical method was chosen for this purpose and a technique was developed for continuous measurement and recording of the currents generated in models of the electrochemical corrosion cells which occur on the metal surface when exposed to the atmosphere. Two types of cells were used, galvanic cells consisting of steel and copper electrodes and electrolytic cells consisting of only one type of electrode, namely, steel, zinc or copper. In the latter type of cell an external emf was applied. The cell current was found to vary between 10^{-10} and 10^{-3} A in accordance with changes in climatic conditions, the changes being at least in qualitative agreement with changes in the rate of atmospheric corrosion as earlier reported in the literature. An inexpensive electronic integrator was developed for estimation of the accumulated quantity of cell current over a certain period of time. This device integrates separately on two counters the amount of current during periods with low current and during periods with high current. A time counter also records the exposure time during which the current exceeds a chosen value. This time counter can be used to measure the time of surface wetness, that is, that part of the period of exposure when the corrosion current is of practical importance. Efforts are now being made to find the quantitative relation between the cell current and the atmospheric corrosion rate. It is believed that the technique will prove to be a useful tool for the investigation of atmospheric corrosion in the laboratory as well as on test sites out of doors and in industrial applications.

KEY WORDS: atmospheric corrosion testing, electrochemical measurements, corrosivity of atmosphere, time of panel wetness, relative humidity, sulfur dioxide, carbon steel, copper, zinc

The rate of atmospheric corrosion is at present generally studied either in long-term field tests in different types of atmosphere or by means of accelerated corrosion tests in the laboratory. Such studies have often been

---

[1] Senior research scientist and director of research, respectively, Swedish Corrosion Institute, Stockholm, Sweden.

criticized, the field tests because they require too much time and do not permit unambiguous conclusions to be drawn, and the accelerated tests because they are not representative of conditions in practice.

The aim of this investigation was to develop a technique and equipment for determination of the instantaneous rate of atmospheric corrosion for metals. Such a technique would permit the determination and recording of the corrosion rate during the hours of the day, at different seasons of the year, at different localities, at different levels above ground level, and also in different industrial installations or inside ventilation systems. It would also be applicable for studies of how the corrosion at various points on a car depends on method of driving, road salting, or garaging conditions. Such a technique might also be useful for studies of atmospheric corrosion under controlled conditions with one-factor variation.

In order to achieve this aim, two methods—measurements of electrical resistance and measurements using electrochemical cells—were considered. Both methods had previously been used for the study of atmospheric corrosion and are described in a number of publications [*1–15*].[2]

In the first group, measurement of changes in the electric resistance of thin wires or foils should primarily be mentioned [*1–6*]. The sensitivity of the method has been improved in recent years [*6*], but it cannot be used for determination of the instantaneous rate of atmospheric corrosion.

The electrochemical method is based on measurement of the current in models of electrochemical corrosion cells, and thus permits determination of the instantaneous value of the current. Galvanic cells with electrodes of different metals have been used in most investigations to date. The Soviet school, represented by Tomashov and his colleagues [*7–11*], and also Sereda [*12–15*] in Canada, should primarily be mentioned among research workers who have used this technique.

The Soviets have used galvanic cells of iron-copper, iron-zinc, iron-aluminum, and copper-aluminum, the most comprehensive tests having been performed with cells of the iron-copper type [*8*]. It was found in these tests that climatic factors affect the current in the cells in a manner similar to that in which they influence the rate of atmospheric corrosion. The authors have therefore come to the conclusion that the method is suitable for fast determination of the corrosivity of the atmosphere, and that it is possible to calibrate the current measuring instrument in such a way that it directly indicates the rate of atmospheric corrosion for the anode material in question [7]. The cells have also been used to determine the total period during which the surface is covered by a film of moisture formed as a result of rain, snow, fog, or dew (period of surface wetness). The total period of surface wetness determined in this way was, for example, 1342 h/year in Moscow and 3161 h/year in Batumi [*11*]. The length of the period

---

[2] The italic numbers in brackets refer to the list of references appended to this paper.

of surface wetness has also been related to the rate of corrosion as found by determinations of weight loss, and it has been found that corrosion is approximately proportional to the period of wetness of the metal surface [*10*].

Sereda has used galvanic cells of the platinum-iron and platinum-zinc type to determine the total period during which the surface is moist [*12–13*]. An instrument, based on the use of a platinum-zinc cell, has been developed and used for recording of the period of surface wetness at test sites in Canada and the United States [*14*]. This instrument records the period during which the voltage across a 100 MΩ resistance that is connected into the cell circuit exceeds the value of 0.1 V. This figure is exceeded when the relative humidity of the atmosphere is greater than about 85 percent. The period of surface wetness has been found by this method to be 29 percent and 55 percent of the total time in Ottawa and Panama, respectively [*15*]. The period of surface wetness, in combination with the sulfur dioxide (SO_2) content and the temperature, has been used as a parameter in developing empirical equations for the relations between the atmospheric corrosion of steel, copper, or zinc and climatic factors. These equations provide a comparatively good description of the corrosion process, at least during the initial period of exposure.

Examination of the literature showed that the electrochemical method had given promising results in studies of atmospheric corrosion outdoors, and it had also been used satisfactorily for determination of the period during which the area subjected to corrosion is moist. In view of this, the electrochemical method was chosen for this investigation, the results published by Tomashov and his colleagues and by Sereda being used as the starting point.

Experimental Procedure

The arrangement of the electrochemical measuring equipment used is shown in Fig. 1. It consists of a measurement cell and equipment for the measurement, recording, and integration of the current produced by this cell. Besides the electrochemical measurements, certain climatic factors which are of significance for atmospheric corrosion, such as relative humidity, temperature, and SO_2 content, were determined.

Electrochemical Measurement Cells

Two different types of electrochemical cell, a galvanic cell and an electrolytic one, were used. Their construction is shown in Fig. 1. Each cell consists of 20 plates (65 by 10 by 0.5 mm) which form a unit encapsulated in epoxy resin. The plates are insulated from one another by means of 0.1-mm foils of polycarbonate or teflon. The cells are polished on one side by a method conventional in metallography in order that the cross sections

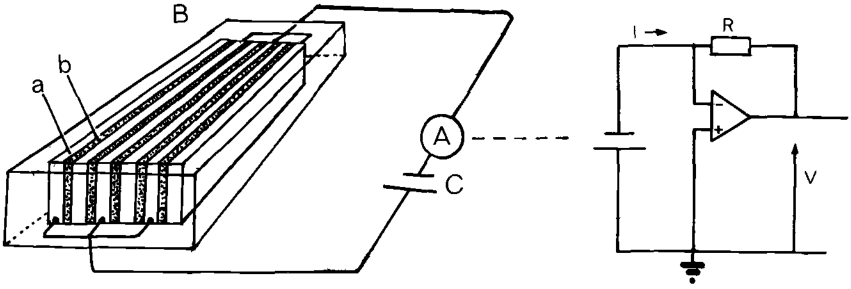

FIG. 1—*General arrangement of electrochemical device for measurement of atmospheric corrosion*: (A) *is a zero resistance ammeter, the circuit of which is shown to the right*; (B) *is an electrochemical cell of electrolytic type* [(a) *electrodes*, (b) *insulators*]; (C) *is an external emf.*

of the plates should be exposed. The overall dimensions of the cell are 80 by 25 by 15 mm, and the total exposed electrode area is 6.5 cm^2. The dimensions of the cell were made small so that it may be used in restricted spaces, for example, in building structures or inside hollow frame members of a car body.

The galvanic cell consists of ten steel plates [carbon steel to SIS (Swedish standard) 14 11 45 containing 0.07C, 0.30Mn, 0.022P, 0.023S, and 0.02Cu] and ten copper plates, the plates in each set being connected in parallel. Its construction is in principle identical with that of the galvanic cells used by Tomashov et al [*7*,*8*].

The electrolytic cell consists of 20 plates of the same metal, that is, steel, zinc, or copper. Ten electrodes are connected in parallel to one terminal, and the other ten are connected in parallel to the other terminal. The terminals are connected to an external emf.

Measurement and Recording of the Cell Current

Initial tests with both types of cell [with an external electromotive force (emf) of 100 mV being imposed on the electrolytic cell] showed that the current, on exposure of the cells to different atmospheric conditions, varies between 10^{-10} and 10^{-3} A. Measurement and recording of such currents by conventional current measuring instruments were found impossible, even when a resistance was incorporated in the cell circuit and the drop in voltage was recorded by means of a recording potentiometer with a sensitivity as high as 1 mV. For, without interfering with the cell current, one may connect a maximum resistance of 10^2 to 10^3 Ω during the wet period and 10^4 to 10^5 Ω during the dry period.

An inexpensive device for zero resistance measurement and recording of the current with the aid of a simple operational amplifier as shown in Fig. 1 was therefore developed. This device, in combination with a 4-channel Linseis line recorder which has automatic changeover between measuring ranges of 1 mV to 10 mV to 100 mV to 1 V to 10 V, was used for continuous recording of the current over extended periods of measurement. This made possible the automatic recording of the current in the ranges 10^{-9} to 10^{-4} or 10^{-8} to 10^{-3} A even under long-term exposure conditions.

Integration of the Cell Current

In order that the cell currents could be automatically integrated over extended periods of time, an electronic integrator was developed. The block diagram of the instrument is shown in Fig. 2 and a detailed wiring diagram in Fig. 3.

The amount of current is integrated over two separate measuring ranges and is directly indicated in ampere-seconds on two digital counters. One current range represents the currents generated during dry periods and the other the currents generated during wet periods. The device automatically switches from one measuring range to the other as the current flowing exceeds, or drops below, a certain preset value which may be varied between 10^{-7} and 10^{-6} A. At the same time as the counter for the wet region comes into action, a timer is also switched on, and in this way the length of the "wet period," that is, the period during which the current exceeds a certain value, is also recorded in addition to the total amount of current. The highest current for which the integrator can be used is 1.5

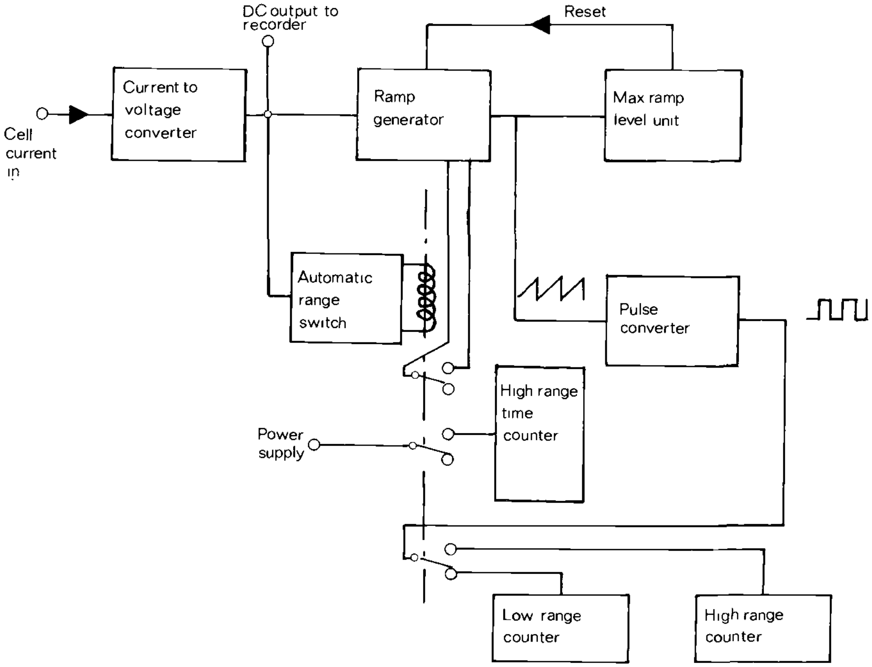

FIG. 2—*Block diagram of the electronic integrator with two current ranges.*

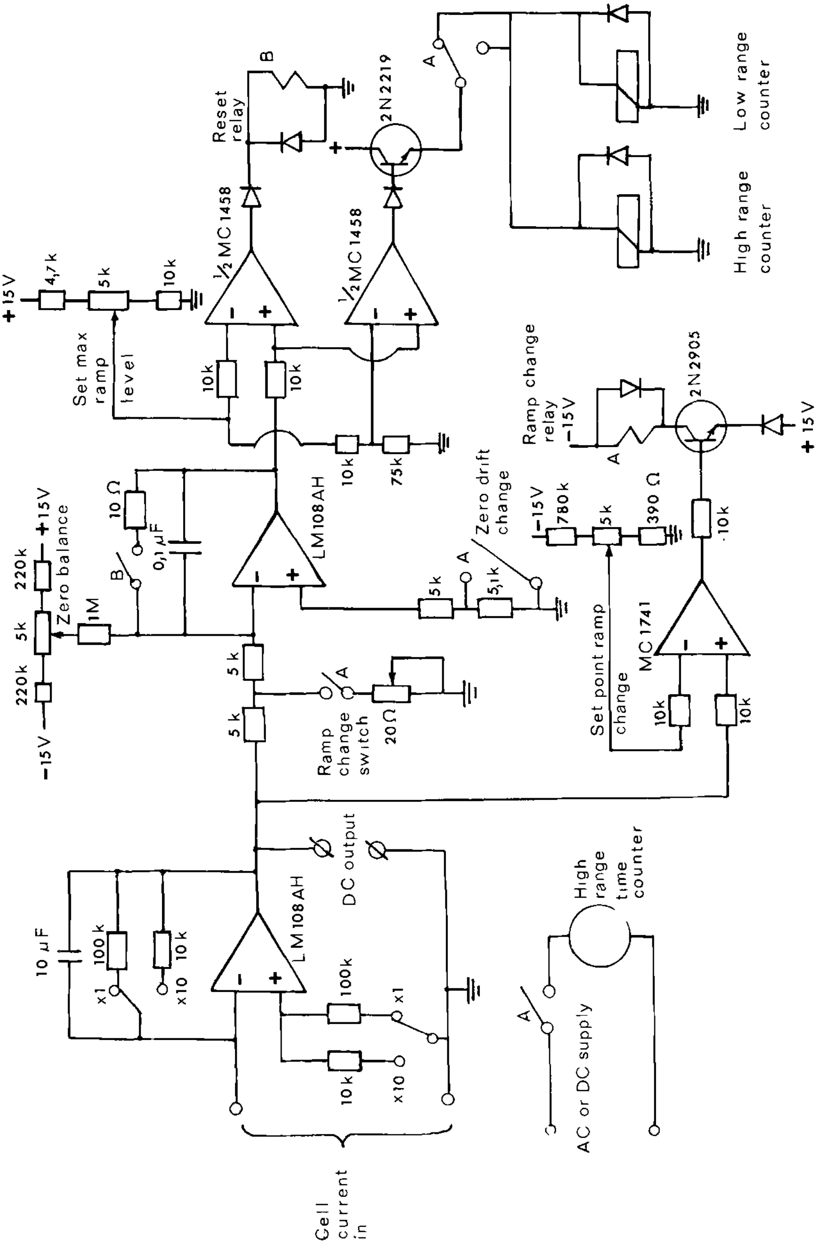

FIG. 3—*Circuit of the electronic integrator with two current ranges.*

or 0.15 mA. The device also has a terminal for recording of the current, and it is therefore also possible at the same time to perform continuous and zero resistance measurement of the current. Provided that the temperature deviates by not more than 20°C (68°F) from room temperature, measurement accuracy is better than about 1 percent when the current region 10^{-8} to 10^{-3} A is used. If the device is set for a maximum current of 1.5 mA the current capacity is 10^2 A.sec for the "dry" measurement region and 10^3 A.sec for the "wet" measurement region. If the maximum current is 0.15 mA the current capacity values are one order of magnitude lower. Owing to this, when for example galvanic iron-copper cells are used in outdoor atmospheres, measurement periods of a minimum duration of about three months can be undertaken without the capacity of the counter unit being exceeded. The instrument can be run on mains or on a battery.

Outdoor Measurements

Most of the outdoor measurements were made outside the laboratory building in central Stockholm while some measurements were carried out at the test sites of the Swedish Corrosion Institute which are representative of different types of atmosphere. The designations of the test sites and climatic data are shown in Table 1. In all cases the cells were placed on stands about 1 m above ground level with their surfaces inclined at 45 deg to the ground.

Temperature, relative humidity, and the SO_2 content were continuously recorded during exposure. A Meloy flame photometer was used for measurement of the SO_2 content of the air.

Laboratory Measurements

Laboratory measurements under controlled conditions were performed in a Feutron 301 climate chamber in which the relative humidity could be set at the desired value over the temperature range −25 to +60°C (−13 to +140°F). The SO_2 content of the atmosphere could also be directly regulated by means of the SO_2 analyzer and dosage of SO_2 from a bottle containing a mixture of SO_2 and gaseous nitrogen.

TABLE 1—*Meteorological and atmospheric-chemical data obtained on the test sites. All data are mean values for the fourth quarter of the year around the middle of the 1960's.*

Test Site	Type of Atmosphere	Sulphur Content, µg S/m^3	Temperature, °C	Relative Humidity, %
Stockholm	urban	35	+3	about 85
Gothenburg	urban-marine	50	+5	
Ryda	rural	2	+2	
Kungsgard				

Results

The galvanic and electrolytic corrosion cells were used for a number of measurements both in outdoor atmospheres and in the climate chamber. Initial tests were concentrated on determination of the sensitivity of the method and its reproducibility and on the influence which different climatic factors exerted on the cell current.

Cell Current Variation with Time

Current varied very extensively when the measuring cells were exposed outdoors, which indicates that the cell current is greatly dependent on climatic factors. As shown in Fig. 4, the cell current can change by about four orders of magnitude in a few minutes, depending primarily on variations in the relative humidity and on occasional wetting of the surface by rain.

Measurements carried out during long-term exposures outdoors, both during the summer and winter seasons, show that time may in principle be divided into two types of periods,

1. "Wet periods," when the cell current is high, usually as a result of the surface having been wetted by rain, snow, fog, or dew.
2. "Dry periods," when the cell current is low.

The boundary between these two regions was not absolutely distinct, but for the galvanic iron-copper cell it was somewhere between 10^{-7} and 10^{-6} A. On the assumption that all the current produced is utilized for oxidation of the metal, this is equivalent to a corrosion rate on the steel of 0.35 and 3.5 μm per year, respectively. The wet period, which has been defined as the period during which the cell current is greater than 10^{-6} A, has so far been found to represent between 10 and 55 percent of the total time in Stockholm over periods of four weeks. It was also found that the difference between the cell currents during dry and wet periods in the summer, when the relative humidity is often below 80 percent, was 2 to 4 orders of magnitude. During the autumn, when relative humidity in Scandinavia is very often greater than 80 percent, the aforementioned difference was only 1 to 2 orders of magnitude.

The reproducibility was studied by measurements on duplicate cells which were exposed outdoors simultaneously. Under stable weather conditions, for example, during dry periods or rainy weather of long duration, differences in current were less than 25 percent. There were, however, larger differences during shorter periods; for instance, during drying up of a film of moisture.

Variation of Cell Current with Relative Humidity

During dry periods, the cell current is considerably influenced by the relative humidity; see Figs. 5 and 6. The values in Fig. 5 show the cell

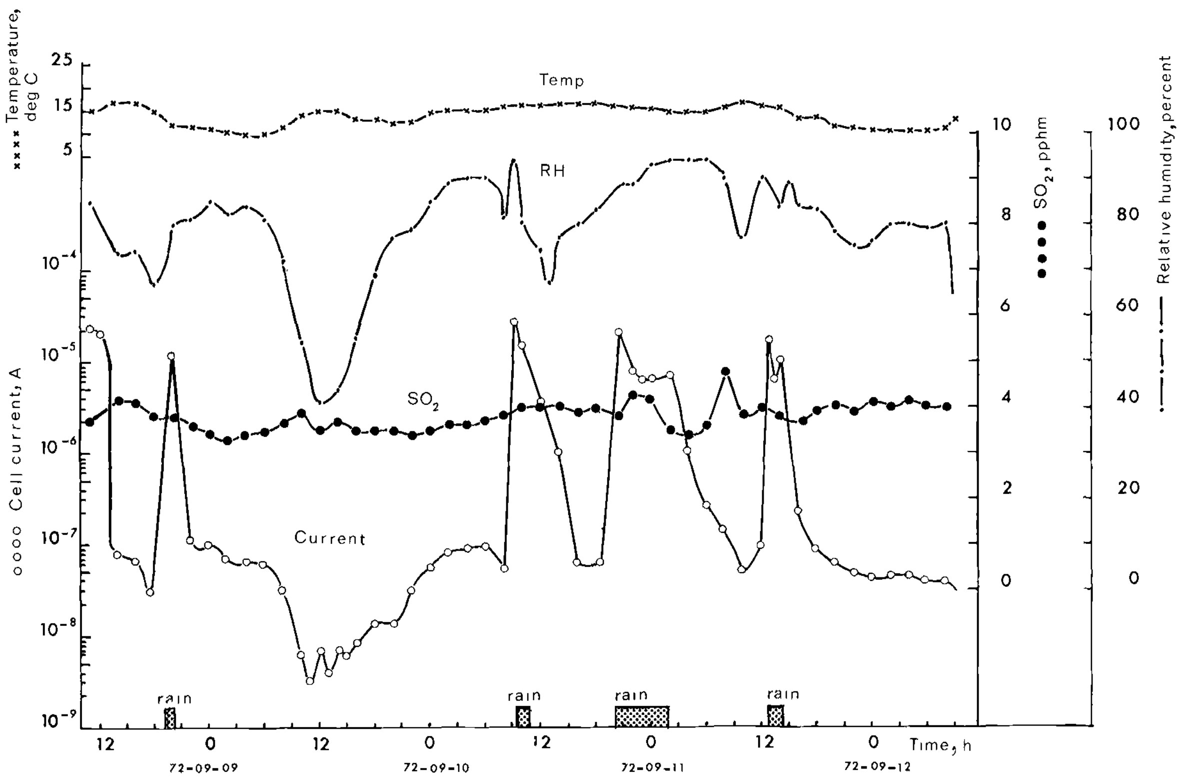

FIG. 4—*Cell current in a galvanic cell of the iron-copper type and the relative humidity, SO_2 content, and temperature in Stockholm over the period 8 Sept. to 13 Sept., 1972.*

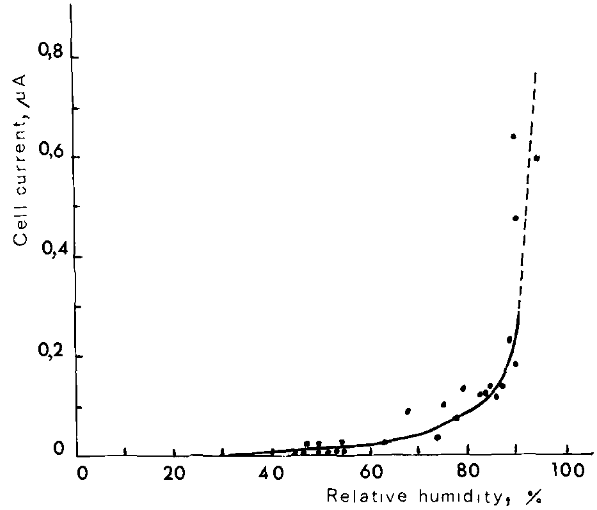

FIG. 5—*Cell current in a galvanic cell of the iron-copper type as a function of the relative humidity out of doors in Stockholm over the period 26 June to 17 July 1972. There was no rain during this period. The values of the cell current relate to the occasions every day when the relative humidity had a maximum or minimum. The dashed portion of the curve represents conditions when the surface may have been affected by dew.*

currents in a galvanic iron-copper cell as a function of the relative humidity. The readings were obtained during a dry summer period of three weeks in Stockholm and consist of maximum and minimum values of the relative humidity and corresponding cell currents for every day during this period. In the dashed portion of the curve, however, the readings may have been affected by dew.

Tests performed in the climate chamber under controlled conditions with regard to temperature and SO_2 content produced similar curves; see Fig. 6. When the relative humidity was high ($\geq$80 percent), however, the values obtained were considerably higher when the SO_2 content was 10 pphm (parts per hundred million) than when it was lower.

Variation in Cell Current During the Wet Period

The cell current also varied with time during wet periods. The curve representing the time dependence of the current during a period of rain has a characteristic shape. This is shown by some examples relating to cells which were exposed at 45 deg to the horizontal with their surfaces directed upward; see Fig. 7. At the beginning of a period of rain, a current maximum usually occurred, after which the current dropped and, during rains of long duration, decreased to an almost constant value which was often only one half to one tenth of the maximum value. The decrease in current after the beginning of a period of rain mainly depended on the

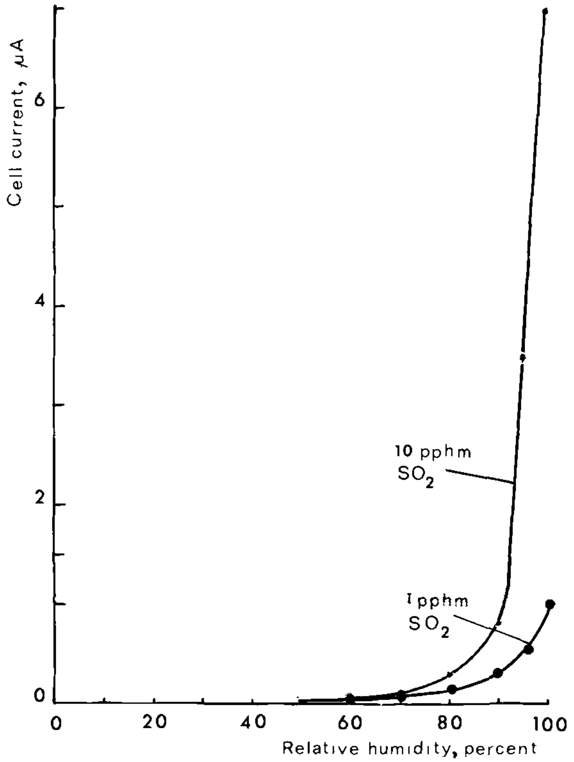

FIG. 6—*Cell current in a galvanic cell of the iron-copper type as a function of the relative humidity for two SO_2 contents during exposure in the climate chamber.*

intensity of rain. During periods of light drizzle, very high current values were observed for several hours, right up to the time when the intensity of rainfall increased; see, for example, Fig. 7*c*.

Cell Current as a Function of the Content of Air Pollution

The SO_2 content of the atmosphere was determined as a measure of the content of air pollutants. It was found in the course of measurements that rapid variations in SO_2 content did not cause obvious changes in the cell current. In the long run, however, sulphur dioxide affected the cell current, probably after it has been adsorbed onto the metal surface and been converted into SO_4^{2-} in accordance with the mechanisms which have been the subject of extensive discussion in the literature.

Particularly during wet periods, the influence of the SO_2 content was evident. This will be seen on comparing cell currents at the beginning of wet periods in Stockholm (urban atmosphere), Gothenburg (marine-urban atmosphere), Ryda (rural atmosphere), and in the climate chamber, where the SO_2 content was kept at 10 pphm. The value of the maximum current

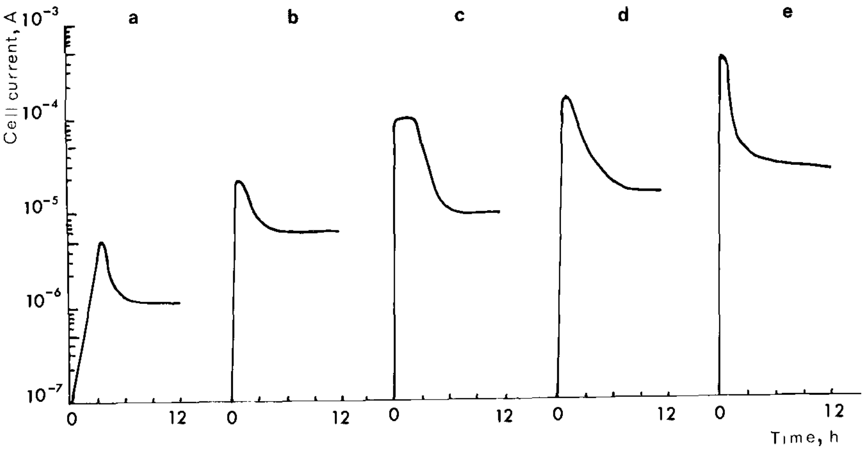

FIG. 7—*Characteristic changes of the cell current in galvanic cells of the iron-copper type at the beginning of a period of rainfall*: (*a*) *Test site Ryda Kungsgard* (*rural atmosphere*); (*b*) *Test site Stockholm* (*urban atmosphere*)—*rain after a short dry period*; (*c*) *Test site Stockholm* (*urban atmosphere*)—*rain after a long dry period*; (*d*) *Test site Gothenburg* (*marine-urban atmosphere*)—*rain after a long dry period*; (*e*) *Climate chamber in an atmosphere with 10 pphm* SO_2—*continuous wetting with distilled water.*

was greatest in the climate chamber, where the SO_2 content had the greatest value. Even after long periods of rain, when the current had stabilized, the average value of current was greater at localities which had a high content of air pollutants than at those where the atmosphere was purer.

It may also be mentioned that the maximum current was usually higher after a long dry period with adsorption of pollutants than after a short one, and that the current during rainfall in Stockholm was most often lower in the summer than in the autumn. The latter phenomenon, however, could not be discerned at the test site with rural atmosphere.

Conditions during dry periods were studied in the climate chamber and in this case also a relationship could be found between the cell current and the SO_2 content in the atmosphere. The influence of the higher SO_2 content, however, was evident only when the relative humidity was at least 80 percent.

Cell Current as a Function of the Electrode Material

Parallel measurements with galvanic iron-copper cells and electrolytic iron-iron cells with an imposed electromotive force of 100 mV showed current-time curves of a similar shape. The values were, however, often higher in iron-copper cells during dry periods and higher in electrolytic iron-iron cells during wet periods; see Fig. 8.

The decisive importance of the anode material was shown during simultaneous exposure of three electrolytic cells of the types iron-iron, copper-

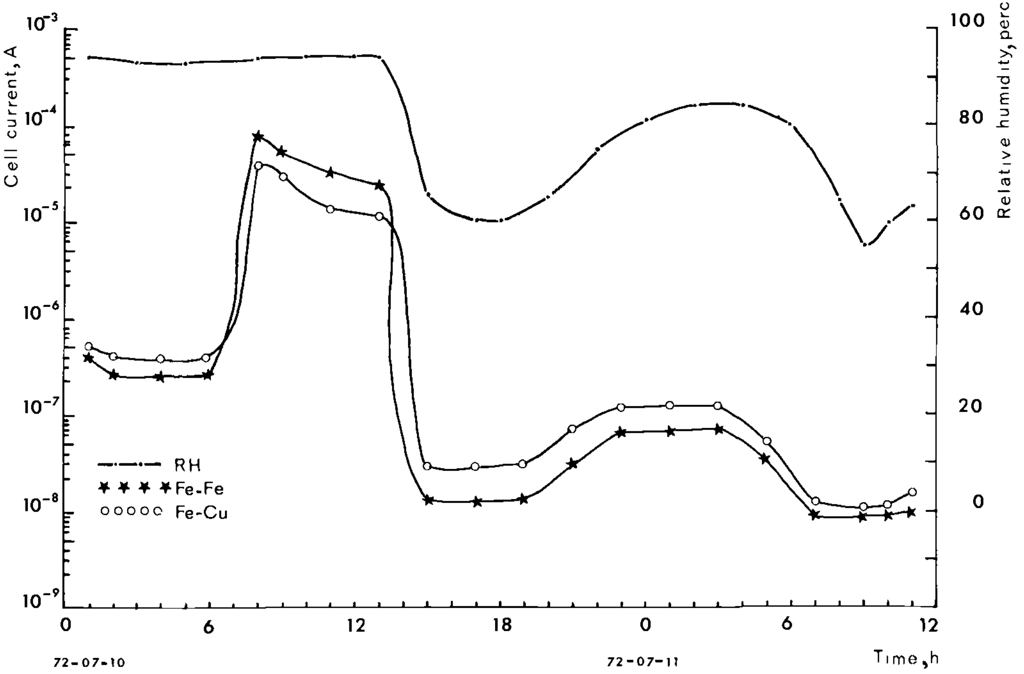

FIG. 8—*Cell current in a galvanic cell of the iron-copper type and an electrolytic cell of type iron-iron with an imposed emf of 100 mV, and the relative humidity in Stockholm over the period 10 July to 11 July 1972.*

copper, and zinc-zinc, all supplied with an imposed emf of 100 mV. As will be seen in Fig. 9, the currents were different both during dry and wet periods, those for the iron-iron cell being appreciably higher than for the other two metals. Over long periods of low relative humidity the currents in the zinc-zinc and copper-copper cells dropped to values below 10^{-9} A.

Influence of the Time of Exposure

When new cells were exposed, there was generally no flow of current even when the relative humidity was high. This was supported during simultaneous exposure of bright steel plates by the fact that there was no visible corrosion attack during an exposure for more than 100 h at a relative humidity of 90 percent. Cells containing steel electrodes were, however, rapidly covered with a film of rust after a few periods of rainfall. Such cells generally produced currents in excess of 10^{-9} A even when the relative humidity was 40 to 50 percent. It was evident that the rust formed during the first six months had no protective effect that reduced the cell current. After the initial six-month period, however, the protection effect of the

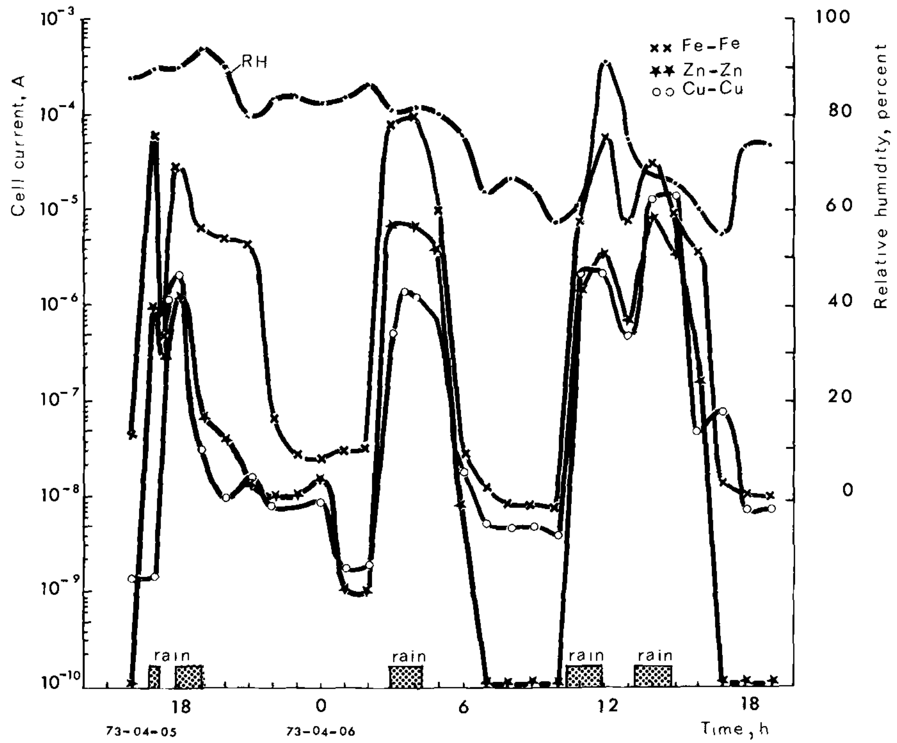

FIG. 9—*Cell current in electrolytic cells of the iron-iron, zinc-zinc, and copper-copper types, all with an imposed emf of 100 mV, and the relative humidity in Stockholm over the period of 5 April to 7 April 1973.*

corrosion products began to exert an influence and the current values during wet periods decreased. After long exposure, corrosion products with electron conducting properties may cause short-circuiting between the electrode systems. In an urban atmosphere the cells could be used without any short-circuiting problems for at least 6 months and usually for 12 months. In a rural atmosphere galvanic iron-copper cells were used for 18 months. After short-circuiting, the cells have to be repolished and can then be used for measurements again.

When electrolytic cells of the copper-copper or zinc-zinc type were exposed to outdoor atmospheres, there was no short-circuiting problem similar to the one in cells containing steel plates. On the other hand short-circuiting occurred in electrolytic zinc cells during exposure in the climate chamber at a high relative humidity and a high SO_2 content.

Influence of the Orientation of the Surface

The influence of the orientation of the surface was studied, *inter alia*, in two galvanic iron-copper cells which were exposed outdoors with their surfaces at 45 deg to the horizontal, one with the surface directed skyward and the other with the surface directed groundward. Figure 10 shows the cell current during part of the exposure, which comprised two rain periods. During the first very brief rain, only the surface of the cell which faced upward was wetted, while during the second period—a rainfall of long

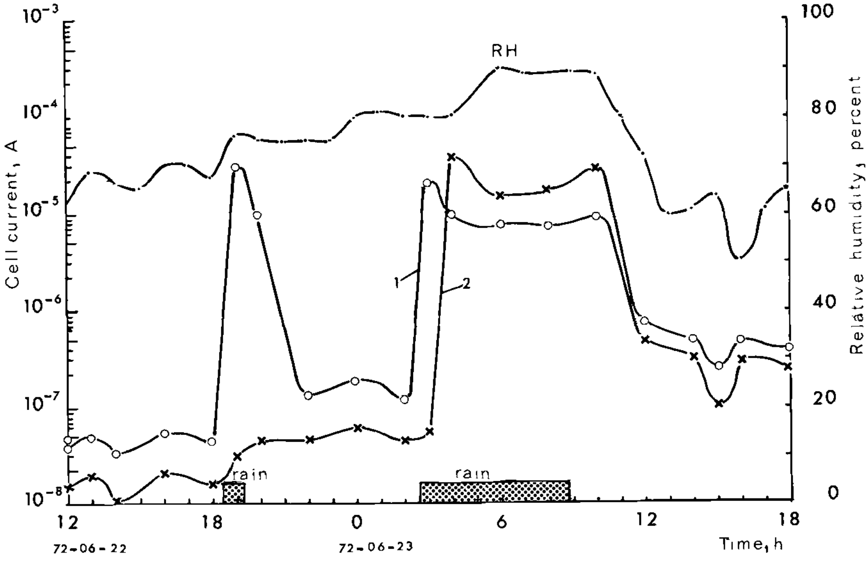

FIG. 10—*Cell current in two galvanic cells of the iron-copper type, exposed at 45 deg to the horizontal, and the relative humidity in Stockholm over the period 22 May to 23 June 1972: Curve 1—cell surface directed skyward; Curve 2—cell surface directed groundward.*

duration—the surface of the cell facing downward also gradually became wet, and this latter cell then exhibited higher values of current all through the remainder of the wet period.

Integrated Values of Current

The current integration devices were put into use recently and were found to perform their duty very well. There are only a few experimental results available at present, however. The initial experiments had the aim of comparing the integrated current value from a galvanic iron-copper cell with weight loss data for exposed steel plates, earlier reported for the Stockholm area [22]. The results applicable to two 4-week periods are shown in Fig. 11. Table 2 gives detailed information which can be obtained about the corrosion process with the aid of the integrator. The period of exposure has been divided into short intervals of 24 or 48 h. The integrator was set for automatic changeover between the wet and dry ranges at 10^{-6} A. The total duration of surface wetness during the two exposure periods was 89 and 138 h, which is equivalent to about 13 and 21 percent of the total time. The total duration of rainfall, as recorded by a pluviograph, was 29 and 77 h. The average cell current calculated for each one of the two exposure periods was 2.7×10^{-6} and 3.9×10^{-6} A, which is equivalent to a corrosion rate of approximately 10 and 14 μm per year,

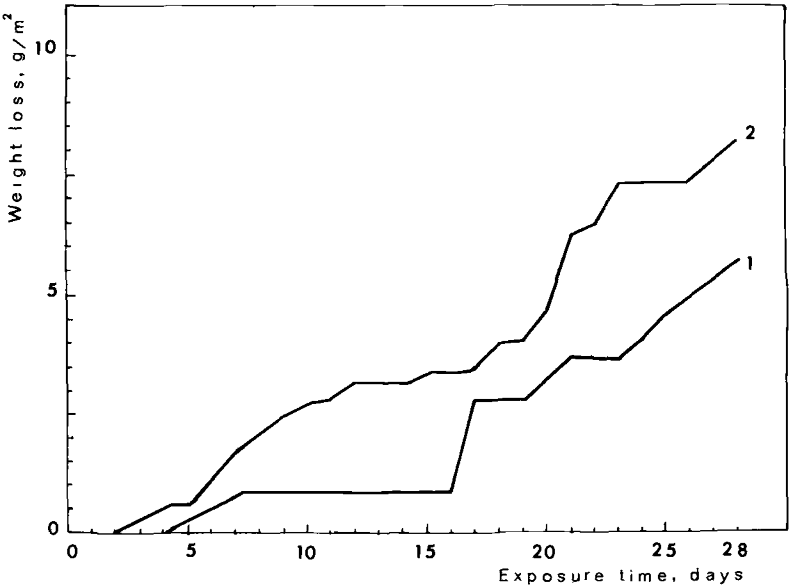

FIG. 11—*Integrated quantities of current obtained during exposure of a galvanic cell of the iron-copper type in Stockholm converted into weight loss of steel: Curve 1—period 12 March to 9 April 1973; Curve 2—period 9 April to 7 May 1973.*

TABLE 2—*Detailed results obtained in integrating the cell current in a galvanic cell of the iron-copper type exposed in Stockholm over the period 9 April to 7 May 1973.*

Date	Period of Exposure, h	Period of Surface Wetness, h	Period of Rain, h	Amount of Current $10^{-4} \times$ A. sec		Average Cell Current, A		Total Amount of Current as Weight Loss, g/m^2
				Wet Periods	Dry Periods	Wet Periods	Whole Periods	
9 April to 10 April	21	...	...	...	76	...	1.0×10^{-7}	6.8×10^{-3}
10 April to 11 April	24	2.3	...	119	11	1.4×10^{-6}	1.5×10^{-7}	1.2×10^{-2}
11 April to 12 April	24	3.4	2.0	3 861	74	3.2×10^{-5}	4.6×10^{-6}	3.5×10^{-1}
12 April to 13 April	24	8.0	4.0	2 962	106	1.0×10^{-5}	3.6×10^{-6}	2.7×10^{-1}
13 April to 14 April	25	0.1	...	22	13	6.1×10^{-6}	3.9×10^{-8}	3.1×10^{-3}
14 April to 16 April	47	17.8	10.0	12 562	56	2.0×10^{-5}	1.5×10^{-5}	1.1
16 April to 17 April	24	7.3	4.0	3 948	51	1.5×10^{-5}	4.6×10^{-6}	3.1×10^{-1}
17 April to 18 April	24	13.7	5.0	4 201	73	8.5×10^{-6}	5.0×10^{-6}	3.8×10^{-1}
18 April to 19 April	24	8.4	2.0	2 729	54	9.0×10^{-6}	3.2×10^{-6}	2.5×10^{-1}
19 April to 20 April	29	4.2	2.0	1 165	128	7.7×10^{-6}	1.2×10^{-6}	1.2×10^{-1}
20 April to 21 April	23	5.4	1.0	3 233	19	1.7×10^{-5}	3.9×10^{-6}	2.9×10^{-1}
21 April to 23 April	48	0.1	...	9	71	2.5×10^{-6}	4.7×10^{-8}	7.1×10^{-3}
23 April to 24 April	20	2.2	...	2 440	71	2.8×10^{-5}	3.2×10^{-6}	2.1×10^{-1}
24 April to 25 April	24	0.6	...	126	124	5.8×10^{-6}	2.9×10^{-7}	2.2×10^{-2}
25 April to 26 April	24	0.6	...	1 401	39	6.5×10^{-5}	1.7×10^{-6}	1.3×10^{-1}
26 April to 27 April	24	7.5	6.0	5 761	83	2.1×10^{-5}	6.8×10^{-6}	5.2×10^{-1}
27 April to 28 April	26	0.4	...	403	46	2.8×10^{-5}	4.8×10^{-7}	4.0×10^{-2}
28 April to 29 April	22	2.4	2.0	6 649	31	7.7×10^{-5}	8.5×10^{-6}	6.0×10^{-1}
29 April to 30 April	25	25.0	16.0	18 079	...	2.0×10^{-5}	2.0×10^{-5}	1.6
30 April to 1 May	24	5.3	4.0	1 826	56	9.6×10^{-6}	2.2×10^{-6}	1.7×10^{-1}
1 May to 2 May	23	14.2	11.0	10 204	100	2.0×10^{-5}	1.2×10^{-5}	9.2×10^{-1}
2 May to 3 May	24	...	...	...	39	...	4.5×10^{-8}	2.0×10^{-3}
3 May to 4 May	24	...	...	...	17	...	2.0×10^{-8}	1.5×10^{-3}
4 May to 5 May	28	...	...	1	8	...	1.0×10^{-8}	8.0×10^{-4}
5 May to 7 May	45	9.0	8.0	9 011	25	2.8×10^{-5}	5.6×10^{-6}	8.0×10^{-1}
Average value						1.8×10^{-5}	3.9×10^{-6}	
Total	670	137.9	77.0	90 512	1371			8.1

that is, 8.6×10^{-3} and 1.2×10^{-2} g/m^2 h. The average cell current during periods of wetness was found to be 2.0×10^{-5} and 1.8×10^{-5} A for the two exposure periods. The atmospheric corrosion rate of steel earlier found through weight loss determinations for panels exposed in Stockholm has been reported to be of the order 30 μm per year [*22*].

Discussion

It is obvious that the rate of atmospheric corrosion out of doors is a very complicated function of a great number of factors; for example, the time of surface wetness, the relative humidity and SO_2 content in the atmosphere, the temperature, the nature of the metal, the amount and structure of corrosion products on the surface, and the content of absorbed atmospheric pollutants in the corrosion products. Many efforts have been made to formulate in mathematical terms the correlation between the atmospheric corrosion rate and these influencing factors [*15,16,17*]. Various accuracies have been claimed for the equations given, but so far nobody seems to have found a completely satisfactory solution, at least in relation to atmospheric corrosion of steel over extended periods of time. One reason has been the difficulty of recording the atmospheric corrosion rate in such a way that one-factor variations can be studied over a reasonable period and unambiguous conclusions drawn.

Meaning of the Electric Current Measured

A key question in this investigation is whether the electric current measured with the electrochemical technique can be considered as a measure of the atmospheric corrosion rate, either on the basis of a straight-line relation or according to some other more complicated mathematical relations. If the relation between the cell current and the atmospheric corrosion rate can be found, the technique should prove a valuable tool for studies of atmospheric corrosion.

To get an idea of the relation between the current measured and the atmospheric corrosion rate we will compare the results obtained in this investigation with earlier reports about atmospheric corrosion:

1. The cell current was found to be considerably higher when the metal surface was moist from rain, fog, or snow than in the absence of such deposition. This is in agreement with experimental results reported by Dearden [*18*] and Schikorr [*19*], which show that the atmospheric corrosion as determined by weight loss is considerably greater when the surface is moist than when it is in contact with an atmosphere of a relative humidity such as 90 percent, but with no deposition. It should also be mentioned, however, that Barton has warned against overemphasizing the importance of rain periods in relation to atmospheric corrosion [*20*].

2. In the absence of moisture deposition the cell current increased with relative humidity in a way similar to the atmospheric corrosion rate as reported by Vernon [*21*].

3. The cell current was found to be influenced by SO_2 content in the atmosphere only when the relative humidity was above about 80 percent, which is in good agreement with Vernon's findings concerning the atmospheric corrosion of steel [*21*].

4. The cell current produced under humid conditions was found to be greatest in the steel cell and considerably smaller in the copper and zinc cells. This is in agreement with the relation between the atmospheric corrosion rates for the three metals found in conventional exposure tests [*22*].

5. Under rain periods other than very short ones a steel cell with the surface directed groundward produced a greater cell current than a similar cell with the surface directed skyward. This agrees with reports from field tests, that the corrosion rate is greater on the groundward side of a steel panel than on the skyward surface [*18*].

6. The integrated amount of cell current during two 4-week periods corresponds to corrosion rates of 10 and 14 μm per year. These values are of the same order of magnitude as average corrosion rates for steel found in preliminary tests on the same site over the same period by weight loss determinations, and also of the same order of magnitude as the average corrosion rates earlier found in the same area.

Thus, the observations made with the electrochemical technique are in qualitative or even semiquantitative agreement with results from atmospheric exposure tests reported earlier. This fact supports the hypothesis that there is a relation between the current measured and the atmospheric corrosion rate. Since we consider additional confirmation of the hypothesis desirable, we plan to carry out further investigations of the electrochemical technique. In the first place the measurement device will be studied under one-factor variations of different climatic factors in the climate chamber. Long-term outdoor tests, with the cell exposed to different types of atmosphere, are also being planned. The amount of current will then be integrated over a period of time and compared with weight loss data determined for the same period. Such experiments might show the quantitative relations between current and atmospheric corrosion rate and provide a basis for the calculation of conversion factors. Even if the meaning of the electric current measured has not been fully interpreted, it appears likely that the current is closely related to the atmospheric corrosion rate.

Measurement Technique

The choice between the galvanic (copper-iron) and electrolytic (iron-iron) types of cell may be discussed. The magnitude of current produced was approximately the same in both types of cell under the chosen conditions. The galvanic cell has the advantage of being easier to handle since it has a built-in emf. The electrolytic type of cell, on the other hand, has the advantage that the anode surface is not contaminated with copper, and the magnitude of the current can be adjusted by changing the external emf applied across the electrolytic cell. Further, different metals can be studied simultaneously.

The characteristics of the cells can also be varied by changing the thickness of the insulator between the electrode plates. When the insulator is made thinner, the current produced is increased, but the risk of short-circuiting owing to bridges of electron-conducting corrosion products is also increased. It may thus be suitable to choose a comparatively thin insulator for a zinc-zinc cell, since the atmospheric corrosion rate of zinc is known to be nearly constant during the exposure, and tests of only short duration are therefore required. In iron-iron cells thicker insulators might be of advantage because the corrosion rate is known to change considerably during the exposure, and tests of long duration—without short-circuiting owing to electron-conducting oxide bridges between the cell plates—are therefore required. The cells now used, with insulators of 100 μm thickness, have proved useful for exposures up to at least six months. By moderately increasing the thickness, the time of exposure might be extended considerably, although one has to be aware of the possibility that the cell current will then be more influenced by the electrolyte resistance. So the modified cell has to be calibrated with respect to the relation between cell current and atmospheric corrosion rate.

Replacement of the recorder by the integrator for determination of the total current produced seems to be an improvement of great practical value. The integrator is much less expensive than the recorder. It is easier to operate, which is of particular importance during long-term exposures. It can also be set to record the accumulated exposure time when the current has exceeded a chosen value, that is, that part of the period during which corrosion has been of practical importance. This period seems to have a similar significance as the time-of-wetness reported by other authors [*10,11,13,14,15*]. In case of interest, a recorder may of course be connected to the recorder terminal of the integrator and the current-time curve plotted simultaneously.

Conclusions

An electrochemical technique has been developed for continuous measuring and recording of the current produced in models of corrosion cells which are formed on the surface of the metals when these are exposed to the atmosphere.

Two types of cells have been used: galvanic cells with electrodes of steel and copper, and electrolytic cells with electrodes of only one metal, for example, steel, zinc, or copper, and with an external emf. The use of electrolytic cells avoids contamination of the rust layer by copper ions and allows adjustment of the current by changing the applied emf.

The current produced in the cells when exposed to different climatic conditions varies from 10^{-10} to 10^{-3} A. The changes in current due to variations in conditions such as time of wetness, relative humidity, and SO_2 content are at least in qualitative agreement with variations in the atmospheric corrosion rate as reported by other authors.

An inexpensive electronic integrator has been developed for the determination of the total amount of current produced over a period. It can also be used to record the accumulated exposure time during which the current has exceeded a chosen value, that is, that part of the period which is often called the "time of wetness."

Using this device, efforts are now being made to find the quantitative relation between the measured cell current and the atmospheric corrosion rate.

It is believed that the technique and equipment will prove to be useful tools for studies of atmospheric corrosion in the laboratory as well as on test sites out of doors and in industrial applications.

Acknowledgment

This investigation was carried out at the Research and Development Laboratory of the Swedish Corrosion Institute, with financial support from the Swedish Board for Technical Development and the Swedish Council for Building Research. The electronic integrator was designed by T. Svensson, and B. Hultman contributed in carrying out the experiments. The project has been given technical support by working group No. 9 70 15 0 at the Swedish Corrosion Institute.

References

[1] Wilson, J. C., *Proceedings of the Physical Society of London*, Vol. 39, 1926, pp. 15–25.

[2] Hudson, J. C., *Proceedings of the Physical Society of London*, Vol. 40, 1927, pp. 107–131.

[3] Burns, R. M. and Campbell, W. E., *Transactions of the Electrochemical Society*, Vol. 55, 1929, pp. 271–286.

[4] Bonwitt, W. F. and Eisen, I., "Quantitative Evaluation of Corrosive Conditions," *ASTM Bulletin*, No. 151, American Society for Testing and Materials, March 1948, pp. 84–88.

[5] Enrico, F., Riccio, V., and Martini, B., *Transactions of the Institute of Metal Finishing*, Vol. 41, 1964, pp. 74–79.

[6] Mikhailovskii, Yu. N., Shuvakhina, L. A., Klark, G. B., and Agafonov, V. V., *Zashchita Metallov.*, Vol. 7, 1971, pp. 154–158.

[7] Tomashov, N. D., Berukshtis, G. K., and Lokotilov, A. A., *Zavodskaia Laboratoriia*, Vol. 22, 1956, pp.345–349.

[8] Tomashov, N. D. and Lokotilov, A. A., "An Electrochemical Study of the Atmospheric Corrosion of Metals," *Corrosion and Protection of Steels, Collection*, Moscow, 1959, pp. 158–170.

[9] Tomashov, N. D. and Berukshtis, G. K., *Trudy Instituta Fizicheskoi Khimii*, No. 6, 1959, pp. 50–55.

[10] Berukshtis, G. K. and Klark, G. B., "The Influence of Meteorological Conditions on the Rate of Atmospheric Corrosion of Metals," *Corrosion of Metals and Alloys, Collection*, Translated from Russian by National Lending Library, Boston Spa, 1964, pp. 379–400.

[11] Berukshtis, G. K. and Klark, G. B., "Atmospheric Corrosion of Steel, Zinc, Cadmium, Copper and Aluminium in Different Coastal and Continental Regions," *Corrosion of Metals and Alloys, Collection No. 2*, Translated from Russian by Israel Program for Scientific Translations, Jerusalem, 1966, pp. 281–297.

[12] Sereda, P. J., "Measurement of Surface Moisture—A Progress Report," *ASTM Bulletin*, No. 228, American Society for Testing and Materials, Feb. 1958, pp. 53–55.

[13] Sereda, P. J., "Measurement of Surface Moisture—Second Progress Report," *ASTM Bulletin*, No. 238, American Society for Testing and Materials, May 1959, pp. 61–63.

[14] Sereda, P. J., "Measurement of Surface Moisture and Sulfur Dioxide Activity of Corrosion Sites," *ASTM Bulletin*, No. 246, American Society for Testing and Materials, May 1960, pp. 47–48.

[15] Guttman, H. and Sereda, P. J. in *Metal Corrosion in the Atmosphere*, *ASTM STP 435*, American Society for Testing and Materials, 1968, pp. 326–359.

[16] Haynie, F. H. and Upham, J. B., *Materials Protection and Performance*, Vol. 9, 1970, pp. 35–40.

[17] Stanners, J. F., *British Corrosion Journal*, Vol. 5, 1970, pp. 117–121.

[18] Dearden, J., *Journal of the Iron and Steel Institute*, Vol. 159, 1948, pp. 241–246.

[19] Schikorr, G., *Werkstoffe und Korrosion*, Vol. 14, 1963, pp. 69–80.

[20] Barton, K., *Verlag Chemie*, Weinheim, Germany, 1973, pp. 64–72.

[21] Vernon, W. H. J., *Transactions of the Faraday Society*, Vol. 31, 1935, pp. 1678–1686.

[22] Mattsson, E. and Kučera, V., "The Influence of Sulphur Compounds on the Atmospheric Corrosion in Sweden, Results of Field Tests and Economic Considerations," Second International Symposium on Modelling the Effect of Climate on Electrical and Mechanical Engineering Equipment, Czechoslovak Academy of Sciences, Liblice, Czechoslovakia, 1971.

R. R. M. Johnston[1] *and C. P. Lloyd*[1]

Accelerated Testing of Marine Grade Steels—A Localized Corrosion Approach

REFERENCE: Johnston, R. R. M. and Lloyd, C. P., "**Accelerated Testing of Marine Grade Steels—A Localized Corrosion Approach,**" *Corrosion in Natural Environments*, *ASTM STP 558*, American Society for Testing and Materials, 1974, pp. 261–278.

ABSTRACT: Factors affecting local cell action such as the presence of nonmetallic inclusions in steel and the contribution of ohmic control (*iR* drop) in the electrolyte are discussed. The importance of local action in the marine environment and the poor reliability of current accelerated tests for marine grade steels are pointed out. An investigative technique, developed from earlier work, is described in which the specimen has been incorporated in the form of a horizontal rotating disk enabling solution hydrodynamics to be readily defined. The intensity of local cells is displayed in real time as a magnified contour map of the corroding specimen surface. Effects of test electrolyte composition including ionic strength and concentration of cathodic species have been studied on a model galvanic system, a steel containing sulphide inclusions, and two low-alloy marine grade steels.

KEY WORDS: corrosion, corrosion environments, accelerated tests, electrolytes, electrodes, kinetics, galvanic corrosion, inclusions, local action cells, marine grade steels

Local cell action as a corrosion process is particularly important in the marine environment. Splash-zone pitting, weld corrosion, and crevice effects are all dependent on the nature of the metal surface and are partly under ohmic (*iR*) control [*1*].[2] Weld corrosion of ships' plates, for example, is reported to be influenced not only by composition of both the plate and the weld electrode, but is also increased by the speed of the seawater [*1*,*2*]; that is, its rate is under intermediate or mixed control due to a combination of mass transport and surface effects [*3*].

Recent controversy [*4*,*5*] over the relative corrosion resistance of ingot and continuously cast steel was centered on localized corrosion supposedly due to various types of sulphide inclusions. This argument arose from the premature deterioration of spray-painted bridge girders which had been transported by floating and then, prior to erection, left standing in brackish

---

[1] Senior research officer and research officer, respectively, BHP Melbourne Research Laboratories, Clayton, Victoria, Australia.

[2] The italic numbers in brackets refer to the list of references appended to this paper.

water for three to six months [*5*,*6*]. A second aspect concerned one particular series of plates in the hull of an icebreaker which had corroded quite seriously in comparison with adjacent plates after the ship had seen only minimal service [*5*,*6*]. The resulting spate of publications [*4*,*5*,*7*] showed not only that little is understood about the contribution of nonmetallic inclusions to corrosion in comparison with other types of local cells, but that very few methods are currently in use (or indeed exist) which can make truly localized measurements on mild or low-alloy steels [*8*].

The accelerated testing of low-alloy marine grades of steel is currently quite unreliable despite the necessity for such a procedure as an aid to development in this area [*9*]. The test performance of a series of alloy steels is often dependent in an unexplained way on such factors as frequency of intermittent immersion or the nature of the test electrolyte [*9*,*10*].

Cron et al [*11*] made an electron microscope study of the phases attacked in a 0.45 weight percent carbon steel immersed in various aqueous electrolytes. Although pH and potential were well defined in this work, the test solutions were unstirred and the results cannot be readily related to service conditions as regards degree of mass transport, surface or ohmic control. It appears, therefore, that careful study and choice of accelerated test parameters are needed to ensure that the actual properties measured in any given test are relevant to practical situations.

In the present work, we sought a technique which would pinpoint and measure the activity of local action cells, initially of unknown location. The method had to be nondestructive to enable regions of activity to be subsequently examined by metallographic and surface analysis techniques and, since we wished to work with mild steels, this meant that it would be necessary to use dilute electrolytes.

In 1951 a rotating electrode (cylinder) technique was described by McAndrew et al [*12*] which appeared to have the potential to fulfill these requirements if some additional development work could be effected. Moreover, since its principle of operation depended upon sensing the ohmic potential differences (iR drop) associated with the ion currents flowing in the local action cells, it provided a true kinetic measure of corrosion activity rather than just a thermodynamic possibility of occurrence.

A detailed evaluation of this technique has hitherto not been reported, and since it appeared to have a number of parameters which could be closely related to important corrosion phenomena, the present work was undertaken to establish the usefulness or otherwise of the method as a test procedure.

Preliminary Development Work

The initial technique used by McAndrew et al [*12*] and others [*13*,*14*] involved a stationary microreference or probe electrode mounted close to a rotating cylindrical specimen. The probe electrode picks up variations in *iR* drop as it cuts the fields set up by the local action cells. The signals induced in the probe may be amplified and fed to the vertical plates of a cathode ray oscilloscope (CRO) where, if the rotation of the specimen is synchronized with the CRO trace, a standing wave is displayed which represents the point-to-point variations in *iR* drop between the local cells around a circumference of the specimen as determined by the position of the probe. These principles are illustrated in terms of an Evans diagram in Fig. 1 (upper half), where E_c and E_a are the equilibrium potentials of the cathodic and anodic reactions and the other terms have their usual meaning. The significance of probe distance from the surface is indicated in the lower half of the figure.

Preliminary work in the authors' laboratories [*15*] was carried out with rotating cylinders to establish a convenient means of quantifying a display of local action cells due to sulphide inclusions in steel. Phelps [*14*] had discussed vertical movement of the probe parallel to the rotating cylinder

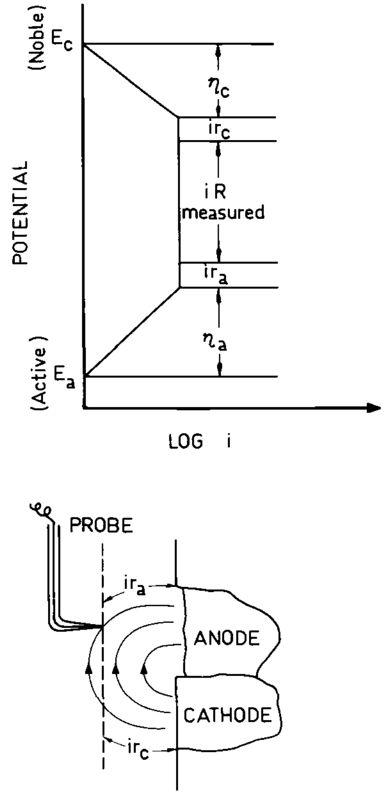

FIG. 1—*Principle of rotating electrode method*: (top) *Evans diagram showing ohmic control of corrosion rate*; (bottom) *schematic representation of probe passing a localized cell.*

axis to enable the surface of the corroding specimen to be scanned in a spiral path. By translating this vertical movement by means of a potentiometer to the vertical (y) plates of the CRO and, using the potential field signal to modulate the trace intensity, a map of corrosion activity could be obtained as light and dark areas (gray scale). This display procedure has been followed only recently by Isaacs [*16*], who actually employed quiescent solutions and a different electrode system, but the result is merely a diffuse gray-scale picture without clarity or definition.

Our work resulted in motorizing the scanning movement of the reference probe, and in the construction of a contour generator [*17*] which is connected between the amplifier and the oscilloscope to modulate the intensity of the oscilloscope trace. This contour generator samples the signal amplitude and selects up to eight voltage levels for simultaneous display as discrete contours on the CRO screen. In addition, we used a specimen in the form of a horizontal rotating disk (Fig. 2) for which mass-transport conditions in solution can be accurately defined [*18*].

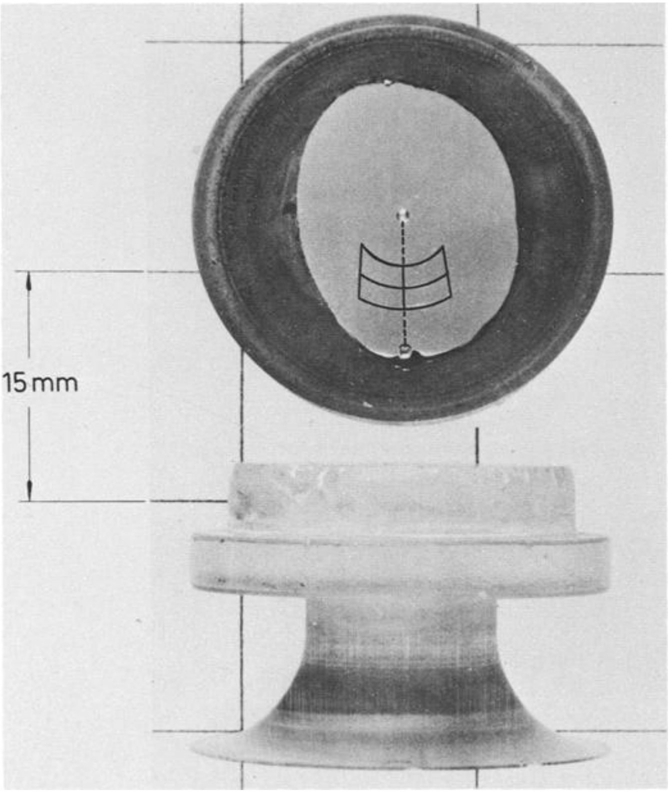

FIG. 2—*Specimen mounting details:* (top) *lower face showing center and peripheral reference marks, and a typical scanned area;* (bottom) *side view showing the RDE shape.*

Experimental

Specimen Composition and Preparation

The compositions of the various steels used are shown in Table 1. The pure iron was prepared from Gliddon melting stock by vacuum-induction melting. It was carbon deoxidized and vacuum cast. All steels were hot-rolled and normalized.

Description of the Apparatus

Figures 3 and 4 show the present apparatus. The motor, D, is connected to the main shaft, C, by a belt drive; T is a feedback tachometer to facilitate speed control; A is a rotary potentiometer linked to C which provides a ramp voltage for driving the horizontal (x) differential amplifier of the CRO (not shown). This use of an x-amplifier (to replace the normal time base) in conjunction with A ensures perfect synchronization of the rotation of the specimen, S, with the CRO trace at all speeds.

Metal specimens (15 mm diameter by 2 mm thick) were mounted in epoxy resin and the epoxy machined to the fluted shape (Fig. 2, bottom) of a rotating disk electrode (RDE) which provides definable hydrodynamic flow. The RDE epoxy former was an accurate push fit in the bottom of C. The disk surface was then prepared by grinding on wet and dry emery paper of successively finer grades to 600 mesh. Prior to the 600-grade a center drill was used to mark the center of the disk surface with a circular pit about 250 μm in diameter. This did not affect the results obtained since measurements were usually made at between 3 mm and 5 mm radius.

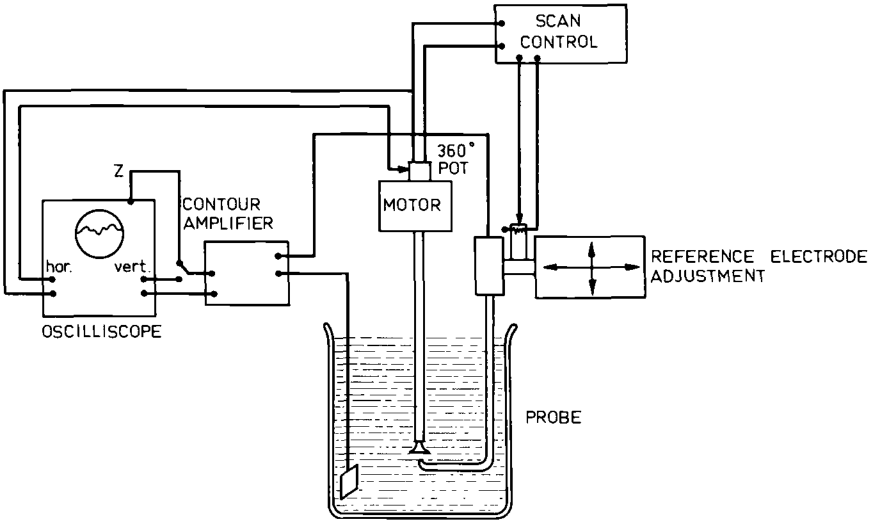

FIG. 3—*Block diagram of apparatus.*

TABLE 1—*Composition of the steels.*

Grade	C	Mn	Si	P	S	Cr	Ni	Cu	Al
High-purity iron	0.023	0.026	0.005	0.003	0.004	<0.05	0.06	0.003	<0.01
Plain carbon	0.09	0.60	<0.01	0.002	<0.01	0.01	0.02	0.03	...
Copper-nickel-phosphorus	0.21	0.96	0.071	0.083	0.024	0.06	0.69	0.58	...
Chromium-aluminum	0.13	0.97	0.41	0.02	0.01	0.96	0.065	0.035	1.03
Resulfurized steel	0.43	0.75	0.22	0.036	0.114	0.09	0.01	...	...

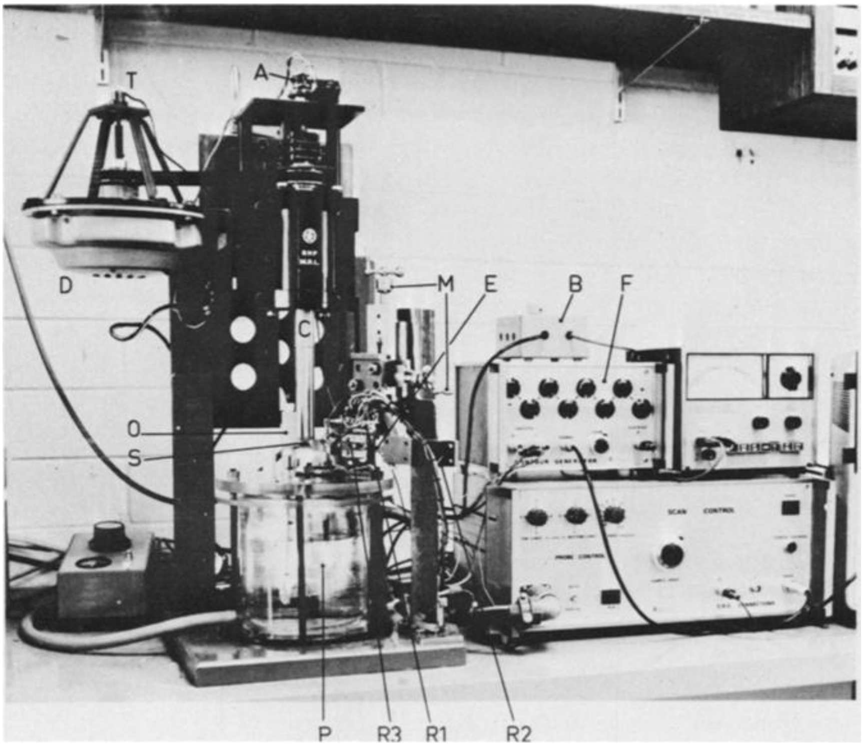

FIG. 4—*Photograph of present apparatus.*

Final polishing was done with 1 to 4 μm then 0 to 1 μm diamond pastes. All specimens were rinsed in alcohol and dried in a stream of air.

The microelectrode probe, P, was constructed by electromachining platinum wire initially 250 μm diameter to a fine tip and sealing into glass capillary tube. The bottom end of this tube was shaped as a "J" and the tip ground back to expose the thinned section of the wire. A typical diameter of the wire tip of these probes was 28 μm. The tip could be set at known distances from the underside of the RDE by the vertical micrometer screw, M, upon which the probe assembly was mounted. In the probe assembly the probe is actually carried on a rack and pinion, E, which could be oscillated horizontally by a small motor powered through the probe control box. This enabled the underside of the RDE to be scanned from the center to the periphery of the metal specimen. The limits of oscillation along this radial path are governed through a linear motion potentiometer, R_3, employed as a transducer in the probe control circuit to monitor the position of E. A typical area scanned is scratched on the surface of the RDE in Fig. 2 (top). The lateral limits of this scan are set by the voltage sensitivity selected on the x-amplifier of the CRO, so that any desired fraction of a full revolution may be displayed across the full CRO screen. As will be detailed elsewhere [*19*], the resistors R_1 and R_2, in conjunction with A, are arranged so that any desired area can be centered on the screen and the lateral (x,y) dimensions of the display are dimensionally consistent. The only distortion present is that associated with the curved, scanned area being displayed as a rectangle.

The reaction vessel of 1 dm^3 capacity contained approximately 0.8 dm^3 of electrolyte and was thermostated at 25°C (77°F) by a water jacket. Solutions were flushed either with high-purity nitrogen alone or nitrogen with a small amount of air (medical grade) bled in to fix the concentration of dissolved oxygen. O (Fig. 4) is an electrode used to monitor oxygen in the electrolyte. B is a mercury cell polarizing unit for O which, when used in conjunction with the differential voltmeter (at the right of the figure), gave a typical sensitivity of 7.4 mV/μ mole (22.2 mV/ppm) and a lower limit of detection of less than 1×10^{-7} mole of dissolved oxygen.

Stock solutions of NaCl, HCl, and H_2SO_4 were prepared from AR grade materials and singly distilled water (resistivity 2.7×10^5 Ω cm^{-1}), and were stored in borosilicate glassware.

Results and Discussion

Pure Iron and Mild Steel

A typical trace for a pure iron RDE is shown in Fig. 5 (top). Since the signal was passed directly into a capacitor at the front end of the amplifier the trace should ideally average out along the zero line of the screen. This behavior for pure iron may be compared with Fig. 6, which shows curves obtained under similar conditions for SS41 plain carbon steel.

In this latter case there is considerable departure of the trace from the zero line. Rice [*13*] drew a horizontal line through the lowest point of the trace and took the area under the curve as a measure of the corrosion activity. In the present work, however, warping from the zero line and instability of the trace were aggravated when the probe tip was brought closer than about 5 to 10 μm of the surface of the RDE specimen. It seems therefore that surface flatness limitations may be in part responsible for such effects. During preliminary work conducted with cylindrical specimens, considerable trace instability and warping were experienced which was not readily associated with any particular parameters. The fact that trueness of rotation is more difficult to achieve with cylinders than with an RDE lends weight to this proposal.

In general, large signals were observed immediately after immersion of the RDE in the electrolyte. These decreased rapidly, reaching a steady state after 2 to 5 min immersion, at which stage they resembled the original trace closely in all respects except size. The signal then remained virtually constant for more than 30 min and measurements were always taken

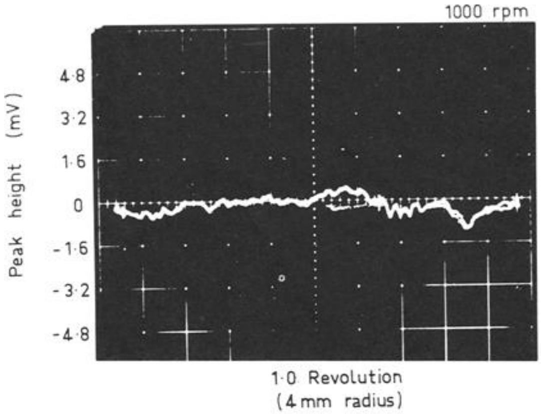

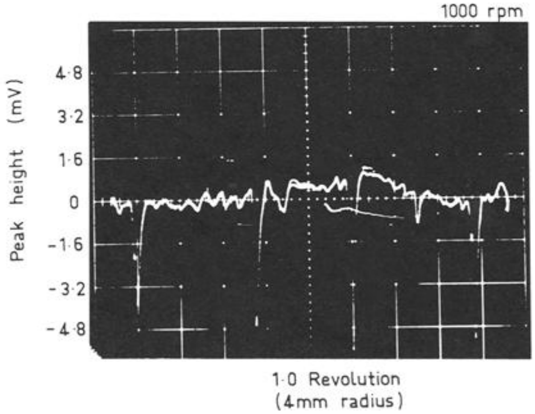

FIG. 5—*CRO traces for pure iron:* (top) *pure iron;* (bottom) *pure iron with two radial gold strips.* (*Experimental conditions:* 10^{-5} *M HCl, 20-μm probe distance, less than* 10^{-7} *M* O_2.)

within this period. Specimens left in contact with the electrolyte for longer periods became covered with a thin tarnish layer which, if immersion was prolonged past the hour mark, developed into thick oxide patches and serious modification of the trace occurred.

A Model Local Cell

Figure 5 (bottom) shows the effect of two gold strips vacuum deposited across the center of a pure iron specimen. As may be deduced from purely physical considerations, with the input signal connected to the positive side of the differential amplifier trough is recorded when the cathodic strip passes the probe tip. Ideally, the shape of these cathodic peaks should be

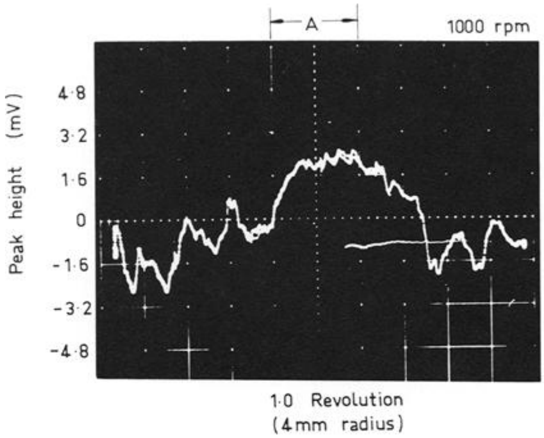

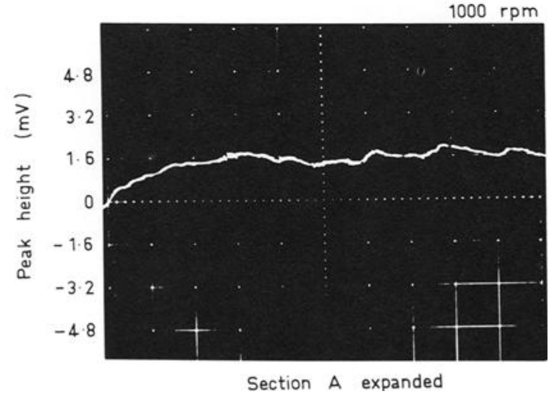

FIG. 6—*CRO traces for SS41 structural carbon steel:* (top) *full revolution;* (bottom) *expansion of Section A. (Experimental conditions: 10^{-5} M HCl, 20-μm probe distance, less than 10^{-7} M O_2.)*

of square wave form, but this could only occur if (*a*) the diameter of the probe tip was small in comparison with the strip width; (*b*) spherical diffusion of hydrogen ion, the cathodic species, did not occur along the side of the strip; and (*c*) the signal amplifier had a perfect response (that is, infinite bandwidth). Undoubtedly, other factors are also involved. The dependence of the amplitude of these peaks on the width of the gold strips is shown in Fig. 7. The signal has been corrected, as indicated in the figure, for amplifier response on the basis of the time required for a strip of given width to pass any point on the tip of the probe. In addition to strip width, this time will also be influenced by radius of scan and the rotation speed of the RDE.

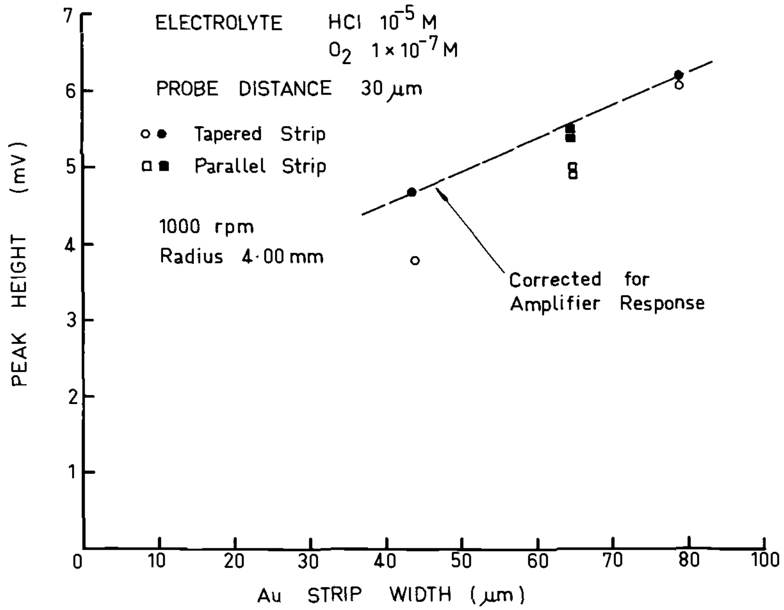

FIG. 7—*Effect of gold strip width on cathodic peak height (pure iron used as base for gold strips).*

The results shown in Figs. 5 and 6 were obtained with 10^{-5} M HCl as electrolyte and similar results were obtained in 5×10^{-6} M H_2SO_4. Since the residual level of oxygen in these runs was typically below 2×10^{-7} M, it is concluded that reduction of hydrogen ion is the essential cathodic process.

Figure 8 shows the effect of changing the rate of mass transport of the cathodic reactant at two concentration levels while keeping the resistivity of the electrolyte constant. An electrolyte of 10^{-5} M NaCl containing known amounts of dissolved oxygen proved to be a convenient way of achieving this. It can be seen that the *iR* signal increases rapidly with rotation speed initially, and then slowly approaches a plateau. The curve for the higher oxygen level must be associated with an increase in *i*, the corrosion current, and therefore its curve lies uppermost since the *iR* product has been increased.

A possible explanation of the effect of rotation speed is given schematically in Fig. 9 in terms of an anodic reaction which is surface controlled and a cathodic reaction under mixed control. It can be seen that increase of the rotation speed ceases to produce a larger *iR* signal once the cathodic reaction also becomes fully surface controlled. This explanation may also apply to similar effects observed in both acid electrolytes with gold strip models and with resulphurized steel.

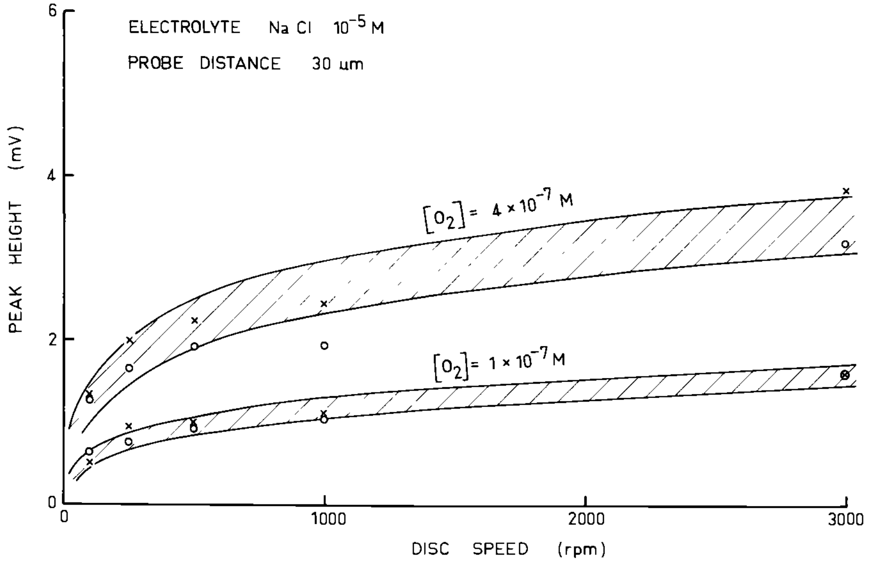

FIG. 8—*Relationship between peak height and RDE rotation speed. (Cathodic peaks arising from 170 μm wide, vacuum-deposited gold strip on pure iron RDE. Peak heights were corrected at 1000 and 3000 rpm for amplifier response by adding, respectively, 10 and 50 percent to the observed peak heights.)*

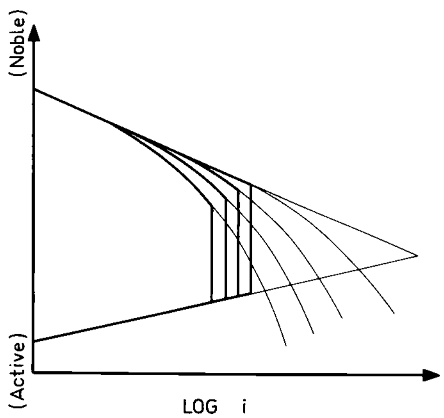

FIG. 9—*Schematic representation on Evans diagram of effect of rotation speed (see Fig. 8).*

Figure 10 (top) shows the effect of changing the concentration of sodium chloride electrolyte in the presence of a fixed concentration of dissolved oxygen. The decrease in peak height from 10^{-4} M down to noise level at 10^{-2} M is readily explained by a fall in the *iR* signal due to a decrease in *R*. The maximum at approximately 10^{-4} M NaCl may be considered barely significant and is certainly difficult to explain, since there appears to be no

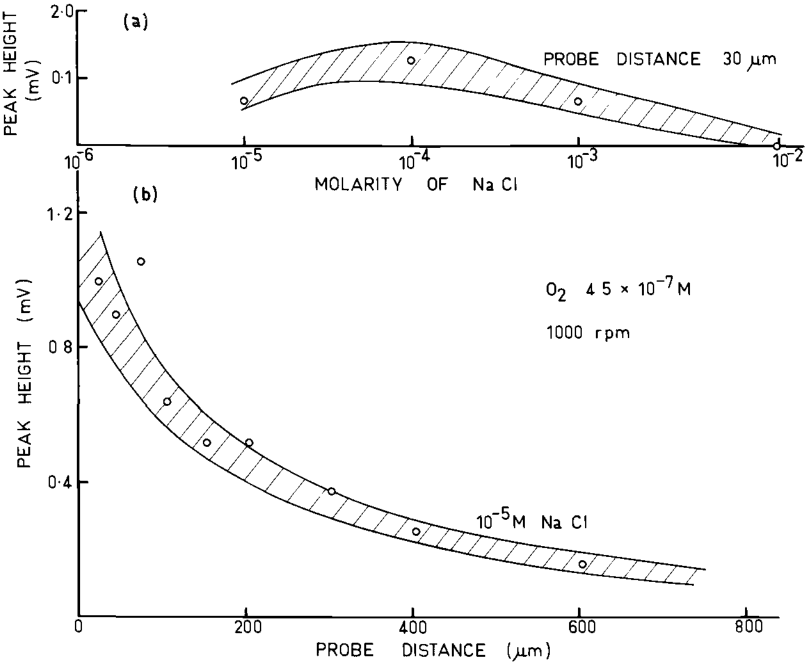

FIG. 10—*Dependence of peak height on NaCl concentrations and distance of probe from specimen surface. (Cathodic peaks arising from vacuum-deposited 60-μm-wide gold strip on pure iron RDE. Peak heights corrected for amplifier response.)*

reason why the product $i \times R$ should increase. The effect of changing electrolyte concentration in acid solution appears to differ for HCl and H_2SO_4, and, at present, no further elucidation can be given.

The effect of variation of the distance between the probe and the surface of the RDE can be seen in Fig. 10 (bottom). On the basis of the amplifier response correction, discussed in the foregoing, the peak height values in Fig. 10 have actually been increased by 100 percent. This smooth decay of peak height with increasing distance of the probe from the RDE surface, while in accordance with expectations from purely physical considerations, contrasts markedly with the positive slope published by Rice [*13*]. However, while the magnitude and sign of the slopes obtained by the latter were reported to depend on the location of the probe opposite the specimen surface, the trend shown in Fig. 10 (bottom) was invariably found with all steels in all three electrolytes used.

Resulphurized and Low Alloy Steels

The results obtained when the resulphurized steel was examined in 10^{-5} MNaCl electrolyte are shown in Fig. 11. The upper trace is for one full revolution of the specimen (about 25 mm in the x-direction) while the center trace is an expansion of 4.2 mm out of the middle. A contour map

Trace at 4·0mm Radius

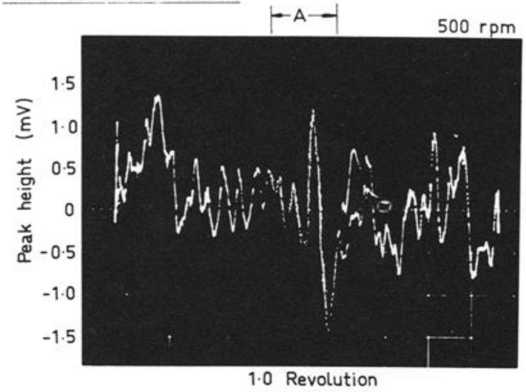

Section A Expanded

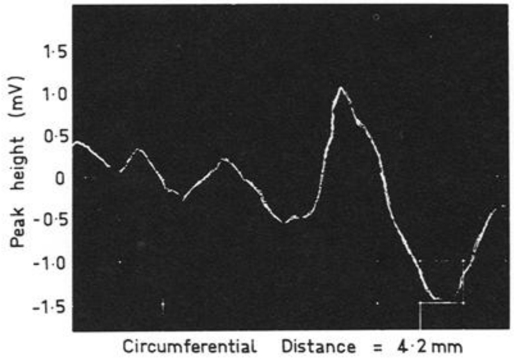

Contour Map around Section A

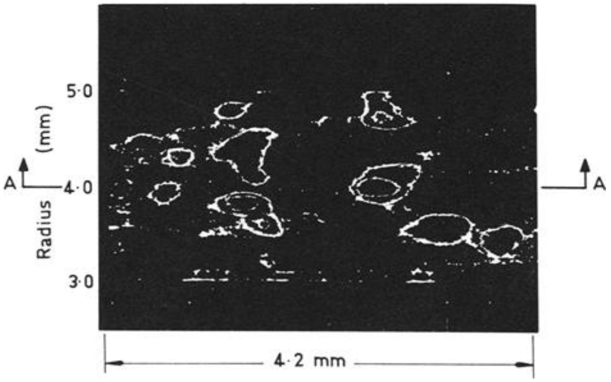

FIG. 11—*Results obtained with sulfide inclusions in mild steel. (Experimental conditions: 10^{-5} M NaCl, 7 × 10^{-7} M O_2, 40-μm probe distance.) Note: contour map shows anodic areas only.*

of the potential field variations in this area is shown in the lower part of Fig. 11, for contour levels at +0.25 and +0.75 mV.

Figure 12 shows photomicrographs of the specimen surface, the curved grid delineating the limits of the scan. The upper plate shows an overlay of the rectilinear map of Fig. 11 cut into four sections to fit the curved area. It can be seen that only about 10 percent of the area has developed anodic activity. Comparison with the lower plate of Fig. 12 shows groups of inclusions associated with these areas of activity. Subsequent electron microprobe analysis, however, has not shown any singularities of composition of the inclusions in these areas in comparison with those analyzed outside.

Figure 13 (top and center) shows a trace and contour map for the chromium-aluminum steel examined in 10^{-5} M HCl, the bottom map being for the copper-nickel-phosphorus steel in a similar electrolyte solution. The contour levels were −1.0 mV, −0.25 mV, and +0.75 mV. The contours obtained for the low-alloy steels are much larger and less frequent on an equivalent area than those in Fig. 11. Electron microprobe analysis, accurate to within ±0.05 percent, has failed to identify any heterogeneities in composition responsible for the activity of these low-alloy steels.

From the relative sizes of the contour circles and the inclusions (Fig. 12) it may be concluded that the technique is a long way from resolving effects due to individual heterogeneities. Nevertheless, it is currently the only means available of providing any quantitative comparison of the intensity, type, and distribution of local action cells on mild and low-alloy steels. It may therefore become invaluable as a tool for assessing development changes in this area.

Summary and Conclusions

1. The usefulness of the rotating electrode technique in the study of local action phenomena has been significantly increased.

2. By quantifying the display of corrosion activity in the form of a magnified contour map, it has become possible to readily identify the area of study.

3. Adaption of the method to scan a horizontal rotating disk electrode has facilitated subsequent examination of the specimen surface by metallographic and other surface analysis techniques.

4. A model local cell system has been examined under conditions of corrosion rate control considered to be important in the marine environment. Parameters studied (*a*) the rate of mass transport of cathodic oxygen and hydrogen ion; (*b*) the concentration of nonelectroactive salt; (*c*) the nature of the anion in the electrolyte; and (*d*) the limitations set by the associated electronic equipment.

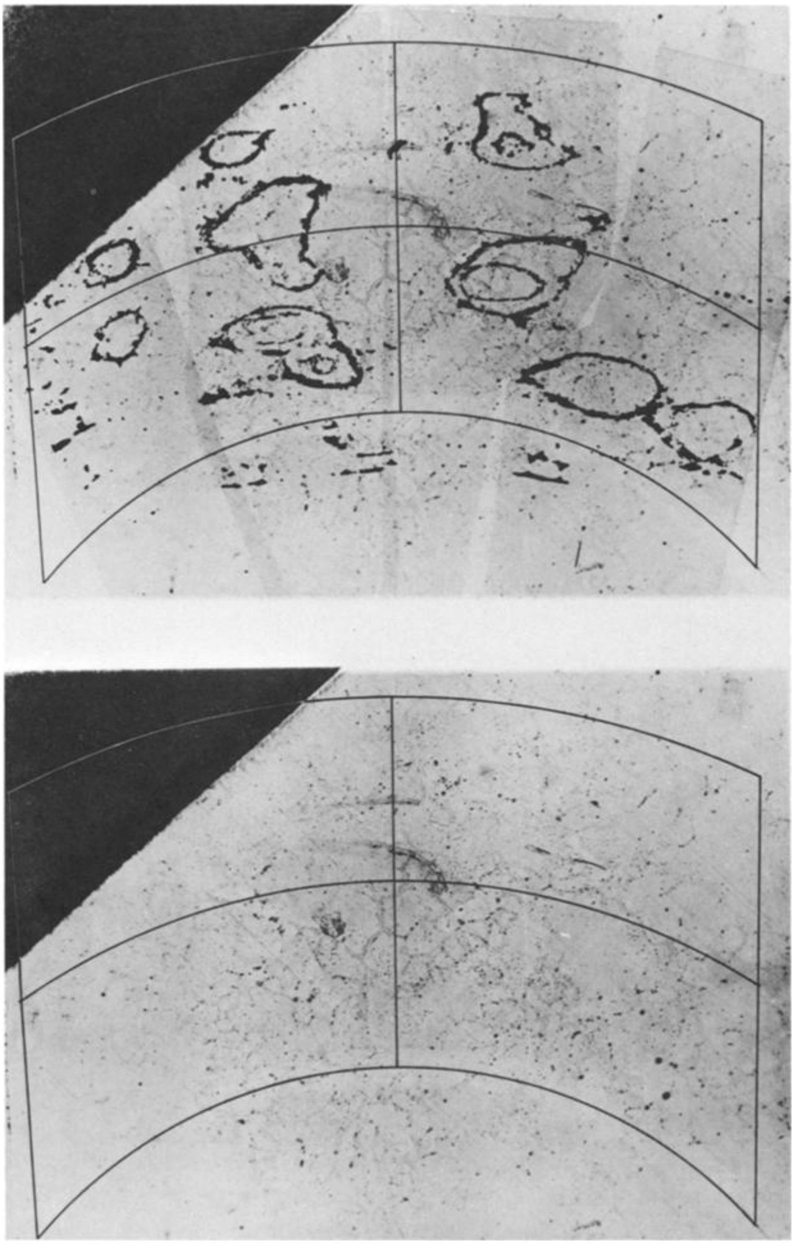

FIG. 12—*Correlation of contour map with sulfide inclusions present in scanned area:* (top) *contour map layed over area scanned;* (bottom) *area scanned.*

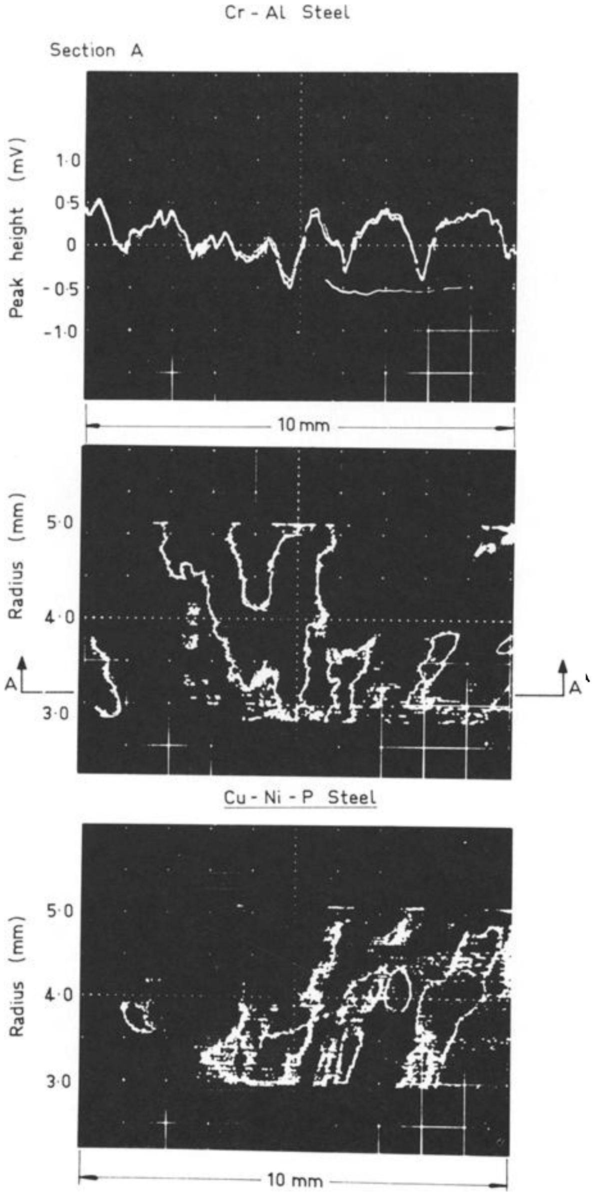

Cr - Al Steel

Section A

Cu - Ni - P Steel

FIG. 13—*Contour maps obtained with two marine grade steels.* (*Experimental conditions:* 10^{-5} *M HCl,* 10^{-7} *M* O_2, *20-μm probe distance.*) *Note: Except for half-formed contour along right-hand border of chromium-aluminum steel at 3.8 mm radius, all closed contour lines in both maps represent areas of cathodic activity.*

5. While the present work has not been completely definitive, experimental conditions have been identified in the laboratory under which sulphide inclusions constitute the predominant local cell activity. It is expected that further work may sufficiently enhance our understanding to correlate laboratory results with field observations.

References

[*1*] Wranglén, G., *Corrosion Science*, Vol. 9, 1969, p. 585.

[*2*] Greenblatt, J. H., *Corrosion*, Vol. 13, 1957, p. 817t.

[*3*] Bircumshaw, L. L. and Riddiford, A. C., *Quarterly Reviews*, Vol. 6, 1952, p. 157.

[*4*] Wallwork, G. R. and Harris, B., U. R. Evans International Conference on Localized Corrosion, 6–10 Dec. 1971.

[*5*] Wranglén, G., U. R. Evans International Conference on Localized Corrosion, 6–10 Dec. 1971.

[*6*] *Engineering and News Record*, 25 Feb. 1971, p. 14; *New Scientist*, Vol. 48, 10 Dec. 1970, p. 440.

[*7*] Janik-Czachor, M., Szummer, A., and Szlarska-Smialowska, Z., *British Corrosion Journal*, Vol. 7, March 1972, p. 90; Kullberg, G., *Iron and Steel*, Vol. 45, No. 2, April 1972, p. 173; Kaneko, N. et al, Nippon Kokan Technical Report—Overseas, March 1969, p. 21.

[*8*] Budd, M. and Booth, F., *Metalloberfläche*, Vol. 19, No. 7, 1965, p. 197.

[*9*] Johnston, R. R. M. and Shackleford, R. E., *Journal of the Australian Institute of Metals*, Vol. 17, No. 4, Dec. 1972, p. 175.

[*10*] Takamura, A. et al, *Transactions of the Iron and Steel Institute of Japan*, Vol. 11, No. 5, 1971, p. 299.

[*11*] Cron, C. J., Payer, J. H., and Staehle, R. W., *Corrosion*, Vol. 27, No. 1, Jan. 1971, p. 1.

[*12*] McAndrew, J. B., Colner, W. H., and Francis, H. T., NACA Technical Note 2523, National Advisory Committee for Aeronautics, Washington, D. C., 1951; *Chemical Engineering*, Vol. 59, 1952, p. 305.

[*13*] Rice, J. K., *Corrosion*, Vol. 10, 1954, p. 25.

[*14*] Phelps, E. H., *Corrosion*, Vol. 18, 1962, p. 239t.

[*15*] Johnston, R. R. M. and Lloyd, C. P., 13th Australasian Corrosion Association Conference, Melbourne, Victoria, Nov. 1972, Paper 18; Johnston, R. R. M., and Lloyd, C. P., 3rd Australian Electrochemistry Conference, Terrigal, New South Wales, Feb. 15–18, 1972.

[*16*] Isaacs, H. S., U. R. Evans International Conference on Localized Corrosion, Dec. 6–10, 1971; Isaacs, H. S. and Kissel, G., *Journal of the Electrochemical Society*, Vol. 119, No. 12, Dec. 1972, p. 1628.

[*17*] Sander, A. J., Australian Patent Office, Provisional Patent No. PB2040, Jan. 1973.

[*18*] Levich, V. G., *Physiochemical Hydrodynamics*, Prentice Hall, Englewood Cliffs, N. J., 1962; Riddiford, A. C., *Advances in Electrochemistry and Electrochemical Engineering* Vol. 4, 1966, p. 47.

[*19*] Paper to be submitted to *Journal of Scientific Instruments*.

J. W. Spence[1] *and F. H. Haynie*[1]

Design of a Laboratory Experiment to Identify the Effects of Environmental Pollutants on Materials

---

REFERENCE: Spence, J. W. and Haynie, F. H., "**Design of a Laboratory Experiment to Identify the Effects of Environmental Pollutants on Materials,**" *Corrosion in Natural Environments, ASTM STP 558*, American Society for Testing and Materials, 1974, pp. 279–291.

ABSTRACT: This paper describes an environmental system consisting of five exposure chambers and an experimental design for studying the effects of gaseous air pollutants [sulfur dioxide (SO_2), nitrogen dioxide (NO_2), and ozone (O_3)] on materials. Each chamber has the means for independent control of six environmental variables (temperature, relative humidity, etc.) as well as the unique feature of chill racks that regulate the formation of dew on the test specimens. An accelerated test is achieved by a dew-light (xenon lamp) cycle to simulate diurnal conditions. Statistical techniques (analysis of variance) were used to correct for differences in light and pollutant distribution within the chambers before initiating a statistically designed environmental experiment. To study the interactions of pollutants and other environmental variables that are likely to have significant effects on materials, a two-level factorial arrangement was selected.

KEY WORDS: corrosion, test chambers, air pollution, sulfur dioxide, nitrogen dioxide, and ozone, materials, damage, statistical tests, factorials positioning

The effects that air pollutants have on materials are currently being investigated by the Environmental Protection Agency (EPA) [*1–5*];[2] however, effects data upon which environmental management decisions can be based are not firmly within our grasp. This paper describes an environmental chamber system developed in our laboratory and an experimental design for studying the effects of air pollutants on materials. Resulting information will be useful in setting secondary ambient air quality standards and in making economic assessments of pollutant damage to property.

Background

Midwest Research Institute (MRI), under contract to EPA, conducted a systems approach study [*6*] to rank materials according to potential

---

[1] Research chemist and chief, respectively, Materials Section, Chemistry and Physics Laboratory, Environmental Protection Agency, National Environmental Research Center, Research Triangle Park, N. C. 27711.

[2] The italic numbers in brackets refer to the list of references appended to this paper.

TABLE 1—*Relative order of pollution damage and available information.*

Materials	Dollar Loss[a]	References with Useful Information
Metals	39	54
Paints	32	7
Textiles	9	14
Elastomers	5	12
Plastics	3	9
All others	12	4

[a] Percent of total.

economic damage by air pollution. Table 1 summarizes the results of this ranking, which pertains only to gaseous pollutants. The potential economic loss for pollutant-damaged metals ranked higher than other materials; published information was also highest. Damage to paints ranked second in economic importance. Equally significant, MRI's study revealed that little has been published on the effects of air pollutants on paints and the remaining materials.

Materials and Effects Measurement Techniques

The MRI study and ranking formed the basis for selecting materials (Table 2) for exposure in our laboratory-controlled environments. All of these materials are used in products with large sales and therefore are commercially important. Except for the drapery goods, these materials are exposed to exterior environments. Previous field and laboratory studies conducted by industry and EPA have shown that dyed fabrics fade in the presence of certain pollutant gases [7–9].

For this exposure study, effect measurement techniques were selected to provide damage data that would reflect loss of service life. For the drapery materials, color change (fade) of the dyed fabric and microscopic determination of fiber deterioration will be observed durmg exposure. Film thickness measurements as described in the ASTM Measurement of Dry Film Thickness of Nonmetallic Coatings of Paint, Varnish, Lacquer, and

TABLE 2—*Materials selected for chamber exposure studies.*

Metals:	Weathering steel, galvanized steel, aluminum
Paints:	Water base, oil base vinyl coil coated, acrylic coil coated
Rubber:	White sidewall radial tire
Plastics:	Vinyl house siding
Textiles:	Drapery materials (cotton, rayon/acetate, and polyester)
Stone:	White Cherokee marble
Cement:	portland

Related Products Applied on a Nonmagnetic Metal Base (D 1400-67) will be used to determine erosion rates for the galvanized steel and exterior paints. Gravimetric measurements will be recorded in order to determine corrosion rates for the weathering steel. The galvanized and weathering steel will be prepared for measurements according to the ASTM Recommended Practice for Preparing, Cleaning, and Evaluating Corrosion Test Specimens (G 1-72). The vinyl house siding, marble, and portland cement specimens will undergo microscopic examination during the exposure. Microprobe analysis of the house siding and marble specimens will be the primary tool for detecting pollutant (SO_2) contamination. Strips of the radial tire will be stressed at two levels during exposure. Tensile measurements will be taken to detect loss of sidewall strength after exposure. Aluminum (C-ring specimens) will be exposed at two levels of stress during exposure. This test procedure is described by ASTM Committee B-3 as Method 2A [*10*]. Time to break for the specimens will be recorded in order to determine failure due to stress corrosion.

Laboratory-Controlled Simulation of Polluted Environments

Precise damage data for the deterioration of materials can best be obtained by means of controlled environmental chambers. The chambers, however, must be designed to accelerate the weathering of materials but at ambient conditions of temperature, humidity, and pollutant concentrations. Weathering may be accelerated by providing a variable day/night cycle. Increasing the cycling rate should yield an accelerated test from which pollutant damage data to materials may be obtained.

Chamber Design

An environmental system consisting of five chambers was designed and constructed for studying the effects of gaseous pollutants on materials. Figure 1 shows the basic flow diagram of this environmental system.

Room air is filtered by charcoal to remove any existing pollutants and cooled to 0.6°C (33°F) to remove moisture. The air then flows into a manifold and splits into five separate air streams, each having heater and humidification systems. Before entering the chambers, the cooled air is heated to the desired temperature [up to 48.9°C (120°F)] and humidified by the introduction of steam. At the back of each chamber the air enters a mixing box that houses temperature and humidity control sensors and three gaseous pollutant (SO_2, NO_2, O_3) injection ports. The reconditioned, polluted air then flows through the chambers over the test specimens into a decontamination exhaust system containing charcoal and Purafil[3] filters, and finally to the outside.

---

[3] Mention of company name commercial products throughout this paper does not constitute endorsement by the Environmental Protection Agency.

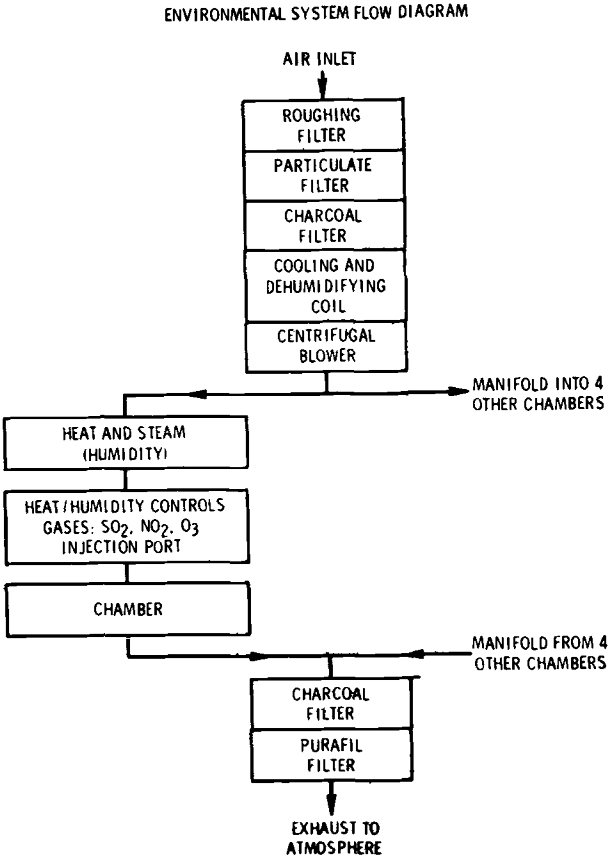

FIG. 1—*Environmental system flow diagram.*

Temperature, humidity, and concentration of sulfur dioxide, nitrogen dioxide, and ozone within each chamber can be independently controlled. Control of temperature and humidity is achieved with commercial hardware. The concentration of each pollutant is controlled by an automatic time-sharing proportional system. Pollutant controllers were specially designed and built for EPA. A time-sharing feature enables the concentration levels in all five chambers to be controlled by a single air-monitoring instrument for each pollutant. Each pollutant controller will continually monitor, record, and control the concentration of one of the three air pollutants within the five environmental chambers.

Chamber Operation

Each of the five chambers is equipped with a xenon arc lamp (6000 W) to simulate sunlight. The chamber and light cap are shown in Fig. 2. The xenon arc lamp is separated and protected from the chamber environment conditions by means of a 4-mil film of clear FEP Teflon. This fluoro-

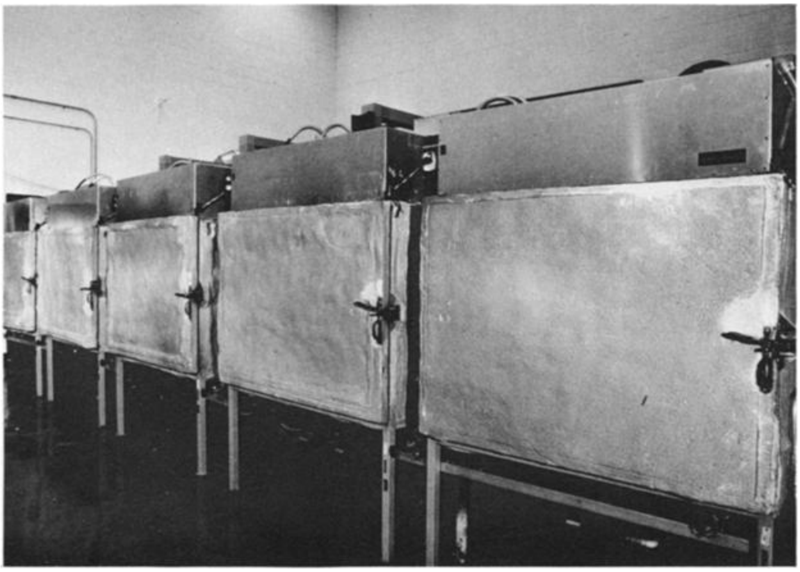

FIG. 2—*Environmental chambers.*

carbon film was selected because it transmits the ultraviolet, visible, and infrared radiation that is emitted by the xenon lamp. Each chamber is also equipped with dew-racks (Fig. 3) upon which the specimens are mounted. Coolant can be circulated through the racks to cause dew formation on the specimens.

During exposure, the air entering the chambers is maintained at preselected temperatures, relative humidities, air flows, and concentration of pollutants. An exposure cycle consists of:

1. Lamp off/dew-rack on—moisture condenses on the test specimens and absorbs pollutants.
2. Lamp on/chill rack off—moisture evaporates and pollutants react with test specimens.

The cycling operation simulates night and day conditions. The temperature and humidity of the reconditioned polluted air are allowed to fluctuate during the dew-light cycle. Increasing the cycle rate should yield an accelerated test.

Evaluation of Environmental Chambers

Results of a statistically designed controlled-environment experiment will only be as good as the control system. Thus, variability from the desired levels of pollutants, temperature, humidity, and light energy

FIG. 3—*Chamber chill racks.*

should be minimized. Statistical techniques can be used to determine what parts of the control system need to be adjusted.

Chamber Lighting

The energy distribution from the xenon lamp within the chambers was measured and recorded as millivolts by a Talley Industries SOL-A-Meter. The distribution of energy on the specimen racks within the five chambers was initially balanced by (1) varying the lamp wattage, (2) placing reflectors in the light cap, and (3) varying the angle of the specimen rack.

Analysis of variance (Table 3) was conducted on the energy data to determine chamber and position effects.

TABLE 3—*Analysis of variance for initial energy data.*

Source	Sum of Squares	Degrees of Freedom	Mean Squares	F_{calc}	F_{table}[a]
Position	311.9379	17	18.3493	6.05	1.76
Chamber	49.4749	4	12.3687	4.08	2.05
Residual[b]	206.2371	68	3.0229		
Total	567.6499	89	6.3781		

[a] 0.05 probability level.

[b] Residual is confounded with a possible chamber *x* position interaction effect because the experiment was not replicated. It is taken as the error term in calculating F values.

The calculated F statistics (Table 3) determined for the positions on the specimen racks and the chambers exceed the F_{table} value (0.05 probability level). Therefore, the observed differences for the positions and chambers are statistically significant and caused by something other than random error. The best estimate of the overall mean ($\bar{x}$) energy was 63.28 mV. Based on 89 degrees of freedom the standard deviation (2S) is 5.05. The coefficient of variation is 4 percent. With these tolerance limits we can be 95 percent certain that less than a 10 percent variation from the mean energy may be expected from 95 percent of the measurements.

High energy readings at particular positions were lowered by selectively reducing the reflectivity of the walls with a light spray of flat, black paint. Individual lamp wattages were adjusted to reduce differences among chambers. Analysis of variance (Table 4) was performed on the new data for the five chambers.

The calculated F statistic (Table 4) now reveals that the chamber differences are statistically insignificant. The position effect, however, is still significant at the 0.05 probability level. The best estimate of the overall mean ($\bar{x}$) energy was 61.51 mV with a standard deviation (2S) of 3.38 for 89 deg of freedom. The coefficient of variation is 3 percent. With these tolerance limits we can be 95 percent certain that less than a 6.8 percent variation from the mean energy exists for 95 percent of the measurements. This relatively small amount of variability does not warrant the stratification of position as a variable. Placing the material test specimens randomly within each of the five chambers minimizes any bias that could be caused by the position effect.

Chamber Pollutant Distribution

It is essential that the movement of polluted air be uniformly distributed across the test specimens. A plenum (sheet of stainless steel with 0.74-cm holes spaced 2.5 cm apart) was installed about 12.7 cm above the base of the chamber. The plenum created a pressure drop in the movement of air across it, thereby facilitating the mixing of pollutants within the chambers. The air flow from each chamber was measured in the exhaust ducts with a

TABLE 4—*Analysis of variance for energy data.*

Source	Sum of Squares	Degrees of Freedom	Mean Squares	F_{calc}	F_{table}[a]
Position	55.5960	17	3.2704	2.05	1.76
Chamber	5.7005	4	1.4251	1.09	2.50
Residual[b]	89.0596	68	1.3097		
Total	150.3560	79	1.6894		

[a] 0.05 probability level.

[b] Residual is confounded with a possible chamber *x* position interaction effect because the experiment was not replicated. It is taken as the error term in calculating the F values.

pitot tube. The air flow to each chamber was then balanced by means of a vane installed in the air supply duct.

In order to establish the distribution pattern of polluted air within the chambers, specimens of blue-colored test ribbon were placed at various locations within the chambers about 15.24 cm above the plenum and parallel to the air flow. The test ribbon was developed by the American Association of Textile Chemists and Colorists and is sensitive to NO_2. All five chambers were operated at constant conditions:

Temperature	35°C (95°F)
Relative humidity	5 percent
Nitrogen dioxide	940 $\mu g/m^3$
Air flow	2.7 m^3 min (2.5 air changes per minute)

After 48 h of exposure, the color of the ribbon specimens was measured photoelectrically with a Hunter Model D25A Color Difference Meter. The magnitude of the color change of each ribbon specimen was recorded as ΔE values. An analysis of variance (Table 5) was conducted to determine the significance of chamber and position effects.

TABLE 5—*Analysis of variance for pollutant (NO_2) distribution within the chambers.*

Source	Sum of Squares	Degrees of Freedom	Mean Squares	F_{calc}	F_{table}[a]
Position	0.02344	8	0.00293	3.84	2.25
Chamber	0.00424	4	0.00106	1.40	2.67
Residual[b]	0.02441	32	0.00076		
Total	0.05209	44	0.00118		

[a] 0.05 probability level.

[b] Residual is confounded with a possible chamber x position interaction effect because the experiment was not replicated. It is taken as the error term in calculating F values.

The calculated F statistic (Table 5) for the pollutant distribution within the chambers indicates that the chamber effect is statistically insignificant; however, position effects exist at the 0.05 probability level. The best estimate of the overall mean ($\bar{x}$) for the ΔE values was 3.50 with a standard deviation (2S) of 0.069 for 8 degrees of freedom. The coefficient of variation is 1 percent. With these tolerance limits we can be 95 percent certain that less than a 2.25 percent variation from the mean color change is expected for 95 percent of the measurements. Again, randomly placing the test specimens within the chambers minimizes bias that this variable may cause.

Control of Chamber Environmental Variables

The control capability of the environmental variables for 24 h of continuous exposure is shown in Table 6. It appears that the variability (2S)

TABLE 6—*Control capability of environmental variables within the chambers.*

Environmental Variable	Control Point	Control Capability	
		$\bar{x}$	2S
Temperature, C°	35 (95°F)	34.8	±2
Humidity, %	90	88.8	±2.2
	50	50.4	±1.1
Ozone, μg/m^3	980	991.8	±31.4
	196	199.9	±11.8
Sulfur dioxide, μg/m^3	1310	1372.9	±131.0
	262	275.1	±23.6
Nitrogen dioxide, μg/m^3	940	930.6	±26.3

for the control capability of the environmental variables may be proportional to some function of level ($\bar{x}$). Such a relationship is not uncommon and is frequently encountered in controlled experimentation. It should pose no problems in the computation of exposure data.

The control of temperature and relative humidity is within the mixing box prior to the air entering the environmental chambers. During the dew-light cycle the temperature and humidity are not controlled but allowed to fluctuate in the chamber. The three gaseous pollutants are injected into the mixing box but are controlled within the chambers. Air samples are continuously taken from each of the chambers by means of a manifold system connected to an air monitoring analyzer. The air monitoring analyzers are specific for measuring concentration of each of the three pollutant gases. The levels of the pollutants are maintained during the dew-light cycle.

Chamber Experiment

A 1000-h exposure experiment involving two chambers was conducted to evaluate (1) effects measurement techniques, and (2) the dew-light cycle for accelerating the weathering rate of materials. The chambers were both operated with clean air at 35°C (95°F) and 90 percent relative humidity. One of the chambers was cycled at 20-min intervals of dew and light, while the remaining chamber was held at constant conditions of temperature and humidity. Materials (Table 2) that were determined to be economically important were exposed in both chamber environments.

The galvanized steel and paint panels were evaluated for loss of film thickness after exposure periods of 250, 500, and 1000 h. The method of least squares was used to statistically analyze the rate of erosion of film thickness of these materials. Tables 7 and 8 present the materials studied and the erosion rate data computed respectively from the two chamber exposure conditions.

TABLE 7—*Erosion rates for exposed materials (dew-light cycle).*

	Number of Observations	Erosion Rate, μm/year	95% Confidence Limits
Galvanized steel	36	0	
Coil acrylic paint	90	6.13	±1.49
Coil vinyl paint	90	4.15	±3.03
Oil-base paint	36	267	±484
Latex paint	36	25.9	±39.0

TABLE 8—*Erosion rates for exposed materials (temperature and humidity constant).*

	Number of Observations	Erosion Rate, μm/year	95% Confidence Limits
Galvanized steel	36	0	
Coil acrylic paint	90	10.37	±0.56
Coil vinyl paint	90	6.15	±1.91
Oil-base paint	36	32.9	±49.4
Latex paint	36	0	

After a small initial loss, the galvanized steel exposed in both chambers had zero erosion rates. An initial zinc loss of 4.40 μm ± 1.30 was recorded for the dew-light cycle condition whereas for the constant temperature/humidity condition only 0.42 μm ± 0.93 was initially lost. The dew-light cycle accelerated the erosion of the painted panels except for the coil coated panels. This anomaly could be the result of the lack of experimental replication; however, it is more likely caused by the inaccuracy in the measurement technique. Film thickness was recorded by a Dermitron instrument that operates on the principle of eddy currents for detecting coating thickness on nonmagnetic surfaces. It now appears that the technique of gravimetric analysis [*4*] should be used in conjunction with the Dermitron measurements.

Tensile strengths (psi) for the tire strips were recorded after the 1000-h exposure period for each environmental condition. Analysis of variance (Table 9) was conducted on the tire cord breaking strength to determine significant effects.

The calculated F statistic (Table 9) revealed that the chamber and stress effects are statistically significant at the 0.05 probability for the tire cord breaking strength. However, the interaction effect of chamber x stress is insignificant. No significant effects on the rubber sidewall breaking were observed.

The dew-light cycle accelerated the weathering of the remaining exposed materials. The measurement techniques for these materials provide damage data for which significant differences were distinguished. Therefore, no additional techniques will be needed in assessing damage of these materials.

TABLE 9—*Analysis of variance for white sidewall cord breaking strength.*

	Sum of Squares	Degrees of Freedom	Mean Squares	F_{calc}	F_{table}
Chamber	9894.4	1	9894.4	21.75[a]	5.32
Stress[b]	3369.8	1	3369.8	7.41[a]	5.32
Chamber x stress	965.7	1	965.7	2.12	
Error[c]	3639.5	8	454.9		
Total	17869.4	11			

[a] Exceeds 0.05 probability value.

[b] Rubber strips were stretched 10 and 20 percent.

[c] Replication error.

Experimental Design

An experimental design [*11-13*] to obtain dose response (materials damage) data must now be selected. A commonly used experimental design is to hold all but one variable constant and study only the effect of that variable. Each variable of interest would then be studied—one at a time. With seven variables to be studied, this approach would require considerable time to complete and the result would be fragmentary. As an example, a damage function may be obtained by varying sulfur dioxide concentrations while holding other variables at some set of constant conditions. The shape and magnitude of this function, however, also depends on relative humidity. If a higher relative humidity is selected, both the slope and magnitude of damage as a function of sulfur dioxide are expected to be greater. In statistical language, the change of slope is an interaction effect between sulfur dioxide and relative humidity. The practice of holding all but one variable constant does not enable the researcher to observe interaction effects.

The experimental design, however, must enable the researcher to determine if interaction effects exist. When the researcher does not know what to expect from an experiment and several variables could possibly have an effect on the results, the two-level factorial arrangement is an excellent statistical tool for determining which variables or combination of variables or both, have significant effects. As many variables as possible that are likely to cause an effect on the outcome should be included in the experiment. In this experiment five variables at two levels or conditions (Table 10) were selected.

This experiment requires 32 (2^5) different tests, one at each combination of variable and level, and does not include replication of the test. The large number of tests is necessary because that many direct and synergistic or interaction effects possibly exist. On the other hand, the probability that all of these effects exist is very small. Since each test involves 1000 h of

TABLE 10—*Environmental variables for the two-level factorial arrangement.*

Environmental Variables	Levels	
	Low	High
Sulfur dioxide, $\mu g/m^3$	78.6	1310
Nitrogen dioxide, $\mu g/m^3$	94.0	940
Ozone, $\mu g/m^3$	156.8	980.0
Temperature, C°	10	32.8
Relative humidity, %	50	90

exposure, it is more practical to perform fewer tests and not try to determine all the possible interaction effects.

The test conditions and the sequence for performing the factorial arrangement for studying the effects of the environmental variables on materials are shown in Table 11. Each of the tests (X_1 through X_{32}) will be conducted at a dew-light cycle of 20 min.

The first 16 tests (X_1 through X_{16}) involve studying the direct and interaction effects of the three pollutants and relative humidity at the high-temperature level. The selection of test conditions at the low temperature (X_{16} through X_{32}) will be based on the results of the first 16 tests. According to reaction kinetics, it is very unlikely that variables that are statistically insignificant at the high temperature will show significant interactions with temperature. Thus, the second half of the factorial arrangement (X_{16} through X_{32}) will be a selected fraction. The entire factorial arrangement of the experiment does not have to be completed in order to produce

TABLE 11—*Two-level factorial arrangement.*[a]

			HH		LH	
			HT	LT	HT	LT
L NO_2	L O_3	L SO_2	X_1	X_{17}	X_2	X_{18}
		H SO_2	X_3	X_{19}	X_4	X_{20}
	H O_3	L SO_2	X_5	X_{21}	X_6	X_{22}
		H SO_2	X_7	X_{23}	X_8	X_{24}
H NO_2	L O_3	L SO_2	X_9	X_{25}	X_{10}	X_{26}
		H SO_2	X_{11}	X_{27}	X_{12}	X_{28}
	H O_3	L SO_2	X_{13}	X_{29}	X_{14}	X_{30}
		H SO_2	X_{15}	X_{31}	X_{16}	X_{32}

[a] Low (L) and high (H) levels for the environmental variables are shown in Table 10.

the desired results. Field exposure of materials as well as continued laboratory investigations will be conducted based on the result obtained from this experiment.

Summary

An environmental exposure system consisting of five chambers has been assembled to conduct statistically designed experimentation to investigate the effects of environmental pollutants (SO_2, NO_2, and O_3) on materials. Control of the environmental variables (temperature, humidity, and pollutant concentrations), as well as chamber differences in lighting and pollutant distribution, was established to be below 10 percent variation for 95 percent of the measurements. Exposure of materials to a dew-light cycle was found to accelerate deterioration as compared with exposure in a constant humidity-temperature environment. To identify the significant effects that the interaction of pollutants and other environment variables have on materials, a two-level factorial arrangement was selected as the statistical experimental tool.

References

[*1*] Haynie, F. H. and Upham, J. B., *Materials Protection and Performance*, Vol. 10, Nov. 1971, pp. 18–21.
[*2*] Haynie, F. H. and Upham, J. B., *Materials Protection and Performance*, Vol. 9, Aug. 1970, pp. 35–40.
[*3*] Stickney, P. B., Mueller, W. J., and Spence, J. W., *Rubber Age*, Vol. 109, Sept. 1971, pp. 41–45.
[*4*] "A Study to Evaluate Techniques of Assessing Air Pollution Damage to Paints, Final Report," Sherwin-Williams Company, Contract No. 68-02-0030, May 1972.
[*5*] "Inquiry into the Economic Effects of Air Pollution on Electrical Contacts, Final Report," Stanford Research Institute, Contract No. Ph-22-68-35, April 1970.
[*6*] "Systems Analysis of the Effects of Air Pollution on Materials, Final Report," Midwest Research Institute," Contract No. CPA-22-69-113, Jan. 1970.
[*7*] Salvin, V. S., *Journal of the Air Pollution Control Association*, Vol. 13, 1963, pp. 416–422
[*8*] Ajax, R. L., Conlee, C. J., and Upham, J. B., *Journal of the Air Pollution Control Association*, Vol. 17, 1967, pp. 220–224.
[*9*] Beloin, N. J., *Textile Chemist and Colorist*, Vol. 4, No. 3, March 1972, pp. 77/43–82/48.
[*10*] "Stress Corrosion Testing Methods—Report of Task Group 1 on Stress Corrosion Testing Methods of Sub-Committee X on Stress Corrosion of Committee B-3 on Corrosion of Nonferrous Metals and Alloys," *Proceedings ASTM*, Vol. 65, 1965, pp. 182–197.
[*11*] Ostle, B., *Statistics in Research*, The Iowa State University Press, 1963.
[*12*] Finney, D. J., *An Introduction to the Theory of Experimental Design*, University Press, Chicago, 1960.
[*13*] Cox, D. R., *Planning of Experiments*, Wiley, New York, 1958.

R. N. Shuler[1] *and W. H. Ailor*[1]

Prediction of Environmental Pitting and Corrosion Rates

REFERENCE: Shuler, R. N. and Ailor, W. H., "**Prediction of Environmental Pitting and Corrosion Rates,**" *Corrosion in Natural Environments, ASTM STP 558*, American Society for Testing and Materials, 1974, pp. 292–305.

ABSTRACT: For nearly 15 years the environmental test results from long-term exposures have been handled by a computer program. Over 1¼-million bits of information representing data from more than 250 metals and alloys on test at fifteen atmospheric and two seawater locations are included in the program. Calculations are made reflecting aging changes, and changes due to the cleaning procedure and to corrosion. A printout then gives corrosion rates and mechanical property changes for each time period. Data points include 1, 2, 7, and 20 years for atmospheric specimens and 1, 2, 5, 10, and 20 years for seawater tests. Exposures of new alloys are made each year as phases of the continuing program along with appropriate removals of exposures from earlier series.

Since at least three data points are now on hand from some test metals, it is feasible to predict both corrosion rates and extreme pitting values for future removals. The corrosion rates and pitting data are subjected to curve fitting techniques through a computer operation. Several models were considered. However, based on earlier published studies on aluminum, we decided to begin with a least-squares fit of the cube-root pitting equation, $d = kt^{1/3}$. Future work with other models may indicate improved reliability.

It is now possible to predict the 20-year corrosion rate for a marine environment and to estimate the time to perforation for a given alloy system. Actual 20-year data, when available, will be compared with these predicted values. Also included in the program is the capability to predict 10-year results when shorter-term data (1, 2, and 5 years) are on hand.

KEY WORDS: corrosion, environmental tests, corrosion tests, seawater tests, atmospheric tests, pitting, predictions, corrosion rates, computer programs

The development of several long-term environmental test programs has been reported in the literature [*1–3*].[2] The test environments include both natural atmospheres [*1,3*] and seawater exposures [*6*]. Detailed results for exposure periods as long as seven years have been published, showing both corrosion rates and pitting depths [*5,6*].

Machine procedures for handling the derived data and making the computations have been discussed elsewhere [*2,4*]. These procedures

---

[1] Engineer-analyst and research scientist, respectively, Metallurgical Research Division, Reynolds Metals Company, Richmond, Va. 23218.

[2] The italic numbers in brackets refer to the list of references appended to this paper.

involve calculations based on panel weight losses and changes in tensile properties for test periods of 1, 2, and 7 years for atmospheric exposures and 1, 2, 5, and 10 years for seawater tests.

While these test periods involve relatively long exposures, there is a continuing need for data involving corrosion rates and pitting tendencies for at least 20 years. In most cases, practical considerations do not permit us to wait for the termination of such long-term tests, especially for developmental alloys.

Since three or more actual test points were available on curves representing environmental tests (1, 2, and 7 years or 1, 2, 5, 10 years) we planned to use statistical methods to predict the 20-year values. Earlier work by Aziz and Godard [*7,8*] had shown how extreme-value theory could be applied to the pitting corrosion of aluminum. Champion [*9*] had used statistical methods, including curve-fitting, for corrosion and tensile values derived from exposures of aluminum and other metals in a number of environments. An evaluation technique called Pitting Index is described by Pathak [*10*]. The Perforation Factor [*11*] was calculated from measured pits to indicate the danger of perforation by pitting.

We decided to use measured values of corrosion rates, tensile changes, and pitting depths for removal periods as long as ten years to predict these same values for periods of twenty years or more. In due course, these predicted values could be checked with actual values obtained at the time of the 20-year removals. For shorter-term verification the three seawater periods (1, 2, and 5 years) would be used to predict the 10-year results (already on hand for a number of aluminum alloys).

In this paper the statistical techniques used are described for three measures of corrosion tendency: loss of weight, changes in tensile properties, and depths of pitting.

Procedure

Triplicate 4 by 12-in. panels of each test alloy are exposed in two seawater locations for each of five test periods (1, 2, 5, 10, and 20 years). The two locations are tidal or half-tide immersion (Site "U"), and full immersion (Site "V") at Wrightsville Beach, North Carolina. At the end of each exposure period the appropriate panels (in triplicate unless one or more panels have been lost) are removed, cleaned by a standard technique, weighed, and the ten deepest pits on each side of a test panel measured [*6*]. Subsequently, tension specimens are cut from the panels and the ultimate tensile and yield strengths and percentage elongation are determined. All data, other than pitting depths, are entered into a computer program which tabulates corrosion rates as milligrams per square decimeter per day (MDD) and mils per year (mpy) and determines the changes in tensile properties as a result of any corrosion due to exposure [*2,4*].

The pitting depths have been recorded in the past but, until now, have not been entered into our computer program. Other studies have indicated that both corrosion rates and pitting depths for aluminum are likely to follow predictable patterns [*7–9*]. While these patterns are applicable to atmospheric as well as seawater exposures, we were persuaded to concern ourselves initially with only seawater results. Four data points were available (1, 2, 5, and 10-year evaluations). Three points could be used for curve fitting and the 10-year point projected on the basis of the resultant curve. This predicted value then could be compared with the actual 10-year evaluation of the panel. Using the four available data points (1, 2, 5, and 10 years) a corrected curve could then be used to predict the 20-year values.

A panel corrosion report printout (discussed in Ref *4*) has been expanded to show pitting data in addition to corrosion rates and tensile data. The display of this information is shown in Fig. 1. Maximum measured and average (of six deepest) pits are shown in the four columns to the right. The first pair of these columns shows values for one side of a 4 by 12-in. panel and the last two columns include data for the reverse side. This distinction is made to enable us to distinguish between skyward and groundward sides of atmospheric test panels—in the seawater tests reported in this paper the sides measured should not represent relevant differences.

Figure 1 further shows the 10-year corrosion rates and pitting depths as projected from the 1, 2, and 5-year data. Then the 20-year projection is obtained from use of the 1, 2, 5, and actual 10-year test results. As noted in the foregoing, the expressions "pits up" and "pits down" are used with seawater test results only to conform with atmospheric data in a later extension of the present program.

All projections represent data from triplicate test panels when all panels were available for evaluation.

The program also has the capability for storing information indicating other than the usual pitting mode of attack. These other corrosion forms include etching, intergranular attack, and delamination or exfoliation attack. If "no apparent attack" is found on a test panel, this information is entered into the program also.

In our discussion here, we shall use only the data involving actual measured pits since the depth of pitting is one of the corrosion criteria that could be most useful if it can be reliably predicted.

A computer program has been written which has the capability for fitting a least-square line between variables X (independent) and Y (dependent), assuming $y = f(x)$. We let X be the time (in months) to some fractional exponent and Y be a corrosion property: 1/MDD, 1/mpy, weight loss per unit area, pitting, or ultimate strength loss. Any of all variables may be selected for plotting. For this reason, and to enhance the usefulness of resulting scales, the reciprocals of MDD and mpy are plotted.

The program develops in this manner:

1. The assumption is made that initial values of Y and T are zero (that is, $Y_1 = 0$ at $T_1 = 0$).
2. Values for Y_i, $i =$ data points from 2 to 10, and $T_i^{1/N}$, $N = 3$, $i =$ data points from 2 to 4 are read from disk storage. The assumed N-value of 3 is consistent with the work of Aziz and Godard [*7,8*].
3. A regression curve is obtained in the form $Y = A + BX$. Assuming weight loss $= 0$ (that is, corrosion rate $= \infty$) at $t = 0$, use this point in the regression (weight loss $= 0$ for time $= 0 \rightarrow t_{ci}$, where t_{ci} is time required for corrosion initiation). The point (0,0) is included because it is known to be true for all data, whereas t_{ci} varies from alloy to alloy and from site to site. By *not* forcing solution through (0,0), A becomes a time value at which weight loss begins. The relationship $y = A + BT^{1/3}$ has been found to fit the data and is not necessarily a better relationship than others such as $Y = AT^n$, $Y = Ae^{nt}$, or $Y = A + BT^n$.
4. Y is calculated for t_5 (10-year values).
5. Values for Y at $X = 10$ years (t_5) are added to the data and a second curve is obtained.
6. Y is calculated for t_6 (20-year values).
7. A program option is exercised to obtain a computer plot of the curve.

The computer-produced graph contains

1. Actual data for 0, 1, 2, and 5 years.
2. Regressed curve for foregoing data.
3. Projected Y-value for 10 years.
4. Data for 10 years.
5. Regressed curve for all data, predicting Y-value for 20 years.

Results

Corrosion Rates

Computer-produced graphs (Figs. 2–5) show the corrosion rate curves for several aluminum alloys exposed for ten years in seawater. The vertical axes are representations of reciprocal values for corrosion rates (1/MDD, 1/mpy) or weight loss (mg/unit area). The horizontal scales show the exposure times as the cube-root values for the exposure periods (in months).

In Figs. 2–5 curves are plotted for both 1/MDD and weight loss/in.^{2}. The ideal fit is a straight-line graph and the projected point ideally should fall on or very close to the experimental curve. Ideally, too, the recomputed curve for four test periods should be congruent with the curve plotted for the first three time periods.

```
CORROSION TESTS
  MARINE   EXPOSURE
                           PANEL CORROSION REPORT
SPECIMAN    ALLOY WEIGHT YEARS    MDD    MPY   TENSILE      YIELD     ELONGATION            PITTING DATA
                   LOSS                       KPSI   0/0   KPSI   0/0    0/0    0/0 DEEPEST AVERAGE DEEPEST AVERAGE


  55A 00 5456H343                             57.1         40.6          11.7
  55A  1 5456H343 0.051                       57.3         40.7          12.0
  55U  1          0.698  0.8  0.344  0.186    57.7  -0.6   40.9  -0.4    11.7    2.5    3.8     2.8     5.0     3.6
  55U  2          0.719  0.8  0.354  0.191    56.6   1.2   39.7   2.4    12.5   -4.1    3.8     2.9     3.2     2.5
  55U  3          0.707  0.8  0.349  0.188    57.0   0.5   40.2   1.2    13.0   -8.3    3.2     2.1     5.5     3.2
  55A  4 5456H343 0.078                       57.1         40.3          12.3
  55U  4          0.675  1.8  0.153  0.082    58.2  -1.9   40.9  -1.4    12.5   -1.6    3.5     2.3     3.2     2.8
  55U  5          0.635  1.8  0.144  0.077    56.4   1.2   40.4  -0.2    13.0   -5.6    3.5     2.6     5.5     3.2
  55U  6          0.633  1.8  0.143  0.077    56.6   0.8   39.4   2.2    12.5   -1.6    2.0     1.6     2.5     2.0
  55A  7 5456H343 0.037                       57.6         40.6          11.5
  55U  7          1.012  4.7  0.087  0.047    57.7  -0.1   40.8  -0.4    12.5   -8.6   14.0    11.5     0.0     0.0
  55U  8          0.954  4.7  0.082  0.044    57.2   0.6   40.9  -0.7    11.5    0.0   20.0    10.3     0.0     0.0
  55U  9          1.002  4.7  0.086  0.046    57.2   0.6   40.4   0.4    12.7  -10.4   18.0    12.5     0.0     0.0
10 YR PROJECTION

                1/MDD           A               B             R
                 14.2778       -2.5995           3.4217         0.9305
                1/MPY           A               B             R
                 26.4294       -4.8119           6.3339         0.9305
                MG/IN           A               B             R
                 12.0043        0.7826           2.2750         0.9470

               PITS DOWN        A               B             R

                  1.5557        3.5591          -0.4061        -0.1991
  55A 10 5456H343 0.024                       57.4         40.4          12.5

  55U 10          1.611  9.8  0.067  0.036    57.8  -0.6   40.2   0.4    11.5    8.0   11.5    10.2    15.5     9.7
  55U 11          1.565  9.8  0.065  0.035    57.9  -0.8   40.2   0.4    11.5    6.0   16.0    13.1    10.5     9.4
  55U 12          1.525  9.8  0.063  0.034    58.0  -1.0   40.4   0.0    11.5    8.0   14.5    10.5    12.0     8.4
20 YR PROJECTION


                1/MDD           A               B             R
                 19.6221       -3.1311           3.6613         0.9645
                1/MPY           A               B             R
                 36.3220       -5.7959           6.7773         0.9645
                MG/IN           A               B             R
                 17.9455       -0.6772           2.9966         0.9603
               PITS DOWN        A               B             R
                 12.1455       -1.6266           2.2161         0.6449
  55A  1 5456H343 0.051                       57.3         40.7          12.0
  55V  1          1.459  0.8  0.720  0.389    56.7   1.0   39.9   1.9    12.7   -5.8    5.5     4.1     7.0     4.9
  55V  2          1.371  0.8  0.676  0.365    56.8   0.8   40.2   1.2    12.0    0.0    5.2     4.3     6.0     5.0
  55V  3          1.359  0.8  0.671  0.362    56.8   0.8   40.2   1.2    12.5   -4.1    5.8     4.9     7.5     5.0
```

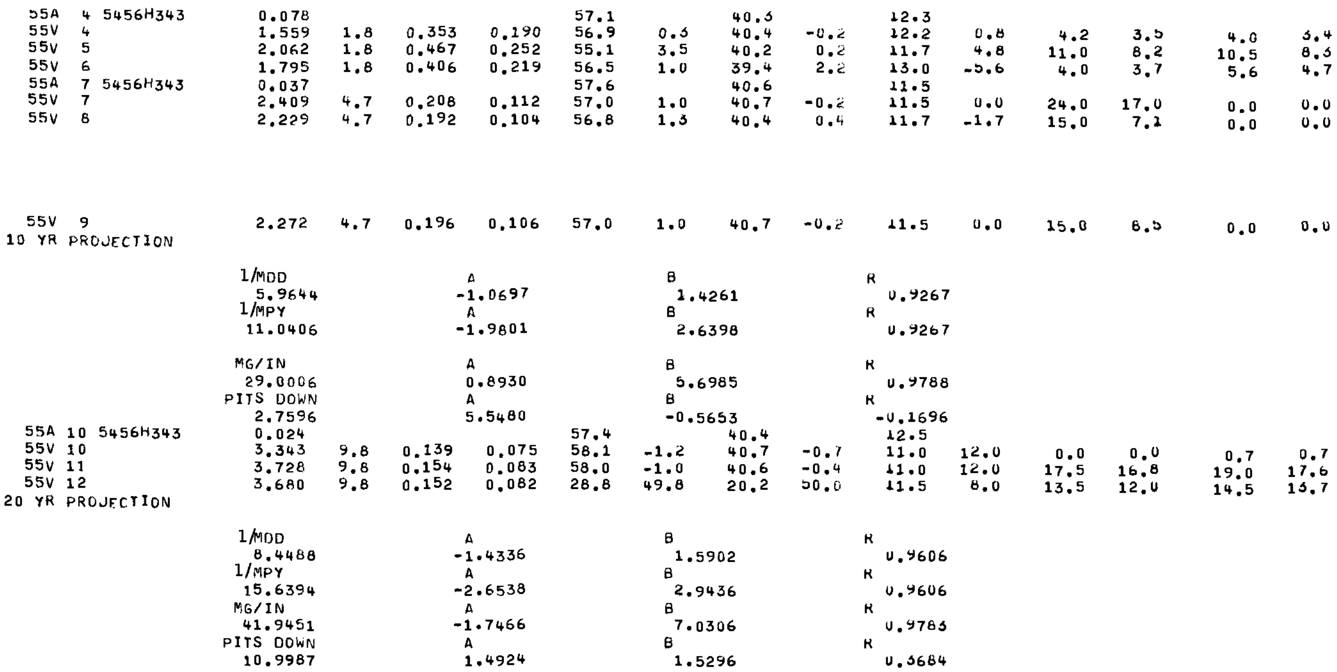

```
55A   4 5456H343     0.078                          57.1          40.3         12.3
55V   4              1.559   1.8   0.353   0.190   56.9   0.3    40.4  -0.2   12.2   0.8    4.2   3.5    4.0   3.4
55V   5              2.062   1.8   0.467   0.252   55.1   3.5    40.2   0.2   11.7   4.8   11.0   8.2   10.5   8.3
55V   6              1.795   1.8   0.406   0.219   56.5   1.0    39.4   2.2   13.0  -5.6    4.0   3.7    5.6   4.7
55A   7 5456H343     0.037                          57.6          40.6         11.5
55V   7              2.409   4.7   0.208   0.112   57.0   1.0    40.7  -0.2   11.5   0.0   24.0  17.0    0.0   0.0
55V   8              2.229   4.7   0.192   0.104   56.8   1.3    40.4   0.4   11.7  -1.7   15.0   7.1    0.0   0.0



 55V  9              2.272   4.7   0.196   0.106   57.0   1.0    40.7  -0.2   11.5   0.0   15.0   6.5    0.0   0.0
10 YR PROJECTION

                    1/MDD             A                   B                  R
                     5.9644          -1.0697               1.4261              0.9267
                    1/MPY             A                   B                  R
                     11.0406         -1.9801               2.6398              0.9267

                    MG/IN             A                   B                  R
                     29.0006          0.8930               5.6985              0.9788
                   PITS DOWN          A                   B                  R
                      2.7596          5.5480              -0.5653             -0.1696
 55A 10 5456H343      0.024                         57.4          40.4         12.5
 55V 10               3.343  9.8   0.139   0.075   58.1  -1.2    40.7  -0.7   11.0  12.0    0.0   0.0    0.7   0.7
 55V 11               3.728  9.8   0.154   0.083   58.0  -1.0    40.6  -0.4   11.0  12.0   17.5  16.8   19.0  17.6
 55V 12               3.680  9.8   0.152   0.082   28.8  49.8    20.2  50.0   11.5   8.0   13.5  12.0   14.5  13.7
20 YR PROJECTION

                    1/MDD             A                   B                  R
                      8.4488         -1.4336               1.5902              0.9606
                    1/MPY             A                   B                  R
                     15.6394         -2.6538               2.9436              0.9606
                    MG/IN             A                   B                  R
                     41.9451         -1.7466               7.0306              0.9783
                   PITS DOWN          A                   B                  R
                     10.9987          1.4924               1.5296              0.3684
```

FIG. 1—*Computer printout showing corrosion rates (MDD and mpy), changes in mechanical properties, pitting data, and 10-year and 20-year projections. Predicted values are shown in rows having coefficients A and B, and factor R. A good curve-fit is indicated by a high R-factor (close to 1.0).*

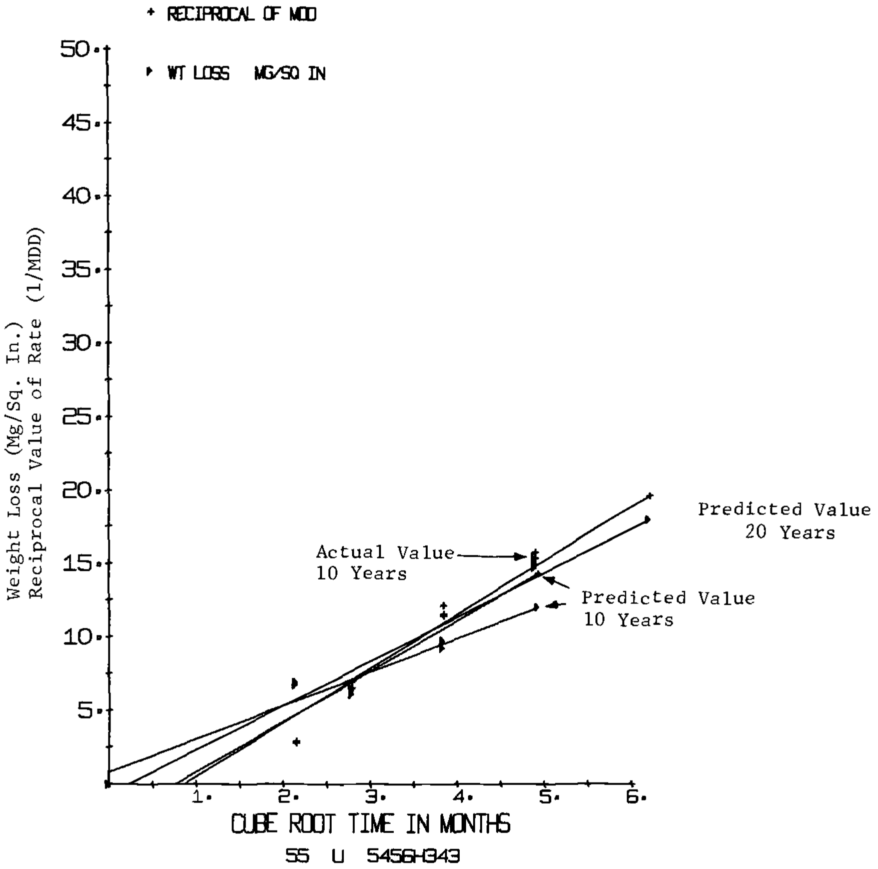

FIG. 2U—*Projected and actual corrosion rate values for 5456-H343 alloy in tidal seawater.*

Graphical representations in Figs. 2–5 are coded "V" for full-immersion test panels and "U" for tidal test panels. It has been noted that test results were generally more reliable for these full-immersion studies than were the results from the half-tide data, based on the coefficient of correlation *R*.

The predicted and actual 10-year values for the reciprocals of corrosion rates and weight losses can be seen in Figs. 2 (5456-H343), Fig. 3 (5086-0), and Fig. 4 (5454-H32). Figure 2U shows nearly ideal predictive results inasmuch as the 10-year predicted and actual values are very close. Figures 3V and 4 illustrate cases when the actual rates and predicted rates are not as close to each other.

As noted earlier, the values obtained for half-tide immersions were not as consistently reliable for predictive purposes. "V" figures show the wider scattering of data as compared with the same alloy in tidal immersion (U figures) in Figs. 2–4.

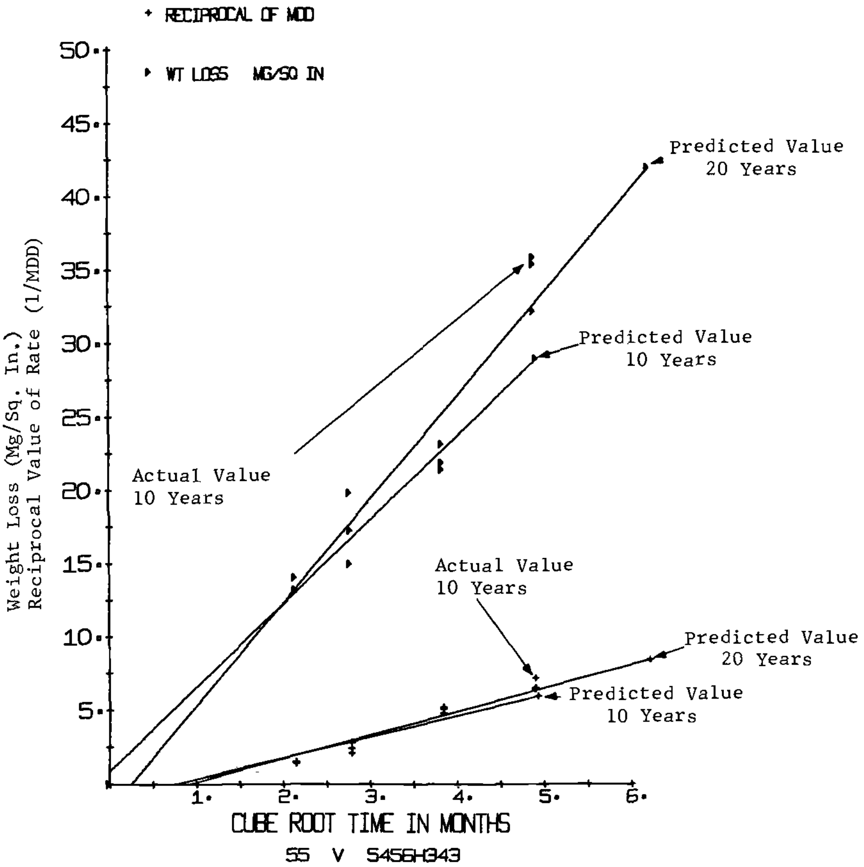

FIG. 2V—*Projected and actual corrosion rate values for 5456-H343 alloy totally immersed in seawater.*

Pitting Depths

Plots for both the MDD rate curve and the maximum measured pit are shown in Fig. 5V for 5454-H32 alloy after total immersion. Here both predicted values are very close to the measured values.

The prediction of pitting depths has been found to be more inconsistent than the projections based on corrosion rates. This difficulty derives from the randomness of pitting and the difficulty frequently encountered in measuring pitting depths. However, projected values enabled us to anticipate the order of magnitude for pitting after ten years.

Tensile Properties

The changes in tensile properties for aluminum alloys (aluminum-magnesium type) exposed to seawater have not shown significant changes over a 10-year period. For this reason no readily predictable losses are

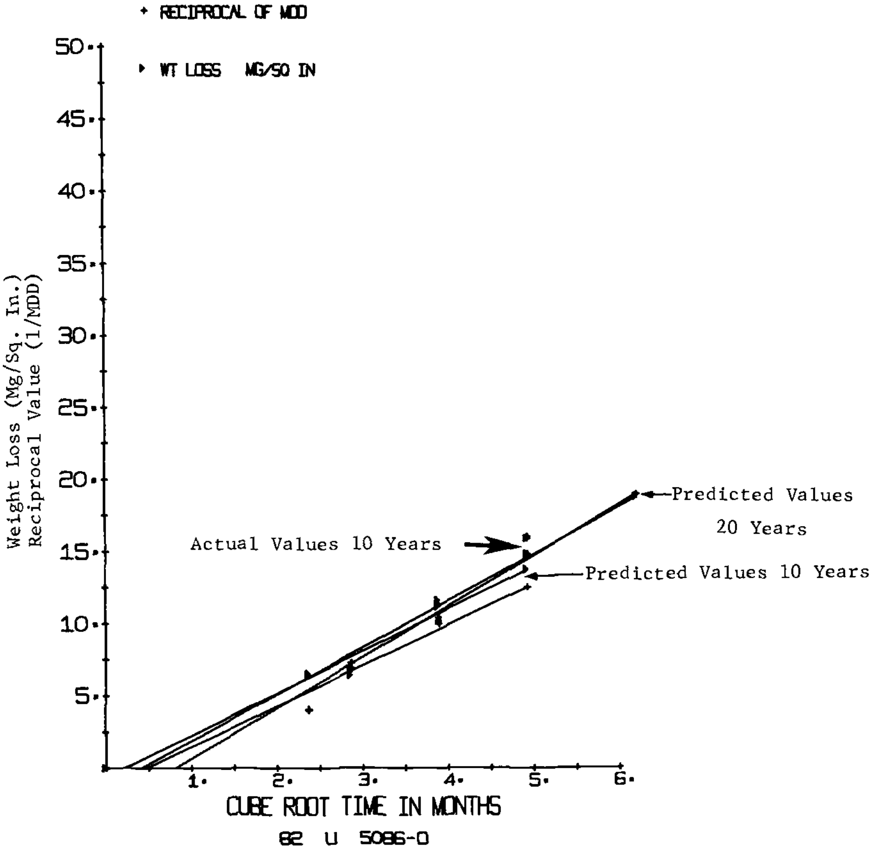

FIG. 3U—*Actual and predicted corrosion rate values for 5086-0 alloy in tidal seawater.*

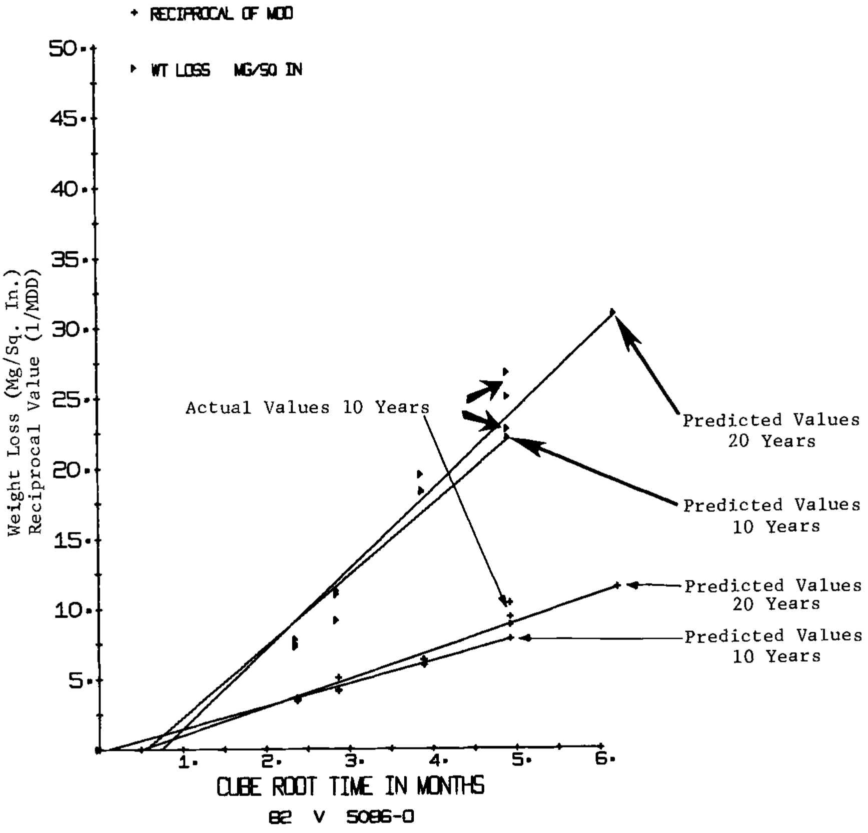

FIG. 3V—*Actual and predicted corrosion rate values for 5086-0 alloy immersed in seawater.*

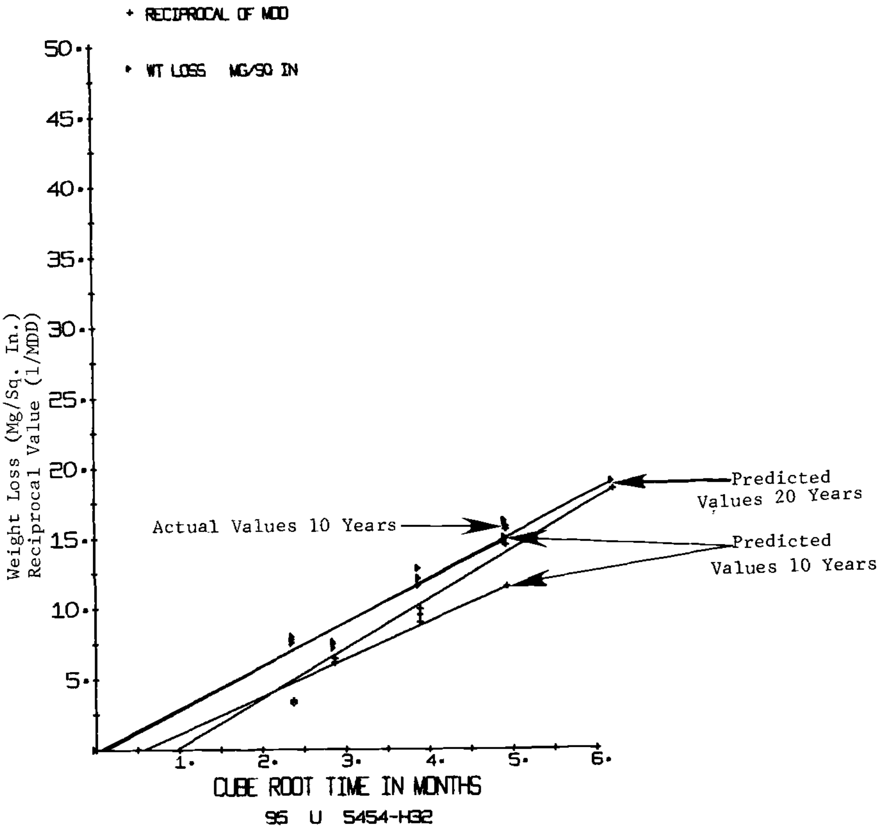

FIG. 4U—*Actual and predicted corrosion rate values for 5454-H32 alloy in tidal seawater.*

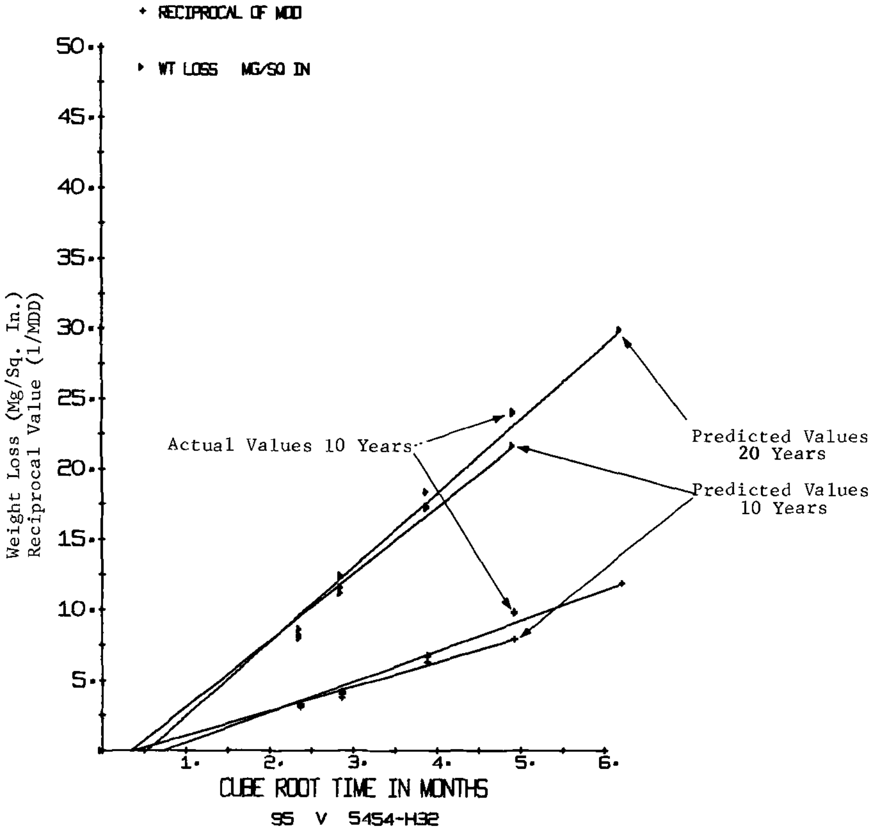

FIG. 4V—*Actual and predicted corrosion rate values for 5454-H32 alloy immersed in seawater.*

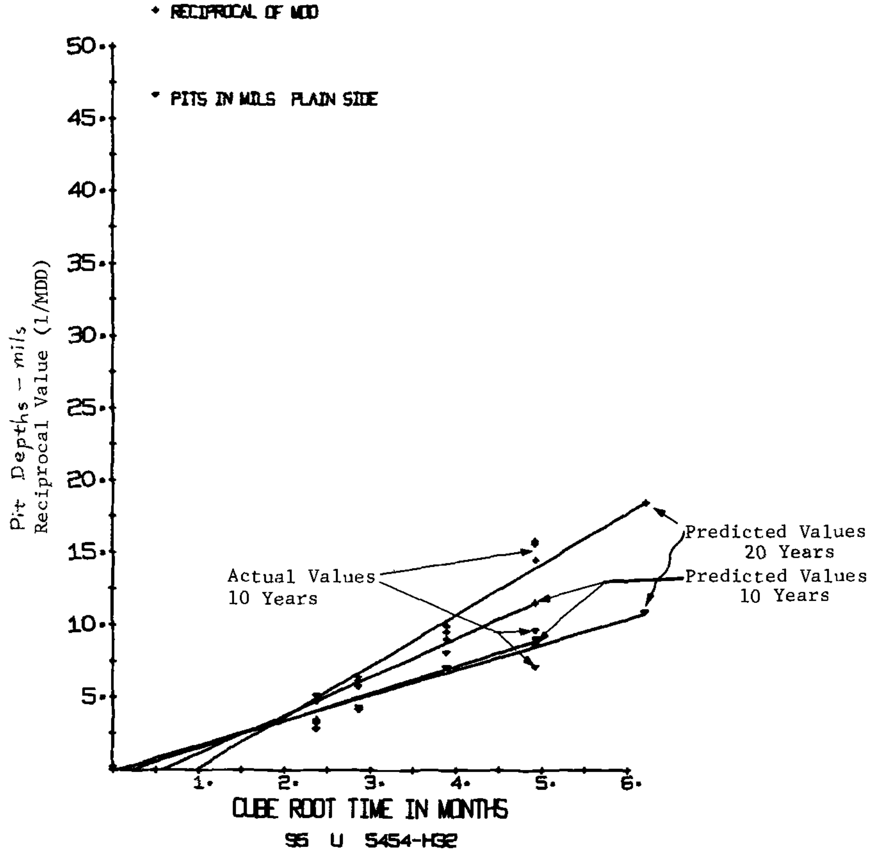

FIG. 5V—*Actual and predicted corrosion rate values for 5454-H32 alloy in tidal seawater.*

anticipated for longer exposures. Alloys of the aluminum-copper (2000 series) and aluminum-zinc-magnesium (7000 series) types do show property losses. However, these losses are often a result of intergranular attack and lamellar or exfoliative attack, making their measurement difficult and often meaningless.

General Comments

The work discussed here includes data from only aluminum alloys in the marine testing program. We plan to test these methods for other metal systems including zinc, iron and steels, and titanium.

Conclusions

The results from data obtained by corrosion rate and pitting analyses lead to the following conclusions for seawater immersion of aluminum alloys (aluminum-magnesium series):

1. The prediction of full-immersion corrosion rates (MDD and mpy) and pitting depths can be more reliably projected than these same factors in tidal immersion.
2. Generally, corrosion-rate predictions are more reliable than pitting-depth projections.
3. In seawater, the corrosion-rate curves tend to follow the equation $y = A + BT^{1/3}$ (that is, a cube root of time relationship).
4. Because of certain inherent difficulties associated with the determination of pitting depths, it appears unlikely that pitting depths can reliably be predicted for aluminum in seawater.

Acknowledgments

The authors thank the Reynolds Data Processing Operations Department and especially F. M. Wheeler for continued support for many years with our work. Also, we thank the management of the Metallurgical Research Division for encouraging the work herein described and for permitting the publication of this material.

References

[*1*] "Atmospheric Exposure of Nonferrous Metals and Alloys," *ASTM Proceedings*, Vol. 59, 1959; Vol. 61, 1961; Vol. 62, 1962; and Vol. 66, 1966.

[*2*] Ailor, W. H. and Hodgson, M. R., "Punch-Card Handling of Atmospheric Test Data," *ASTM Bulletin*, Dec. 1960.

[*3*] Ailor, W. H., "World-Wide Atmospheric Test Program," *Corrosion Technology*, Nov. 1965.

[*4*] Spatig, D. O. and Ailor, W. H., *Metal Corrosion in the Atmosphere*, *ASTM STP 435*, American Society for Testing and Materials, 1968, pp. 43–60.

[*5*] McGeary, F. L., Summerson, T. J., and Ailor, W. H., *Metal Corrosion in the Atmosphere*, *ASTM STP 435*, American Society for Testing and Materials, 1968, pp. 141–174.

[*6*] Ailor, W. H., *Materials Performance and the Deep Sea*, *ASTM STP 445*, American Society for Testing and Materials, 1969, pp. 115–130.

[*7*] Godard, H. P., "Corrosion Behaviour of Aluminum in Natural Waters," *Canadian Journal of Chemical Engineering*, Oct. 1960.

[*8*] Aziz, P. M. and Godard, H. P., *Corrosion*, Vol. 10, Sept. 1954, pp. 269–272.

[*9*] Champion, F. A., *Corrosion Testing Procedures*, Wiley, New York, 1952.

[*10*] *Handbook on Corrosion Testing and Evaluation*, W. H. Ailor, Ed., Wiley, New York, Chapter 20, 1971.

[*11*] "Aluminum in the Chemical and Food Industries," The British Aluminium Co., Ltd., 1959.

B. W. Lifka[1] *and D. O. Sprowls*[1]

Relationship of Accelerated Test Methods for Exfoliation Resistance in 7XXX Series Aluminum Alloys with Exposure to a Seacoast Atmosphere

---

REFERENCE: Lifka, B. W. and Sprowls, D. O., "**Relationship of Accelerated Test Methods for Exfoliation Resistance in 7XXX Series Aluminum Alloys with Exposure to a Seacoast Atmosphere,**" *Corrosion in Natural Environments, ASTM STP 558*, American Society for Testing and Materials, 1974, pp. 306–333.

ABSTRACT: Accelerated corrosion tests are necessary and an invaluable aid to research and quality control engineers, provided that the test has adequate discriminatory ability and the test results relate to serviceability of the metal. An inherent problem associated with accelerated exfoliation tests is the definition of different degrees of susceptibility and the interpretation of borderline performances. The concern in the present instance is that truly insignificant exfoliation tendencies may be magnified out of proportion by the very rapid exfoliation tests now being used in materials specifications for exfoliation resistant 7XXX-T7 alloy products.

Correlation of accelerated tests with service environments or the equivalent is necessary, and it is highly desirable that the range of performances observed in the accelerated test be related to a similar range of performances under service conditions. This paper contains the results of relatively long exposures of test panels to the salt atmosphere at a location about 100 yd from a stony beach at Point Judith, Rhode Island, where the corrosive conditions are representative of other very corrosive environments. These extended exposures are of particular interest because they furnish a basis of evaluating indications of borderline susceptibility to exfoliation revealed in the accelerated corrosion tests.

Four- to eight-year exposures to this aggressive seacoast atmosphere have demonstrated the excellent resistance to exfoliation of 7075-T73 and T76 and 7178-T76 products, whereas exfoliation susceptible T6 temper materials displayed considerable exfoliation after short exposures, sometimes after only three to six months. Both the EXCO immersion test (ASTM G 34-72) and the salt spray test (modified ASTM acetic acid salt intermittent spray) developed the same basic type of corrosion that occurred in the seacoast atmosphere. It was shown, however, that the accelerated tests, especially the spray test, tend to magnify slight indications of susceptibility to exfoliation that are of doubtful practical consequence. Suggestions are made for determining more realistic visual acceptance criteria in 7XXX-T7X materials specifications.

KEY WORDS: corrosion, exfoliation corrosion, marine environments, accelerated corrosion tests, correlation, exfoliation resistant tempers, aluminum alloys, zinc alloys, magnesium alloys, copper alloys

---

[1] Senior research engineer and section head, respectively, Chemical Metallurgy Division, Alcoa Laboratories, Alcoa Center, Pa. 15069.

Accelerated corrosion tests are a necessary tool for research and quality control engineers. The validity of accelerated tests depends upon their relationship to anticipated service and their sensitivity to varying degrees of the particular form of corrosion being investigated. The test must be discriminatory and yet not so drastic as to be unrealistic.

For the majority of engineered structures, except when subjected to certain highly specific chemical environments, exposure to outdoor atmosphere provides a baseline that is representative of service conditions. Unfortunately, long exposures are usually required and the corrosiveness of the atmosphere at specific test sites can vary widely depending on marine and industrial influences [*1*,*2*].[2] Experience has shown that seacoast conditions tend to be more corrosive than do the conditions at inland urban and industrial locations [*3*]. Usually the most corrosive conditions exist where there is a combination of seacoast and industrial effects, while the mildest conditions are found in rural areas.

The purpose of this paper is to report the resistance to exfoliation after four or more years' exposure to seacoast atmosphere of 7075-T73, T76, and 7178-T76 materials that have also been evaluated with the accelerated tests stipulated in material specifications for T76 temper products. These results provide a useful supplement to the Interim Report of the AA-ASTM G01.05.02 Task Group on Exfoliation Corrosion Testing of Aluminum Alloys, also presented in this symposium [*4*], and to other recent papers on improved exfoliation tests [*3*,*5*].

Alcoa Seacoast Weathering Station at Point Judith, Rhode Island

The seacoast atmosphere test site used for this study is the Alcoa station at Point Judith, Rhode Island. This site is at the tip of a small peninsula, in a sparsely populated area with little industrial influences, at the entrance to Narragansett Bay, about 30 miles due south of Providence (Fig. 1). The exposure racks face south, inclined at an angle of 45 deg from vertical and are located about 300 ft from the ocean (Fig.2). Prevailing winds are from the sea, usually from the southwest, with an average velocity of 17 mph. The shore area is stony and the sea is often rough so that generally there is considerable salt mist in the air. Thus, the combined wind-wave action results in the specimens coming in direct contact with salt spray and salt-laden fog—conditions particularly conducive to development of exfoliation corrosion in aluminum base alloys. Other average weather conditions at the Point Judith site are given in Table 1 [*6*].

Dix and Mears have shown [*1*] that the corrosivity at a particular location is influenced more by environmental factors such as proximity to the ocean, type of beach, local topography, possible industrial pollution, and the direction of prevailing winds, than by the particular geographic

---

[2] The italic numbers in brackets refer to the list of references appended to this paper.

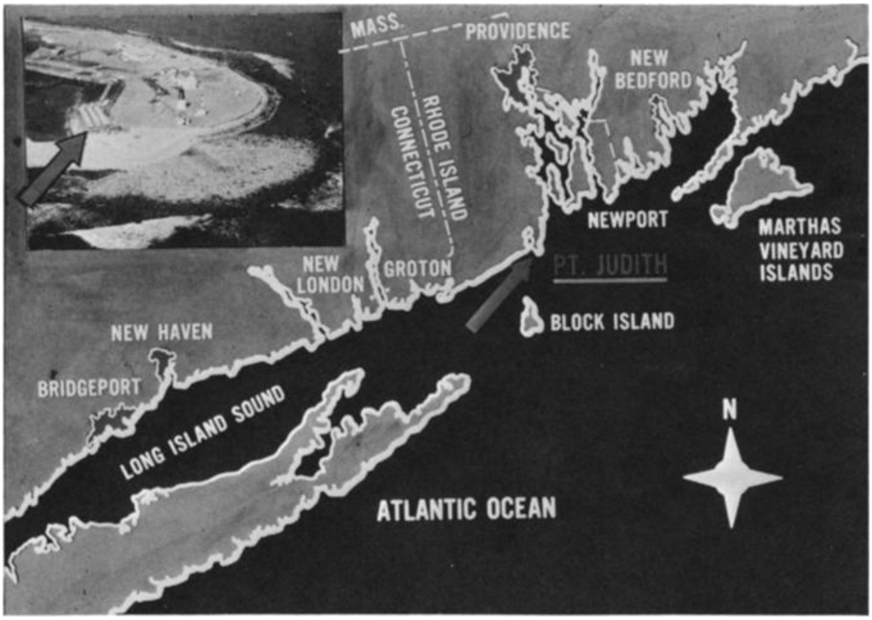

FIG. 1—*Location of the Point Judith, Rhode Island exposure site* (insert) *on the Atlantic seacoast at the entrance to Narragansett Bay, 30 miles due south of Providence, Rhode Island. Arrow indicates test site and direction of prevailing wind.*

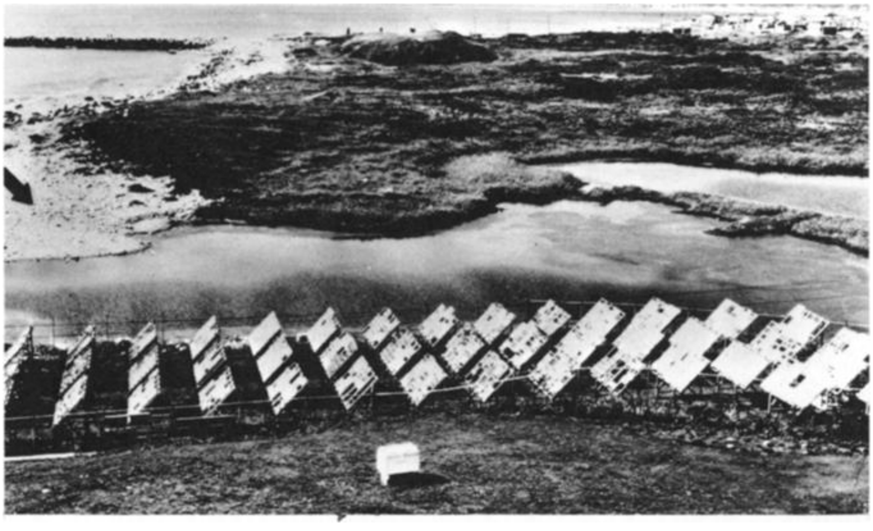

FIG. 2—*Close-up of the Point Judith station showing test racks inclinded at a 45-deg angle and the proximity of the racks to the beach. Arrow indicates direction of the prevailing wind from the sea.*

TABLE 1—*Average weather conditions at two basic Alcoa weathering test stations compared with some other cities.*

	Mean Temperature, °F		Rainfall		Avg. Relative Humidity		Record Temperature	
	Jan.	July	in./year	days/year	a.m.	p.m.	High	Low
New Kensington, Pa.[a] (Pittsburgh)	31 (−1°C)	75 (24°C)	36	150	77	65	103 (39°C)	−20 (−29°C)
Point Judith, R. I.[b] (Block Island)	29 (−2°C)	72 (22°C)	41	125	79	67	91 (32°C)	−4 (−20°C)
Boston	30 (−2°C)	72 (22°C)	39	125	73	61	104 (40°C)	−18 (−28°C)
Chicago	26 (−3°C)	74 (23°C)	32	124	78	69	104 (40°C)	−15 (−26°C)
Houston	54 (12°C)	83 (28°C)	45	99	86	59	105 (40°C)	10 (−12°C)
Los Angeles	54 (12°C)	71 (21°C)	15	37	77	51	110 (43°C)	28 (−2°C)
Miami	68 (20°C)	82 (28°C)	59	135	78	74	98 (37°C)	32 (0°C)
New York City	32 (0°C)	74 (23°C)	42	127	74	67	102 (39°C)	−14 (26°C)

[a] During winter months, about a fourth of the precipitation occurs as snow and there is a 50 percent chance of measurable precipitation on any day. Seven months of the year, April through October, have sunshine more than 50 percent of the time. During the remaining five months, cloudiness is heavier. There is frequent early morning fog, particularly along the Allegheny River valley. The Alcoa test station is on the roof of the Alcoa Research Laboratories where chemical hood exhausts aggravate the industrial character of the atmosphere. Specimens are exposed facing south, at a 45-deg angle.

[b] Summers are usually dry but the highest rainfall in any one month (12.93 in.) fell in June 1881. The record low amount (trace) was in June also, 1949 and 1957. Fog occurs on one out of four days in early summer. Winters are distinguished for their comparative mildness, with maxima averaging 4° to 10° above freezing and minima averaging 25° in February. Surface winds are usually from the southwest. The wind velocity averages 17 mph for the year (20 mph in winter, with 40 mph during gales). This area is frequently affected by tropical storms moving up the coast, in the early fall. The Alcoa test site is in a sparsely populated area, about 300 ft from and facing the Atlantic Ocean to the south.

TABLE 2—*Description of various seacoast exposure stations.*

Location	Climatic Zone	Distance From Ocean or Bay	Type of Shore	Direction of Prevailing Winds	Remarks	Station Operated by
Kure Beach, N. C.	temperate	80 ft	sandy	from ocean	sea rough, considerable salt mist	International Nickel Co.
La Jolla, Calif.	temperate	"several hundred feet"	rocky	from ocean	sea rough, frequent fogs, little rain to wash specimens	ASTM
Point Judith, R. I.	temperate	300 ft	stony	from ocean	sea rough, considerable salt mist and fogs	Alcoa
Miami Beach, Fla.	subtropical	300 ft	sandy	from ocean	warm, humid without fogs	South Florida Test Service
Sandy Hook, N. J.	temperate	300 ft	sandy	from bay	station at tip of hook jutting into bay	ASTM
Georgetown, British Guiana	tropical	1.5 miles	. . .	from ocean	on low building by Demerara River; hot, humid.	Alcoa
Key West, Fla.	subtropical	"close to ocean"	sandy	across island	station on leeward side of island.	ASTM

location. It is necessary, therefore, to establish the severity of the conditions at a particular atmospheric test site before data obtained there can be meaningfully evaluated. The weathering characteristics at the Point Judith station have been evaluated by comparing the effects noted on 1100 and 3003 aluminum alloys, annealed copper, and mild steel with results obtained at various other seacoast stations [*1,2,6,7*]. Seven test sites that were compared are listed in Table 2, and examples of the results are given in Fig. 3. The corrosivity at Point Judith is quite severe, approaching that of the former ASTM site at La Jolla, California—La Jolla most likely being more severe because of the warmer winter temperatures, less rainfall, and the rocky cliff shoreline that results in more salt spray (compare weather conditions for Point Judith and Los Angeles areas in Table 1). Although these comparative tests were conducted many years ago, the immediate area of the Point Judith station is sparsely populated and the

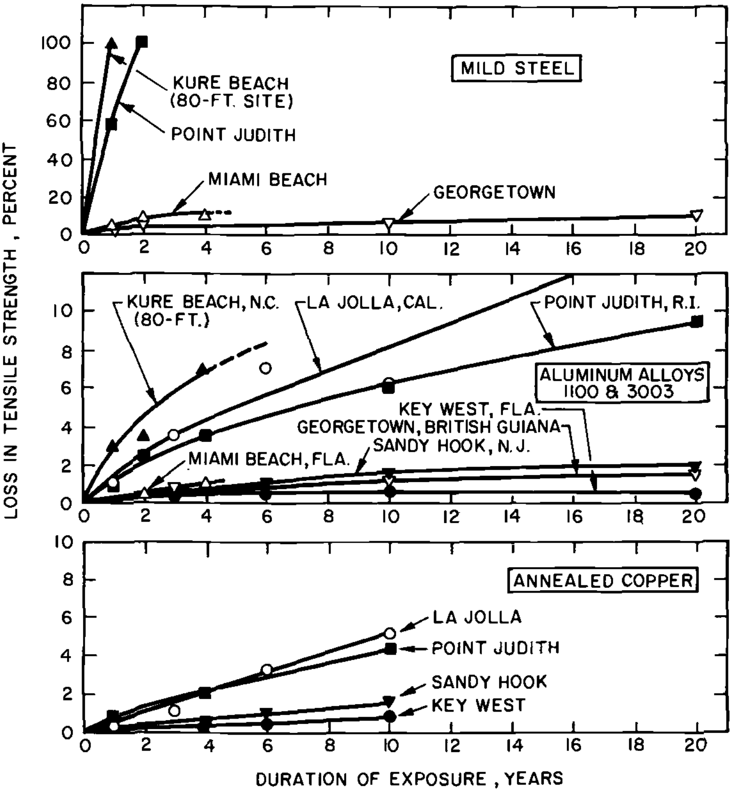

FIG. 3—*Graphs comparing severity of Point Judith test site with several other seacoast stations, using loss in tensile strength of premachined 0.064-in. sheet specimens or of 0.035-in. sheet specimens converted to an equivalent loss for 0.064 in. thickness. Point Judith is somewhat milder than Kure Beach, about the same as the ASTM site at La Jolla, and more severe than the remaining sites.*

adjacent land use has been virtually unaltered during the ensuing years. As a result of this and the fact that prevailing winds are from the sea, the atmospheric effects have not changed notably since the inception of the test station. This is fortunate in that data obtained over the years at the Point Judith station can be used with confidence to predict the performance of aluminum alloys in most seacoast environments.

Experience gained from over 40 years of testing a wide variety of aluminum alloys and products at Point Judith has shown that 2XXX and 7XXX aluminum alloy products with appreciable susceptibility to exfoliation will show evidence of this form of corrosive attack within a year. Often the initial signs of exfoliation are seen after an exposure as brief as three to six months and the attack will be quite severe after one to two years' exposure. The general experience has been that items that do not show appreciable exfoliation within two years will not exfoliate to any major degree with continued exposure. Consequently, freedom from exfoliation after four or more years is convincing evidence of high resistance to this form of corrosion. This paper is based on the premise that four years' exposure at Point Judith may be regarded as sufficient exposure to reliably predict service performance of aluminum alloys in aircraft structures, which is the principal use of T76 temper products.

Performance of Commercial Products in the Seacoast Atmosphere

Test Materials and Procedure

In developing the exfoliation-resistant T76 and T73 tempers for copper-containing aluminum 7XXX alloys, it was necessary to conduct many accelerated exfoliation tests on a number of materials given various precipitation heat treatments. Corroborative exfoliation tests in a seacoast atmosphere were then performed on samples from production runs of various 7075 and 7178 alloy products. This paper deals with the results obtained with both the outdoor and accelerated tests of such materials. The chemical composition of alloys 7075 and 7178, along with typical heat treatments for commercial tempers of sheet, plate, and extrusions, is listed in Table 3.

The tendency for exfoliation corrosion is most pronounced in fabricated products that have a highly directional grain structure in which the shape of the grain is elongated and relatively thin compared with its width. Exfoliation tests in the seacoast atmosphere were concentrated on products most likely to contain this type of grain structure; namely, intermediate section thicknesses of about 0.1 to 1.0 in. thick, along with a width-to-thickness ratio of 10 or greater. The directional grain structure observed in rolled products such as sheet and plate (Fig. 4) occurs primarily as a result of ingot reduction and tends to be uniform throughout the length and width. For extruded and forged shapes, the directionality of the grain structure may vary throughout the cross section, as shown in Fig. 5, as

TABLE 3—*Principal aluminum alloys evaluated.*

Part A—Chemical Composition Limits[a]

AA Designation	Si	Fe	Cu	Mn	Mg	Cr	Zn	Ti	Others	
									Each	Total
7075	0.40	0.50	1.2–2.0	0.30	2.1–2.9	0.18–0.35	5.1–6.1	0.20	0.05	0.15
7178	0.40	0.50	1.6–2.4	0.30	2.4–3.1	0.18–0.35	6.3–7.3	0.20	0.05	0.15

Part B—Typical Heat Treatments[a]

		Solution Heat Treatment		Precipitation Heat Treatment			
		Metal Temperature				Metal Temperature	
Alloy	Product	°F	°C	Temper Designation	Time at Temperature, h	°F	°C
7075	Sheet	900	482	T6	24	250	121
				T76	3+	250	121
					15–18	325	163
				T73	6+	225	107
					24–30	325	163
	Plate	900	482	T651	24	250	121
				T7651	3+	250	121
					15–18	325	163
				T7351	6+	225	107
					24–30	325	163
	Extrusions	870	466	T6510	24	250	121
				T76510	3+	225	121
					18–21	320	160
				T73510	6+	225	107
					6–8	350	177
7178	Sheet	875	468	T6	24	250	121
				T76	3+	250	121
					15–18	325	163
	Plate	875	468	T651	24	250	121
				T7651	3+	250	121
					15–18	325	163
	Extrusions	870	466	T6510	24	250	121
				T76510	3+	250	121
					18–21	320	160

[a] Aluminum Standards and Data, 1972–73 Edition, The Aluminum Association.

well as for different thicknesses. Therefore, test panels were always machined from locations in the product having the most directional grain structure.

Susceptibility to exfoliation of 7075-T6 and 7178-T6 alloy products is also dependent on the cooling rate during quenching from the solution heat-treat temperature, a slow cooling rate being adverse. A natural

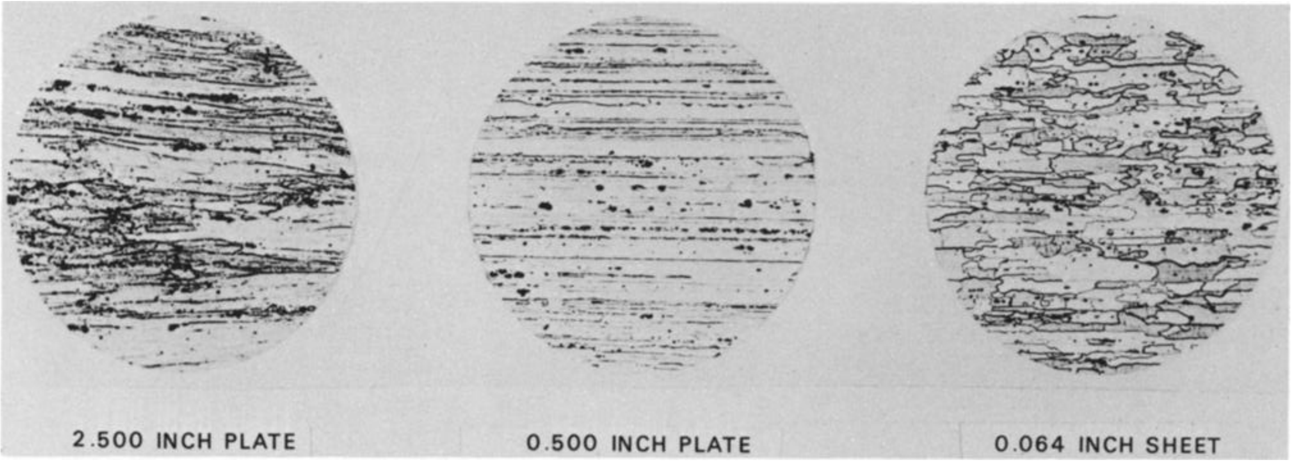

FIG. 4—*Photomicrographs (×70, Keller's etch) of longitudinal slices taken at the midplane of three thicknesses of 7075-T651 sheet and plate. The increased directionality of the grain structure observed with decreasing plate thickness results from increased reduction of the ingot. This in turn results in increased susceptibility to exfoliation. With further reduction to thin sheet gages, recrystallization reduces the directionality and the susceptibility to exfoliation. Improved resistance to exfoliation of thin sheet also is favored by a more rapid cooling rate during quenching after solution heat treatment. (The rolling direction is horizontal and the thickness direction vertical.)*

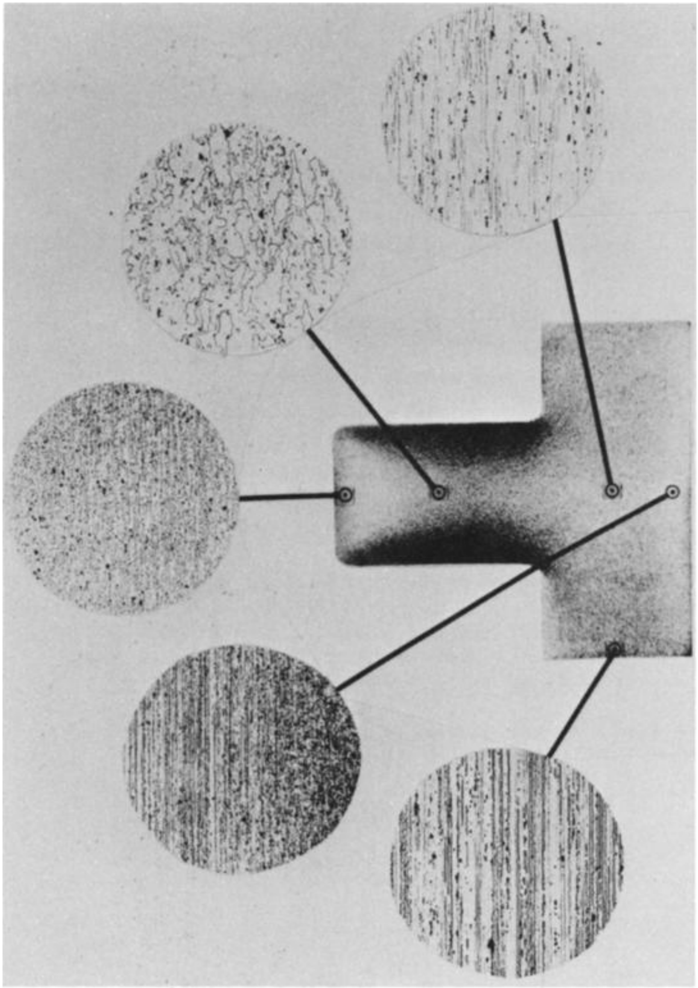

FIG. 5—*Transverse sections from a 17-in.-wide extrusion with outstanding ribs showing examples of the various microstructures present (macrosection ×1, photomicrographs ×50, Keller's etch).*

gradation in quench cooling rate exists through the thickness in all but very thin products. Thus the tendency for exfoliation is greater at subsurface locations exposed by machining. Test panels were machined from several depths in the products to evaluate possible effects of differences in grain structure and quench cooling rate.

Panel specimens exposed at Point Judith were mounted so that the test surface faced skyward. An open framework was used so that the earthward surface was also freely exposed, although not facing the ocean. Exfoliation sometimes occurs slightly faster on the earthward surface because of less washing by rainfall, but the corrosive conditions can be less uniform on the earthward surface.

Results of Prolonged Exposure to Seacoast Atmosphere

A summary of the various T76 and T73 temper materials exposed to seacoast atmosphere with accumulated periods of two or more years is given in Table 4. These panels were examined on site at least twice a year and were returned to the laboratory for evaluation after 1, 2, 4, and 8 years of exposure. Thus far, not the slightest evidence of exfoliation has been detected on any T73 temper panel, even after the prolonged exposure of 11 years, as shown in Fig. 6. Likewise, for the T76 temper materials, no exfoliation has been noted on panels representative of the surface or near-surface planes, down to and including the T/10 plane. The longest-term T76 specimen is shown after eight years of exposure in Fig. 6. Slight exfoliation occurred on certain T76 midplane (T/2) panels but this was

TABLE 4—*Summary of 7075 and 7178 alloy products in T73 and T76 tempers that are being tested at the Point Judith, Rhode Island seacoast test site for resistance to exfoliation corrosion.*

Product	Alloy	Temper	No. of Lots	Gages Tested, in.	Years in Test
Sheet	7075	T73	1	0.063	8
	7075	T76	2	0.063 and 0.125	4
	7178	T76	2	0.125 and 0.150	3
Plate	7075	T7351	28[a]	0.250–2.500	2–11
	7075	T7651	16[b]	0.250–1.750	2–8
	7178	T7651	8	0.250–1.750	2–8
Extrusions	7075	T73510	13	0.688–3.500	2–9
	7075	T76510	4[c]	0.563–3.750	2–4
	7178	T76510	23	0.050–3.500	2–7
Total—All Products	7075	T73	42	0.063–3.500	2–11
	7075	T76	22	0.063–3.750	2–8
	7178	T76	33	0.050–3.500	2–8

[a] Two additional lots in test with less than two years' exposure.
[b] Four additional lots in test with less than two years' exposure.
[c] Eight additional lots in test with less than two years' exposure.

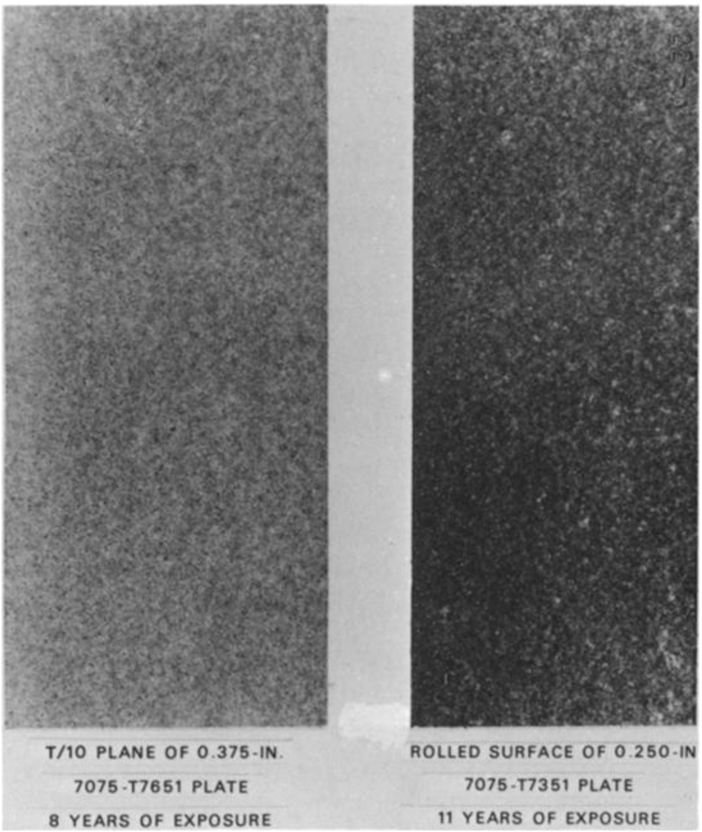

FIG. 6—*Photographs* (×0.4) *showing the excellent condition of the T76 and T73 specimens with the longest exposure to seacoast atmosphere at Point Judith. The opposite sides exposed earthward (rolled surface in both cases) also were completely free of exfoliation.*

minor (Fig. 7). It is concluded, therefore, that for all practical purposes 7075-T73, 7075-T76, and 7178-T76 products that are correctly heat treated can be expected to provide very high resistance to exfoliation corrosion in seacoast atmosphere. While T76 temper products may show slight susceptibility when machined to midthickness (Fig. 7), the effect is probably negligible and the performance vastly superior to that of T6 temper products.

If freedom from exfoliation after exposures of four or more years in the seacoast atmosphere at Point Judith is regarded as ample assurance of required service performance, then an accelerated exfoliation test should be able not only to detect materials that are less resistant to exfoliation, but also should not produce a form or degree of corrosive attack that would cause undue concern for material verified as resistant in seacoast atmosphere.

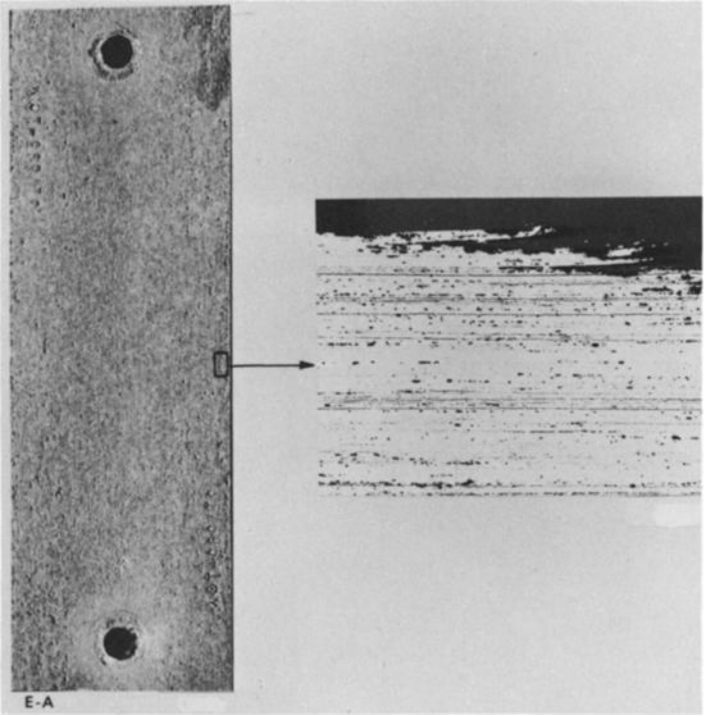

FIG. 7—*Midplane panel* (left, ×*0.4;* right, ×*50) from a 0.688-in.-thick 7178-T76510 extrusion representative of the maximum amount of exfoliation noted for the T76 temper after four years' exposure to seacoast atmosphere at Point Judith. Scattered sites of very mild exfoliation are present that penetrate only to a depth of about 0.006 in. The as-extruded surface exposed earthward showed no evidence of exfoliation. Code letters underneath the panel in this and subsequent figures rate the visual degree of corrosion against the ASTM photographic standards in Fig. 8.*

Comparative Performances in Seacoast Atmosphere and in Accelerated Test Media

Test Materials and Procedure

The objective of the T73 temper for 7075 alloy is very high resistance to stress-corrosion crakcing (SCC) at the high stress of 75 percent of the yield strength. During development of the temper it was learned that achievement of this degree of resistance to SCC required longer precipitation heat treatment than is needed for high resistance to exfoliation. Thus, procurement specifications for 7075-T73 products only state SCC requirements, as it is expected that such material also has high resistance to exfoliation. Unfortunately the T73 temper necessitates a 10 to 15 percent decrease in strength from that of 7075-T6 material.

The T76 temper for 7075 and 7178 alloy products was needed to provide a significantly higher resistance to exfoliation than the T6 temper with a minimum decrease in strength. Development of the T76 temper involved extensive use of the acidified 5 percent NaCl intermittent-spray exfoliation test described in Ref *3*. This test subsequently was incorporated in product specifications to ensure adequate heat treatment of T76 temper products. Expanded use of this test for quality control in various laboratories revealed some difficulties [*8*]. One of the problems is associated with the strong tendency for pit-blistering corrosion and the difficulty in distinguishing performances of materials with borderline resistance to exfoliation.

Recently a new laboratory test, ASTM Test for Exfoliation Corrosion Susceptibility in 7XXX Series Copper Containing Aluminum Alloys (EXCO Test) (G 34-72), was evaluated by an ASTM task group [*8*] for determining the resistance to exfoliation corrosion in copper-containing 7XXX alloys. This test involves 48-h immersion in an acidified salt solution, and its advantages over the spray test are better reproducibility, speed, simplicity, and low cost. Both the EXCO and spray tests are used at the Alcoa Laboratories. Good agreement between the two tests has been noted with material having either very good or poor resistance to exfoliation. Some disparity in results was observed when the material evaluated gave indications of slight susceptibility to exfoliation

In order to resolve the minor differences noted between results from the EXCO and spray tests, repeat tests were made on certain specimens whose performance in seacoast atmosphere was well established by virtue of four or more years of exposure at the Point Judith test site. This was done for two reasons:

(*a*) To determine which test result corresponds most closely to performance in seacoast atmosphere.

(*b*) To develop a basis for establishment of realistic visual acceptance criteria for material specifications covering T76 temper products.

This latter objective is needed to ensure that the criteria used with the laboratory tests are not so stringent as to reject serviceable material.

The atmospheric test panels recalled for retest were visually rated using the ASTM Method G 34-72 photographic standards shown in Fig. 8, photographed, and the type of corrosion present determined metallographically. The panels were then sectioned into three portions as shown in Fig. 9 and the portion labeled "seacoast atmosphere" was reexposed at Point Judith. The other two portions were machined just enough to remove corroded metal, tested by the spray and EXCO methods, visually rated and photographed, and the resultant type of corrosion determined metallographically. Panels used for this purpose represented test planes that were

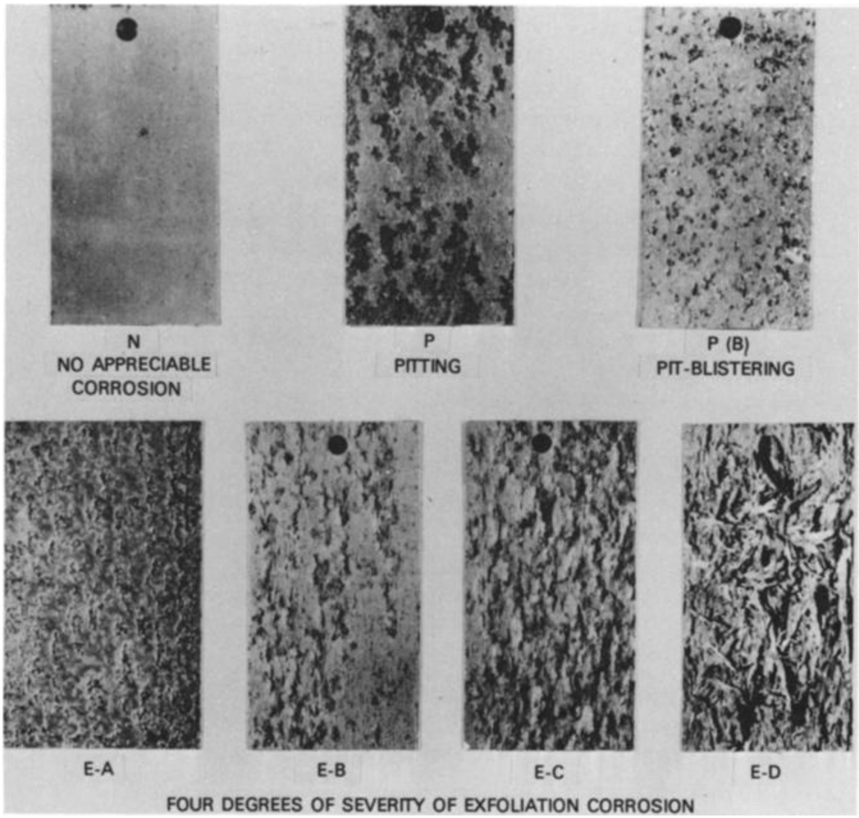

FIG. 8—*Rating codes and photographic standards in ASTM Standard Method of Test G 34-72 for use in reporting visual examination of corroded specimens.*

at least 0.063 in. and generally more than 0.250 in. beneath the extruded surface. Thus, the small amount of additional machining required did not significantly alter the location of the test plane and the inherent resistance to exfoliation. It is noteworthy that the maximum depth of machining required to remove all corroded metal from all the T7-type temper panels was only 0.010 in. This in itself is strong evidence of the good corrosion resistance of 7075-T73, 7075-T76, and 7178-T76 materials in seacoast atmosphere.

Specimens from two extruded shapes (section 113292 in 7075 alloy and 86366 in 7178 alloy) were selected to provide a photographic record of the results obtained. The configurations of these shapes and locations of test panels are shown in Fig. 10, while pertinent fabrication practices and metal properties are given in Table 5.

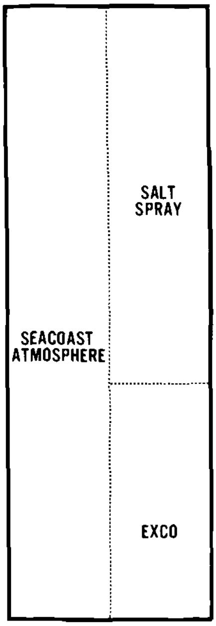

FIG. 9—*Sketch showing manner in which the 3 by 9-in. panels from the seacoast atmosphere were divided for retesting in accelerated exfoliation tests.*

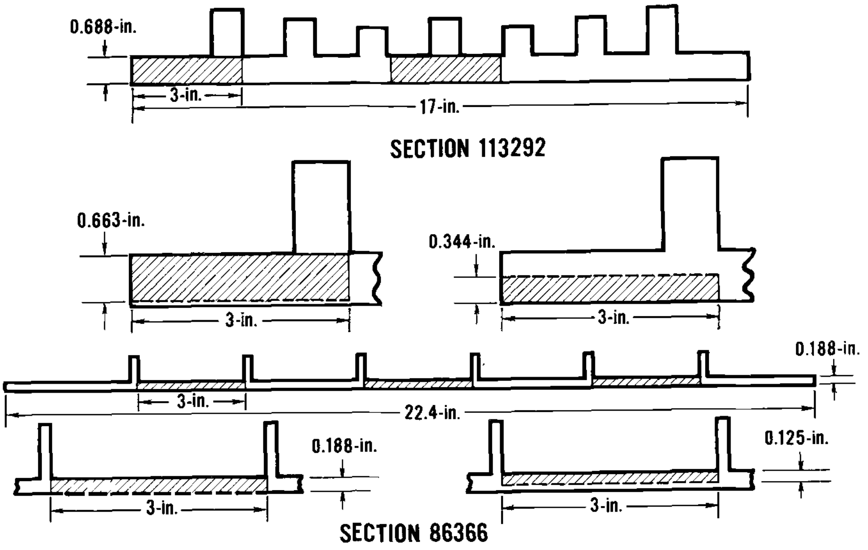

FIG. 10—*Cross sections of two integrally stiffened extruded shapes that were tested for resistance to exfoliation in accelerated environments and in seacoast atmosphere. Full cross-section views show positions at which test panels were obtained. Partial cross-section views indicate the depth to which the test surface* (dashed line) *was machined prior to exposure.*

TABLE 5—*Composition, heat-treat practices, longitudinal mechanical properties, and electrical conductivity of extruded sections 86366 and 113292.*[a]

Identification			Remelt Composition, %							
Section	Alloy	Temper	Si	Fe	Cu	Mg	Zn	Cr	Mn	Ti
86366 0.188-in. thick	7178	T6510	0.11	0.18	1.94	2.60	6.72	0.18	0.03	0.03
		T7X510	0.12	0.19	1.94	2.65	6.59	0.18	0.03	0.03
		T73510	0.11	0.18	1.92	2.69	6.72	0.19	0.02	0.02
113292 0.688-in. thick	7075	T6510	0.10	0.17	1.71	2.56	5.73	0.19	0.03	0.02
		T76510	0.10	0.17	1.69	2.55	5.69	0.20	0.04	0.02
		T73510	0.10	0.17	1.71	2.56	5.73	0.19	0.03	0.02

Identification			Heat Treat Practices	
Section	Alloy	Temper	Solution Heat Treatment	Precipitation Heat Treatment
86366	7178	T6510	15-min soak at 870°F (466°C)	24 h at 250°F (121°C)
		T7X510	15-min soak at 870°F	3 h at 250°F plus 10 h at 320°F (160°C)
		T76510	15-min soak at 870°F	3 h at 250°F plus 15 h at 320°F
113292	7075	T6510	20 min soak at 870°F (466°C)	24 h at 250°F (121°C)
		T76510	20-min soak at 870°F	3 h at 250°F plus 15 h at 320°F (160°C)
		T73510	20-min soak at 870°F	6 h at 225°F (107°C) plus 8 h at 350°F (177°C)

Identification			Longitudinal Properties			Conductivity, % IACS			
Section	Alloy	Temper	TS, ksi	YS, ksi	El, %	Surface	Near Surface[b]	T/3[c]	T/2[d]
86366	7178	T6510	91.3	82.2	11.0	32.8	...	32.3	...
		T7X510	87.4	79.5	9.0	38.3	...	37.8	...
		T76510	83.8	75.1	9.0	39.4	...	39.3	...
113292	7075	T6510	87.6	80.5	11.0	32.8	32.0	...	32.3
		T76510	79.4	69.9	11.0	40.2	39.5	...	39.2
		T73510	74.7	63.5	12.5	41.6	41.6	...	40.3

[a] Configuration of these sections shown in Fig. 10.

[b] 0.025-in. machined off surface.

[c] 0.063-in. machined off surface.

[d] 0.344-in. machined off surface.

Comparative Results

Alloy 7075—The original salt spray tests of specimens from extruded section 113292 in alloy 7075 were conducted for two weeks, twice the exposure time required by subsequent procurement specifications for the T76510 temper. The appearance of these specimens after the test is shown in Fig. 11.

Both the T76510 and T73510 temper materials are expected to be resistant to exfoliation at the near surface and, indeed, both were re-

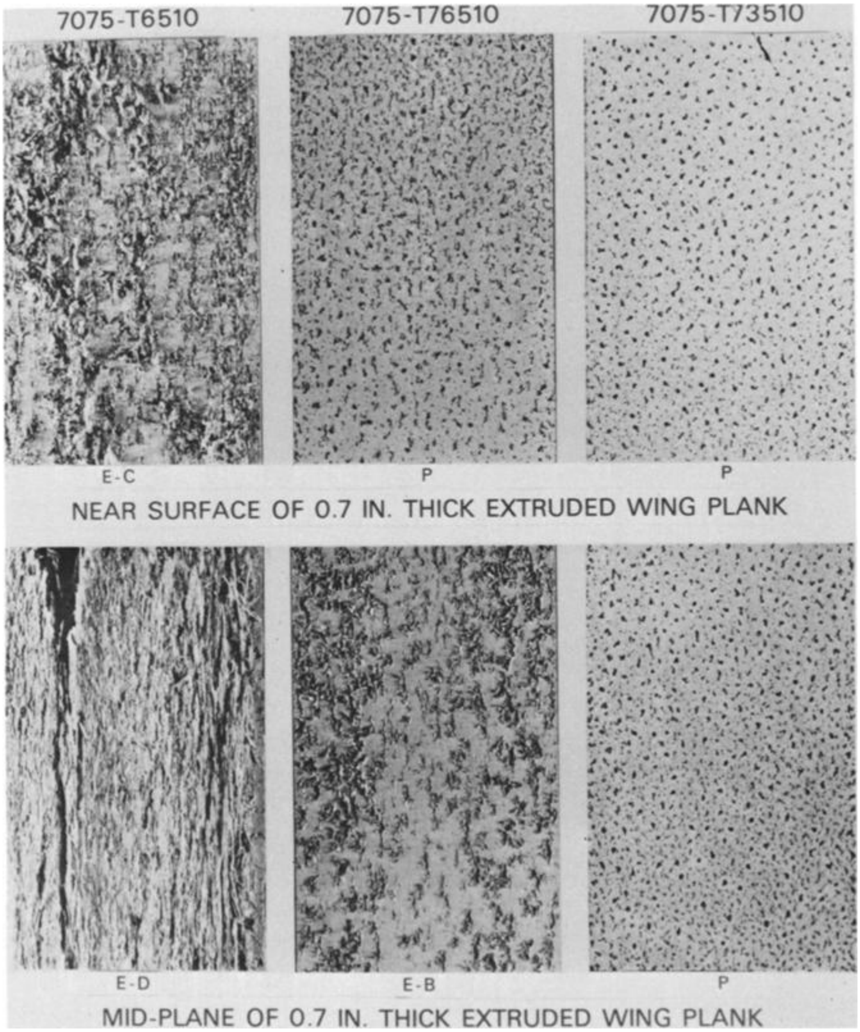

FIG. 11—*Appearance (×0.63) of panels from extruded section 113292 after two weeks' exposure to the salt spray test. Complete freedom from exfoliation was provided by the T73510 temper and greatly improved resistance by the T76510 temper.*

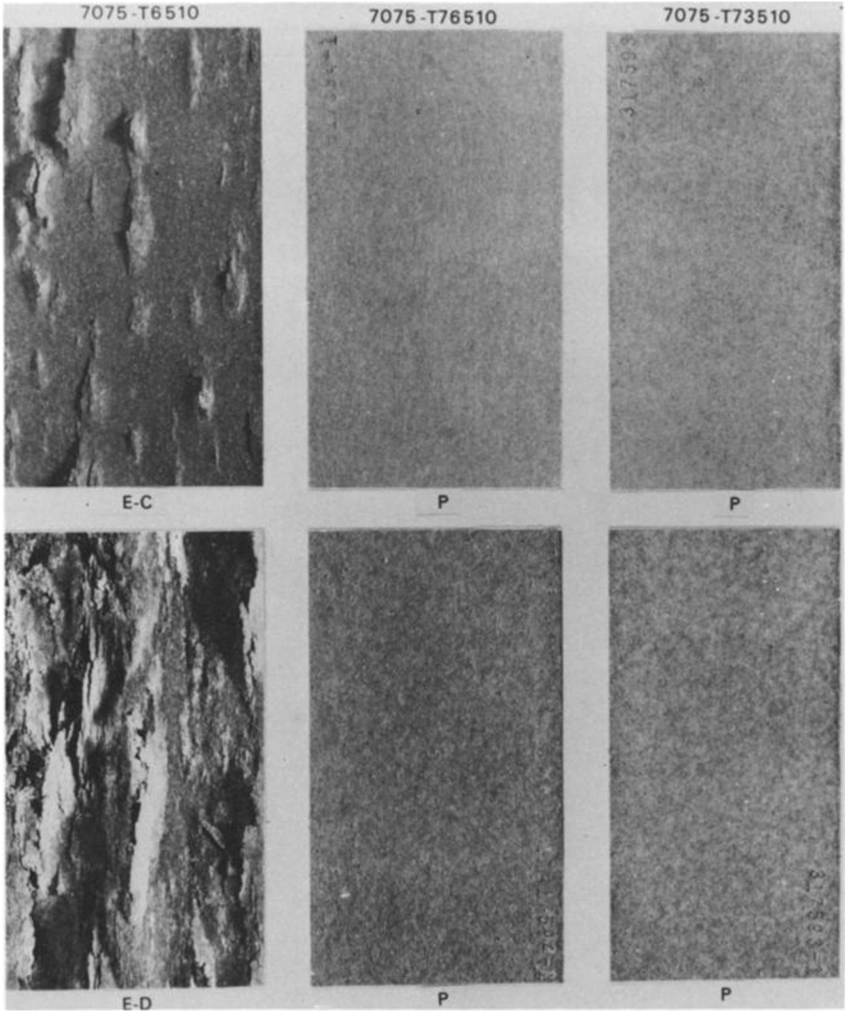

FIG. 12—*Appearance* (×*0.63*) *of midplane panels from extruded section 113292 exposed skyward to seacoast atmosphere at Point Judith for one year* (top) *and four years* (bottom). *The T6510 panel first showed exfoliation after only five months. After four years the T76510 and T73510 panels are still completely free of exfoliation.*

sistant. At this test plane the T6510 temper specimen incurred exfoliation to about a C degree.[3]

Only T73510 temper material is expected to be completely resistant to exfoliation at the midplane. The spray test did not cause any exfoliation of the midplane of the T73510 specimen, but resulted in a B degree[3] of ex-

---

[3] The condition of the near-surface T6510 specimen was intermediate between E-B and E-C, while that of the midplane T76510 specimen was intermediate between E-A and E-B. In keeping with the guidelines of G 34-72, such intermediate specimens were rated in the category of greater susceptibility, E-C and E-B, respectively.

foliation on the T76510 specimen and a D degree of exfoliation on the T6510 specimen (Fig. 11).

When midplane specimens were exposed to seacoast atmosphere the T6510 specimen was susceptible to severe exfoliation and the T73510 specimen immune, as in the spray test; but the T76510 material was also quite resistant (Fig. 12).

When midplane panels recalled from atmospheric exposure were retested by the EXCO and spray methods, the T6510 specimen incurred severe exfoliation (D degree) in both tests (Fig. 13). Results obtained on the T76510 and T73510 specimens were in good agreement for the seacoast atmosphere and the EXCO test. In these two environments the corrosion of T76510 and T73510 material was pitting, not exfoliation, but with a tendency for the pitting attack to undermine the surface (Figs. 14 and 15).

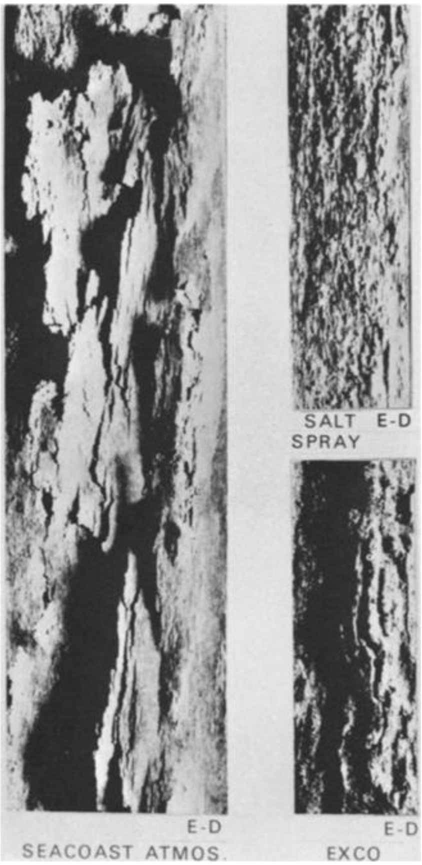

FIG. 13—*7075-T6510 panels from extruded section 113292. Severe exfoliation occurred in all three test environments.*

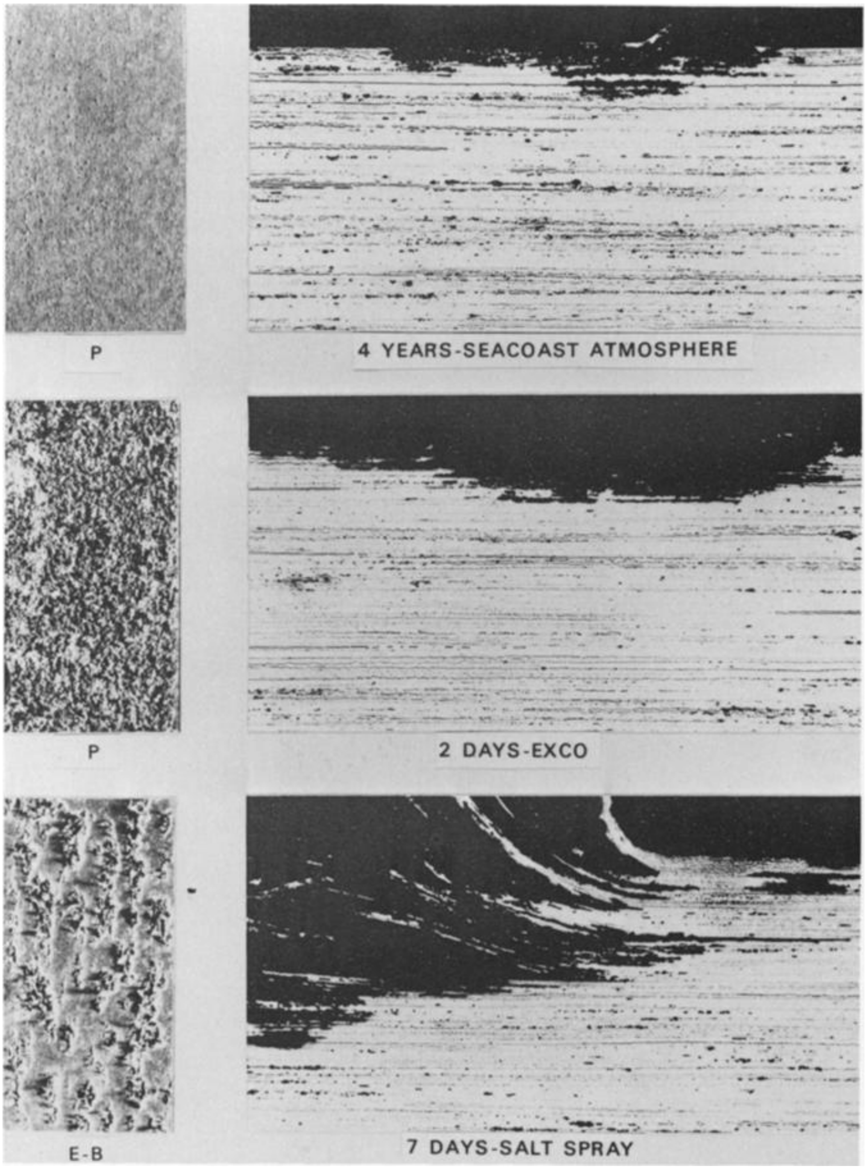

FIG. 14—*Appearance (×0.68) and metallographic type of attack (×68) of specimens from the 7075-T76510 panel; extruded section 113292.*

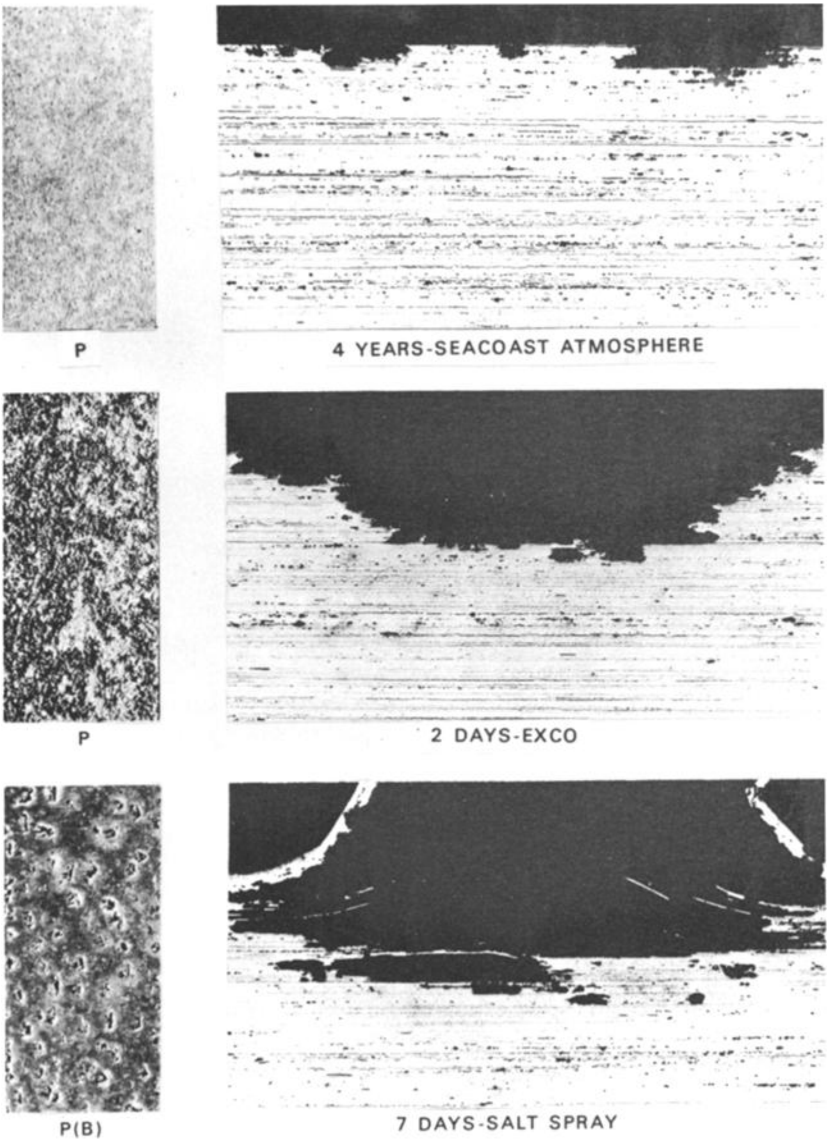

FIG. 15—*Appearance* ($\times 0.68$) *and metallographic type of attack* ($\times 68$) *of specimens from the 7075-T73510 panel; extruded section 113292.*

The only real difference was deeper attack into specimens exposed to the EXCO test.

The spray test, however, greatly aggravated the tendency for lateral undermining. The attack in the T76510 specimen (Fig. 14) was not confined solely to grain boundaries, but it did progress faster at the boundary and grain margins than within the grains. This resulted in exfoliation of a B degree on the T76510 specimen. The aggravated nature of the lateral attack is even more apparent on the T73510 specimen (Fig. 15). Lateral attack here was quite broad, consuming many grains in width, so that it clearly is pitting in nature, not intergranular corrosion. The undermined metal tended to blister up before opening into a pit (pit-blistering) so that there is a possibility of the visual appearance of this specimen being misinterpreted as exfoliation.

Alloy 7178—The same general comparison between the three environments was obtained on the 7178 alloy extrusions. The appearance of these specimens after exposure to seacoast atmosphere is shown in Fig. 16. The T6510 specimen showed severe exfoliation (D degree) after one year's exposure and was removed from test at that time. After four years, the T76510 specimen showed no exfoliation. Even the T7X510 specimen, intentionally underaged, showed no exfoliation after one year and only slight exfoliation (A degree) after four years.

When the 7178 specimens were retested there was good agreement between results in seacoast atmosphere and in the EXCO test, just as has been noted for alloy 7075. The T7X510 specimen developed exfoliation to an A degree in both tests (Fig. 17) while the T76510 specimen showed only pitting (Fig. 18). The spray test, however, accelerated exfoliation of the T7X510 specimen to a C degree (Fig. 17) and aggravated the undermining tendency of the pitting corrosion in the T76510 specimen, resulting in a marked degree of pit-blistering (Fig. 18).

Discussion of Results

As stated earlier, the validity of any accelerated test must be considered in the light of the intended applications of the metal and the anticipated service environments. For the purpose of this paper, aircraft structures are the assumed application with the premise that a four-year exposure to a seacoast atmosphere such as the Alcoa station at Point Judith is representative of the most severe conditions encountered with any regularity. Experience supports this premise for the overall aircraft structure, with the possible exception of certain sump areas or tanks where unusual chemical or bacteriological conditions can exist. The possibility of encountering unusual conditions generally is known and special protective measures are used in these cases. The logical conclusion, then, is that an aluminum alloy which performs well during a four-year exposure in a

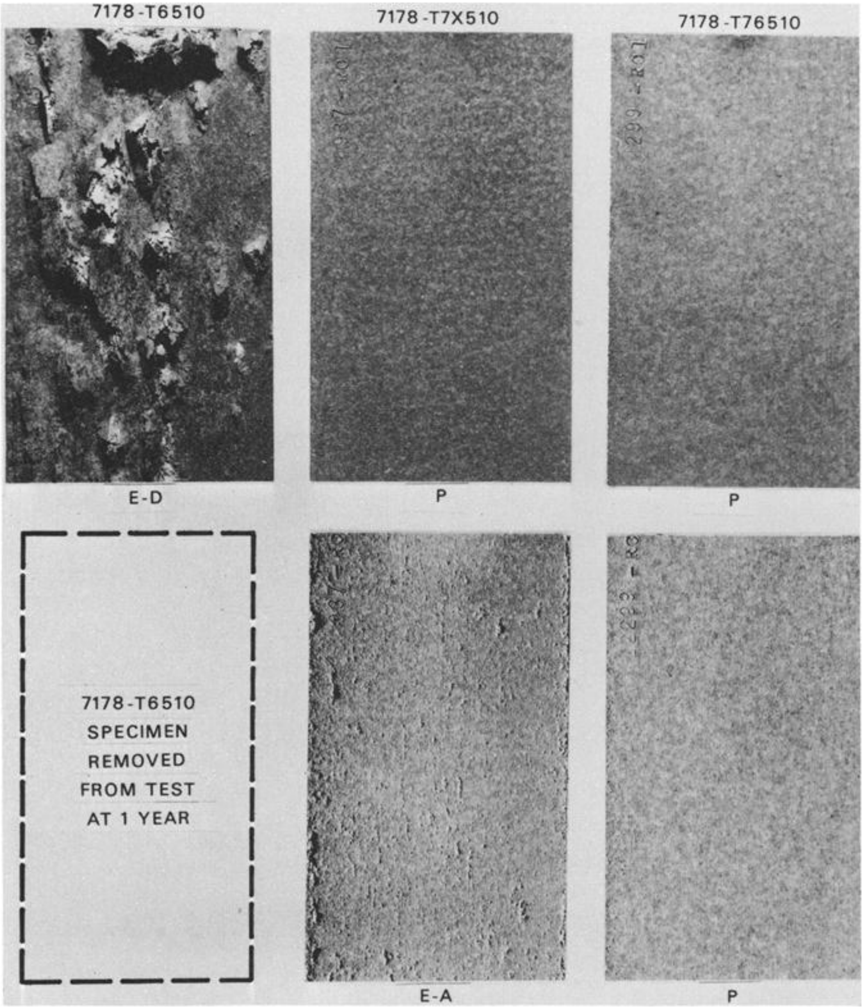

FIG. 16—*Appearance* ($\times 0.73$) *of T/3 panels from extruded section 86366 exposed to seacoast atmosphere at Point Judith for one year* (top) *and four years* (bottom). *The T6510 panel showed exfoliation after three months. After four years the T7X510 panel shows a slight amount of exfoliation and the T76510 panel is completely free of exfoliation.*

severe seacoast atmosphere, such as Point Judith, should be satisfactory for use in aircraft structures.

It is gratifying that the newly adopted EXCO test for determination of exfoliation corrosion of 7XXX series aluminum alloys appears to correlate well with exposures to an aggressive seacoast atmosphere. A review of the behavior of a number of lots of material, including some not identified in this paper, leads to the following observations. Materials in the T6 temper that exfoliated severely within six months to one year in the sea-

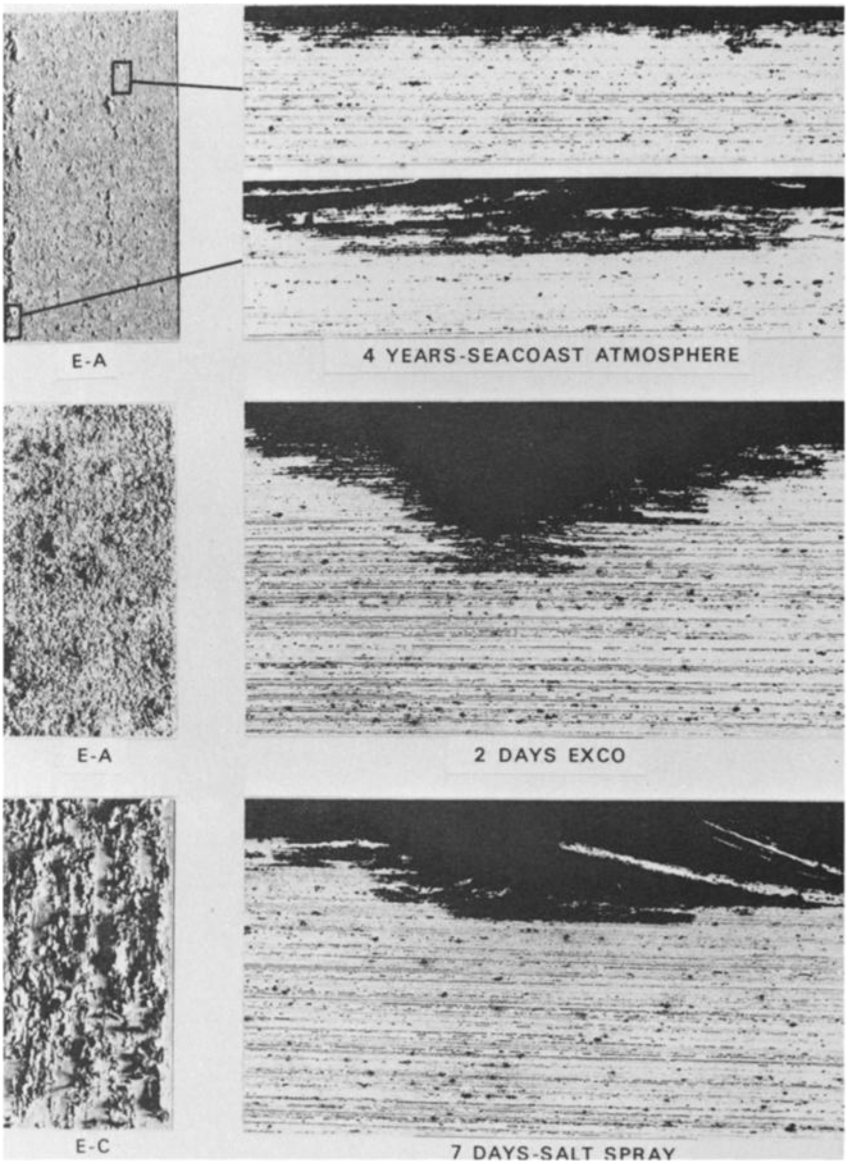

FIG. 17—*Appearance (×0.68) and metallographic type of attack (×68) of specimens from the 7178-T7X510 panel; extruded section 86366.*

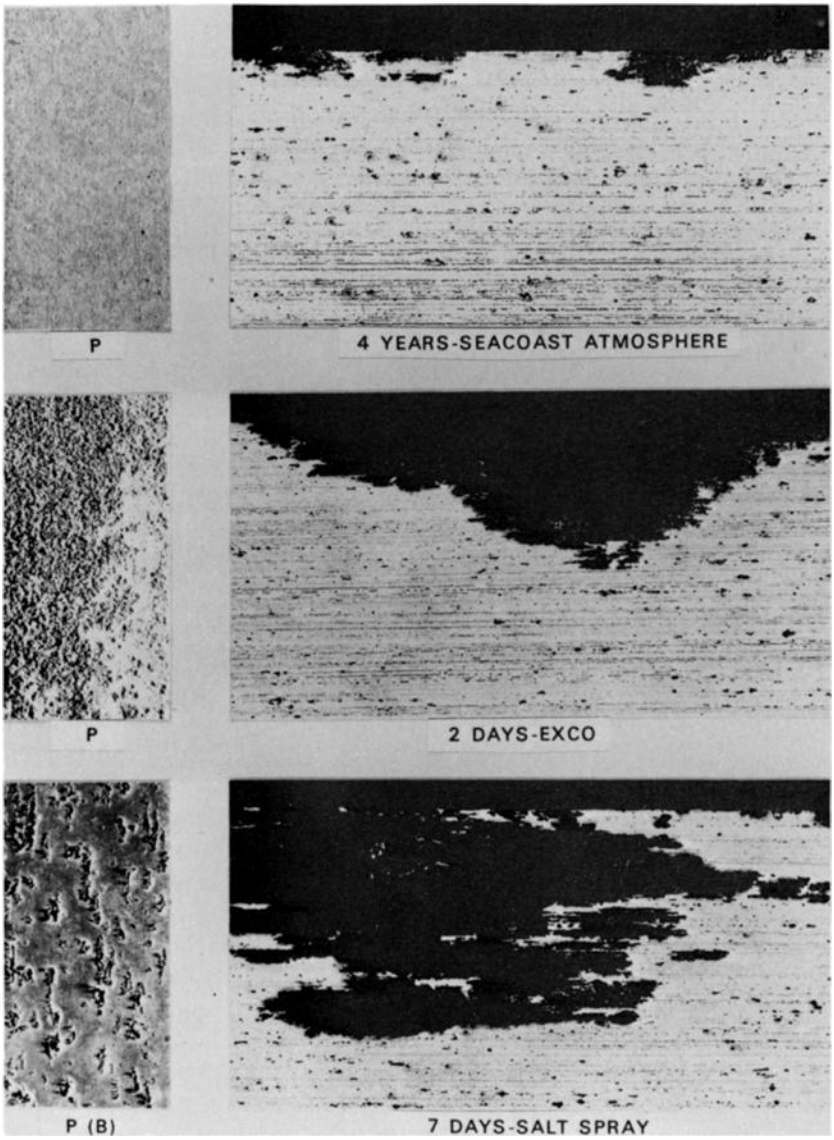

FIG. 18—*Appearance* (×*0.68*) *and metallographic type of attack* (×*68*) *of specimens from the 7178-T76510 panel; extruded section 86366.*

coast atmosphere also exfoliated severely in the EXCO test. Materials in the T73 and T76 tempers that showed no exfoliation after exposures of four years in the seacoast atmosphere showed either no exfoliation or slight (E-A) exfoliation in the EXCO test. Materials that show evidence of incipient exfoliation after four years' exposure (slight blistering similar to that shown in Fig. 17) may show slight exfoliation (E-A or E-B) in the EXCO test. Usually the spray test will emphasize such minor attack still more (Figs. 14, 17, 18).

A precaution that must be taken in using these accelerated tests, and especially the spray test, is to recognize the tendency to exaggerate undermining pitting and to cause pit-blistering in material that has no susceptibility to exfoliation. When the degree of pit-blistering is slight, it can usually be recognized visually as a different form of corrosion than exfoliation. In some cases, though, the appearance of a specimen with severe pit-blistering is similar to a mild degree of exfoliation, and metallographic examination is necessary to establish the primary type of corrosion present.

Finally, a factor of all laboratory tests for resistance to exfoliation that requires better resolution for quality control testing is definition of the limiting conditions for acceptance and rejection. Precise definition is complicated because there is no workable quantitative measure of degree of exfoliation; hence, the use in ASTM Method G 34-72 of photographic standards to illustrate varying degrees of exfoliation. This has shortcomings, three principal ones being (*a*) the influence of personal interpretation, (*b*) the difficulty in rating a specimen that has a degree of exfoliation in between two illustrated standards, and (*c*) differences in appearance that result from the extent and manner in which the exfoliated metal is dislodged. For example, the entire surface may lift off in layers, or it may come off in slivers, patches, or flakes, or it may merely result in swelling and bulging of the surface.

Material specifications have attempted to avoid these problems by stipulating that for an acceptable material no visible evidence of exfoliation shall be present on a specified test surface. The T/10 plane was selected to provide a more reproducible test plane than the fabricated surface. The extremely good performance to date of not only T/10 but also other such interior panels of 7075-T76 and 7178-T76 in exposures of four years and longer to the seacoast atmosphere at Point Judith raises serious doubt as to the practical significance in either of the accelerated tests of a minor tendency to exfoliation such as the degree A in the ASTM Method G 34-72 rating system. It is suggested, therefore, that specifications be revised to accept material showing exfoliation of degree A in the accelerated tests. This would also eliminate the need for metallographic examination to distinguish between pit-blistering and minor exfoliation. Possibly even the B degree of exfoliation may be allowed in the accelerated test if further testing establishes that such material will not exfoliate to any significant extent in service. However, the available experience shows that, in order to ensure performance significantly better than that of T6 temper material, the C and D degrees of exfoliation should not be allowed.

Conclusion

In review, it has been shown that commercially fabricated 7075-T73, 7075-T76, and 7178-T76 aluminum alloy products have excellent resistance to exfoliation corrosion when exposed to seacoast atmosphere at a relatively severe test site. Thus, these products should provide many years of trouble-free service in aircraft applications. Limited evaluations indicate that both the EXCO test, and the acidified salt spray test for determining resistance to exfoliation correlate well with results obtained in seacoast atmosphere. However, both tests can produce very slight exfoliation on material that as yet has not exfoliated in seacoast atmosphere and also exaggerate the tendency for undermining-pitting corrosion of material that is resistant to exfoliation.

Thus, it is concluded that a very slight tendency for exfoliation in these two accelerated tests, as represented by the ASTM visual standard for exfoliation of degree A, is of dubious concern for practical aircraft applications. It is suggested that consideration be given to tolerating this degree of susceptibility in 7075-T76 and 7178-T76 materials so as to maintain the optimum balance between resistance to exfoliation and strength.

References

[*1*] Dix, E. H., Jr. and Mears, R. B. in *ASTM Sympsosium on Atmospheric Exposure Tests on Non-Ferrous Metals*, American Society for Testing and Materials, 1946, p. 57.

[*2*] Walton, C. J. and King, W. in *Atmospheric Corrosion of Non-Ferrous Metals, ASTM STP 175*, American Society for Testing and Materials, 1955, p. 21.

[*3*] Lifka, B. W. and Sprowls, D. O., *Corrosion*, Vol. 22, No. 1, 1966, p. 7.

[*4*] Sprowls, D. O., Summerson, T. J., and Loftin, F. E., this symposium, pp. 99–113.

[*5*] Sprowls, D. O., Walsh, J. D., and Shumaker, M. B. in *Localized Corrosion—Cause of Metal Failure, ASTM STP 516*, American Society for Testing and Materials, 1972, p. 38.

[*6*] McGeary, F. L., Englehart, E. T., and Ging, P. J., *Materials Protection*, Vol. 6, No. 6, 1967, p. 33.

[*7*] Walton, C. J., Sprowls, D. O., and Nock, J. A., Jr., *Corrosion*, Vol. 9, No. 10, 1953, p. 345.

[*8*] Ketcham, S. J. and Jeffrey, P. W. in *Localized Corrosion—Cause of Metal Failure, ASTM STP 516*, American Society for Testing and Materials, 1972, p. 273.

R. A. Legault[1] *and H. P. Leckie*[1]

Effect of Alloy Composition on the Atmospheric Corrosion Behavior of Steels Based on a Statistical Analysis of the Larrabee-Coburn Data Set

REFERENCE: Legault, R. A. and Leckie, H. P., "**Effect of Alloy Composition on the Atmospheric Corrosion Behavior of Steels Based on a Statistical Analysis of the Larrabee-Coburn Data Set,**" *Corrosion in Natural Environments, ASTM STP 558*, American Soicety for Testing and Materials, 1974, pp. 334–347.

ABSTRACT: In 1962 C. P. Larrabee and S. K. Coburn published an extensive collection of atmospheric exposure data showing the effect of variations in copper, nickel, chromium, silicon, and phosphorus content on the corrosion resistance of low-alloy steel. Two hundred and seventy steel alloys of different composition were exposed for 15½ years at three separate locations representing industrial, semirural, and marine atmospheres. Among these experimental steel compositions there were five levels of copper concentration, two levels of nickel concentration, three levels of chromium concentration, three levels of silicon concentration, and three levels of phosphorus concentration represented. A statistical analysis of these data has been conducted and the results of the analysis are presented and discussed.

KEY WORDS: corrosion, alloy steels, atmospheric corrosion, chromium steels, copper steels, corrosion statistics, industrial atmospheres, low-alloy steels, marine atmospheres, nickel steels, phosphorus steels, regression analysis, semirural atmospheres, silicon steels, statistical analysis, steel alloy development, steel compositions, predictions, weathering steels

In 1962, Larrabee and Coburn[2] published a very comprehensive collection of atmospheric exposure data showing the effect of variations in the content of copper, nickel, chromium, silicon, and phosphorus on the atmospheric corrosion resistance of low-alloy steel. Two hundred and seventy low-alloy steels of different compositions were exposed for 15½ years at three separate locations representing industrial, semirural, and marine atmospheres. Although generalized conclusions were drawn from

---

[1] Senior research engineer and director, Coated Products Division, respectively, Inland Steel Research Laboratories, Inland Steel Company, East Chicago, Ind. 46312.

[2] Larrabee, C. P. and Coburn, S. K., *First International Congress on Metallic Corrosion*, Butterworths, London, p. 276, 1962.

the data in the initial publication of test results, no thorough statistical analysis of this remarkable data set has, to our knowledge, ever been published. Such an analysis, designed to establish the contributions of main effects, binary interaction effects, and quadratic effects of the five alloying elements to the total effect on corrosion rate, has now been completed. Reliable predictive equations were developed for corrosion rate as a function of composition for all three test site conditions.

Experimental Details

All 270 experimental steels were reported to have been made in a 30-lb high-frequency induction furnace utilizing an aluminum deoxidation prior to addition of the alloying elements, and then cast into 1 by 6 by 12-in. slabs. The slabs were reheated and cross-rolled to about a ⅛ in. thickness, normalized at 1850°F (1010°C) and pickled. The sheets were sheared into 4 by 6-in. specimens and weighed. Exposure was initiated in October and November of 1942 and all of the specimens at each location were placed on the test racks during the same day. During exposure, the specimens were supported on porcelain insulators mounted on metal frames placed at 30 deg to the horizontal facing south. The exposure sites are described in Table 1.

TABLE 1—*Exposure sites.*

Industrial:	Kearny, New Jersey (five miles west of Lower Manhattan)
Semirural:	South Bend, Pennsylvania (thirty-six miles northeast of Pittsburgh)
Marine:	Kure Beach, North Carolina (800 ft from the ocean surf)

TABLE 2—*Relative corrosivity of exposure sites.*

Site	1 Year	2 Years	4 Years	8 Years
State College, Pa. (rural)	1.0	1.0	1.0	1.0
South Bend, Pa. (semirural)	1.5	1.5	1.6	1.7
Kure Beach, N. C. (marine)	2.0	2.5	3.5	5.8
Kearny, N. J. (industrial)	3.3	2.7	2.5	2.6

The relative aggressiveness or corrosivity of these three sites has been reported by an ASTM committee[3] and is shown in Table 2. It should be noted that the relative corrosivity decreases with time at Kearny, New Jersey; increases slowly with time at South Bend, Pennsylvania; and increases rapidly with time at Kure Beach, North Carolina. These changes in site corrosivity with time are shown graphically in Fig. 1.

Although it might be intuitively felt on the basis of short-term comparisons that an industrial atmospheric site should be significantly more

---

[3] *Proceedings ASTM*, Report of Committee B-3, Vol. 59, 1959.

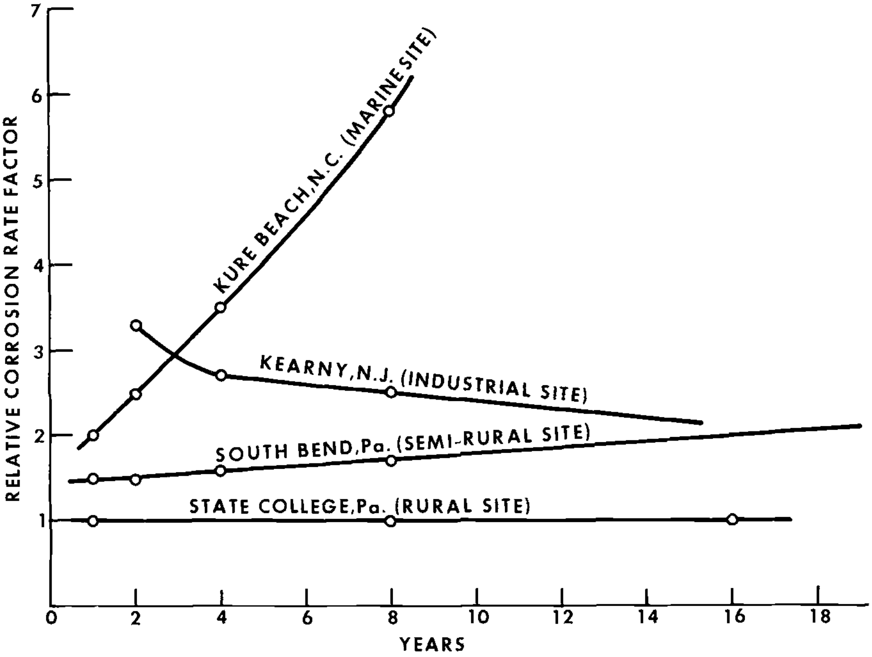

FIG. 1—*Change in relative atmospheric corrosion test site corrosivity with time.*

aggressive than a semirural site, the data shown in Fig. 1 indicate that after 15½ years' exposure little difference in aggressiveness exists between the two sites. A marine site, on the other hand, can be expected to be significantly more corrosive than the other two types of sites when long-term exposure data are compared. This is borne out in the Larrabee-Coburn 15½-year data as given in Table 3.

TABLE 3—*15½-year corrosion rates for each exposure site.*

Location	Type	Median of 260 Values (mils)	Low Value	High Value
South Bend, Pa.	Semi-Rural	3.905	1.3	7.9
Kearny, N. J.	Industrial	3.965	1.6	10.4
Kure Beach, N. C.	Marine	6.213	3.1	14.3

Ten of the 270 experimental steels were omitted from this statistical analysis either because the data reported was estimated at one or more sites or because the data reported for one or more sites clearly represented statistical outliers.

In all of the steel compositions investigated, carbon was present at less than 0.1 percent, manganese at 0.25 to 0.40 percent and sulfur at less than 0.02 percent. The experimental response reported, and the dependent variable used in this analysis, was the average reduction in thickness for the entire 15½-year exposure period expressed in mils and calculated from weight losses. For convenience, this response is referred to herein as corrosion rate.

The experimental steels used in the study represented five concentration levels of copper, two levels of nickel, three levels of chromium, three levels of silicon and three levels of phosphorus. Extreme compositional levels are shown in Table 4. The smallest concentration range, that for silicon, still involves a factor of more than six, and the widest range, that for copper involves a factor of more than forty.

TABLE 4—*Compositional limits represented in the data set.*

Additive	Low	High
Copper	0.012	0.51
Nickel	0.05	1.1
Chromium	0.1	1.3
Silicon	0.1	0.64
Phosphorus	0.01	0.12

Statistical Procedures Used

The first step in the process of statistically analyzing the three sets of empirical data provided by Larrabee and Coburn was the curve fitting of each data set to obtain mathematical expressions which accurately describe the data. Several, essentially linear, models were tried and discarded before the decision was made to settle on a quadratic model. Such a model for a five-additive system involves an equation of twenty terms: five main effect terms, ten binary-interaction terms, and five squared main effect terms. The curve fitting itself was accomplished using standard multiple-regression analysis techniques. The procedure used was the "stepwise regression" recommended by Draper and Smith.[4] The basic steps in the procedure are as follows:

1. A regression equation is computed by inserting variables in turn until the regression equation is satisfactory. The order of insertion is determined by using the partial correlation coefficient as a measure of the importance of variables not yet in the equation.

2. As each variable is entered into the regression, the following values are examined: first, R^2, the multiple correlation coefficient which is defined as the ratio of the sum of squares due to regression to the sum of squares about the mean; and second, the partial F-test value for the variable most recently entered, which shows whether that variable has taken up a sig-

---

[4] Draper, N. R. and Smith, H., *Applied Regression Analysis*, Wiley, New York, 1966, p. 171.

nificant amount of variation over that removed by variables previously in the regression.

3. Variables which were incorporated into the model in previous stages are reexamined at every stage in the regression. A variable which may have been the best single variable to enter at an early stage may, at a later stage, be superfluous because of the relationships between it and other variables now in the regression.

4. Sequential F-test values at each stage are compared with a preselected significance level and this provides the criterion for acceptance or rejection of a particular variable.

5. This stepwise process is continued until no more variables will be admitted to the equation and no more are rejected.

For the data sets in question, a sequential F statistic equal to 6.7 corresponds to a 99 percent confidence level and this was the significance level selected as the criterion for both the acceptance and the rejection of variables in the stepwise regression procedure used.

TABLE 5—*Quadratic model regression statistics for marine exposure.*

Sequential-F to enter	6.7	(99% Confidence)
Sequential-F to remove	6.7	(99% Confidence)
Multiple correlation coefficient (R^2)	0.950	
Equation F statistic	307	
Constant term	15.49	

	Coefficient	Student-T
Copper	−16.30	16.99
Nickel	−4.34	25.69
Chromium	−4.79	16.54
Silicon	−12.41	11.79
Phosphorus	−32.01	16.63
Copper-nickel	2.93	7.58
Copper-chromium	2.46	6.31
Copper-silicon	4.36	4.25
Nickel-silicon	2.74	8.07
Nickel-phosphorus	12.82	7.18
Chromium-silicon	1.75	4.99
Silicon-phosphorus	20.88	4.61
(Copper)^2	16.60	10.47
(Chromium)^2	1.20	6.42
(Silicon)^2	4.25	2.89

In the more customary form, the equation would appear as follows:

$$\begin{aligned}\text{Corrosion rate (mils)} = {} & 15.49 - 16.30\,(\%\ \text{Cu}) - 4.34\,(\%\ \text{Ni}) \\ & - 4.79\,(\%\ \text{Cr}) - 12.41\,(\%\ \text{Si}) - 32.01 \\ & (\%\ \text{P}) + 2.93\,(\%\ \text{Cu}\ \%\ \text{Ni}) + 2.46 \\ & (\%\ \text{Cu}\ \%\ \text{Cr}) + 4.36\,(\%\ \text{Cu}\ \%\ \text{Si}) \\ & + 2.74\,(\%\ \text{Ni}\ \%\ \text{Si}) + 12.82\,(\%\ \text{Ni}\ \%\ \text{P}) \\ & + 1.75\,(\%\ \text{Si}\ \%\text{P}) + 16.60\,(\%\ \text{Cu})^2 \\ & + 1.20\,(\%\ \text{Cr})^2 + 4.25\,(\%\ \text{Si})^2\end{aligned}$$

Results Obtained from Statistical Procedures

The equation obtained using these procedures together with pertinent statistical information on the data gathered at Kure Beach, North Carolina is shown in Table 5. It should be noted that despite the rather severe criteria imposed for the inclusion of variables in this equation, 15 of the 20 possible terms are represented here. The values listed for R^2 and for the F-statistic testify to the quality of the fit obtained. It should also be noted that only the main effect terms tend to decrease the corrosion rate; all of the interaction terms tend to increase the rate.

Similar information obtained from the data gathered at South Bend, Pennsylvania is given in Table 6. Only ten of the possible twenty terms appear in this equation and it should be noted that two of the additives, chromium and silicon, appear only in interaction terms. Every term which appears in this equation also appears in the marine exposure equation, suggesting that this set of variables is a subset of the grouping present in the marine exposure equation. This equation produced the only interaction terms with negative coefficients. It must be pointed out that these terms involved only chromium and silicon or both for which no negative main effect terms appear.

Analogous information obtained from the data gathered at Kearny, New Jersey is given in Table 7. Here only eight of the possible twenty

TABLE 6—*Quadratic model regression statistics for semirural exposure.*

Sequential-F to enter	6.7	(99% Confidence)
Sequential-F to remove	6.7	(99% Confidence)
Multiple correlation coefficient (R^2)	0.911	
Equation F statistic	256	
Constant term	8.50	

	Coefficient	Student-T
Copper	−13.39	16.29
Nickel	−3.03	24.22
Phosphorus	−21.27	18.22
Copper-nickel	3.48	9.89
Copper-silicon	2.41	2.62
Nickel-phosphorus	9.55	5.88
Chromium-silicon	−1.11	3.73
(Copper)^2	15.31	10.65
(Chromium)^2	−0.65	8.96
(Silicon)^2	−2.82	6.17

This equation can be written as follows:

$$\begin{aligned}\text{Corrosion rate (mils)} = {} & 8.50 - 13.39\ (\%\ \text{Cu}) - 3.03\ (\%\ \text{Ni}) \\ & - 21.27\ (\%\ \text{P}) + 3.48\ (\%\ \text{Cu}\ \%\ \text{Ni}) \\ & + 2.41\ (\%\ \text{Cu}\ \%\ \text{Si}) + 9.55\ (\%\ \text{Ni}\ \%\text{P}) \\ & - 1.11\ (\%\ \text{Cr}\ \%\ \text{Si}) + 15.31\ (\%\ \text{Cu})^2 \\ & - 0.65\ (\%\ \text{Cr})^2 - 2.82\ (\%\ \text{Si})^2\end{aligned}$$

TABLE 7—*Quadratic model regression statistics for industrial exposure.*

Sequential-F to enter	6.7	(99% Confidence)
Sequential-F to remove	6.7	(99% Confidence)
Multiple Correlation Coefficient (R^2)	0.804	
Equation F statistic	128	
Constant term	10.00	

	Coefficient	Student-T
Copper	−26.01	17.63
Nickel	−3.88	15.76
Chromium	−1.20	9.97
Silicon	−1.49	5.22
Phosphorus	−17.28	7.52
Copper-nickel	7.29	10.78
Nickel-phosphorus	9.10	2.91
(Copper)^2	33.39	12.07

This equation would be written as follows:

$$\begin{aligned}\text{Corrosion rate (mils)} = {} & 10.00 - 26.01\,(\%\ \text{Cu}) - 3.88\,(\%\ \text{Ni}) \\ & - 1.20\,(\%\,\text{Cr}) - 1.49\,(\%\,\text{Si}) - 17.28\,(\%\,\text{P}) \\ & + 7.29\,(\%\ \text{Cu}\ \%\ \text{Ni}) + 9.10\,(\%\ \text{Ni}\ \%\ \text{P}) \\ & + 33.39\,(\%\ \text{Cu})^2\end{aligned}$$

terms appear in the equation, with only three interaction terms represented, each of which tends to increase the corrosion rate. Again, every term which appears in this equation also appears in the marine exposure equation, suggesting that this set of variables is also a subset of the grouping present in the marine exposure equation.

The effect of dropping terms not meeting the $F \geqq 6.7$ criterion is shown in Table 8. The headings labelled 6.7, 6.7 indicate that the F-statistic criterion for entry as well as for removal was 6.7; the 0, 0 headings indicate that all of the variables were allowed to enter and that none were removed. Decreases in the values of the multiple correlation coefficients as variables are omitted, are insignificant. For instance, in the New Jersey data, although 12 of the 20 variables were omitted, the R^2 value decreased by only 0.015. The 3σ (99 percent) criterion for acceptance and for rejection of variables, taken together with the highly significant values obtained for both multiple correlation coefficients and F-statistics, indicates that a highly satisfactory fit of the data has been obtained in each case.

TABLE 8—*Effect of dropping equation terms.*

	Pennsylvania		New Jersey		North Carolina	
	0, 0	6.7, 6.7	0, 0	6.7, 6.7	0, 0	6.7, 6.7
M.C.C. (R^2)	0.921	0.911	0.819	0.804	0.955	0.950
F-Statistic	139	256	54	128	256	307
No. of terms	20	10	20	8	20	15

A measure of how reliable these predictive equations are is shown in Fig. 2, in which the observed corrosion rates for the Kure Beach, North Carolina site are plotted against values calculated using the 3σ predictive equation. Similar plots for the other two sites show that satisfactory fits have been obtained for all three sites, although there is somewhat more scatter evident in the New Jersey data than from the other two exposure sites.

Table 9 shows a comparison of the equation coefficients obtained for the three types of exposures. This table provides us with a measure of the relative effect of a given alloying element in each environment. It should be remembered that the effect of a given additive cannot be obtained

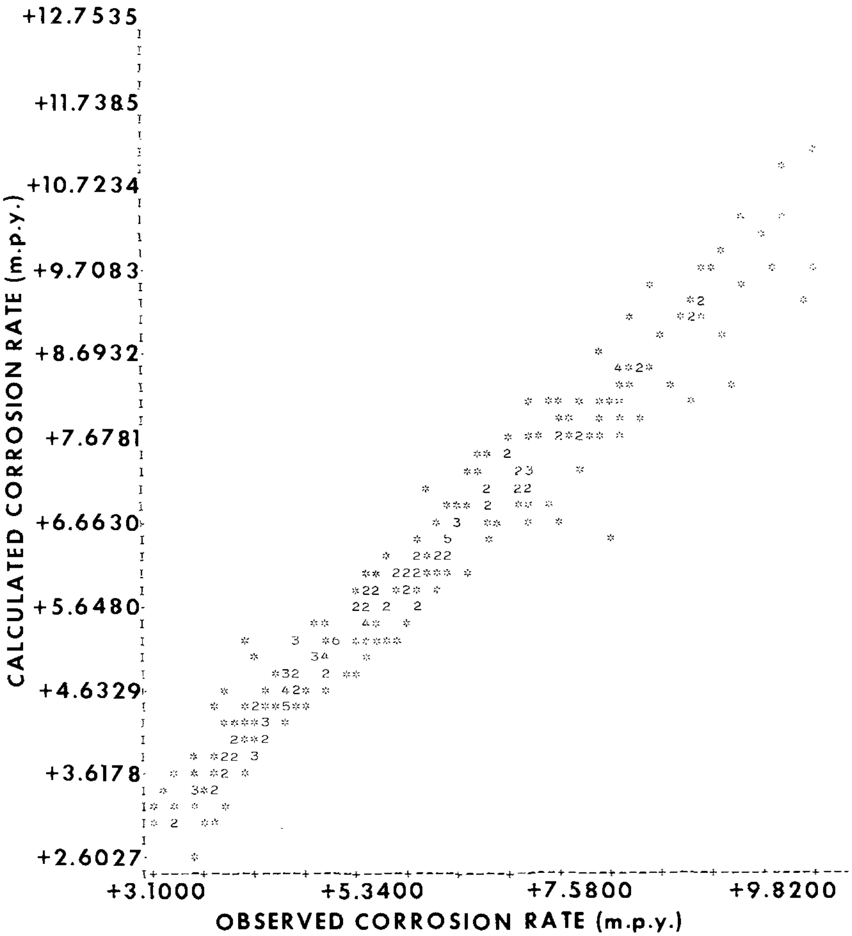

FIG. 2—*Plot of calculated corrosion rates versus observed corrosion rates at Kure Beach, North Carolina.*

TABLE 9—*Comparison of coefficients obtained for each site.*

	Pennsylvania	New Jersey	North Carolina
Constant	8.50	10.00	15.49
Cu coefficient	−13.39	−26.01	−16.30
Ni coefficient	−3.03	−3.88	−4.34
Cr coefficient	...	−1.20	−4.79
Si coefficient	...	−1.49	−12.41
P coefficient	−21.57	−17.28	−32.01
Cu Ni coefficient	3.48	7.29	2.93
Cu Cr coefficient	...	...	2.46
Cu Si coefficient	2.41	...	4.36
Ni Si coefficient	...	...	2.74
Ni P coefficient	9.55	9.10	12.82
Cr Si coefficient	−1.11	...	1.75
Si P coefficient	...	...	20.88
Cu^2 coefficient	15.31	33.39	16.60
Cr^2 coefficient	−0.65	...	1.20
Si^2 coefficient	−2.82	...	4.25

simply by noting the approximate main effect coefficient; every variable which involves that additive must be taken into account. It should also be noted that the effect of a squared term coefficient being greater than zero is to impose an upper concentration limit on that particular additive above which it will tend to increase the corrosion rate rather than to lower it.

Analysis of the Results

Having produced a satisfactory equation for each of the three exposure sites, attention was directed toward a determination of optimum additive levels based on these equations. Optimum additive levels are defined here as those included within the compositional levels evaluated in the Larrabee-Coburn data set; no attempt was made to extrapolate to compositional levels outside these values.

For each of the three corrosion rate equations, the partial derivative was taken with respect to each of the five additives. Each rate equation thus produced five partial derivatives which were set equal to zero and then solved simultaneously to obtain the optimum concentration levels for that exposure site. The optimum additive levels determined by this procedure are shown in Table 10. The letter "m" signifies here that the concentration level in question is the maximum level represented in the data set. For the Kearny, New Jersey and the South Bend, Pennsylvania exposure sites, only copper shows an optimum level other than the highest one represented in the data set. At the Kure Beach, North Carolina exposure site, silicon joins copper in showing an optimum concentration at an intermediate level.

TABLE 10—*Optimum additive concentration levels.*

	Pennsylvania	New Jersey	North Carolina
Copper	0.17	0.18	0.25
Nickel	1.1 (m)	1.1 (m)	1.1 (m)
Chromium	1.3 (m)	1.3 (m)	1.3 (m)
Silicon	0.64 (m)	0.64 (m)	0.42
Phosphorus	0.12 (m)	0.12 (m)	0.12 (m)

Accordingly, Fig. 3 shows the variation in corrosion rate at Kure Beach, North Carolina with changes in copper and silicon concentration when the other three additives are present at maximum levels for the data set; that is, nickel at 1.1 percent, phosphorus at 0.12 percent, and chromium at 1.3 percent. This is a three-dimensional plot in which corrosion rate is plotted vertically, thus producing a surface which depicts corrosion rate changes. It is interesting to note that whereas at the lowest level of copper shown (0.05 percent) the corrosion rate decreases with increasing silicon content, the opposite is true at the highest level of copper shown (0.4 percent). A minimum corrosion rate is produced, therefore, at an intermediate level of both copper and silicon. This effect can be seen in Fig. 4, in which a series of contour lines (iso-corrosion rate lines) for various corrosion rate levels at Kure Beach is depicted. The minimum corrosion rate occurs at lower and lower silicon levels as the copper concentration is increased.

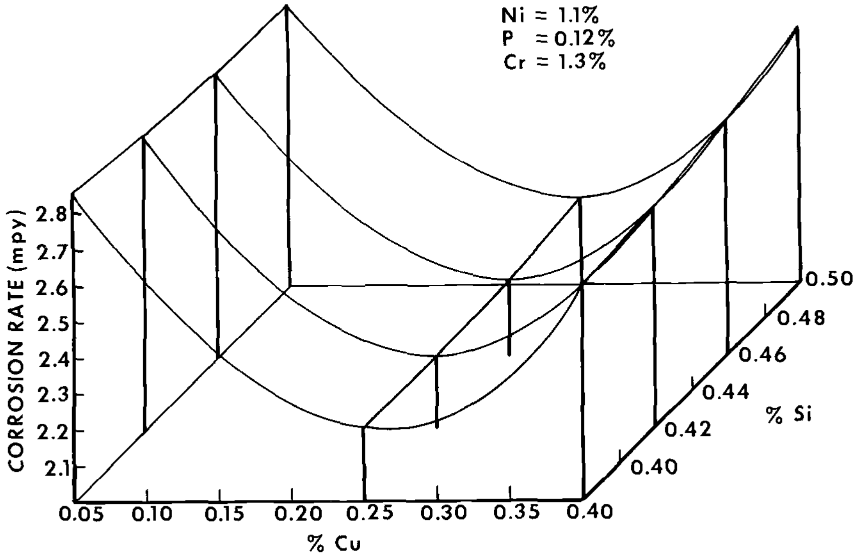

FIG. 3—*Three-dimensional plot showing the effect of corrosion rate at a marine test site as both copper and silicon concentrations are varied.*

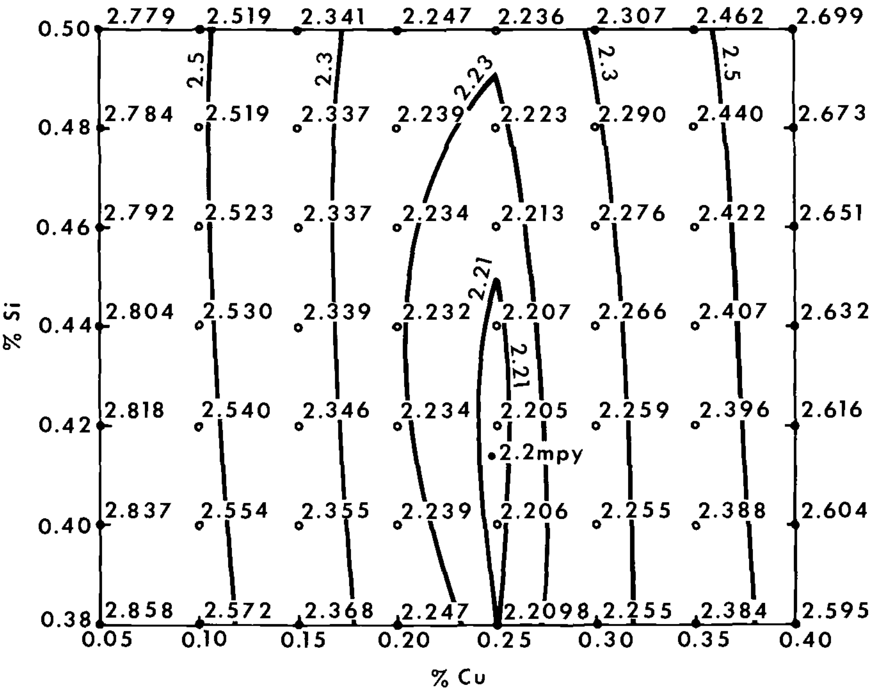

FIG. 4—*ISO-corrosion rate lines for a marine test site as both copper and silicon concentrations are varied.*

Figure 5 shows the variation in corrosion rate with copper content at Kure Beach when the other four additives are at the highest levels represented in the data set (Ni = 1.1 percent, Cr = 1.3 percent, P = 0.12 percent and Si = 0.64 percent), and again when they are at the optimum levels represented in the data set (Ni = 1.1 percent, Cr = 1.3 percent, P = 0.12 percent and Si = 0.42 percent). The advantage derived from using the lower silicon concentration is shown clearly in Fig. 5.

A three-dimensional plot such as that shown in Fig. 3 makes it possible to examine interaction effects on corrosion rate in the concentration regions of greatest interest. A large number of such plots have been constructed using each of the three equations derived in the present study. Figure 6 shows the effect of copper and silicon at an industrial site. A comparison of Fig. 3 with Fig. 6 thus allows an examination of behavior differences noted between marine and industrial exposures. The highest level of copper shown (0.4 percent) is clearly more effective in lowering corrosion rate at an industrial site than at a marine site.

Another example of a three-dimensional plot is shown in Fig. 7 in which the effect of copper and nickel concentration changes at an industrial site is depicted. It is interesting to note that, at Kure Beach, for the highest

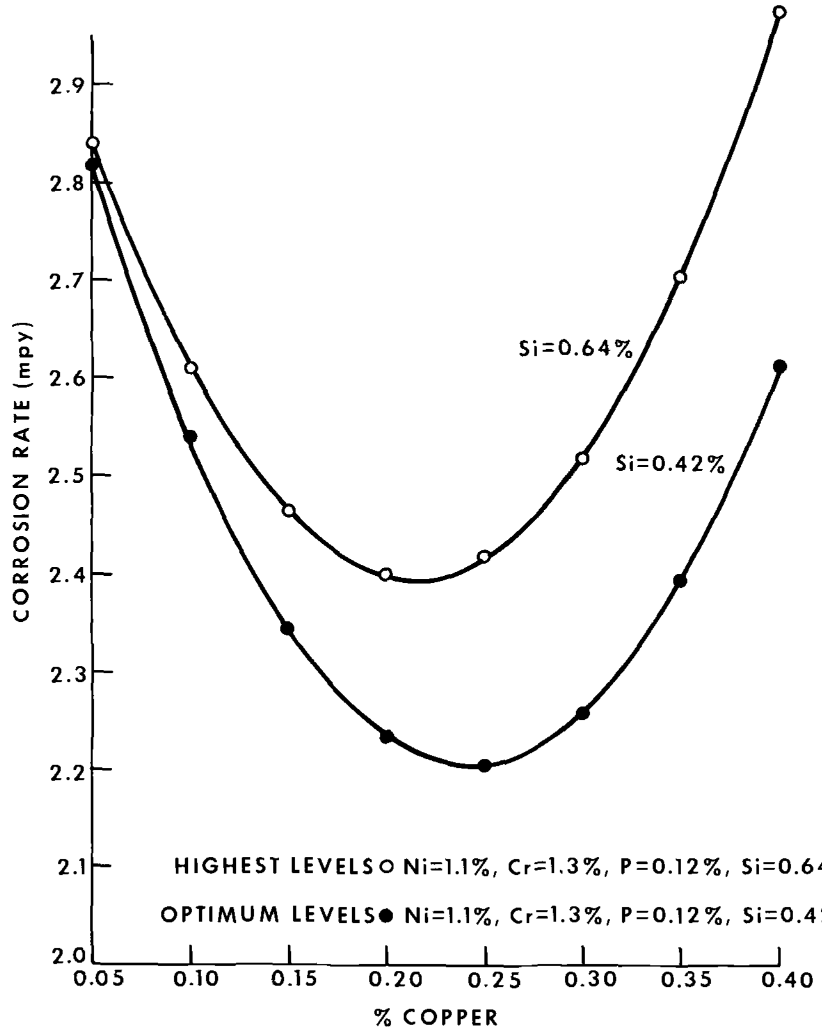

FIG. 5—*Effect of copper concentration on corrosion rate at a marine test site—comparison of the optimum levels of the other four additives with the highest levels represented in the data set.*

level of copper shown (0.4 percent), the corrosion rate decreases with increasing nickel concentration. The reverse effect was calculated for the Kearny, New Jersey site.

These considerations allow not only the selection of optimum concentration levels for a given type of exposure, but also provide information concerning how much the corrosion rate can be expected to change as the additive concentrations are varied from their optimum values.

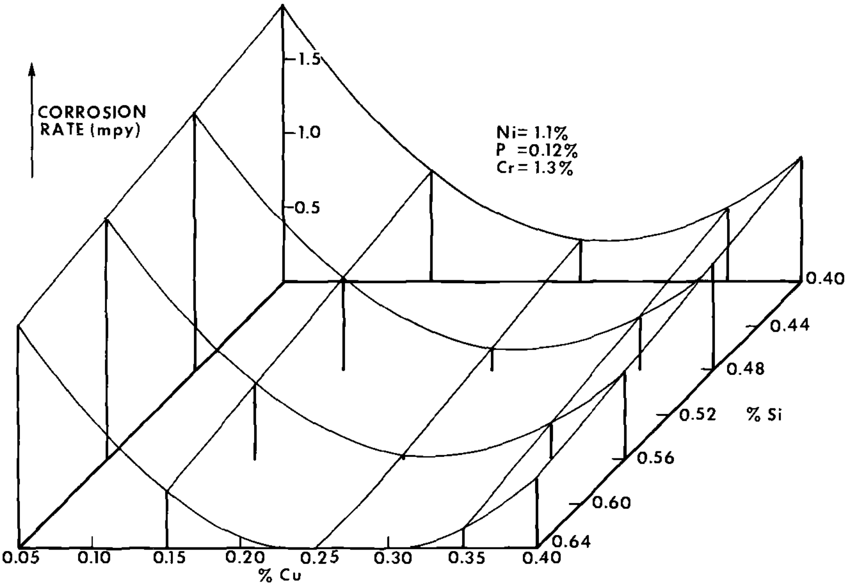

FIG. 6—*Three-dimensional plot showing the effect on corrosion rate at an industrial test site as both copper and silicon concentrations are varied.*

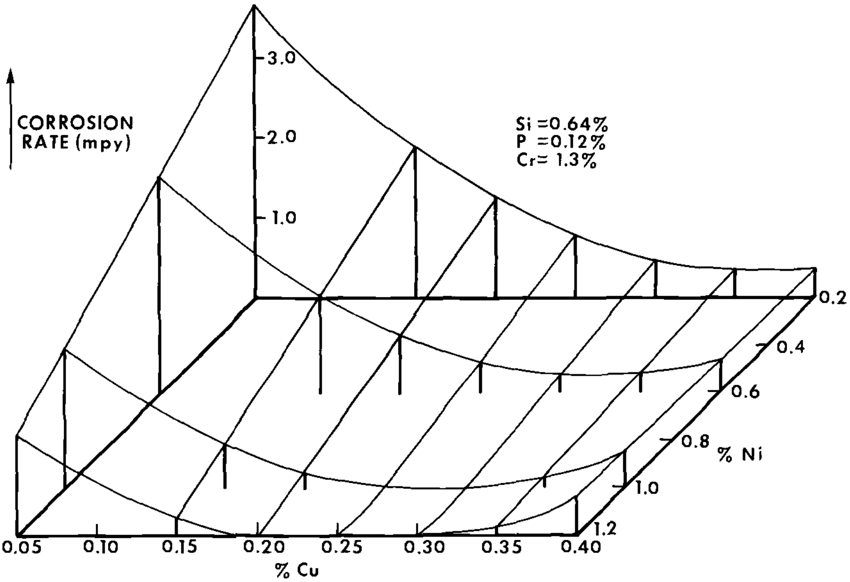

FIG. 7—*Three-dimensional plot showing the effect on corrosion rate at an industrial test site as both copper and nickel concentrations are varied.*

Summary

1. A reliable predictive equation relating corrosion rate to composition has been obtained for each of the three exposure sites (marine, industrial, and semirural) used in the Larrabee-Coburn atmospheric corrosion study.
2. For both the industrial exposure site at Kearny, New Jersey and the semirural site at South Bend, Pennsylvania, only copper among the five additives studied produces a minimum in corrosion rate at a concentration level other than the highest level represented in the data set.
3. For the marine exposure site at Kure Beach, North Carolina both copper and silicon produce corrosion rate minima at intermediate concentrations.
4. Within the compositional limits of the data set, statistical analysis shows corrosion rates to vary over a wide range.
5. A statistical analysis of the type described here makes possible the delineation of optimum compositional ranges with respect to corrosion resistance under environmental conditions corresponding to the three exposure sites described.

Acknowledgment

The authors wish to acknowledge the helpful discussions and suggestions of J. Dalal and A. G. Preban of the Inland Steel Research Laboratory.